INVESTIGATING ASPECTS OF HLA-DR ANTIGENS ON T CELLS

PHD THESIS

by

Anne Louise S. Revenfeld

AALBORG UNIVERSITY
DENMARK

Dissertation submitted June 17, 2015

- IMPOSSIBLE THINGS MAY CAUSE A SLIGHT DELAY -

Thesis title: Investigating aspects of HLA-DR antigens on T cells

Name of PhD student: Anne Louise Schacht Revenfeld

Name of supervisors:

Allan Stensballe, PhD, Associate Professor, Laboratory for Medical Mass Spectrometry, Department of Health Science and Technology, Aalborg University, Aalborg, Denmark

Malene M. Jørgensen, PhD, Senior Scientist, Department of Clinical Immunology, Aalborg University Hospital, Aalborg, Denmark

Kim Varming, MD, Head of Department, Department of Clinical Immunology, Aalborg University Hospital, Aalborg, Denmark

Papers included in the thesis:

Revenfeld, A.L.S., Bæk, R., Nielsen, M. H., Stensballe, A., Varming, K., Jørgensen, M. (2014): *Diagnostic and prognostic potential of extracellular vesicles in peripheral blood*. Clin Ther; 36, 6, pp. 830-46.
Revenfeld, A.L.S., Steffensen, R., Pugholm, L. H., Stensballe, A., Jørgensen, M.M, Varming, K. (2015): *The existence of HLA-DR on circulating CD4+ T cells cannot be explained by a concurrent presence of HLA-DRB1 expression.* BMC Immunology. Accepted with revisions.
Revenfeld, A.L.S., Bæk, R., Varming, K., Jørgensen, M.M, Stensballe, A. (2015): *Phenotypic characterization of extracellular vesicles and CD4+ HLA-DR+ responder T cells following contact-dependent and –independent allogeneic MLC*. Journal of Leukocyte Biology. In preparation.
Revenfeld, A.L.S., Søndergaard, E.K.L., Stensballe, A., Bæk, R., Jørgensen, M.M, Varming, K. (2015): *Characterization of a cell culturing system for the study of contact-independent vesicle communication. Journal of Extracellular Vesicles.* Submitted.

This thesis has been submitted for assessment in partial fulfillment of the PhD degree. The thesis is based on the prepared, submitted, or published scientific papers, which are listed above. In addition, the parts of the papers are used directly or indirectly in the extended summary of the thesis. As part of the assessment, co-author statements have been made available to the assessment committee and are also available at the Faculty. The thesis is not in its present form acceptable for open publication but only in limited and closed circulation as copyright may not be ensured.

PREFACE

This PhD thesis has been submitted to the Faculty of Engineering and Science, Aalborg University, Denmark. The work presented in the thesis is the outcome of research conducted at the Laboratory for Medical Mass Spectrometry, Aalborg University, Aalborg, Denmark and at the Department of Clinical Immunology, Aalborg University Hospital, Aalborg, Denmark. Moreover, a research visit of three months was carried out at the laboratory of Associate Professor Leonard J. Foster at the Department of Biochemistry and Molecular Biology, University of British Colombia, Vancouver, Canada.

This PhD thesis investigates aspects of HLA-DR on human T cells. First, this is achieved through elucidating the endogenous protein and mRNA expression. Moreover, some of the consequential functional features are also characterized.

The thesis is sectioned into five chapters. Initially, the introductory section provides the reader with an overview of the known and unknown aspects of the investigated area. Next, the aims of the PhD study and each of the included manuscripts are elaborated. In the methodology section, additional aspects of techniques and methods not covered by the manuscripts are described in more detail. Subsequently, the major findings of the PhD study are presented, followed by a discussion of the results and an outline of the implications of these. Finally, future work based on the results of the PhD study is put forward. The thesis also contains two appendices, which hold all information about additional scientific work carried out along with the manuscripts included in the thesis.

Aalborg, 17th of June 2015

Anne Louise Schacht Revenfeld

ABSTRACT

For more than four decades it has been observed that T cells can present major histocompatibility complex II (MHCII) and that this phenomenon increases upon activation. Currently, the human MHC class II isotype, human leukocyte antigen DR (HLA-DR) is a well-accepted marker for T cells activation. Nonetheless, an increasing amount of research points to a more pronounced role for HLA-DR than being an activation marker. The constitutive expression of HLA-DR is limited to professional antigen-presenting cells (APCs) and in this context the functions of HLA-DR are well described. These cells use HLA-DR to present antigenic peptides to CD4+ T cells and HLA-DR is involved in many facets of immune homeostasis, including T cell activation, peripheral tolerance, and induction of apoptosis. However, the functional consequences and physiological relevance of HLA-DR on T cells remain enigmatic. It has been demonstrated that mouse T cells cannot endogenously express MHCII but rather acquire it from APCs and a similar protein transfer has been observed for human T cells. Consequently, there is still no consensus of whether an endogenous protein expression or a molecular acquisition accounts for the presence of HLA-DR on human T cells.

The aim of the present PhD study was to investigate the endogenous expression and/or acquisition of HLA-DR by human T cells. The key methods applied in this investigation included flow cytometry to determine cellular phenotypes, qPCR to quantify gene expression, and the EV Array, which is a novel technique for characterizing the protein phenotype of cell-derived vesicles. The research presented in the thesis indicates that human T cells in peripheral blood do not express HLA-DR endogenously, based on investigations at both the protein and transcript level. Furthermore, the functional phenotype of these HLA-DR presenting T cells points to a role in down-regulating the activity of other T cells. This has a major impact in understanding the regulation of the immune system, since a likely role of these HLA-DR presenting T cells is to be involved in the induction and maintenance of peripheral tolerance. Thus, the research presented in this thesis has implications for both fundamental immunology as well as several pathological conditions, including autoimmune diseases and cancer.

DANSK RESUMÉ

I mere end fire årtier er det blevet observeret, at T-celler kan præsentere vævstype-proteinet MHCII (major histocompatibility complex) i deres cellemembran og at antallet af disse celler stiger ved en aktivering af immunforsvaret. Den humane udgave af MHCII proteinet, kaldet humant leukocytantigen DR (HLA-DR), benyttes en markør for aktiverede T celler. Forskning peger dog i stigende grad på, at HLA-DR er mere en blot en aktiveringsmarkør. Den konstitutive udtrykkelse af HLA-DR er forbeholdt professionelle antigen-præsenterende celler (APC) og disse celler anvender HLA-DR til at præsentere antigener til CD4 + T-celler, som aktiveres, hvis antigenet genkendes. Dette igangsætter et immunrespons og dermed er HLA-DR et protein med en meget vigtig funktion. Det er stadig uvist, hvilke funktionelle konsekvenser, samt hvilken fysiologiske relevans, det har, at HLA-DR kan findes på T celler. Det er blevet vist, at T-celler fra mus ikke selv kan udtrykke MHCII proteinet, men i stedet erhverver det fra APC. Desuden er en tilsvarende observation blevet gjort for humane T celler. Der er derfor stadig uenighed omkring, hvorvidt humane T celler har evnen til selv at udtrykke HLA-DR proteinet, dvs. en endogen udtrykkelse, eller om en proteinoverførsel forklarer tilstedeværelsen af HLA-DR på disse celler.

Formålet med denne Ph.d. afhandling var at undersøge humane T cellers endogene udtrykkelse og / eller erhvervelse af HLA-DR. Til denne undersøgelse blev en række metoder anvendt, hvoraf de centrale inkluderede flowcytometri til bestemmelse af cellernes proteinudtryk, qPCR til kvantificering af genudtrykkelse, samt EV Arrayet, der er en ny teknik til at karakterisere tilstedeværelsen af proteiner på celle-deriverede vesikler. Resultaterne, der præsenteres i afhandlingen, indikerer, at humane T celler, som findes i perifært blod, ikke selv udtrykker de HLA-DR proteiner, der findes i deres cellemembran. Endvidere tyder den samtidige tilstedeværelse af en række cellemembran-proteiner på, at T-celler, som præsenterer HLA-DR har en rolle i at nedregulere aktiviteten af andre T-celler. Dette har stor betydning for forståelsen af, hvordan immunsystemet reguleres, da disse HLA-DR præsenterende T-celler sandsynligvis kan være involveret i at skabe og opretholde perifær tolerance. Derfor har den præsenterede forskning i denne afhandling konsekvenser for både grundlæggende immunologi samt for flere patologiske tilstande, herunder autoimmune sygdomme og kræft.

ACKNOWLEDGEMENTS

I have many people to thank for being involved and investing their time and resources in me throughout my time as a PhD student. First, I would like to express my gratitude to my supervisors Associate Professor, PhD, Allan Stensballe, Senior Scientist, PhD, Malene M. Jørgensen, and MD, Kim Varming for providing me with the opportunity to carry out this PhD study. I also thank my supervisors for allowing me to pursue my ideas, for their guidance, their constant support, and our exciting discussions.

I would also like to thank all my great and indispensable colleagues at the Department of Clinical Immunology, Aalborg University Hospital, Denmark. Evo K.L. Søndergaard, Lotte H. Pugholm, Anne Elbæk, and Rikke Bæk – thank you for always keeping a positive attitude, for providing me with important input on both work- and non-work-related subjects, and for your help with countless proof readings. Moreover, I would like to thank my current and former colleagues at the Laboratory for Medical Mass Spectrometry, Aalborg University, including Tue B. Bennike, Michael K. Meyer, Lau Sennels, Thomas G. Carlsen, Kasper B. Lauridsen, Professor Svend Birkelund, and Professor Gunna Christensen for their valuable input and assistance in my work. In addition, I would like to thank Associate Professor Leonard J. Foster, Department of Biochemistry and Molecular Biology, UBC for welcoming me to into his laboratory, which was a very rewarding and memorable experience.

Finally, I would like to express my deepest gratitude to my family and friends for their unconditional support and encouragements. In particular, I am thankful for my greatest supporter, Jens Christian. Without his believe in me and without providing me with the most necessary support of all, this thesis would not have been.

ABBREVIATIONS

AEP	Asparagine endopeptidase
AF	Alexa Fluor
APC	Antigen-presenting cell
BLS	Bare lymphocyte syndrome
CatS	Cathepsin S
CD	Cluster of differentiation
cDNA	Complementary DNA
CIITA	Class II *trans*-activator
CIITA-p	Promoter for class II *trans*-activator
CLIP	Class II-associated invariant chain peptide
cSMAC	Central supramolecular activation complex
CTLA-4	Cytotoxic T-lymphocyte-associated protein 4
DC	Dendritic cell
ER	Endoplasmic reticulum
EV	Extracellular vesicle
FCM	Flow cytometry
FITC	Fluorescein isothiocyanate
FSS	Forward scatter
FMO	Fluorescence minus one
GM-CSF	Granulocyte-macrophage colony-stimulating factor
HLA	Human leukocyte antigen
HLA-DRB	Human leukocyte antigen, β-chain
ICAM-1	Intercellular adhesion molecule 1
iDC	Immature dendritic cell
IFN-γ	Interferon-γ
Ii	Invariant chain
IL	Interleukin
IL-R	Interleukin receptor

IS	Immunological synapse
LFA-1	Lymphocyte function-associated antigen 1
LPS	Lipopolysaccharide
mDC	Mature dendritic cell
MFI	Median fluorescence intensity
MGB	Minor groove binder
MHC	Major histocompatability complex
MIIC	MHC class II compartment
MLC	Mixed lymphocyte culture
MLR	Mixed lymphocyte reaction
PBMC	Peripheral blood mononuclear cells
PD-1	Programmed death-1
PD-L	PD-1 ligand
PE	Phycoerythrin
PHA	Phytohemagglutinin
PMA	Phorbol 12-myristate acetate
pMHCII	Peptide:MHC class II complex
pSMAC	Peripheral supramolecular activation complex
SD	Standard deviation
SSC	Side scatter
T-APC	Antigen-presenting T cell
TCR	T cells receptor
TNFRII	Tumor necrosis factor receptor 2
Teff	Effector T cell
Treg	Regulatory T cell
qPCR	Real-time quantitative polymerase chain reaction

TABLE OF CONTENTS

CHAPTER 1. INTRODUCTION

1.1. THE ANTIGEN-SPECIFIC IMMUNE SYSTEM

The immune system of the human body has a fundamental role in protection against pathogenic challenges as well as defeating them. The immune system thus encompasses a complex array of barriers, cells, and processes, which are dedicated to defense. In general, the immune system can be divided into two parts, namely the innate immune system and the adaptive immune system. Though not completely separated, one very key feature distinguishing these two systems is their mechanism for pathogen recognition. Accordingly, the innate immune system utilizes a limited number of specificities, while the adaptive immune system is highly specialized and antigen-specific (1). Two different aspects account for this antigen specificity. The first aspect relates to the effector cells of the adaptive immune system, the T cells. Two separate lineages of T cells exist, the CD4+ T cells and the CD8+ T cells, and common for both is their activation upon recognition of their specific antigen through interaction of the T cell receptor (TCR) and the antigen bound to a major histocompatibility complex (MHC) molecules. The antigens are peptide fragments derived from degraded proteins of either endogenous or exogenous origin and can be presented on MHC class I (MHCI) or class II (MHCII) molecules, respectively. Whereas the TCR comprises one half of the antigen specificity, the antigen presentation on the MHC molecules constitutes the other. In line with this, any given T cell is specific for the complex of a particular peptide bound to a particular MHC molecule, a phenomenon called MHC restriction (1). This is one of the intricate regulatory mechanisms used by the immune system that allows for initiation of finely tuned and precise immune responses.

All nucleated cells in the body express MHCI, however, the constitutive expression of MHCII is limited to the professional antigen-presenting cells (APCs): Dendritic cells (DCs), B cells, and monocytes/macrophages (2, 3). Moreover, inducible MHCII expression is possible in a number of non-APCs, including endothelial cells and fibroblast (3, 4). T cells constantly monitor the body for infections and other abnormalities, such as cancers, and consequently T cells make many temporary interactions with other cells. At the interface between these the interacting cells, a supramolecular structure is created, termed the immunological synapse (IS) (Figure 1A). The formation of the IS facilitates extensive reorganization of the receptors involved in adhesion and antigen recognition (5). Within the IS, a peptide and a MHCII molecule complex (pMHCII) interacts with the cognate TCR on CD4+ T cells, informing the T cells about the presence of an infection. This interaction provides stimulatory signals to the involved T cells, which consequently differentiate. Depending on the nature of the co-stimulatory signals also received, the T cell differentiation can lead to the formation of activated effector cells, the creation of anergic cells, or even the induction of apoptosis (Figure 1B). Regardless of the outcome of the differentiation, it is apparent that MHCII molecules hold pivotal

roles in the initiation, advancement, and termination of an adaptive immune response.

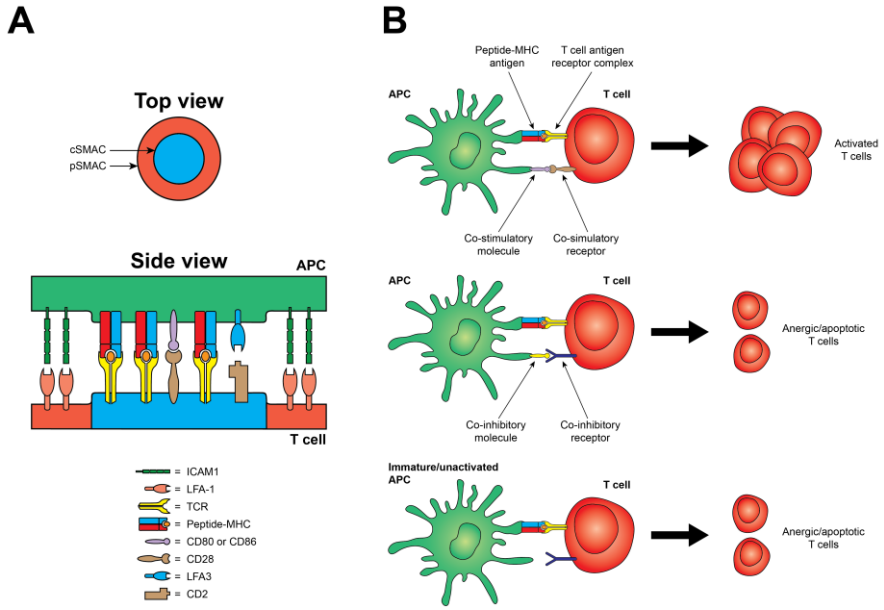

Figure 1 The immunological synapse (IS) and the interaction between pMHCII and the cognate TCR is essential for T cell activation. A | The IS is organized in a central supramolecular activation complex (cSMAC) and a peripheral SMAC (pSMAC). While the cSMAC harbors clusters of TCR, MHC determinants, and co-stimulatory molecules, the pSMAC is rich in molecules, which facilitate a tight adhesion of the interacting cells (5, 6). An important protein interaction in the pSMAC is that between lymphocyte function-associated antigen 1 (LFA-1) on the T cell and intercellular adhesion molecule 1 (ICAM-1) on the APC (7). **B** | Depending on the co-stimulatory signals received alongside the TCR:pMHCII ligation, the resulting fate of the T cell is quite different. Top panel: If the TCR:pMHCII ligation is accompanied by co-stimulatory signal via CD28 (T cell) and a B7 molecule (CD80/CD86, APC), the target T cell is activated. Once activated, the T cell undergoes clonal expasion and differentiation, acquiring its effector functions, such as cytokine production. This is under the control of IL-2, which is produced by the T cell itself only after receiving both the antigen-specific and co-stimulatory signals. Middle panel: The TCR:pMHCII interaction can also be accompanied by a co-inhibitory signal, such as that mediated by cytotoxic T-lymphocyte-associated protein 4 (CTLA-4) on the T cells and CD80 or CD86. The co-inhibitory signal can in some cases outcompete the co-stimulatory signal. This is the case for CTLA-4 (CD152), which has a much higher affinity for B7 molecules than CD28. The result of the co-inhibition is functional unresponsiveness, called anergy, or apoptosis. Lower panel: When the TCR:pMHCII ligation is not accompanied by a co-stimulatory signal, the target T cell becomes anergic or undergoes apoptosis.

1.2. THE EXPRESSION AND REGULATION OF HLA-DR

1.2.1. HLA-D ANTIGENS

In humans, MHC molecules are also known as human leukocyte antigens (HLA). This term was coined due to the observation that antibodies identifying MHC molecules targeted antigens on leukocytes. There are three classical and highly polymorphic isotypes of MHCII molecules, called HLA-DP, HLA-DQ, and HLA-DR (8) and all isotypes are all involved in antigen presentation to CD4+ T cells (9, 10). Two non-classical and less polymorphic isotypes of MHCII molecules also exist and these are HLA-DM and HLA-DO (8). These isotypes are involved in the loading of antigenic peptides to HLA-DP, HLA-DQ, and HLA-DR molecules (1). Several similarities exist for all HLA-D molecules, related to both genetic sequence and protein structure. In line with this, all HLA-D molecules are heterodimeric, transmembrane glycoproteins (11), which consist of one α-chain and one β-chain (Figure 2A). For HLA-DP, HLA-DQ, and HLA-DR it is the extracellular domains of both chains that form the peptide-binding groove, enabling antigen presentation (Figure 2A). Both polypeptide chains are encoded by distinct set of genes located on the short arm of chromosome 6. These genes are part of a genetic cluster, which is involved in the expression of other proteins also involved in antigen processing and presentation (1, 9). The genetic diversity of HLA-D molecules arises from both the presence of numerous genes encoding the α- and β-chains and extensive allelic polymorphism. Though the extent of this diversity is not as great as that for immunoglobulins and TCRs, it has both functional and medical implications related to aspects such as disease susceptibility and transplantations (1, 8, 10).

1.2.2. THE GENETIC BASIS OF HLA-DR

Of the HLA-D antigens, HLA-DR is the most widely studied isotype (10). It is subject to the largest extent of allelic polymorphism and is characterized by having a monomorphic α-chain and a highly polymorphic β-chain (1). Consequently, the β-chain makes by far the largest contribution to the diversity of HLA-DR (10). Only one gene exist for the α-chain (*HLA-DRA)* whereas four different loci encode functional HLA-DR β-chains (*HLA-DRB*). These comprise *HLA-DRB1*, *HLA-DRB3*, *HLADR-B4*, and *HLA-DRB5* (Figure 2A). Also five genes exist encoding non-functional β-chains; *HLA-DRB2*, *HLA-DRB6*, *HLA-DRB7*, *HLA-DRB8*, and *HLA-DRB9* (8). All humans carry *HLA-DRB1* on their chromosome 6, while the presence of any of the three remaining functional genes varies from individual to individual. Furthermore, the *HLA-DRB1* locus has the most identified alleles (Figure 2A). However, any of these functional HLA-DR β-chains can pair up with an HLA-DR α-chain to form a heterodimeric HLA-DR molecule. Despite the diversity of *HLA-DRB*, it is possible to divide individuals into five different HLA-DR haplo-

types, which denote a particular combination of HLA-DR alleles (8)(Figure 2B). These groups are characterized by their sole expression of *HLA-DRB1* or *HLA-DRB1* in combination with *HLA-DRB3*, *HLADR-B4*, or *HLA-DRB5*.

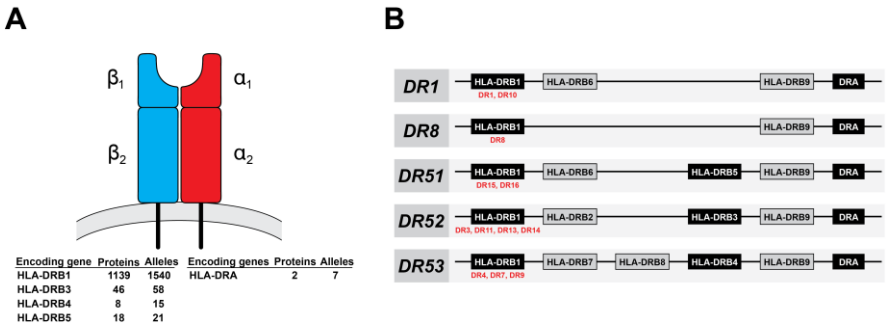

Figure 2 A | Structure and expression of HLA-D molecules, as exemplified by HLA-DR. Top panel: HLA-DR is a type I membrane protein consisting of an α/β heterodimer (12). The α-chain and β-chain are approximately 35 kDa and 27 kDa, respectively (12). In the extracellular part of HLA-DR, each of these chains consists of two domains of which one contributes to the peptide binding groove (α-1 and a β-1) and one to the immunoglobulin-like support (α-2 and a β-2). The latter provides a binding site for the CD4 co-receptor. HLA-DR is anchored to the cell surface by a transmembrane domain and has a C-terminal cytoplasmic tail, which can transmit intracellular signals (13). Lower panel: One gene encodes the α-chain (HLA-DRA), whereas four genes encode functional β- chains (HLA-DRB) of the HLA-DR protein. For each of these loci, a varying number of alleles and protein products exist **(14). B | The five major HLA-DR haplogroups (DR1, DR8, DR51, DR52, and DR53).** Each haplotype has been defined by the presence of a varying number of functional genes (black boxes) and pseudogenes (grey boxes) on chromosome 6. The DRB1 alleles can also be divided into five families, which relate to the haplogroups. For each haplogroup, the corresponding DRB1 allelic lineage is noted in red text, as exemplified by the DR1 haplogroup containing the *HLA-DRB1*01* and *HLA-DRB1*10* alleles (8).

1.2.3. MODULATION OF HLA-DR EXPRESSION

The expression of HLA-DR is subject to intricate regulation, consistent with the essential role in determining the specificity of the adaptive immune system. Accordingly, defects in this regulation have severe immunopathological consequences (8). A great number of biochemical and genetic mechanisms control the modulation of HLA-DR expression and new aspects continues to be unraveled.

The modulation of HLA-DR expression occurs mainly at the transcriptional level (8, 11). The majority of the knowledge about this modulation is based on studies of the bare lymphocyte syndrome (BLS), a severe combined immunodeficiency characterized by the lack of *HLA-D* gene expression (8, 11, 15). The transcriptional

control involves several highly conserved sequences located in the proximal promoter region upstream of both classical and non-classical *HLA-D* genes (8). The sequences are called the SXY module and four different bindings factors cooperatively bind to these sequences, forming a complex called the MHC class II enhanceosome. It is the result of multiple protein-protein and protein-DNA interactions and, when assembled, it serves as a scaffold to which the class II *trans*-activator (CIITA) can be recruited. It is CIITA, which then directs the subsequent transcription (8, 15). In effect, CIITA has been named the master regulator of *MHCII* gene expression, controlling both the constitutive and inducible *HLA-DR* expression (11, 15). Accordingly, out of all the *trans*-acting elements required for *HLA-DR* gene expression, CIITA is the only element that is not expressed ubiquitously (15). Hence, the protein synthesis of HLA-DR correlates with the presence of CIITA. Adding another level of complexity, the expression of the gene encoding CIITA, called *MHC2TA*, is also complex and involves the engagement of at least three different promoters (CIITA-pI,- pIII, and -pIV), which each transcribe a unique first exon (16). The employment of the different promoters depends on both the cell type and the particular stimuli (3, 8, 17). Furthermore, CIITA requires several post-translational modifications before it acquires its functional form (18-20). Interestingly, also several examples of CIITA-independent MHCII expression can be found for both professional APCs and non-APCs. Accordingly, the expression of MHCII was observed for both mouse B cells and DCs in the absence of CIITA, although the levels were five-fold reduced as compared to cells co-expression of CIITA and MHCII (21). Moreover, mouse corneal endothelium has been shown to express MHCII in a CIITA-independent manner and the resulting MHCII molecules were found to present antigens primarily of endogenous origin (4). Finally, it has been recognized that parameters such as epigenetic modifications and non-coding RNAs, e.g. miRNAs, are also important aspects of gene regulation (8, 22, 23). However, for the expression of *HLA-DR* genes the importance of these parameters remains to be investigated.

Several biochemical mechanisms also modulate the expression of HLA-DR molecules, although they are interdependent with those directly related to the genetics. These biochemical mediators also encompass a quite complex system of stimuli, where one mediator can exhibit different effects on two cell types, which impedes simple categorization. Nonetheless, the effects on the *HLA-DR* expression can be divided into two overall parts: An effect on the basal, constitutive expression or an effect on the induction or the enhancement the *HLA-DR* expression.

It is known that the basal expression can be enhanced or down-regulated by a number of immune and neuroendocrine mediators. As examples of the former, granulocyte-macrophage colony-stimulating factor (GM-CSF) can stimulate *HLA-DR* gene expression in DCs (24, 25), whereas glucocorticoids and prostaglandins down-regulate *HLA-DR* expression in B cells (11, 26). Related to the effects of biochemical mediators on the inducible *HLA-DR* expression, interferon-γ (IFN-γ) is reported as a potent inducer of this expression in non-APCs, including endothelial cells,

epithelial cells, and fibroblasts (11, 22, 27-29). It is believed that these HLA-DR expressing non-APCs are involved in maintaining peripheral tolerance, when co-stimulatory molecules are not concomitantly present (30), which can be related back to the same effect exerted by APCs on T cells (Figure 1B).

1.2.4. THE MHCII ANTIGEN PRESENTATION PATHWAY

Of great relevance to the function of HLA-DR is the entire pathway that directs its trafficking to intracellular compartments associated with antigen processing, loading of antigenic peptides, and ultimately transport to the cell surface. The molecular mechanisms involved in this pathway have been comprehensively investigated with the majority of the work focusing on HLA-DR or mouse MHCII (I-A and I-E)(2).

After synthesis, the HLA-DR heterodimer assembles in the endoplasmic reticulum (ER) together with the invariant chain (Ii, CD74) (Figure 3). The Ii protein forms a heterotrimer and acts as a chaperone for three HLA-DR heterodimers by carrying out a number of important tasks. First, Ii enhances the formation of stable HLA-DR heterodimers and also prevents premature binding of peptides by blocking the peptide-binding groove of the HLA-DR molecule. Moreover, Ii directs HLA-DR to and within the endosomal pathway (12, 31). From the ER, the HLA-DR:Ii complex is transported from the Golgi to the MHC class II compartment (MIIC). The MIIC is a late endosomal compartment, which contains a high density of MHCII molecules, HLA-DM, and proteolytic enzymes, called cathepsins, as the minimal prerequisite for loading of antigenic peptides to HLA-DR (32). The transport of the HLA-DR:Ii complex to the MIIC occurs either directly or via the cell surface (Figure 3)(2, 12, 31). Upon entry into the endosomal pathway, Ii is degraded by resident proteases, leaving only a small peptide fragment, called the class II-associated invariant chain peptide (CLIP), in the peptide-binding groove of HLA-DR (32, 33). Within the MIIC, CLIP is exchanged for antigenic peptides, which is a process supported by HLA-DM, and in some cells also HLA-DO (2). Subsequently, the antigen-loaded HLA-DR molecule is transported to the plasma membrane where if functions to present antigens to CD4+ T cells (Figure 3). A fraction of the cell surface HLA-DR molecules may yet again enter the endosomal pathway for re-loading and recycling back to the plasma membrane (34). However, the exact mechanism by which the complex is targeted for degradation or recycling and how these processes are regulated still remains elusive (2, 32). As a final point, HLA-DR is internalized and degraded, most likely following ubiquitination (2, 35).

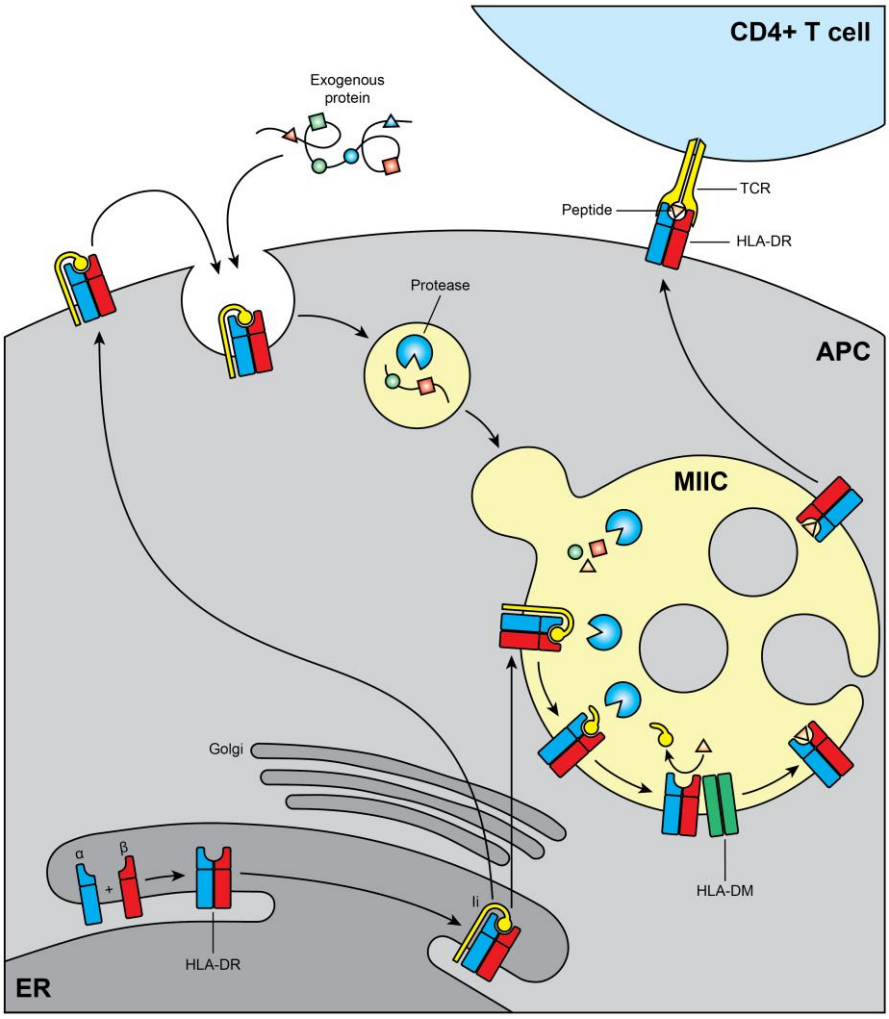

Figure 3 The MHCII antigen presentation pathway. The HLA-DR α/β heterodimer assembles in the ER, forming a stable complex Ii. The complex enters the endocytotic pathway either directly or via the cell surface. In the MIIC, Ii is degraded, leaving only the small peptide fragment CLIP in the peptide-binding groove of HLA-DR. The chaperone HLA-DM assists the exchange of CLIP for antigenic peptides, thus creating the mature HLA-DR, which is ultimately transported to the plasma membrane to exert its function in antigen presentation to CD4+ T cells.

1.2.5. HLA-DR ANTIGENS ON T CELLS

For more than four decades it has been observed that T cells in peripheral blood can present HLA-DR molecules on their cell surface. In addition, the number of these

cells increases upon activation (36). Accordingly, HLA-DR is often used as a marker for T cell activation, along with other molecules, such as CD69 and CD25 (37, 38). While the expression of HLA-DR is well described in the context of professional APCs, the expressional features of HLA-DR in T cells are still a topic of discussion. Furthermore, the possible functional implications of HLA-DR antigens on T cells remain poorly understood.

The first observation of MHCII molecules on T cells was made in the late 1970's (36, 39-41) and since then, several aspects pertaining to this observation have been investigated. It is widely accepted that HLA-DR marks activated T cell subsets. Moreover, both the percent-wise and the density of HLA-DR molecules on T cells increase following both mitogenic and antigenic stimulation (37). Commonly used mitogens, *i.e.* inducers of proliferation (mitosis), include phytohemagglutinin (PHA) and phorbol 12-myristate acetatate (PMA) in the combination with ionomycin. These two mitogenic stimulators activate T cells in a TCR-dependent or TCR-independent manner, respectively (37, 42). In terms of antigenic/antigen-like stimulation, either a combination of anti-CD3 and anti-CD28 antibodies or irradiated allogeneic peripheral blood mononuclear cells (PBMC) are often used (37, 43). When using the latter, the cellular assay is denoted a mixed lymphocyte culture (MLC) or reaction (MLR). This cellular assay has been employed for over four decades to investigate the proliferation and activation of responder PBMCs to allogeneic stimulator PBMCs. This has often been used to test the tissue compatibility of two individuals for the purpose of transplantation. The allospecific responder T cells, which constitute approximately 5% (44), recognize allogeneic pMHC complexes on the stimulator cells and become activated. The stimulator cells are typically irradiated, leaving them incapable of dividing, so that the read-out of the assay only relates to the responder cells.

HLA-DR is considered to be a late activation marker because its presence on T cells is detected approximately 3 to 5 days after activation (3, 37, 45). In contrast, CD69 is an early activation marker, detectable within hours or few days after T cell activation (3, 37). Despite somewhat contrasting results, the presence of the HLA-DR protein on T cells can be caused by the occurrence of either of two events. In the first event, an inducible *de novo* endogenous synthesis is reported, sharing several similarities to that found in APCs. In contrast, the second event involves an acquisition of HLA-DR from adjacent cells by mechanisms that are yet to be resolved. In the following, each of these two events will be elaborated.

1.2.6. CHARACTERISTICS OF ENDOGENOUS *DE NOVO* SYNTHESIS OF HLA-DR MOLECULES BY T CELLS

Studies supporting the endogenous expression of HLA-DR molecules in T cells often highlight the role of CIITA as the master regulator of HLA-DR expression (see section 1.2.3). Thus, the regulation and expression of CIITA in T cells has received particular attention. It has been demonstrated that isolated and activated

human T cells use the CIITA-pIII for the expression of *MHC2TA*, following PHA stimulation either with (46) or without (47) simultaneous stimulation with allogeneic, irradiated PBMCs, i.e. with or without an MLC. Furthermore, unstimulated T cells investigated in the same studies lacked CIITA expression (46, 47). The expression of MHCII molecules has been reported for T cells in several other species than humans, including bovine, (48) equine, (49) guinea pig, (50), and rat (51, 52). Interestingly, mouse T cells are not able to synthesize MHCII molecules, even upon *in vitro* activation (53). This has been explained by a failure to express *MHC2TA* (33, 54), of which a contributing factor is methylation at the CIITA-pIII region (22). However, contradictory results also exist. As an example, it has been demonstrated that mouse T cells can present MHCII antigens following both mitogenic and antigen-like (anti-CD3/anti-CD28) stimulation (55). Furthermore, a study noted that the preponderance of isolated primary CD4+ T cells do not express CIITA *ex vivo* (33).

1.2.7. CHARACTERISTICS OF A MOLECULAR ACQUISITION OF HLA-DR BY T CELL

The phenomenon of intercellular transfer of molecules has received increasing attention within the last decades. In relation to the immune system, the current understanding of this cellular event is that it comprises a cell-to-cell communication of great importance in the orchestration and regulation of immune responses (56-58). The interacting cells can acquire cell surface proteins and other molecules, including small RNAs, and entire membrane patches from each other. As a consequence of this, the recipient cell can acquire a new functional phenotype. Accordingly, this challenges the common perception of cellular autonomy, in the meaning that each cell is characterized by having a particular transcriptome and proteome (57, 59). In the context of HLA-DR, several investigations have shown that T cells from a number of species can acquire MHCII molecules from APCs (60-62). However, before elaborating on this particular process, the general features of intercellular exchange of molecules will be covered with regards to T cell:APCs interactions.

Mechanisms of intercellular transfer of molecules

It has been proposed that the transfer of proteins and other molecules between two cells can happen by either of four mechanisms. These include gap junctions, nanotubes, the process of trogocytosis, and the uptake of extracellular vesicles (Figure 4) (56, 57, 63). Gap junctions can be formed between cells in solid tissue, but also between immune cells (64). This creates a connection, which allows for the transfer of genetic material and other small molecules between cells (63). Nanotubes can be formed as membrane extensions between two interacting cells, thus creating a direct connection that facilitates a bi-directional exchange of vesicles, surface proteins, and small molecules (56). It is thought that the nanotubes may be formed either as membrane bridges upon termination of the IS, when the cells move apart, or by newly formed membrane outgrowths (56, 63). Trogocytosis (Greek *trogo;* gnaw/nibble) denotes the process in which entire membrane fragments are acquired by lymphocytes from the interacting APC (Figure 4) (65). Trogocytosis occurs at

the IS (section 1.1) and is triggered by signals conveyed through antigen receptors (65). The molecular transfer can be initiated only minutes after IS formation, after which the acquired molecules is either internalized, left in the membrane, or returned to the cell surface in a functional form (56). Extracellular vesicles (EVs) comprise the final and most extensively studied transfer mechanism. Furthermore, one subgroup of these vesicles, termed exosomes, has received the most attention (Figure 4)(63, 66, 67). These membrane-enclosed entities have been shown to play important roles in cellular communication by virtue of their protein, RNA, and lipid content (66, 68-71). In relation to the immune system, EVs have well documented immunomodulatory effects (63). This can be accomplished either by direct receptor-ligand signaling on the target cell or by being internalized or integrated into the plasma membrane, thus bestowing a new functional phenotype on the recipient cell. The vesicular transfer of molecules can occur either within the IS, in its close vicinity, or by transport from more distant locations in the body, which means that direct cell contact is not a prerequisite (63, 67, 72, 73).

T cells can aquire MHCII molecules from APCs

Shortly after the first observation of MHCII proteins on T cells were made, it was described how APC-derived MHCII molecules could be acquired by T cell clones *in vitro* (74). Since then, several groups have investigated this cellular phenomenon for both primary cells and cell lines, demonstrating the transfer of a fully functional protein complex, occasionally accompanied by a simultaneous transfer of co-stimulatory molecules (61, 75).

As previously mentioned, it has been demonstrated that mouse T cells cannot actively synthesize MHCII molecules (section 1.3.1). This observation initiated the continued discussion about the physiological relevance of MHCII on T cells because the immune system of mice seemingly was not impaired by this significant difference. One explanation, which could account for this cellular variation, is that the mouse T cells acquire MHCII molecules from APCs. In effect, the first indications of such a transfer occurring in mice was made in the early 1980´s (74). Subsequent research has confirmed and elaborated on this event (62, 76-78). Also for both rat (60) and human T cells (61), the acquisition of functional pMHCII complexes has been found. The requirements for the molecular transfer demonstrated in all species are currently not fully established and several contradictory results exist. A number of studies have reported that cell contact between T cell and APC is necessary for the molecular acquisition (61, 79). Furthermore, both trogocytosis (80) and vesicular transfer (60, 79, 81) has been indicated as the mechanisms responsible for the acquisition. While some studies report that the transfer is dependent on TCR-ligation (81), other studies draw contradictory conclusions (61, 79). Nonetheless, the activation status of the T cells continues to be underlined for its importance and is has been demonstrated that the acquisition of pMHCII is enhanced, when the T cell is activated and also when the cognate interaction between TCR and pMHCII is involved (62, 77, 81). In line with this, it has been observed that only activated mouse T cells could acquire MHCII-containing vesicles from

APC and that the acquisition was dependent on the presence of LFA-1 on these T cells. Hence, this may indicate that a vesicle-mediated acquisition of MHCII could be regulated by means of only targeting activated T cells. Nonetheless, it may seem like there exist bimodal pathways for synthesis and acquisition of HLA-DR by human T cells. These may be complementary and account for distinct functionalities, though this is currently unverified.

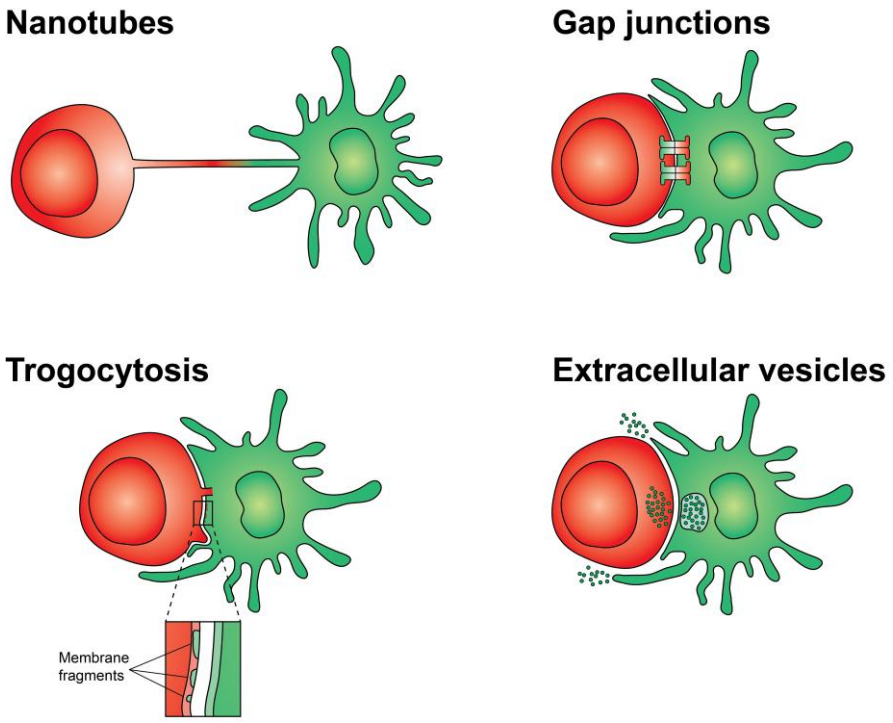

Figure 4 Mechanisms of intercellular transfer of molecules. Upon interaction between two immune cells, the exchange of proteins and genetic material can occur. Currently, four mechanisms have been suggested to account for this molecular transfer. Nanotubes creates a direct passage, enabling a possible molecular transfer of proteins and vesicles. The formation of gap junctions facilitates the transfer of small molecules, including genetic material by directly connecting the cytoplasm of the interacting cells. Trogocytosis is the exchange of entire patches of plasma membrane occurring within the immunological synapse (IS). This can result in the transfer of several proteins to the recipient cell. Extracellular vesicles (EVs) can also enable intercellular communication and transfer of molecules. The EVs can be secreted either directly within the IS or into the extracellular space.

1.2.8. FUNCTION OF HLA-DR ON T CELLS

In terms of functionality, it has been stated that MHCII characterizes the antigen-presenting capacity of a cell (55). Hence, HLA-DR may be more than a mere activation marker for human T cells, regardless of whether the protein is acquired or synthesized endogenously. It could be reasonably assumed that some of the functional features of HLA-DR on APCs could be directly extrapolated to T cells presenting this protein. The finding of several co-stimulatory molecules on T cells (61) could further warrant a hypothesis of the existence and importance of antigen-presenting T cells (T-APCs).

Antigen-presentation by T-APCs has classically been associated with down-regulatory signals (3, 82, 83). As such, T-APCs have been shown to induce either anergy (84-86) or apoptosis (87). Furthermore, in a study of mouse regulatory T cells (Tregs) it was described that the CD4+ $CD25^{hi}$ MHCII+ phenotype identified a functionally distinct Treg population with the ability to suppress proliferation and cytokine production in responder T cells (83). Another study also connects the presence of HLA-DR on CD4+ CD25+ tumor necrosis factor 2 (TNFRII)+ with the strongest suppressive activity, as compared to CD4+ HLA-DR- subsets (88). Conversely, several studies report that T-APCs can activate responder T cells, (61, 62) thus indicating diversity in the possible functions of T-APCs.

APC features of T cells

If a T cell has the capacity of an APC, it is only natural to assume that it possesses a number of key features related to this function. Consequently, the central components of the MHCII antigen presentation pathway would be expected to exist in T-APCs, including the ability to express HLA-DR and also uptake, process, load, and present antigens (section 1.2.4). Finally, the simultaneous presence or absence of co-stimulatory molecules could provide indications of the functional capabilities of T-APCs.

Related to the uptake of antigens, there are currently no unambiguous conclusions for T cells. While some state that T cells hold the ability to capture antigens (47), others claim that there is no known mechanism for this (33) and as a consequence of this, only present self-peptides, such as CLIP, or T cell tropic viruses (33, 89, 90). The capacity to process and load peptides onto HLA-DR molecules requires the MIIC and its constituents (section 1.2.4). Accordingly, it has been demonstrated that T cells can express cathepsin S (CatS) (33), which is an enzyme that degrades Ii to CLIP (91, 92). The same study made the additional observation that T cells did not express the enzyme asparagine endopeptidase (AEP). This is relevant because AEP is the sole protease that, at the time of the study, had been proven necessary for the creation of antigenic peptides (33, 93). For a proper loading of antigenic peptides, within the peptide-binding groove of HLA-DR, the presence of HLA-DM is required. In line with this, HLA-DM has been detected within the CD3+ CD4+ HLA-DR+ T cells (33), however, no further studies on this expression are currently

available. A final requirement for the MIIC, and also for the entire MHCII antigen-presenting pathway, is a high density of HLA-DR molecules. According to our own investigations, out of the CD3+ T cells in peripheral blood, which present HLA-DR on their cell surface, only a fraction of these also contain HLA-DR in the intracellular compartment (Manuscript 1, Figure 2, Appendix B1). Ultimately, the function of HLA-DR on T cells resides with its presence in the plasma membrane, where antigen presentation can occur. However, the outcome of a potential antigen presentation is highly dependent on the co-stimulatory or co-inhibitory signals provided in parallel (Figure 1). The most well described co-stimulatory molecules are those belonging to the B7 family of which B7-1/CD80 and B7-2/CD86 are typical examples (94). They both interact with CD28, which is expressed by the majority of T cells in both human and mouse (95). Professional APCs express CD80 and CD86 constitutively and this expression is increased upon activation of T cells (95). For the presence of co-stimulatory molecules on T cell, diverging reports have been put forward. On one hand, an active protein synthesis has been described (3). On the other hand, a molecular acquisition has been demonstrated by both human (61, 96) and mouse T cells (75, 97).

Differences between T-APCs and APCs

In order to delineate the possible functions of T-APCs, it seems reasonable to look for similarities between professional APCs and T-APCs. Even so, the differences observed between these two cellular subtypes might also provide relevant information in that regard. The involvement of TCR, HLA-DR, and co-stimulatory molecules are present in both the case, where two T cells interact (T:T), and in the interaction between T cells and APC (T:APC). However, the consequential production of IL-2 is not induced following T:T interaction, while IL-4 production is induced in both scenarios (98, 99). This reduced IL-2 synthesis is believed to be associated with the reduced influx of Ca^{2+} observed after T:T interactions, when compared to T:APC interactions (3, 98). Furthermore, the magnitude of TCR and CD3 down-regulation was much greater after T:T interactions, as compared T:APC interactions (84). This down-regulation has been proposed to correlate with the degree of anergy induced in the responder cell (100). Finally, the up-regulation or presence of co-stimulatory molecules CD80 and CD86 on T cells could only be detected following T:APC interaction (84). Taken together, this suggests that the functions of APCs and T-APCs are dissimilar.

CHAPTER 2. AIMS OF THE PHD STUDY

The overall aim of this PhD study is to investigate the endogenous expression and/or acquisition of HLA-DR by human T cells. In line with this, the study is based on the following hypotheses:

Human T cells do not express HLA-DR endogenously

HLA-DR is transferred to T cells from APCs, predominantly mediated by direct cell contact

The main function of HLA-DR presenting T cells is to down-regulate the activity of other T cells

The specific aims of each of the four manuscripts included in the thesis are as follows:

MANUSCRIPT 1
Revenfeld, A.L.S, Steffensen, R., Pugholm, L. H., Stensballe, A., Jørgensen, M.M, Varming, K. (2015): *The existence of HLA-DR on circulating CD4+ T cells cannot be explained by a concurrent presence of HLA-DRB1 expression.* BMC Immunology. Accepted with revisions.

The aim of the study in this manuscript is to **evaluate the expression of HLA-DR at the transcriptional (mRNA) level and protein level in human T cells** obtained from peripheral blood. If an endogenous protein expression occurs in human T cells, it can reasonably be expected that the corresponding mRNA also will be present within this cell population. As a positive control, the simultaneous expression of HLA-DR mRNA and protein is evaluated in autologous B cells. Furthermore, the investigations are carried out with cells directly isolated from peripheral blood to approximate the *in vivo* conditions to the greatest extent.

MANUSCRIPT 2

Revenfeld, A.L.S, Bæk, R., Varming, K., Jørgensen, M.M, Stensballe, A. (2015): *Phenotypic characterization of extracellular vesicles and CD4+ HLA-DR+ responder T cells following contact-dependent and -independent allogeneic MLC*. Journal of Leukocyte Biology. In preparation.

This manuscript contains two aspects to further elucidate the presence of HLA-DR on T cells. Consequently, the first aim is to **determine whether the expression of HLA-DR can be induced in monocultures of CD4+ T cells** from peripheral blood as a measure of the possible endogenous HLA-DR expression. The obtained results should support those presented in Manuscript 1 (as described above). The second aim relates to the requirements of physical contact between T cells and APCs. Hence, the second aim is to **investigate whether allogeneic cells can elicit any effects on each other without physical contact**. In the applied experimental setup the responder and stimulator cells are separated by a membrane, which allows for the passage of molecules up to a particular size, including cytokines and small EVs, such as exosomes. Hence, the phenotype of the secreted EVs is determined to obtain information about their role in the communication between responder and stimulator cells. Moreover, the cellular phenotype of the responder CD4+ HLA-DR+ T cells is in focus in order to evaluate their possible functionality. As for the expression analysis described in Manuscript 1, the applied cells are primary, instead of clones or stable cell lines, to maximize the physiologic relevance.

MANUSCRIPT 3

Revenfeld, A.L.S., Bæk, R., Nielsen, M. H., Stensballe, A., Varming, K., Jørgensen, M. (2014): *Diagnostic and prognostic potential of extracellular vesicles in peripheral blood*. Clin Ther; 36, 6, pp. 830-46.

This scientific review elaborates on the clinical potential of utilizing analyses of EVs from a blood sample. The aim of the review is to **describe selected and useful techniques to create a platform for EV analysis of blood samples in a clinical setting**. Among others, the review includes the description of an EV analysis method developed at the Department of Clinical Immunology, Aalborg University Hospital, Aalborg, Denmark, called the EV Array. This technique can be used to phenotype EVs from a multitude of biological fluids, including blood and cell culture supernatant and has been used throughout the PhD study and in particular for the results presented in Manuscript 2. In addition, the review includes a section in which the role of EVs in the immune system is described, which is very relevant for the experimental work carried out in the present PhD study.

MANUSCRIPT 4

Revenfeld, A.L.S., Søndergaard, E.K.L., Stensballe, A., Bæk, R., Jørgensen, M.M, Varming, K. (2015): *Characterization of a cell culturing system for the study of contact-independent vesicle communication*. *Journal of Extracellular Vesicles.* Submitted.

The content of this manuscript, which is a technical report, should support the results presented in Manuscript 2. The aim of the study is to **describe an experimental system, where dynamic, vesicle-based communication between cells can be investigated**. This is important since appropriate *in vitro* cell culturing systems are necessary to study the activity and biological function of EVs, not only in the context of HLA-DR, as was the focus of Manuscript 2. Many existing studies, which investigate aspects of contact-independent cell communication, do not justify the choice of the relative placement of the cells in the cell culturing setup. This may be relevant for the biological hypothesis being tested. Consequently, the study can serve to illustrate this importance for the design and validation of future studies.

2.1. METHODOLOGY

A number of key methods and analyses have been employed to address the objectives and aims in this thesis. For each original manuscript these methods are described in the "Materials and Methods" section (Appendix B1, B2, and B4). However, additional background information not covered in the manuscripts, concerning methodological considerations and data interpretation, will be elaborated in the subsequent sections.

2.1.1. CELLULAR PHENOTYPING BY FLOW CYTOMETRY

Within the field of immunology, flow cytometry (FCM) is an indispensable technique. It facilitates rapid, multiparametric analysis of single particles, often cells, in a suspension. The particles are focused hydrodynamically, creating a flow of single particles, which subsequently pass a beam of light. The properties measured include the relative size, relative granularity (internal complexity), and relative fluorescence intensity. In terms of cellular analyses, the use of multiple fluorochrome-conjugated antibodies provides the opportunity for simultaneous measurements of several proteins located at the cell surface and intracellularly of a single cell in a larger population. The use of >10 different antibodies in a composite stain is used routinely (101) and the possibility to expand this number exists (102). Ultimately, the use of multicolor FCM analysis allows for functionally distinct cellular subsets to be separated.

In this thesis, FCM holds a central place. As such, this technique has been applied throughout the majority of the presented original work. Moreover, a new assay was developed and validated and applied to obtain the FCM results shown in Manuscript 1. Several aspects of this new assay demanded a thorough investigation of features relating to technique, staining, and gating to ensure that proper conclusions could be made from the obtained results. The following components from the development/ validation of the FCM assay were evaluated and are presented in more detail below:

- Choice of anti-HLA-DR antibody (specificity and fluorophore conjugation)
- Choice of fixation and permeabilization conditions
- Choice of incubation temperature and time
- Choice of gating strategy
- Test of antibody saturation (+/- fixation, +/- permeabilization, antibody concentration)
- Test of reversing the two anti-HLA-DR-antibodies with different fluorophores

Development of a flow cytometric assay for the identification of membrane-bound and intracellular HLA-DR in T and B cells

As stated in the beginning of Chapter 2, the overall aim of this thesis is to investigate the endogenous expression of HLA-DR by human T cells. To facilitate this, a FCM assay was developed in which the aim was to separate the plasma membrane-bound HLA-DR (HLA-DR mem) from the intracellular HLA-DR (HLA-DR IC). As pointed out in Manuscript 1 (Appendix B1), the hypothesis driving such an assay design is that T cells would only present HLA-DR in both cellular compartments if they possess the ability to express the HLA-DR protein endogenously. In line with this, the expression of HLA-DR mem and HLA-DR IC by autologous CD19+ B cells was used as a positive control, due to the constitutive HLA-DR expression by these cells.

The starting point was to choose a monospecific antibody, which would identify mature and functional HLA-DR, since the presence of this protein on the T cells could also provide possible functional clues, aside from those related to expression. Accordingly, the monoclonal mouse anti-human HLA-DR antibody L243 was selected. L243 recognizes mature and non-Ii associated HLA-DR (12) by binding to a conformational epitope on the α-chain of HLA-DR (section 1.2.2). The binding requires the correct assembly of the HLA-DR $\alpha\beta$-heterodimer (103-105). Furthermore, L243 selectively targets HLA-DR and not other MHCII molecules, including HLA-DP and HLA-DQ (section 1.2.1) (105). The L243 antibody was chosen conjugated to two different fluorophores (explained in a subsequent section) and the staining setup included a primary targeting of the HLA-DR mem with one antibody followed by fixation and a subsequent permeabilization of the plasma membrane and identification of HLA-DR IC with the second antibody.

To facilitate the access to the intracellular target, a cell fixation/permeabilization kit from Invitrogen was chosen, since it had previously been used successfully in our laboratories. Though Invitrogen does not provide the constituents of the included solutions, the kit supposedly provides mild fixation and permeabilization of cells. This preserves their side (SSC) and forward scatter (FSC) properties, which is relevant from a flow cytometric point-of-view, since these two properties often are used as an initial identification of the cell populations of interest. Moreover, the autofluorescence of the cells has been reported as low after using the kit (106). This is a desirable trade, because the increased autofluorescence, which is often associated with cellular fixation, can lead to overlap with the emission spectra in the green region of the spectrum, affecting the use of fluorophores such as fluorescein isothiocyanate (FITC) and Alexa Fluor 488 (AF488) (107). The manufacturer of the kit provided the incubation temperature and time and these were used only with minor changes (see final protocol after Figure 10), since they had previously been applied successfully for other applications in our laboratories.

Identification of positive events with the Fluoresence Minus One method

The use of several different fluorophore in a multiparametric FCM analysis calls for the need to estimate and correct the amount of spectral overlaps, also called fluorescence compensation. The overlaps occur since the light emitted from one fluorophore may be detected within the wavelength range assigned to another fluorophore (108, 109). Compensation is usually an obligate step performed as the instrument is started. It is carried out with compensation control samples stained with only one of the fluorochromes used in the composite stain (109). With more complex stain sets, the inclusion of a Fluorescence Minus One (FMO) sample is very useful, especially when there is a need to distinguish weakly positive events from the negative events. The FMO control includes all the staining reagents but one and in some cases replacing it with an isotype control antibody (109). Thereby, it is possible to estimate the cumulative contribution of all other fluorophore into the channel of the one omitted and the threshold for non-stained cells can consequently be determined (108). When a cell is unstained or has no cell-associated fluorescence for a particular dye, the compensation results in a population distributed symmetrically around zero in the corresponding channel (109). This is termed autofluorescence. The width of this distribution can vary considerably depending on the fluorescence compensation, making it difficult to establish whether a cell is weakly positive or unstained. Hence, an FMO control should always be included, when this is an issue.

In this PhD study, the FMO is an essential control in the FCM analysis of HLA-DR on T cells, as presented in Manuscript 1 (Figure 1, Appendix B1). This is the case, since the distribution of HLA-DR+ events across a T cell population is heterogeneous with no clear separation to the HLA-DR- population. Therefore, the FMO is necessary for a more unbiased determination of the threshold defining the HLA-DR+ and HLA-DR- populations than by merely using isotype antibody controls. These controls are otherwise commonly used to evaluate non-specific binding by the target antibodies and are applied to set the threshold, which defines when a population stains positively with a target antibody (109). However, the isotype control antibodies are often used in a composite stain, thus considerably underestimating the background staining in each channel (101). A subsequent placing of the staining boundaries for the antigen specific antibodies, based only on the isotype controls, would thus erroneously indentify false-positive events. For the data presented in Manuscript 1, the FMO sample was used to set the gate for HLA-DR mem and HLA-DR IC so that the positive gate for these markers did not contain more than 1% of the negative events (Figure 1, Manuscript 1). Consequently, this boundary level is placed between two and three standard deviations (SD) from the mean value of the negative population. This is based in the principles of normal distribution and standard deviation in which 0.1% of the events in a distribution are over three SD above the mean of the population, while approximately 2% of the data are two SD above.

Choice of fluorophores for the anti-HLA-DR antibody

Initially, FITC- and phycoerythrin (PE)-conjugated L243 (L243-FITC and L243-PE) were applied to target HLA-DR mem and HLA-DR IC, respectively. Of the two fluorophores, PE has the highest intrinsic brightness (110), which is useful, when a low density of the target antigen is expected, such as HLA-DR on T cells. Although PE is a bulky molecule (~240 kDa), compared to FITC (~390 Da), it has been used successfully for intracellular staining (111). The combination of L243-FITC for staining HLA-DR mem and L243-PE for staining DR IC, identified 18% CD3+ HLA-DR mem+ and >1% CD3+ HLA-DR mem+ DR IC+ T cells (n=3) (Figure 5, left panel). All CD19+ B cells stained positive for HLA-DR mem. Nonetheless, >1% of the B cells from one donor were also HLA-DR IC+, while this number was 45% for a second donor (Figure 5, left panel).

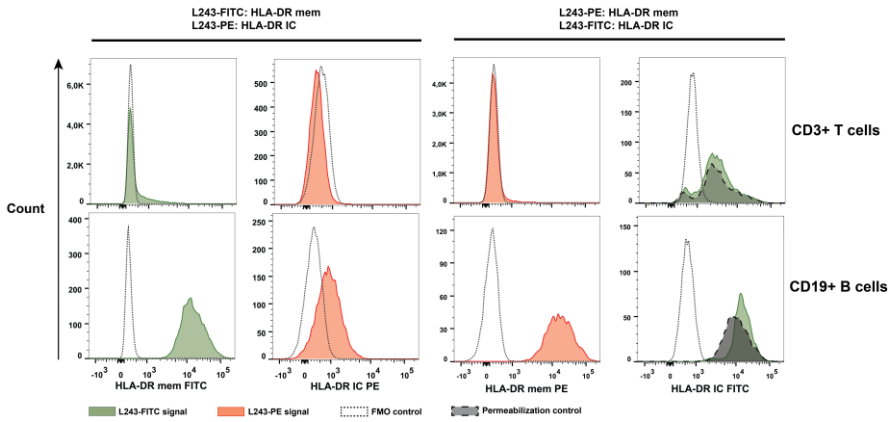

Figure 5 Staining of HLA-DR in the membrane and cytoplasm of T and B cells with two different anti-HLA-DR antibodies. A flow cytometric assay was developed to separate the membrane-bound (HLA-DR mem) HLA-DR from the HLA-DR found in the intracellular compartment (HLA-DR IC) of human T and B cells. The setup included staining PBMCs with anti-CD3, anti-CD19, and two different anti-HLA-DR antibodies of the same clone (L243) but with different fluorophores. As described in Manuscript 1 and the sections above, one L243 antibody was used initially along with the antibodies against the cell-specific surface markers. Subsequently, the cells were permeabilized and the second L243 antibody was applied. In the subsequent flow cytometric analysis, the number of CD3+ T cells and CD19+ B cells presenting HLA-DR were determined using the FMO gating strategy described in the previous section and in Manuscript 1. Left panel: The histograms show the results obtained with the combination of L243-FITC to stain HLA-DR mem and L243-PE to stain HLA-DR IC. Note, that no permeabilization control (*i.e.* entire staining procedure with permeabilization omitted) is included in this panel. n = 3 (T cells), n = 2 (B cells). Right panel: The histograms show the results of switching the two antibodies used in the top panel with cells from the same donor. n = 3.

The observations found for the latter donor were confirmed several times and an increase in the amount of antibody for HLA-DR IC did not increase the amount of B cells staining positive (data not shown). It was unexpected not to identify more B cells presenting HLA-DR IC and to further investigate this observation, the two L243 antibodies were switched (Figure 5, right panel). With this combination, 5% CD3+ HLA-DR mem+ and 69% CD3+ HLA-DR mem+ DR IC+ T cells were identified, while all CD19+ B cells were double positive (n=3). However, in the sample, where no permeabilization agent was added, an equal sized HLA-DR IC signal was also found for both CD3+ T cells and CD19+ B cells (Figure 5, right panel, histograms with dashed lines). This permeabilization control was only included for one of the three donors in the first L243-FITC HLA-DR mem/L243-PE HLA-DR IC combination presented in Figure 5, left panel (though not for the donor included in the figure). Yet, it demonstrated that the HLA-DR IC signal in the permeabilization control for that combination was not greater than the signal from the FMO control (data not shown). Hence, this indicated that the increased HLA-DR IC signal observed in the permeabilization control for the second antibody combination (L243-PE for HLA-DR mem/ L243-FITC for HLA-DR IC) could be fluorophore-specific.

Subsequently, two new antibodies, L243-AF488 and L243-AF647, were tested to further investigate this phenomenon. The AF conjugates are reported to be chemically resistant and very photostable, making them useful for both staining of intracellular targets and for microscopy. Similar to the initial choice of antibodies, the brighter of the two fluorophores was chosen for the staining of HLA-DR IC. Here, this was the L243-AF647 antibody. An additional advantage of AF647 over PE is its relatively low molecular weight of 1250 Da, making it more suitable for intracellular staining than PE. Finally, the emission spectra of AF488 and AF647 fluorophores are very different (107), providing optimal conditions for non-overlapping signals from the staining of HLA-DR mem and HLA-DR IC. The combination of L243-AF488 for staining HLA-DR mem and L243-AF647 for staining of HLA-DR IC resulted in the identification of approximately 18% CD3+ HLA-DR mem+ and 3% CD3+ HLA-DR IC+ (Table 2, Manuscript 1, n = 10). A positive correlation between HLA-DR mem and HLA-DR IC was observed for CD3+T cells (Figure 2, Manuscript 1). Accordingly, the T cells presenting HLA-DR IC were all HLA-DR mem+, but not vice versa (Figure 13). This yielded 18% double positive CD3+ T cells (i.e. HLA-DR mem+ HLA-DR IC+). The subsequent focus on HLA-DR IC in T cells was therefore placed on the T cells also presenting the membrane-bound protein (i.e. CD3+ HLA-DR mem+ HLA-DR IC+ T cells). The analysis of the CD19+ B cells showed that these cells expressed both markers. Representative results of this analysis can be seen in Figure 6, left panel.

When switching the two antibodies, approximately 19% CD3+ HLA-DR mem+ and 10% CD3+ HLA-DR IC+ T cells were identified for cells from the 2 included donors (Figure 6, right panel). This corresponded to roughly 45% of the CD3+ HLA-DR mem+ T cells also being HLA-DR IC+. All B cells were double positive. As can be deduced, a higher number of T cells presenting HLA-DR IC were observed with combination 2 of the L243 antibodies, when compared to combination 1 (Fig-

ure 6). However, the HLA-DR IC signal from the permeabilization control also increased, when switching the two antibodies (Figure 6, histograms with dashed lines). Nonetheless, the specific HLA-DR IC signals did not increase by the same magnitude (Figure 6, filled histograms). For combination 1, the specific HLA-DR IC signal for the CD3+ HLA-DR mem+ T cells was ~ seven times higher than the signal in the permeabilization control. The corresponding increase was only two-fold higher, when using combination 2, yielding a lower resolution between the two signals from combination 2. The difference was even more pronounced for the B cells. Here, the specific HLA-DR IC signal obtained with combination 1 was approximately 10-15 times higher than the permeabilization control, while the increment was five times higher for combination 2.

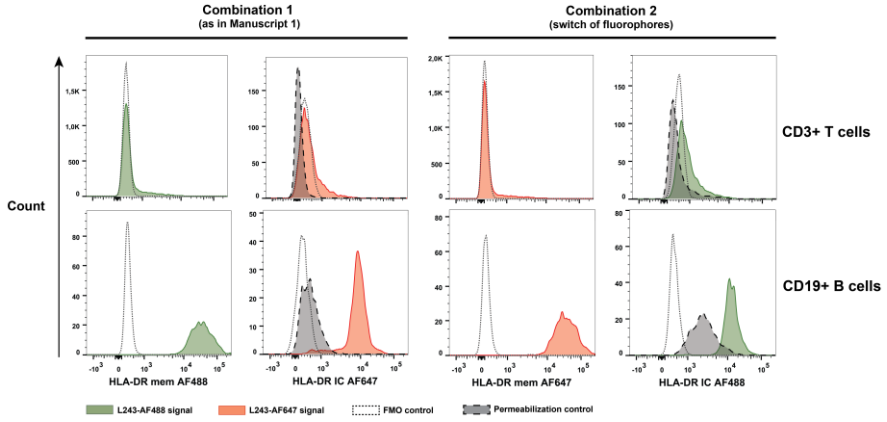

Figure 6 New fluorophores for staining of HLA-DR in the membrane and cytoplasm of T and B cells. PBMCs were stained with antibodies against CD3, CD19, and HLA-DR (L243) to target HLA-DR mem. The cells were permeabilized and a second L243 antibody was applied to identify HLA-DR IC. In contrast to the results presented in Figure 5, two new conjugates for the HLA-DR antibody were applied (AF488 and AF647). In the subsequent flow cytometric analysis, the number of CD3+ T cells and CD19+ B cells presenting HLA-DR were determined using the FMO gating strategy described in the previous section and in Manuscript 1. Left panel: The histograms are representative examples of results obtained with the combination of the two L243 antibodies described in Manuscript 1 (Appendix B1). Here, L243-AF488 was used to target HLA-DR mem and L243-AF647 was applied to stain HLA-DR IC. n = 10. Right panel: The histograms show the results of switching the two antibodies used in the top panel with cells from the same donor. Similar results were obtained with cells from another individual (see Figure 7, left panel). n = 2.

Next, a blocking step was tested in order to investigate, whether the HLA-DR IC signal observed in the permeabilization control was due to non-specific binding. Accordingly, blocking was performed with 20% heat-inactivated human serum after the initial HLA-DR mem targeting with L243-AF647. The blocking step was introduced at this stage, and not before the initial staining step, because the issue with the increased background seemingly originated from the second antibody incubation step. Nonetheless, the blocking of the cells did not decrease the HLA-DR IC (L243-AF488) signal in the permeabilization control. In effect, the median fluorescence intensity (MFI) value of the HLA-DR IC signals in this sample increased approximately 50% for both T and B cells, as compared to the scenario, where no blocking agent was used (Figure 7, histograms with dashed lines). The blocking agent was not included in the final and optimized staining protocol and no other blocking agents and setups were tested.

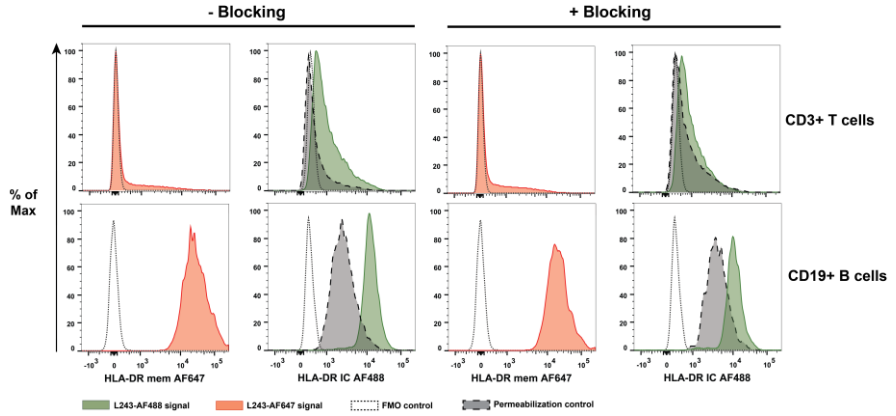

Figure 7 Effect of blocking with human serum to reduce any non-specific antibody binding. PBMCs were stained with antibodies against CD3, CD19, and L243-AF647 for 30 min. Subsequently, the cells were blocked in 20% heat-inactivated human Ab serum for 20 min at room temperature, followed by two washes in PBS. Next, fixation, permeabilization, and incubation with L243-AF488 were carried out, as previously described. In the subsequent flow cytometric analysis, the number of CD3+ T cells and CD19+ B cells presenting HLA-DR were determined using the FMO gating strategy described in the previous section and in Manuscript 1. Left panel: The histograms represent the observed signals from HLA-DR mem and HLA-DR IC on T and B cells without any blocking step added to the staining procedure. Right panel: The histograms represent the corresponding signals to those in the top panel, when adding a blocking step after the initial HLA-DR staining. n = 1.

Due to the results obtained for the L243-AF488 and L243-AF647 antibodies presented above, and the knowledge about the fluorophore properties, the optimal combination for the assay was chosen to be L243-AF488 for targeting HLA-DR mem and L243-AF647 for HLA-DR IC. This decision was primarily based on the lowest degree of binding in the permeabilization control for L243-AF647 (Figure 6). The highest degree of background binding was present, when using either L243-

AF488 or L243-FITC to target HLA-DR IC, indicating a possible link between the non-specific binding and the any shared properties of these two fluorophores that have similar structure and emission spectra. However, this link was not further investigated. The remaining optimization of the assay was carried out only for the selected antibody combination.

Validation to ensure saturation of membrane-bound HLA-DR with the applied antibody

The ultimate condition, which must be fulfilled to validate the presented flow cytometric assay, is that the primarily used anti-HLA-DR antibody must saturate HLA-DR mem. Otherwise, the subsequent staining with a second antibody against HLA-DR would result in a detection of a fraction of false-positive HLA-DR IC+ cells. In addition, the number of HLA-DR mem+ cells may be underestimated. Several controls were included to investigate, if the saturation of HLA-DR mem was present. First, one control was included in most optimization and all final experiments (presented in Manuscript 1 and in the section above). In this control, the entire staining procedure was performed, only omitting the permeabilization agent. Typical results of this permeabilization control can be seen in Figure 3 (Manuscript 1) and in Figure 6. With the applied combination 1 of the L243 antibodies (Figure 6, left panel), the HLA-DR IC signal (L243-AF647) in the permeabilization control was negligible for the T cells. For the B cells, the signal for HLA-DR IC in the control was slightly elevated, when compared to the FMO sample. This was a general feature for all donors. However, the intensity of the signals recorded for HLA-DR IC in the permeabilization control and in the full stain sample was always separated by at least a decade in the resulting histograms for the B cells, as depicted in Figure 6. Moreover, the permeabilization control was included as a part of validating confocal microscopy experiments. These experiments were performed to visualize HLA-DR in the two cellular compartments and to validate the staining setup used for FCM. The results of the microscopy are depicted in Figure 4 (Manuscript 1) and in Figure 8, where all the controls are included. As can be seen in this figure, no HLA-DR IC signal could be detected in the permeabilization control and no non-specific binding from the secondary antibody used for CD3 was detected. Hence, the microscopy validated the staining procedure used in the flow cytometric analysis.

However, to address the signal present in the FCM analysis, it was investigated whether this unexpected HLA-DR IC signal was present due to non-saturated HLA-DR mem from the first antibody incubation. Consequently, the amount of both L243 antibodies was doubled from 1 μg/ 1 million cells to 2 μg/ 1 million cells. The former was the amount recommended by the vendor of the antibodies and the amount used in the final protocol in Manuscript 1. In addition, the effect of an increased incubation time of the initial HLA-DR mem staining from 15 to 30 min was also tested.

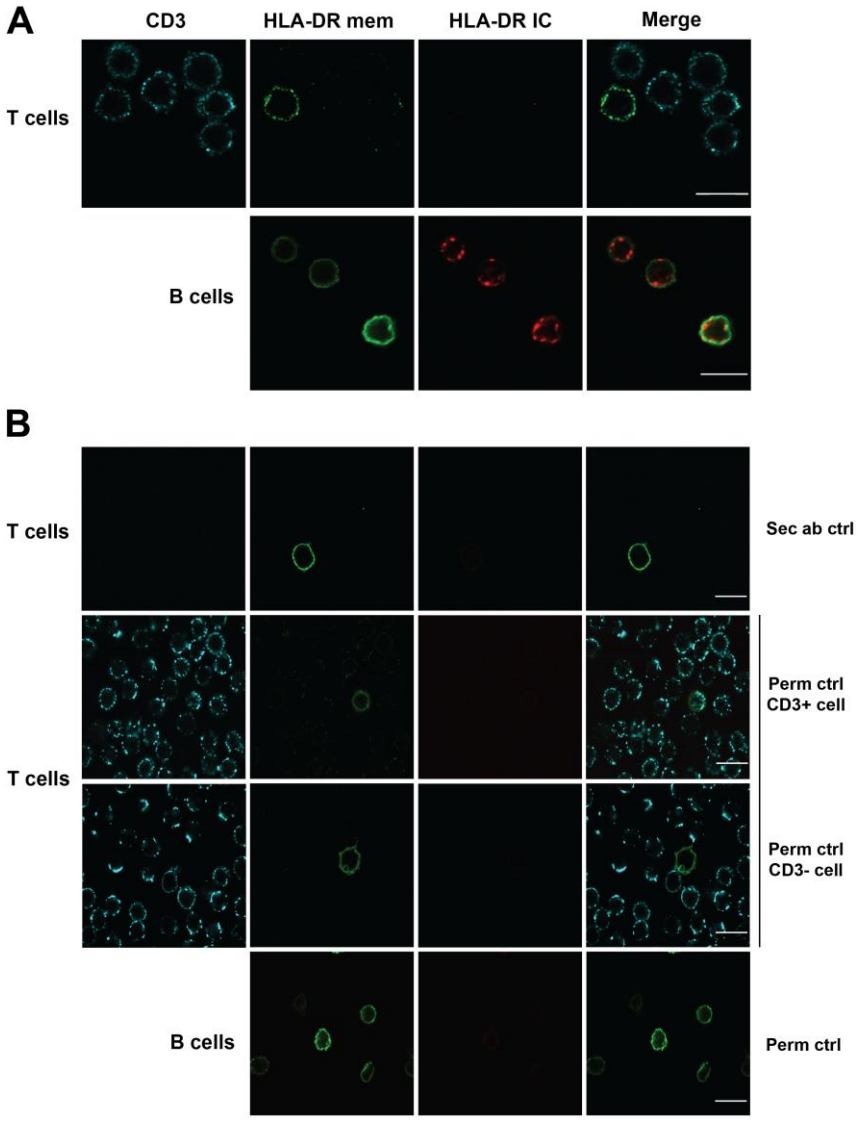

Figure 8 Confocal microscopy of membrane-bound and intracellular HLA-DR. Isolated CD4+ T cells and CD19+ B cells were stained with L243-AF488 (green) and L243-AF647 (red) to target HLA-DR mem and HLA-IC, respectively. Anti-CD3 was also used in the T cell samples (turquoise) A) Full stain of the CD4+ T and CD19+ B cells (also found in Figure 4, Manuscript 1). B) The secondary antibody control (towards anti-CD3) and permeabilization controls. For the T cell permeabilization control, pictures of both a CD3+ HLA-DR mem+ and a contaminating CD3- HLA-DR mem+ has been included to illustrate the absence of a HLA-DR IC signal. The pictures are representative examples from one of the two donors included. The size bar is 10 μm.

The results of increasing the antibody amount are presented in Figure 9. A doubling of the amount of applied HLA-DR antibodies did neither reduce nor increase the specific L243-AF488 and L243-AF647 signals. Accordingly, the number identified HLA-DR mem+ and HLA-DR IC+ T and B cells were similar for the two experimental conditions, as were the corresponding MFI values. Furthermore, the HLA-DR IC signal observed in the permeabilization control did not decrease with an increasing amount of L243 antibodies. In fact, the signal was marginally increased, when using 2 µg of the two antibodies (Figure 9, right panel). For the experiment, which produced the results presented in Figure 9, an increased incubation time of 30 min was applied in the initial HLA-DR mem staining. Only very subtle changes could be observed, when comparing the results obtained with 1 µg of each L243 antibody (Figure 9, left panel) to those previously acquired with a shorter 15 min of incubation time and with the same amount of antibody used. Consequently, a similar amount of HLA-DR mem and HLA-DR IC presenting T and B cells were identified with the two incubation times and the MFI values for these were also comparable (data not shown). However, the MFI values of the HLA-DR IC signal in the permeabilization controls were identical for the B cells but slightly decreased for the T cells, when using an incubation time of 30 min (data not shown). Therefore, an incubation time of 30 min was used in the subsequent analyses and in the final protocol.

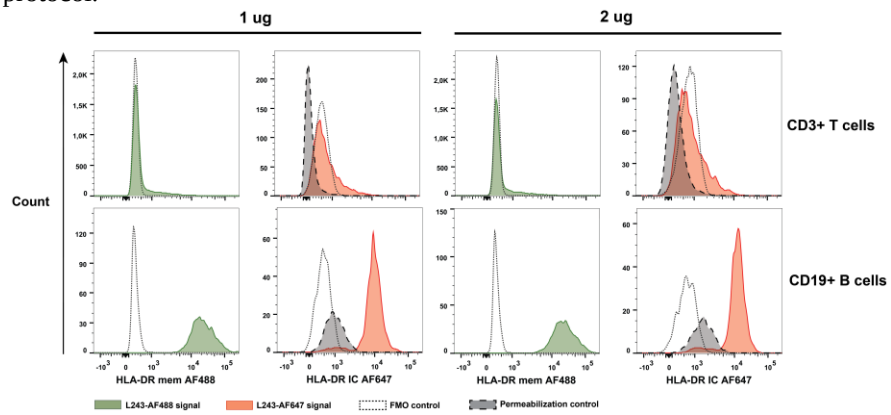

Figure 9 Effect of increasing the amount of anti-HLA-DR antibodies on specific and non-specific signals. PBMCs were stained with anit-CD3, -CD19, and either 1 µg or 2 µg of L243-AF488, as described in Manuscript 1 and in the sections above. For this experiment, an increased incubation time of 30 min (compared 15 min in previous experiments) was used for the initial staining step. The cells were fixed and permeabilized and the L243-AF647 antibody was applied to stain HLA-DR IC. In the subsequent flow cytometric analysis, the number of CD3+ T cells and CD19+ B cells presenting HLA-DR were determined using the FMO gating strategy described in the previous section and in Manuscript 1. Left panel: The histograms show the observed signals from HLA-DR mem and HLA-DR IC for T and B cells when using 1 µg of both L243 antibodies per 1 million cells, as was applied in Manuscript 1. Right panel: The histograms represent the corresponding signals to those in the left panel, when doubling the amount of both L243 antibodies to 2 µg per 1 million cells. n = 1.

The final control experiment evaluated the effect of the fixation step after the staining of HLA-DR mem. In this experiment, the entire staining procedure was applied, however, the fixation of the cells was omitted (Figure 10). In the subsequent FCM analysis, no events could be detected in the samples, where the cells had been permeabilized but not fixed, indicating that these cells had undergone lysis. Hence, the fixation step seemingly stabilized the cells prior to permeabilization, which has also been observed in other intracellular staining protocols (107). Consequently, the only sample providing any information from the non-fixed cells was the permeabilization control, i.e. no fixation and no permeabilization added (Figure 10, solid black line). With this sample, it was possible to see that fixation of the cells seemingly also had an impact on the detected HLA-DR mem signal. As a consistent observation done across many experiments, the HLA-DR mem signal in the fully stained sample and the signal in the corresponding permeabilization control were very similar (data not shown). In contrast, a decreased HLA-DR mem signal was observed in the permeabilization control for the non-fixed cells, when compared to the fixed cells (Figure 10, L243-AF488 histograms).

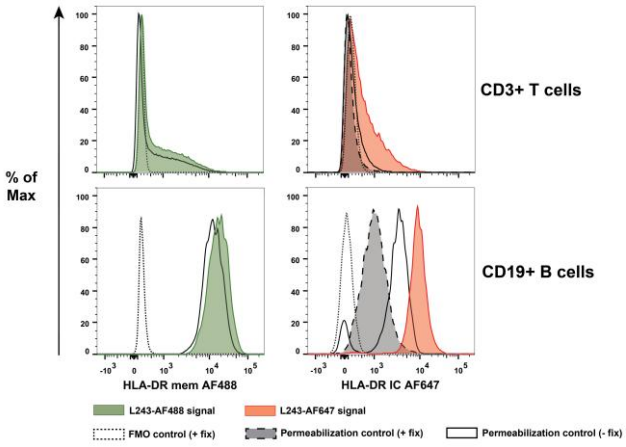

Figure 10 Effect of fixation to separate membrane and intracellular HLA-DR in the flow cytometric assay. The PBMCs were stained with antibodies against CD3, CD19, and L243-AF488 for 30 min. To evaluate the effect of the subsequent fixation step, the cells were either fixed for 15 min or resuspended in PBS. The cells were permeabilized and the L243-AF647 antibody was applied to stain HLA-DR IC. In the subsequent flow cytometric analysis, the number of CD3+ T cells and CD19+ B cells presenting HLA-DR were determined using the FMO gating strategy described in the previous section and in Manuscript 1. Since the cells underwent lysis if they were permeabilized without any prior fixation, the only results presented for the non-fixed cells are those obtained with the non-fixed permeabilization control (i.e.. no fixation and no permeabilization). n = 2

This was the case for both CD3+ T and CD19+ B cells, for which the MFI values of the HLA-DR mem signal decreased with approximately 45% and 30%, respectively, when compared to the fully stained sample (n=2). In addition, the HLA-DR IC signal observed for the HLA-DR mem+ T and B cells increased in the permeabilization control for the non-fixed cells as compared to the corresponding fixed sample (Figure 10, L243-AF647 histograms). The increase observed for the T cells amounted to approximately 60%, while for the B cells it was 50% for one donor (data not shown) and as much as 300% for the second donor included (Figure 10). Hence, it seems likely that the fixation increases the ability to retain the antibody bound to HLA-DR mem on the cells after the initial staining step.

The optimization and validation experiments lead to the protocol for the FCM assay described in Manuscript 1, in which membrane HLA-DR can be separated from HLA-DR found in the intracellular compartment of human T and B cells. In short, the protocol is as follows:

1. Peripheral blood mononuclear cells are isolated from heparinized blood withdrawn from healthy blood donors.

2. The cells incubate with antibodies against CD3, CD19, HLA-DR (L243-AF488, 1 $\mu g/10^6$ cells), or the corresponding isotype control antibodies (FMO; 1 $\mu g/10^6$ cells for HLA-DR control) for 30 min at room temperature.

3. Fixation solution is added and the samples incubate for an additional 15 min at room temperature.

4. Cells are washed with PBS.

5. The second antibody against HLA-DR (L243-AF647, 1 $\mu g/10^6$ cells) or the corresponding isotype control antibody (FMO; 1 $\mu g/10^6$ cells) is added along with permeabilization solution. Incubate for 20 min at room temperature.

6. Cells are washed with PBS, resuspended, and analyzed by flow cytometry on the same day as the staining procedure is carried out.

7. The gates, defining if an event stains positive for HLA-DR mem or HLA-DR IC, are defined with the FMO control samples.

2.1.2. REAL TIME QUANTITATIVE POLYMERASE CHAIN REACTION

Real-time quantitative polymerase chain reaction (PCR), or in short qPCR, is a technique that allows for simultaneous amplification and quantification of nucleic acid sequences (DNA, complementary DNA (cDNA), RNA). The method measures PCR product accumulation through a dual-labeled, fluorogenic probe (e.g. TaqMan probes) or from a non-specific, DNA-binding dye (e.g. SYBR Green) (112). Using TaqMan probes provides very accurate and reproducible quantitation of gene expression. Unlike other quantitative PCR methods, real-time PCR does generally not require post-PCR sample handling, preventing potential PCR-product carry-over contamination and resulting in much faster and higher throughput assays. The output value of qPCR is the threshold cycle (Ct), which marks the cycle number of the PCR in which the fluorescent signal passes a defined threshold (113). In this PhD study, qPCR has been employed to investigate and compare the expression of *HLA-DRB1* mRNA (section 1.2.2) in human CD4+ T cells and CD19+ B cells. The results of this investigation are presented in Manuscript 1 (Appendix B1).

Design of primers for HLA-DRB1*03 qPCR

As a part of the investigation of *HLA-DRB1* expression in human T and B cells, a new qPCR assay was created at the Department of Clinical Immunology, Aalborg University Hospital, Aalborg, Denmark. This assay is specific for the *HLA-DRB1*03* allele and consists of a set of primers and a TaqMan probe (Figure 11) with a FAM dye label and a minor groove binder (MGB). The MGB moiety stabilizes the hybridized probe and effectively raises the melting temperature. It was expected that this custom designed assay would eliminate any potential detection of mRNA from other alleles by only targeting one specific HLA-DRB1 allele, thus simplifying the read-out. This is relevant because of the extensive homology between the different *HLA-DRB1* transcripts, potentially creating false positive results. Also, an initial investigation using commercial primers and probe to *HLA-DRB1* yielded several non-specific results, which motivated the wish to design new primers and specific probes for qPCR of *HLA-DRB1*.

The HLA-DRB1 protein is encoded by 6 exons (114). Exon 1 encodes the leader peptide, exons 2 and 3 encode the two extracellular domains, exon 4 encodes the transmembrane domain, and exon 5 encodes the cytoplasmic tail. In order to make allele-specific primers, it is necessary to target the polymorphic part of the transcript, which is constituted by the extracellular domains. Consequently, the specificity of the assay is based on the design of the forward primer, which targets a sequence of exon 2 in the *DRB1*03:01:01:01* mRNA sequence from the IMGT/HLA database (Figure 11). In contrast, the reverse primer targets a generic sequence of *HLA-DRB1* mRNA. The applied probe was chosen, since it targets the exon-exon boundary of exon 2 and 3 (Figure 11), which also ensures that only mRNA and not genomic DNA is amplified. The newly designed assay was tested on a broad panel of donors representing the five major HLA-DR haplogroups (Figure 2B). These experiments, and subsequent sequence homology analyses, demon-

strated that the assay, aside from *HLA-DRB1*03* mRNA, also amplified transcripts from a number of other HLA-DRB1 alleles. Consequently, these alleles were excluded from further analyses and only alleles, which did not produce any detectable PCR products, were included as negative controls (Manuscript 1).

Analysis of qPCR data

Two commonly used methods can be applied to analyze data from qPCR experiments. These are absolute quantification and relative quantification, yielding either an exact copy number of the input material or a relative change in gene expression as compared to that of another sample, respectively (115). For the qPCR experiments carried out in this PhD study, the relative quantification method has been employed. In relative quantification, data is often analyzed using the comparative Ct method, also called the $2^{-\Delta\Delta Ct}$ method (113). By using this method of analysis, the relative changes in gene expression between two samples, i.e. before and after a treatment, can be shown. ΔΔCt is calculated as (Ct target gene – Ct reference gene)$_{\text{Time X}}$ – (Ct target gene – Ct reference gene)$_{\text{Time 0}}$. As a note, the use of endogenous reference genes to normalize data provides a way to correct for differences in the amount of template input (113). If equal amounts of nucleic acid are analyzed for each sample, and if amplification efficiency before the quantitative analysis is equal for each sample, the gene expression of the reference gene(s) should yield equal signals for all samples. Since the purpose of the qPCR investigation included in this PhD study is to detect expression levels and not expression changes, a derivative of the $2^{-\Delta\Delta Ct}$ method is applied for the data analysis. This is simply denoted $2^{-\Delta Ct}$ and it should be used, when qPCR data is presented as individual data points (115). Here, ΔCt is calculated as (Ct target gene – Ct reference).

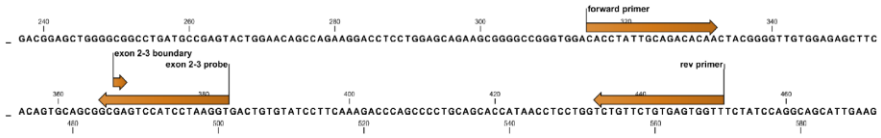

Figure 11 Target sequences of the forward primer, reverse primer, and Taqman probe of the HLA-DRB1*03 specific qPCR assay. A section of the relevant sequence (exon 2 and 3) of the mRNA of *HLA-DRB1*03* is shown along with the specific target sequences of the primers and probe applied in the assay.

2.1.3. VESICLE PHENOTYPING USING THE EV ARRAY

The characterization of EVs can comprise analyses of their biochemical and biophysical features, including size, cargo, and protein phenotype (66). The results of such analyses can be used to extract important information about their origin, amount and possible function, which are useful for both clinical and research purposes. In the present PhD study, extensive phenotyping of the proteins found on EVs has been carried out using a newly developed technique, the EV Array (116), from the Department of Clinical Immunology, Aalborg University Hospital, Aalborg, Denmark. As such, the EV phenotypes presented in Manuscript 2 and 4 were determined using this technique. The EV Array is an antibody-based protein microarray for multiplexed phenotyping of EVs using unpurified starting material (116), including plasma, saliva, urine, and cell culture supernatants (Figure 12). It is an open platform, but the current setup detects the vesicles, which contain CD9, CD63, and/or CD81, which are all accepted exosome markers (66). Furthermore, more than 60 protein markers can be detected simultaneously in the present setup (117).

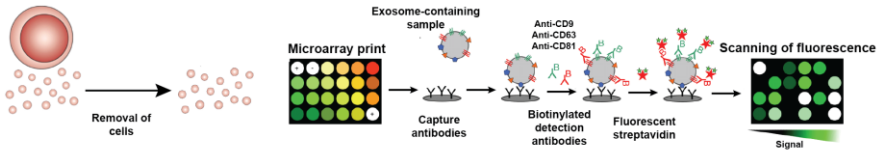

Figure 12 Principle of phenotyping EVs using the EV Array. The EVs are produced by cells from a multitude of biological systems and released into the extracellular space such as culture medium used for *in vitro* cellular assays. From here, the only preparation of the sample prior to analysis is removal of the cellular components. Capture antibodies against target protein are printed onto microarray glass slides after which EVs displaying these target proteins are captured onto the surface of the glass slide. In the current setup, a cocktail of biotinylated antibodies against CD9, CD63, and CD81 are used for the detection of the surface-bound EVs. Fluorescent streptavidin is finally applied to create a detectable signal, which can be used to determine the relative amount of the target protein present on the EVs.

CHAPTER 3. MAIN FINDINGS OF THE PHD STUDY

The research presented in this PhD thesis has focused on delineating some of the yet unknown aspects of HLA-DR in the context of T cells. In the following section, the original work of the thesis will be summarized and additional results not included in Manuscript 1, 2, and 4 are presented (Appendix B1, B2, and B4).

3.1. ENDOGENOUS EXPRESSION OF HLA-DR BY HUMAN T CELLS

Before deriving any functional information about the presence of HLA-DR on human T cells, it was important to establish whether these cells express HLA-DR antigens endogenously. To investigate this, a correlation between the presence of the functional molecule, i.e. the HLA-DR protein, and the transcription of the *HLA-DR* gene, determined by its mRNA, was performed (Manuscript 1). As a reference point/ positive control to the T cells, a simultaneous investigation of autologous B cells was included, due to their constitutive expression of *HLA-DR*. For the protein investigation, a subcellular distribution of HLA-DR was determined for CD3+ T and CD19+ B cells, distinguishing the HLA-DR found in the plasma membrane from that found in the intracellular compartment by using an optimized protocol for FCM (Manuscript 1 and section 2.1.1). The staining setup applied in this protocol was confirmed by confocal microscopy. The FCM investigation demonstrated that HLA-DR could be detected both at the cell surface and intracellularly in all CD19+ B cells, whereas only a fraction of the CD3+ T cells presented HLA-DR in the cell membrane and an even smaller part of these also contained HLA-DR in the cytoplasm (Table II, Manuscript 1 and Figure 13A). Moreover, the densities of HLA-DR molecules found it these two cellular compartments were considerably higher for the B cells, as compared to the T cell levels. To relate the amount of HLA-DR presenting CD3+ T cells in peripheral blood to the two T cell lineages CD4+ and CD8+, it was demonstrated that these two populations each contribute with roughly 50% to the total number of CD3+ HLA-DR mem+ cells (Figure 13B). Of the HLA-DR mem+ CD4+ and CD8+, 23% and 1% also presented another T cell activation marker CD25, respectively.

The transcriptional analysis of *HLA-DRB1* expression was carried out with a novel qPCR assay targeting only one *HLA-DRB1* allele; *HLA-DRB1*03*. The analyzed cells included CD4+ T cells and CD19+ B cells, isolated from peripheral blood. This analysis revealed that the CD19+ B cells express *HLA-DRB1* (Figure 5, Manuscript 1), while only negligible amount of mRNA for HLA-DRB1 could be detected in the isolated CD4+ T cells, which was likely to be explained by a monocyte contamination.

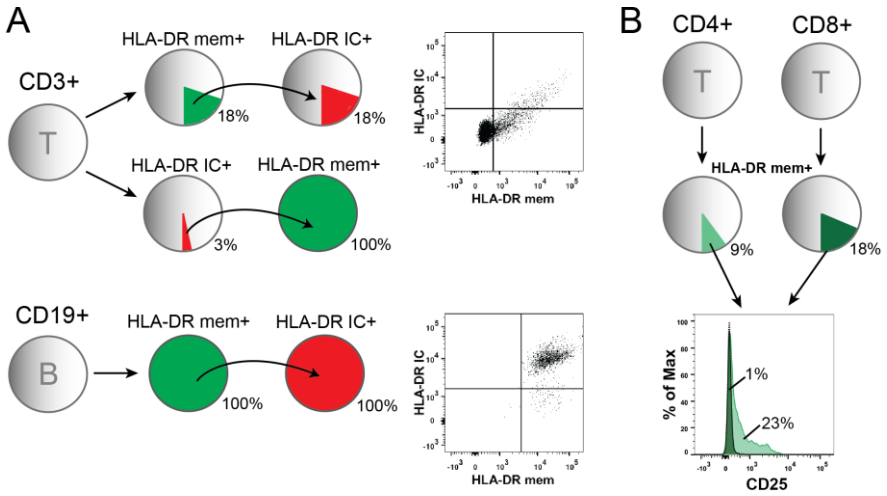

Figure 13 Schematic illustrations of the FCM results presented in Manuscript 1 (Appendix B1). A | Presence of HLA-DR in the membrane (HLA-DR mem) and intracellular compartment (HLA-DR IC) in human CD3+ T cells and CD19+ B cells were determined by FCM. As presented in Table II in Manuscript 1, HLA-DR mem can be detected on approximately 18% of CD3+ T cells in peripheral blood. Out of these, HLA-DR IC can be found in an additional 18% (double positive). Of all CD3+ T cells, 3% present HLA-DR IC, while all of these are HLA-DR mem+. This is in concordance with the positive correlation found between HLA-DR mem and HLA-DR IC (dot plot; from Figure 2, Manuscript 1). The gates in the plots denote the FMO boundaries for HLA-DR mem and HLA-DR IC. **B** | In order to relate the presence of HLA-DR on CD3+ T cells to the two T cell lineages, CD4+ and CD8+ T cells, an additional flow cytometric analysis was made. These results are also presented in Manuscript 1. Here, it was determined that of all CD3+ CD4+ T cells, 9% presented HLA-DR mem, while this number was 18% for the CD3+ CD8+. Moreover, of these HLA-DR mem+ cells, 23% and 1% also co-expressed CD25, respectively. However, since CD4+ T cells constitute a larger part of the total CD3+ T cell population than CD8+ cells (CD4/CD8 ratio is approximately 2 in peripheral blood of adults (118, 119)), the two cell T cell lineages each contribute roughly equally to the total amount of CD3+ HLA-DR+ T cells. n = 6.

3.2. THE ROLE OF APCS FOR THE PRESENCE OF HLA-DR ON T CELLS

To further characterize the presence of HLA-DR on T cells, the role of APCs in this context was addressed. It was demonstrated by FCM that the presence of HLA-DR could not be increased in the plasma membrane after mitogenic or antigen-like stimulated monocultures of CD4+ T cells. However, when APCs and accessory cells were present, both types of stimuli increased the presence of HLA-DR on the T cells (Figure 1, Manuscript 2). Furthermore, it was demonstrated that physical contact between APC and T cells is required to induce proliferation and increase the number of CD4+ HLA-DR+ T cells following an alloresponse (Figure 2 and 3, Manuscript 2).

3.3. EXTRACELLULAR VESICLES IN PROTEIN TRANSFER AND CELLULAR COMMUNICATION INVOLVES HLA-DR

The phenotype of extracellular vesicles produced during alloresponses was characterized, since a vesicle-mediated acquisition of HLA-DR by T cells is a possible mechanism for explaining the presence of HLA-DR on these cells (60, 79, 81). The EV phenotype was also determined to derive functional clues of the vesicle-mediated cell communication and possible transfer of other proteins (Figure 5, Manuscript 2). A summary of the main findings for the EV phenotype is outlined in Table I below. Moreover, it was possible to demonstrate that the experimental design affects this EV phenotype (Figure 4, Manuscript 4). Hence, when studying contact-independent cell communication any effects of this should be determined. In addition to the EV phenotyping results from Manuscript 2, phenotyping of EVs from allogeneic MLCs of isolated CD4+ T cells and immature (iDC) or lipopolysaccharide (LPS)-matured DCs (mDC) derived from monocyte are also included. Furthermore, it was established that it is possible to detect a sufficient signal on the EV Array from only 20.000 DCs (data not shown).

Table I Summary of the EV phenotype following contact-dependent and contact-independent allogeneic MLCs (Manuscript 2). The EV Array was applied to phenotype EVs from the cell supernatants from the classic MLC and TW MLC. For the classic MLC, one value exists for each marker, since only one cell supernatant could be harvested. For the TW MLC, two values exist for each marker, since both stimulator cells (S) and responder cells (R) produced supernatants. Furthermore, observations from a similar analysis from MLCs of CD4+ T cells and immature or LPS-matured monocyte-derived dendritic (MDDCs; here denoted iDCs and mDCs) are also included. The values, which are being referred to, are the intensity of the log2 signals from the EV Array. (+) : minimal expression (0-1; 0 not included); + : low expression (value 1-2); + + : intermediate expression (value 3-4); + + +: high expression (value 5-7; 7 is max value).

EV marker	Contact-dependent MLC	Contact-independent MLC	Additional results: EVs from DC/CD4+ T cell MLC
CD9	+ +	S & R: + + +	Detected in all DC-containing cultures
CD63		S: + ; R: (+)	Detected only in co-cultures
CD81	+ +	S: + + + ; R: + +	Detected in all cell cultures
CD82	+ +	S: + + + ; R: + +	Detected in co-cultures and mDC monoculture
CD3	+	S: (+)	Detected only in co-cultures
CD11a	+	S & R: +	Detected in all cell cultures
ICAM-1	+	S & R: (+)	Detected in co-cultures and mDC monoculture
HLA-DR	+	S: + ; R: (+)	Detected in co-cultures and mDC monoculture

In addition to the EV phenotype, a cellular phenotyping of the included cells in the DC/CD4+ T cell MLCs was also performed. In Figure 14, the results of a selected panel of this cellular phenotyping can be seen. The markers included the tetraspanin family members CD9, CD63, and CD81, being key exosomal markers, along with a cell-specific marker; ICAM-1. For the CD4+ T cells, CD63 and in particular CD81 was detected in these cells in both the mono- and co-cultures. For the DCs, while all three of the exosomal markers were present on DCs, regardless of their maturation state. As an interesting observation, the CD4+ T cells co-cultured with allogeneic iDCs were phenotypically positive for ICAM-1 after the MLC, which was not the case for the CD4+ T cells co-cultured with the mDCs (Figure 14).

<

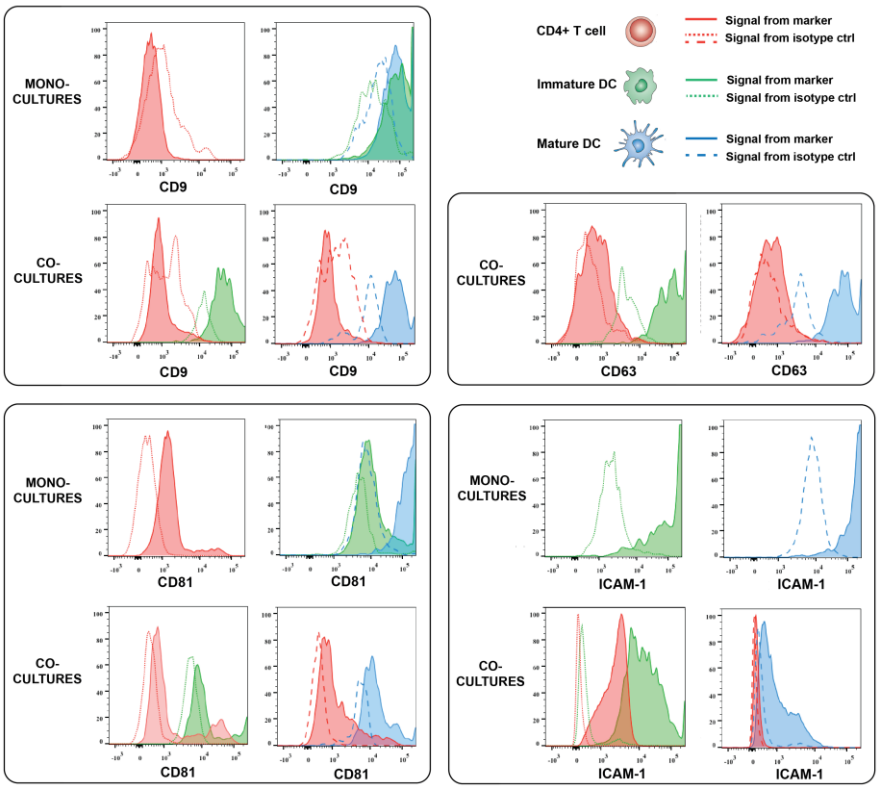

Figure 14 Cellular expression of the exosomal markers CD9, CD63, CD81, and ICAM-1 by CD4+ T cells, immature DCs, and LPS-matured DCs. Following 6 days of co-culture (MLC) between isolated CD4+ T cells and allogeneic DCs (iDCs and mDCs), derived from monocytes, the expression of CD9, CD63, CD81, and ICAM-1 was determined by FCM. For the monocultures, the expression of these markers was evaluated after 48h of culturing. For CD63, the expression was only determined for the co-cultures of T cells and DCs. The expression of ICAM-1 was determined for all cell cultures except for T cell monocultures. Unpublished data. n = 1.

3.4. FUNCTIONAL PHENOTYPE OF HLA-DR+ CD4+ T CELLS

In order to derive information about the possible functionality of the CD4+ T cell that present HLA-DR antigens, the phenotype of these cells was characterized by FCM (Figure 3B, Manuscript 2). Consequently, the presence of seven different cell surface markers was determined for the CD4+ HLA-DR+ responder T cells following a 6 day-allogeneic MLC with or without physical contact between the stimulator cells and the responder cells. A summary of this cellular phenotyping is shown in Table II, while the background for the choice of these markers can be seen in Table III. Furthermore, when comparing the HLA-DR- and the HLA-DR+ CD4+ subsets in both types of MLCs, the HLA-DR+ population was enriched in five out of the eight investigated markers, encompassing CD11a, CD25, CTLA-4, programmed death-1 (PD-1; CD279), and TNFRII.

Table II The phenotype of the CD4+ HLA-DR+ responder T cells following a 6-day allogeneic MLC. The presence of seven markers were determined for the CD4+ HLA-DR+ responder T cells from contact-dependent and contact-independent MLCs (Figure 3B and 3C, Manuscript 2). These markers are related to activation and regulation of T cells and to various effector functions (Table III). Selected markers were also investigated for the responder cell control (i.e. responder cells cultured without the presence of stimulator cells) to account for any culture-induced protein expression. Also, the baseline expression was evaluated for each responder cell donor. For each cellular condition, the % positive events of parent gate ± SEM is given. n = 3.
* The CD4+ HLA-DR+ T cell population was initially gated from lymphocytes as shown in Figure 3A (Manuscript 2) after which the HLA-DR+ cells were determined using an FMO approach, as described in section 2.1.1 and Figure 1, Manuscript 1.

Cell population	Contact-dependent MLC	Contact-independent MLC	Responder control	Baseline
CD4+HLA-DR+*	20.5 ± 2.4	13.3 ± 3.3	18.0 ± 1.3	6.9 ± 2.0
CD11a+	99.0 ± 0.1	97.3 ± 1.5	N/A	99.7 ± 0.0
CD25+	28.8 ± 5.6	15.3 ± 3.8	9.0 ± 0.3	18.6 ± 4.1
CD62L+	69.3 ± 11.2	72.4 ± 6.4	N/A	32.7 ± 0.8
CD127$^{neg/low}$	44.3 ± 4.8	39.7 ± 4.8	N/A	54.2 ± 1.8
CTLA-4+	40.5 ± 3.3	26.6 ± 4.6	6.8 ± 0.3	2.6 ± 0.4
PD-1+	65.2 ± 8.1	52.1 ± 10.4	N/A	42.8 ± 4.0
TNFRII+	51.9 ± 0.9	38.0 ± 5.4	N/A	24.6 ± 3.5

Table III Notes about the seven cell surface markers included in the phenotyping of CD4+ HLA-DR+ responder cells following a 6-day allogeneic MLC. As presented in Table II and Manuscript 2 (Appendix B2), the CD4+ HLA-DR+ respoder T cells from the contact-dependent and –independent MLCs were phenotyped to obtain functional information. The choice of the seven included markers was based on their involvement in effector T cell (Teff) and Treg activation and function, which is described in this table along with some general features of these proteins. FoxP3: Forkhead box P3 (Treg-associated transcription factor).

Surface marker	General notes	Relation to activation and/or regulation of T cells
CD11a	The α-chain of the integrin and adhesion molecule, LFA-1. CD18 constitutes the β-chain. Major ligand: ICAM-1 on APCs (Figure 1, section 1.1) (120, 121).	LFA-1 is constitutively expressed by T cells, switching to a high-affinity state upon T cell activation (120). Has been associated with the uptake of MHCII-enriched, DC-derived exosomes by activated T cells (76).
CD25	The α-chain of the IL-2 receptor (IL2-R), which also comprise a β- and a γ-chain (45). T cells can also produce IL-2, working both in an autocrine and paracrine way to drive proliferation and onset of effector functions in activated T cells (122) (Figure 1B).	Upregulated transiently on activated T cells and is called a T cell activation marker (37, 38, 123). CD4+ CD25+ T cells are often used to define a population of Tregs with suppressive activity (83, 124). The expression of CD25 on Tregs is more stable than for other T cells (123).
CD62L	Adhesion molecule. Also called L-selectin. A homing receptor and a marker of T-cell development. Ligands: Peripheral node adressins (125).	Upon TCR-engagement, the expression of CD62L is down-regulated in T cells. A suppressive capacity has been demonstrated for CD4+ CD25+ CD62L+ Tregs (125). Also, a group of CD4+ CD25+ HLA-DR+ CD62L+ Tregs exist in peripheral blood (83).
CD127	The α-chain of the IL-7R, which also comprises a γ-chain (shared with IL-2R). Binding of IL-7 to IL-7R induces the transcription of anti-apototic genes and initiates proliferation and IL-2 production in activated T cells (126).	$CD127^{neg/low}$ expression is often used as an additional identification marker of CD4+ CD25+ FoxP3+ Tregs. However, for *in vitro* activated Tregs a higher CD127 expression has been observed (127).
CTLA-4	Co-inhibitory molecule. Part of the CD28-family of proteins. Ligands: B7 molecules (CD80, CD86) on APCs. Competes with the co-stimulatory molecule CD28 for their shared ligands (128).	CTLA-4 is expressed shortly after T cell activation (94). For Teffs, CTLA-4 facilitates down-regulation of these cells. For Tregs, CTLA-4 is an important molecule related to the suppressive function of Tregs (129) (Manuscript 2, Discussion).
PD-1	Co-inhibitory molecule. Part of the CD28 family. Ligands (PD-Ls): PD-L1 and PD-L2 (similarity to B7 molecules). PD-L1 is expressed in T cells, B cells, macrophages and DC. PD-L2 is expressed by activated macrophages and DCs (130).	While T cells exclusively express CTLA-4, PD-1 expression can be induced in T cells, B cells, and myeloid cells (130). T cells can express both PD-1 and PD-L1. The PD-1-PD-L1 pathway has been associated with both induction and maintenance of immunological tolerance (129, 130).
TNFRII	Co-stimulatory molecule. Mediates the function of the cytokine TNF (124).	The expression of TNFRII is limited to lymphocytes. It enhances TCR-mediated signaling in T cells (131). TNFRII enriched in Tregs marks a highly suppressive cell population (124).

CHAPTER 4. DISCUSSION

The overall aim of this PhD thesis was to elucidate the endogenous expression and/or acquisition of HLA-DR by human T cells. The incentive for such an investigation is based on two factors; 1) It still remains unclear whether human T cells possess a HLA-DR expression machinery similar to that found in APCs and 2) if the functions of HLA-DR on APCs can be directly extrapolated to HLA-DR on T cells. The subsequent discussion of the theory and data included in this thesis is divided into three sections, which overall relates to the result sections found in Chapter 3, where the main findings of the PhD study are presented.

4.1. FUNCTIONAL PHENOTYPE OF CD4+ HLA-DR+ T CELLS

4.1.1. PRESENCE OF THE FUNCTIONAL HLA-DR PROTEIN

Preceding any functional investigation, it was important to study the endogenous expression of HLA-DR by human T cells. To elucidate this matter from several angles, the presence of HLA-DR at the protein level was compared to the presence of *HLA-DRB1* transcripts in human T and B cells, of which the latter served as a positive reference. The protein-based FCM analysis distinguished between the presence of HLA-DR in the membrane and in the intracellular compartment. This separation was interesting, since it was hypothesized that if the cell contained the protein in both compartments it was likely that it possessed the ability to endogenously express HLA-DR antigens. Even though the reported percentages of HLA-DR+ T cells in peripheral blood vary somewhat from less than 5% (118, 119) to more than 15% (132), it was expected to observe that only a part of the T cells present HLA-DR in the cell membrane. The expectations correlated with the actual observations, however, it was also demonstrated that only a fraction of the CD3+ T cells with membrane-associated HLA-DR also contained HLA-DR in the intracellular compartment. In contrast, all CD19+ B cells were double positive for HLA-DR in the membrane and intracellular. Supposing that the aforementioned hypothesis is true, these collected results served as the first line of evidence indicating that human T cells in peripheral blood do not possess the same endogenous expression machinery of HLA-DR antigens as APCs.

4.1.2. VALIDATION OF FLOW CYTOMETRIC ANALYSIS OF HLA-DR

Before drawing any conclusions, it was important to validate the applied FCM analysis. The assay was based on targeting HLA-DR mem with one anti-HLA-DR followed by permeabilization of the cells and targeting HLA-DR IC with a second anti-HLA-DR. The assay was developed and evaluated through a number of steps, as demonstrated in section 2.1.1. First of all, the selected anti-HLA-DR antibody, L243, was chosen based on the fact that it selectively recognizes all mature and

correctly assembled HLA-DR molecules (12, 103-105). Several other anti-HLA-DR antibodies exist, although with different specificities. However, with L243, the HLA-DR identified on both types of lymphocytes would be a functional molecule, which in the context of T cells is very interesting, since it provides possible functional clues aside from those related to expression.

The entire setup also relied on the ability to separate between two HLA-DR signals; One originating from the membrane-associated protein and one originating from the intracellular compartment. This entailed two aspects. The first was to access the proteins in both cellular compartments, while the other was to have reliable signals from each compartment. Consequently, this demanded that the cells could be sufficiently permeabilized without changing the relevant HLA-DR epitope. Moreover, the fluorophore-conjugated antibodies should also both be resilient to the fixation/ permeabilization process and be able to pass the permeabilized plasma membrane. The last and most important requirement was, however, that the membrane-associated HLA-DR should be saturated with antibodies prior to targeting of the intracellular HLA-DR. Otherwise the HLA-DR mem would be underestimated, while HLA-DR IC would be overestimated.

The intracellular compartment was accessed using a commercially available fixation and permeabilization kit, which had previously been used successfully for other applications in our laboratories. In addition, a simultaneous conservation of FSC and SSC properties of the cells was achieved, which was a desirable trait. In terms of fluorophores, FITC- and PE-conjugated L243 were initially tested in the staining setup. However, the results were non-optimal, most likely related to both size and chemical properties of these fluorophores (Figure 5, section 2.1.1). The results lead to the search for another fluorophore-combination, ending up with AF488 and AF647. Some of the attributes accounting for their choice included a high degree of photostability, their brightness, and their recommendation for intracellular staining. In addition, the emission spectra of the two fluorophores do not overlap, creating favorable conditions for separating the signals from HLA-DR in the two cellular compartments. The results presented in Manuscript 1 are based on using L243-AF488 to target HLA-DR mem and L243-AF647 to stain HLA-DR IC (Table II, Manuscript 1; Figure 6, section 2.1.1). The validity of these results were tested from several angles with the main goal of ensuring that HLA-DR mem was saturated with antibody prior to targeting of HLA-DR IC. Accordingly, the most important control sample for this was the one in which the entire staining procedure was carried out, only omitting the permeabilization of the cells. Hence, in this permeabilization control, no signal from the HLA-DR IC-targeting antibody should be the present if the HLA-DR mem molecules were saturated with the initially applied L243 antibody. As can be seen in Figure 6 (left panel), the HLA-DR IC signal in the permeabilization control (dashed line) separated from the specific HLA-DR IC signal for both CD3+ T cells and CD19+ B cells, when using the antibody combination presented in Manuscript 1. However, it was noted for the B cells that the HLA-DR IC signal in the permeabilization control was slightly elevated, when compared to the FMO control, though with no major overlap to the specific

HLA-DR IC signal. When switching the two antibodies, equal sized HLA-DR mem+ populations were identified, while more CD3+ HLA-DR IC+ T cells were found with the second combination of antibodies (Figure 6, right panel). Nevertheless, also a higher HLA-DR IC signal was detected in the permeabilization control with this antibody combination. In fact, the resolution between the specific HLA-DR IC signal and that from the permeabilization control was reduced to 1/3 of that obtained with the antibody combination from Manuscript 1. Introducing a blocking step after the initial HLA-DR mem staining and increasing the incubation time did not reduce the HLA-DR IC signal in the permeabilization control (Figure 7). This was expected for the B cells, due to their Fc receptor expression (133); a protein, which is not expressed by T cells (134). Moreover, an increase in the amount of applied antibodies did not reduce the HLA-DR IC signal in the permeabilization control (Figure 9), thus indicating that this signal in the control sample was not due to HLA-DR mem antibody shortage. Also, the specific HLA-DR mem and HLA-DR IC signals in the fully stained sample did not increase, when a larger amount of antibodies was applied. It was also demonstrated that fixation of the cells was required for maintaining the structural integrity of the cells prior to permeabilization and also to retain the antibody, which initially targeted HLA-DR mem (Figure 10). Finally, the staining procedure used in the FCM assay was validated using confocal microscopy (Figure 8). No HLA-DR IC signal was observed for the permeabilization control with this assay. Taken together, the results from the validation of the FCM assay indicates that the HLA-DR mem molecules were saturated prior to the staining for HLA-DR IC. Consequently, the supposed non-specific HLA-DR IC signal observed in the permeabilization control could either originate from fluorophores-related features or from cross-reactivity of the L243 antibody. It can be deduced from Figure 6 that the HLA-DR IC signal in the permeabilization control was greatest, when L243-AF488 was applied to target HLA-DR IC, as compared to the situation when L243-AF647 was used (as in Manuscript 1). When comparing this to the HLA-DR IC signal observed in the permeabilization control with L243-FITC (Figure 5, right panel), there is a similarity to the L243-AF488 results. The FITC and AF488 molecules are similar in structure and have nearly identical emission spectra, so they are likely to share some properties. It has been demonstrated that FITC molecules under some conditions can bind non-specifically to intracellular components, making them very difficult to remove by washing (133). This may also be the case for AF488, however, in this study, this feature was not tested further. In relation to the specificity of L243, it has been shown that L243 only recognizes a conformational epitope on the native HLA-DR protein (105). However, it has also been demonstrated that it recognizes a linear epitope on the N-terminal of denatured HLA-DP (135), though not on the native HLA-DP molecule (105, 136). Both the fixation and permeabilization procedure applied to the cells in the presented FCM analysis may unintentionally have created some of these linear epitopes. Consequently, a low degree of cross-reactivity cannot be excluded. The application of an HLA-DP-specific antibody or a pre-incubation with the relevant peptide could be interesting additional tests not already included in the present PhD study. Also, the inclusion of an anti-HLA-DR of a different clone than L243 could also have been performed. Nevertheless, for the results presented in Manuscript 1,

the combination of L243-AF488 to stain HLA-DR mem and L243-AF647 to target HLA-DR IC yielded the best resolution of the specific and non-specific signals (Figure 6). Based on the validation tests carried out and with the stringent gating protocol applied, this antibody combination provides reliable results for a flow cytometric evaluation of HLA-DR mem and HLA-DR IC in CD3+ T cells and CD19+ B cells from peripheral blood.

4.1.3. TRANSCRIPTION OF HLA-DR MRNA

The presence of the HLA-DR protein on the surface of human T cells has been observed for many decades and has also been evaluated in this PhD study, as described above. However, in the context of this thesis, the presence of the protein was correlated to the transcription of its mRNA, as a way of further investigating the endogenous expression of HLA-DR by T cells. In essence, the transcriptional analysis was performed to confirm or deny that the protein found on the surface of T cells could be explained by an active protein synthesis. A novel qPCR assay targeting the *HLA-DRB1*03* allele was developed for this purpose. While the main focus of the protein analysis was the CD3+ T cells, the qPCR analysis was centered on CD4 lineage of the CD3+ T cells. Consequently, the basis of this analysis was a T cell population in which approximately 9% presented HLA-DR in the membrane (Figure 13B and Manuscript 1). In terms of correlating the results from the protein analysis of HLA-DR mem and HLA-DR IC and those from the qPCR assay, it is important to remember one aspect. While the applied L243 antibody targeted all functional HLA-DR αβ-heterodimers (HLA-DRA in complex with either HLA-DRB1, -DRB3, DRB4, or DRB5; Figure 2A, section 1.2.2), the qPCR assay focused on the expression of only one of the functional β-chains; *HLA-DRB1*. All humans carry the *HLA-DRB1* gene on their chromosome 6, while the genes encoding the remaining three functional β-chains are found in a varying degree, depending on the haplotype (section 1.2.2). With the applied FCM analysis it was not possible to determine which β-chain(s) was present on the HLA-DR+ T cells. However, if the T cells can express HLA-DR endogenously, it would be very unlikely that they exclusively expressed all other β-chain genes than *HLA-DRB1*, since one haplogroup (DR8) only contain the *HLA-DRB1* gene (Figure 2B, section 1.2.2). Therefore, it can be reasonably expected that *HLA-DRB1* mRNA would be detected in T cells if these cells express the HLA-DR proteins found on their surface. With the applied transcriptional analysis it was found that B cells clearly encompassed an active transcription of *HLA-DRB1*, while this did not seem to be the case for the CD4+ T cells (Figure 6A, Manuscript 1). The minimal amounts of mRNA for *HLA-DRB1*03* detected in the isolated CD4+ T cells was very likely to be caused by a contamination of monocytes, which are known to express HLA-DR (137) and to some extent CD4 (138). Therefore, these cells would be isolated with the applied isolation kit, which positively selected CD4 expressing cells. It was confirmed by FCM, that approximately 1% of CD14+ monocytes was present in the isolated CD4+ T cell population. Similar to the evaluation of contaminating B cells by qPCR of *CD19* mRNA (Figure 6B, Manuscript 1), a quantification of *CD14* mRNA

could further estimate the extent of this problem. Furthermore, including an incubation step between the cell isolation and the qPCR could minimize the monocyte contamination, since these cells adhere to cell culture plastic (139), thus removing them from the non-adherent CD4+ T cells.

4.1.4. INDUCTION OF HLA-DR EXPRESSION IN HUMAN T CELLS

As a third investigation of the endogenous expression of HLA-DR antigens by human T cells, it was observed that isolated CD4+ T cells does not possess the ability to up-regulate the presence of HLA-DR antigens upon stimulation with either PHA or anti-CD3/anti-CD28 (Figure 1, Manuscript 2). In contrast, the presence of HLA-DR increased on stimulated CD4+ T cells while being a part of a PBMC population. Even though, this latter investigation does not provide direct proof of a non-existing endogenous expression of HLA-DR antigens by human T cells, it underlines the apparent differences in the underlying mechanisms explaining the presence of HLA-DR on T cell, when compared to APCs. This further implies that it is difficult to draw any immediate conclusions of HLA-DR on T cells, as we know it from APCs. Nonetheless, the observations about the induction of HLA-DR protein expression indicate an important role of APCs, and perhaps accessory cells, in this context (further addressed in section 4.2). The observed differences between T cells and APC, in the context of HLA-DR, were also apparent from both the FCM analysis of HLA-DR mem and HLA-DR IC and from the transcriptional analysis of *HLA-DRB1* mRNA (Manuscript 1).

With the collected investigation about the presence of HLA-DR on human T cells presented in this PhD thesis, it has been made very probable that human CD4+ T cells in peripheral blood do not express HLA-DR endogenously. As a natural next step, this trend should be investigated with similar protein and transcript analyses in T cells, which have been activated *in vitro*, like the isolated CD4+ T cells subjected to PHA or anti-CD3/anti-CD28 stimulation. Also an investigation of T cells from other relevant tissues, such as the palatine tonsils (140), could improve the understanding of HLA-DR on T cells.

4.2. ROLE OF APC AND VESICLES IN T CELL ACTIVATION AND FUNCTION

To investigate the role of APCs in relation to HLA-DR on T cells, a number of experiments were carried out. Here, the proliferation and functional phenotype of the HLA-DR+ CD4+ T cells was characterized following an allogeneic MLC in which the responder and stimulator cells were co-cultured with or without physical contact. Furthermore, the phenotype of the EVs produced during the MLCs was characterized, in order to derive information of the importance of vesicle-mediated communication and possible transfer of HLA-DR from APCs to T cells. It was demonstrated and confirmed (61, 79) that physical contact is required to observe an increase in the presence of HLA-DR on CD4+ T cells following an alloresponse. In

addition, the proliferation of responder cells was contact-dependent. The two types of MLCs produced distinct vesicle populations, indicating a potential difference in the functionality of intercellular communication facilitated by vesicles. Although the overall EV phenotypes were quite heterogeneous, there were contact-dependent differences in the levels of the detected HLA-DR bearing EVs. Interestingly, the majority of these EVs were detected in the transwell chamber holding the irradiated stimulator cells. Additionally, EVs from this chamber also contained high levels of CD9 and CD81, thereby indicating that the stimulator cells are capable of producing EVs and that these vesicles can contain HLA-DR. Moreover, it has been observed that HLA-DR+ EVs are produced by DCs in monoculture and also during DC:T cells co-cultures, but not by isolated CD4+ T cells (Table I). This could indicate that the HLA-DR-bearing vesicles observed from the stimulator cells in the transwell chamber are produced by the APCs in this cell population. Since it has been demonstrated that activated T cells can acquire such vesicles (76), a priming of the responder T cells prior to the MLC may change the entire outcome of such a contact-independent alloresponse. Nevertheless, this remains to be investigated. However, with the results presented in this thesis, it is not possible to unambiguously determine that vesicle-mediated cellular communication is important for the presence of HLA-DR on T cells.

4.2.1. EV PHENOTYPE AS AN INDICATOR OF CELLULAR AND ENVIRONMENTAL STRESS

In line with priming of T cells, an additional observation from this PhD study indicates an importance of the inflammatory status of the T cell milieu. This relates to the adhesion molecule ICAM-1, which is normally expressed by APCs and has an important role in establishing the synapse formed between T cell and APC (Figure 1, section 1.1). As noted in Table I (section 3.3), ICAM-1 was detected on EVs from co-cultures of both CD4+ T cells and iDCs and mDCs and also from the monocultures of mDCs. However, ICAM-1 was not detected on EVs from monocultures of either CD4+ T cell or iDCs, thus indicating both cell- and maturation-state-specific differences for this protein on EVs. When relating these EV phenotypes to the cellular phenotypes, a different pattern occurred (Figure 14). Here, ICAM-1 was highly expressed by DCs in monoculture, which was interesting since no ICAM-1-presenting EVs were detected for the iDC monoculture. Moreover, ICAM-1 was present on both CD4+ T cells and iDCs after co-culture, while ICAM-1 was down-regulated on mDCs and absent on the co-cultured CD4+ T cells. Whether or not ICAM-1 was transferred from the iDCs to the CD4+ T cells can only be speculated at the moment. However, the phenomenon is interesting. To further characterize any vesicle-mediated transfer, an indirect way of measuring this is to investigate the possible transfer of APC-derived proteins, including HLA-DR, to T cells by trogocytosis. Such an investigation could be facilitated with a FCM analysis described and employed in other studies (141-143). Nonetheless, the observations with ICAM-1 illustrates two points; First, different inflammatory milieus can create different cellular and EV phenotypes. This suggests that the cells are capable of

adapting and differentiating both the cellular and the vesicular response relative to the present situation. This is ultimately bound to have an impact of the functional outcomes. Second, EVs are not complete mirror images of the parent cell, which is otherwise a general assumption in the EV research field.

Aside from the observation about ICAM-1, an interesting notion about CD3 can also be found. From Table I it can be deduced that CD3 was detected on EVs from the contact-dependent MLC and in the co-cultures of CD4+ T cells and both iDCs and mDCs. Also, a very weak signal was detected for the EVs from the stimulator cells in the contact-independent MLC. In contrast, CD3 was not detected on EVs from the responder cells of the contact-independent MLC and from the CD4+ T cell monocultures; a control cell sample from the CD4+ T-DC experiments. Hence, it could seem as though the T cells, which assumingly produce the CD3-presenting EVs, only produce these, when a physical interaction between T cells and APC can be formed and an activation of the T cells occurs. This can be correlated with the observation that T cells down-regulate CD3 (TCR) upon activation (144, 145) and that this process has been associated with the production of CD3-enriched EVs, as a tool of the down-regulation (73). This yet again correlates with the results found in Figure 2 in Manuscript 2, which demonstrates that cellular proliferation, which is an indication of activation, only occurs in the contact-dependent MLC. In summary, this once again demonstrates how the cells are able to adjust the vesicle-associated proteins according to a given situation and also points to EVs having numerous functionalities, which may not all be associated with communication.

In relation to the more general EV/ exosome markers, here including CD9, CD63, CD81, and CD82 (Table I), all the included experiments indicate that these markers are ubiquitously present on the analyzed EVs, except for CD63. In general, CD63 is the most applied exosome marker, probably due to its initial discovery and description in the 1990s (66, 146). However, similar to the observation made here, the presence of CD63 on EVs from plasma has been found to be far more heterogeneous, when compared to CD9 and CD81 (116). Nevertheless, CD63 is still often found in relation to EVs, thus indicating a role in this context. This role could likely be more specific than the one for CD9 and CD81, thus making CD63 a poor general EV marker. The EV phenotyping presented in Manuscript 2 (Appendix B2) included a panel of 25 markers, comprising both the general EV markers as well as a selection of cell-specific markers. With these markers, several contact-dependent differences were identified. However, only a fraction of these potential differences has probably been identified. Here, a total protein profile of the EV proteins, obtained by proteomics, would aid in selecting new candidate antibodies for a second round of EV Array analysis and pinpoint interesting targets in an extended cellular phenotyping as well. Mass spectrometry has been deemed a powerful method for such a profiling of EV proteins and has demonstrated the heterogeneity of EV proteins, even though particular protein subsets also seem to be enriched in these vesicles (66, 147, 148). This underlines the complexity of EV-based cellular communication and unraveling its roles in physiological and pathophysiological scenarios are still in its infancy.

4.3. FUNCTIONALITY OF HLA-DR ON T CELLS

An essential aspect of HLA-DR on T cells is the functional consequences of this phenomenon. It is becoming increasingly evident that HLA-DR is probably more than an activation marker for T cells and may provide the T cell with APC-like functions. Currently, the role of such T-APCs has mainly been associated with down-regulating the activity of the responder T cell (3, 82, 83). However, it is also possible that T-APCs can activate other T cells (61, 62) (Figure 15). In the present PhD study, it was attempted to add information to the functionality of HLA-DR-presenting CD4+ T cells by characterizing the phenotype of these cells following contact-dependent and -independent allogeneic MLCs. The phenotyping included seven cell surface markers related to T cell activation and regulation (Table II and III, section 3.4). With the obtained results it is obvious that the CD4+ HLA-DR+ T cells from each of the MLCs are quite heterogeneous cell populations. This was not unexpected since the CD4+ HLA-DR+ responder T cells were not a clearly defined population, but overlapped with the CD4+ HLA-DR- T cells. This feature was also observed for T cells in peripheral blood (both for the entire CD3+ population and within each T cell lineage; Figure 13 and Manuscript 1). However, two observations emerged from the phenotyping characterization of the responder T cells in the MLCs. First, practically all the investigated markers were enriched in the CD4+ HLA-DR+ responder T cells from the contact-dependent MLC, compared to the contact-independent counterpart (Figure 3C, Manuscript 2). Secondly, several of the markers were predominantly expressed in the HLA-DR-presenting CD3+ CD4+ subsets of the MLCs than in the corresponding HLA-DR- subsets (Figure 4, Manuscript 4). Most noteworthy was the four differentially expressed markers, which separated the CD4+ HLA-DR+ T cells from the two types of MLCs; CD25, CTLA-4, PD-1, and TNFRII (Table II, section 3.4; Figure 3B, Manuscript 2). As previously mentioned, all of these were present to the greatest extent in the contact-dependent MLC. Both effector T cells (Teffs) and Tregs can express all of these proteins, though with different functional outcomes. Hence, it is difficult to make any immediate conclusions to determine if the CD4+ HLA-DR+ belongs to either of the two T cells subsets. A simultaneous expression analysis of the Treg-associated FoxP3 transcription factor (88) could have aided to solve this issue, though some controversy about FoxP3 as Treg identifier also exists (149).

4.3.1. POSSIBLE ROLES OF HLA-DR-PRESENTING T-APCS/TREGS

It is, nevertheless, possible to deduce some functional clues about the CD4+ HLA-DR+ T cells based on the results of the present study, particularly focusing on CTLA-4 and PD-1. Both CTLA-4 and PD-1 are co-inhibitory molecules involved in down-regulation of T cell activity, consequently involved in induction and maintenance of immune tolerance and homeostasis (Table III, section 3.4) (129, 150). Moreover, it has been demonstrated that blocking HLA-DR on Treg impairs their suppressive activity (151), while blocking CTLA-4 and PD-1 reduces Treg activity in melanoma (152). This suggests a link between HLA-DR, CTLA-4, PD-1, and Tregs and indicates a probable role for these cells in tolerance induction. Addition-

ally, a correlation between PD-1 and TNFRII was detected for the CD4+ HLA-DR+ T cells from both MLCs (Figure 4A, Manuscript 2). A suppressive activity of CD4+ CD25+ TNFRII+ HLA-DR+ T cells has previously been determined and these cells also presented high levels of CTLA-4 (88). Taken together, the simultaneous presence of HLA-DR, CD25, CTLA-4, PD-1, and TNFRII on CD4+ T cells could very likely identify a subset of cells with suppressive activity. T cells with such regulatory functions are frequently known as Tregs and not T-APCs, since the investigated mechanisms of suppression most often do not include any related to antigen-specificity. However, this does not exclude a possible role of antigen-specific suppression by Tregs/T-APCs. The Treg subset is a heterogeneous group of cells, which can be quite difficult to categorize, since their functional phenotypes depend on several factors, including cell lineage (natural versus induced) and status of the surrounding environment (153-155). Hence, these cells can seemingly be tailored for the situation at hand. This feature correlates with the presented results from the contact-dependent and –independent MLCs, which produced different CD4+ HLA-DR+ T cell subsets, though both with a suppressive molecular profile (Figure 3, Manuscript 2). However, any suppressive activity of the investigated CD4+ HLA-DR+ responder T cells remains to be established. Moreover, an investigation of the co-stimulatory molecules CD80 and CD86, which are two APC-related co-stimulatory molecules (section 1.3.3), would further elucidate their putative T-APCs/Tregs function.

4.4. IMPLICATIONS

Delineating all aspects of HLA-DR is pivotal, since HLA-DR in essence controls the specificity of the adaptive immune system. Despite the longstanding observation, HLA-DR on T cells is still a topic of debate, containing several contradictory opinions and results. The results presented in this PhD thesis indicates that CD4+ T cells in peripheral blood do not possess an active, endogenous expression of the HLA-DR protein. Moreover, APCs have an important role in the presence of HLA-DR on CD4+ T cells, since an increase in CD4+ HLA-DR+ cells can only be observed, when T:APC interaction can occur. By combining the expression results with those from investigating the role of APCs, it is warranted to hypothesize that a major mechanism accounting for the HLA-DR on CD4+ T cells could be a molecular transfer from APCs. On a general note, this phenomenon of intercellular transfer of molecules adds another layer of complexity to the function of the immune system and it could possibly necessitate a paradigm shift in relation to immune regulationterms of how this system is regulated. The work of this PhD thesis also points to a down-regulatory function of HLA-DR-presenting T cells. A likely role of these HLA-DR+ T cells is participating in the induction of peripheral tolerance, either to limit autoreactive T cells, with a consequent implication in autoimmunity, or to limit clonal expansion of Teffs, which could serve to terminate an ongoing immune response (Figure 15). Aside from the basic mechanisms of the immune system, understanding the function and dynamics of HLA-DR+ T cells could be used to expand the knowledge of how cancer cells escape immune recognition, which may identify targets of new therapeutic strategies.

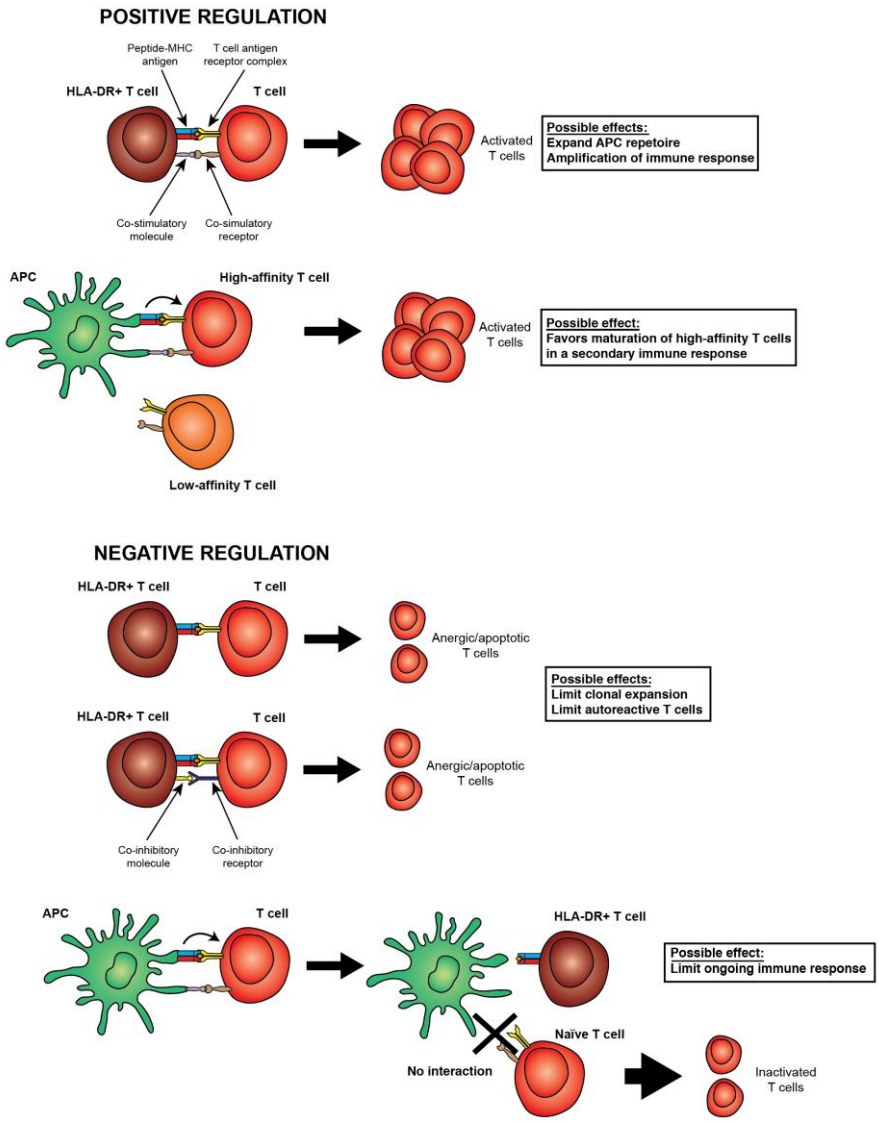
POSITIVE REGULATION
Peptide-MHC antigen
T cell antigen receptor complex
HLA-DR+ T cell
T cell
Co-stimulatory molecule
Co-simulatory receptor
Activated T cells
Possible effects:
Expand APC repetoire
Amplification of immune response
APC
High-affinity T cell
Low-affinity T cell
Activated T cells
Possible effect:
Favors maturation of high-affinity T cells in a secondary immune response
NEGATIVE REGULATION
HLA-DR+ T cell
T cell
Anergic/apoptotic T cells
Possible effects:
Limit clonal expansion
Limit autoreactive T cells
HLA-DR+ T cell
T cell
Co-inhibitory molecule
Co-inhibitory receptor
Anergic/apoptotic T cells
APC
T cell
HLA-DR+ T cell
Possible effect:
Limit ongoing immune response
Naïve T cell
No interaction
Inactivated T cells

Figure 15 Functional consequences of HLA-DR on T cells. As described with the existing literature and the experimental results of PhD thesis, HLA-DR on T cells may play a yet unknown role in regulating the immune system. The possible effects of such a role can be categorized as being either immunostimulatory (positive regulation) or immunosuppressive (negative regulation). The positive regulation involves HLA-DR+ T cells acting as T-APCs with a consequent possibility to activate other T cells upon interaction. This requires the simultaneous presence of the antigen-specific and co-stimulatory signals (also see Figure 1). The function of an HLA-DR+ T-APCs could be to expand the APC repertoire, thereby amplifying an immune response. Moreover, acquisition of HLA-DR from APCs may limit the amount of cognate peptide-HLA-DR complexes available in a secondary immune response, thus favoring the maturation of high-affinity memory T cells (156, 157). As previously mentioned, HLA-DR on T cells has mainly been associated with down-regulatory activity and the induction of tolerance or anergy in other T cells. Consequently, the proposed effects of such a negative regulation includes limiting clonal expansion by ligation of the TCR without a concurrent co-stimulatory signal (Figure 1). This could serve to terminate an ongoing immune reaction. Moreover, a similar scenario could limit autoreactive T cells. In addition, the simultaneous presence of co-inhibitory molecules, such as PD-1, could also negatively regulate the responder T cell. Finally, an acquisition of HLA-DR by T cells from an APC could make HLA-DR inaccessible for another interaction between a naïve T cell and the APC, causing a limit to the degree of T cell activation.

CHAPTER 5. FUTURE WORK

The work presented in this PhD thesis has investigated several aspects of HLA-DR on human T cells, indicating the absence of an endogenous HLA-DR expression and a down-regulatory function of HLA-DR+ CD4+ T cells. To support and elaborate on these results, a number of additional investigations could be carried out:

1. To investigate the transfer of HLA-DR from APCs to T cells, the use of antibodies specific for the protein products of particular *HLA-DR* alleles could be applied. These antibodies are available at the Department of Clinical Immunology, Aalborg University Hospital, Denmark, and their specificities have already been tested. With the antibodies it will hopefully be possible to determine whether the HLA-DR found on responder cells following an allogeneic MLC is the HLA-DR type of the responder cell or that of the stimulator cell. This would be indicative of an endogenous protein expression or a molecular acquisition, respectively. Subsequently, a proteomic analysis of the HLA-DR found on the responder cells, using mass spectrometry, could further validate the findings from this investigation. This setup is currently being optimized at the Laboratory for Medical Mass Spectrometry, Aalborg University, Denmark.

2. Since proliferation is expected for the CD4+ T cells stimulated with PHA or anti-CD3/anti-CD28 (Manuscript 2), it would be reasonable to include this experimental outcome in the future work. Moreover, it would be relevant to include an experiment in which the cells were stimulated for at least three days in order to ensure that the observations presented in Manuscript 2 (Figure 1) is not caused by a delay in the expression of HLA-DR, since HLA-DR typically is used as a late activation marker (section 1.3).

3. To further evaluate the similarities of APCs and T-APCs, it would be interesting to use flow cytometry and fluorescence microscopy to investigate the co-expression/ co-localization of HLA-DR and Ii in T cells. Since Ii is an important chaperone for HLA-DR in APCs, a similar role could be expected in T cells if these cells possess the ability to process and present antigens. In addition, the investigation of a possible transfer/presence of the co-stimulatory molecules CD80 and CD86 would increase the knowledge of the APC function of HLA-DR+ T cells.

4. An evaluation of the suppressive activity of HLA-DR+ T cells would expand the findings from the phenotyping of these cells into a functional context. Classically, this activity is measured by following the proliferation of the responder cells (158), as described in Manuscript 2. With the results presented in this thesis, it would be natural to investigate the possible role of PD-1 in this suppression. Interestingly, it has also been demonstrated vesicle-mediated suppression by Tregs can occur (159), warranting EV analysis in the context of a functional analysis of HLA-DR presenting T cells.

5. Since it was shown that CD4+ T cells in peripheral blood most likely do not express the HLA-DR protein found in their membrane, it would be interesting to see if this was also valid for both *in vivo* and *in vitro* activated T cells. Hence, the correlation between HLA-DR mem/HLA-DR IC and *HLA-DRB1*03* mRNA (as in Manuscript 1) for activated T cells could considerably improve the understanding of HLA-DR on T cells and its validity as a T cell activation marker.

CHAPTER 6. REFERENCES

1. Parham, P. 2009. *The Immune System*. Garland Science, New York.
2. Neefjes, J., M. L. Jongsma, P. Paul, and O. Bakke. 2011. Towards a systems understanding of MHC class I and MHC class II antigen presentation. *Nat Rev Immunol* 11:823-836.
3. Holling, T. M., E. Schooten, and P. J. van Den Elsen. 2004. Function and regulation of MHC class II molecules in T-lymphocytes: of mice and men. *Hum Immunol* 65:282-290.
4. Arancibia-Carcamo, C. V., H. Osawa, H. A. Arnett, Z. Haskova, A. J. George, S. J. Ono, J. P. Ting, and J. W. Streilein. 2004. A CIITA-independent pathway that promotes expression of endogenous rather than exogenous peptides in immune-privileged sites. *Eur J Immunol* 34:471-480.
5. Griffiths, G. M., A. Tsun, and J. C. Stinchcombe. 2010. The immunological synapse: a focal point for endocytosis and exocytosis. *J Cell Biol* 189:399-406.
6. Yokosuka, T., W. Kobayashi, M. Takamatsu, K. Sakata-Sogawa, H. Zeng, A. Hashimoto-Tane, H. Yagita, M. Tokunaga, and T. Saito. 2010. Spatiotemporal basis of CTLA-4 costimulatory molecule-mediated negative regulation of T cell activation. *Immunity* 33:326-339.
7. Rodriguez-Fernandez, J. L., L. Riol-Blanco, and C. Delgado-Martin. 2010. What is an immunological synapse? *Microbes Infect* 12:438-445.
8. Handunnetthi, L., S. V. Ramagopalan, G. C. Ebers, and J. C. Knight. 2010. Regulation of major histocompatibility complex class II gene expression, genetic variation and disease. *Genes Immun* 11:99-112.
9. Horton, R., L. Wilming, V. Rand, R. C. Lovering, E. A. Bruford, V. K. Khodiyar, M. J. Lush, S. Povey, C. C. Talbot, Jr., M. W. Wright, H. M. Wain, J. Trowsdale, A. Ziegler, and S. Beck. 2004. Gene map of the extended human MHC. *Nat Rev Genet* 5:889-899.
10. van Lith, M., R. M. McEwen-Smith, and A. M. Benham. 2010. HLA-DP, HLA-DQ, and HLA-DR have different requirements for invariant chain and HLA-DM. *J Biol Chem* 285:40800-40808.
11. Mach, B., V. Steimle, E. Martinez-Soria, and W. Reith. 1996. Regulation of MHC class II genes: lessons from a disease. *Annu Rev Immunol* 14:301-331.
12. Landsverk, O. J., N. Barois, T. F. Gregers, and O. Bakke. 2011. Invariant chain increases the half-life of MHC II by delaying endosomal maturation. *Immunol Cell Biol* 89:619-629.
13. Al-Daccak, R., N. Mooney, and D. Charron. 2004. MHC class II signaling in antigen-presenting cells. *Curr Opin Immunol* 16:108-113.
14. HLA Informatics Group, A. N. T. 2014. HLA Alleles Number.
15. Drozina, G., J. Kohoutek, N. Jabran-Ferrat, and B. M. Peterlin. 2005. Expression of MHC II genes. In *Molecular Analysis of B Lymphocyte Development and Activation*. H. Singh, and R. Grosschedl, eds. Springer Berlin Heidelberg. 147-170.
16. Muhlethaler-Mottet, A., L. A. Otten, V. Steimle, and B. Mach. 1997. Expression of MHC class II molecules in different cellular and functional compartments is controlled by differential usage of multiple promoters of the transactivator CIITA. *EMBO J* 16:2851-2860.
17. van Eggermond, M. C., D. R. Boom, P. Klous, E. Schooten, V. E. Marquez, R. J. Wierda, T. M. Holling, and P. J. van den Elsen. 2011. Epigenetic regulation of CIITA expression in human T-cells. *Biochem Pharmacol* 82:1430-1437.

18. Sisk, T. J., K. Nickerson, R. P. Kwok, and C. H. Chang. 2003. Phosphorylation of class II transactivator regulates its interaction ability and transactivation function. *Int Immunol* 15:1195-1205.
19. Greer, S. F., J. A. Harton, M. W. Linhoff, C. A. Janczak, J. P. Ting, and D. E. Cressman. 2004. Serine residues 286, 288, and 293 within the CIITA: a mechanism for down-regulating CIITA activity through phosphorylation. *J Immunol* 173:376-383.
20. Bhat, K. P., A. D. Truax, and S. F. Greer. 2010. Phosphorylation and ubiquitination of degron proximal residues are essential for class II transactivator (CIITA) transactivation and major histocompatibility class II expression. *J Biol Chem* 285:25893-25903.
21. Williams, G. S., M. Malin, D. Vremec, C. H. Chang, R. Boyd, C. Benoist, and D. Mathis. 1998. Mice lacking the transcription factor CIITA--a second look. *Int Immunol* 10:1957-1967.
22. Schooten, E., P. Klous, P. J. van den Elsen, and T. M. Holling. 2005. Lack of MHC-II expression in activated mouse T cells correlates with DNA methylation at the CIITA-PIII region. *Immunogenetics* 57:795-799.
23. Kurokawa, R., M. G. Rosenfeld, and C. K. Glass. 2009. Transcriptional regulation through noncoding RNAs and epigenetic modifications. *RNA Biol* 6:233-236.
24. Paglia, P., G. Girolomoni, F. Robbiati, F. Granucci, and P. Ricciardi-Castagnoli. 1993. Immortalized dendritic cell line fully competent in antigen presentation initiates primary T cell responses in vivo. *J Exp Med* 178:1893-1901.
25. Sallusto, F., and A. Lanzavecchia. 1994. Efficient presentation of soluble antigen by cultured human dendritic cells is maintained by granulocyte/macrophage colony-stimulating factor plus interleukin 4 and downregulated by tumor necrosis factor alpha. *J Exp Med* 179:1109-1118.
26. Guardiola, J., and A. Maffei. 1993. Control of MHC class II gene expression in autoimmune, infectious, and neoplastic diseases. *Crit Rev Immunol* 13:247-268.
27. Gaspari, A. A., M. K. Jenkins, and S. I. Katz. 1988. Class II MHC-bearing keratinocytes induce antigen-specific unresponsiveness in hapten-specific Th1 clones. *J Immunol* 141:2216-2220.
28. Frasca, L., F. Marelli-Berg, N. Imami, I. Potolicchio, P. Carmichael, G. Lombardi, and R. Lechler. 1998. Interferon-gamma-treated renal tubular epithelial cells induce allospecific tolerance. *Kidney Int* 53:679-689.
29. Bal, V., A. McIndoe, G. Denton, D. Hudson, G. Lombardi, J. Lamb, and R. Lechler. 1990. Antigen presentation by keratinocytes induces tolerance in human T cells. *Eur J Immunol* 20:1893-1897.
30. Kreisel, D., S. B. Richardson, W. Li, X. Lin, C. G. Kornfeld, S. Sugimoto, C. S. Hsieh, A. E. Gelman, and A. S. Krupnick. 2010. Cutting edge: MHC class II expression by pulmonary nonhematopoietic cells plays a critical role in controlling local inflammatory responses. *J Immunol* 185:3809-3813.
31. Fortin, J. S., M. Cloutier, and J. Thibodeau. 2013. Exposing the Specific Roles of the Invariant Chain Isoforms in Shaping the MHC Class II Peptidome. *Front Immunol* 4:443.
32. Garstka, M. A., and J. Neefjes. 2013. How to target MHC class II into the MIIC compartment. *Mol Immunol* 55:162-165.
33. Costantino, C. M., H. L. Ploegh, and D. A. Hafler. 2009. Cathepsin S regulates class II MHC processing in human CD4+ HLA-DR+ T cells. *J Immunol* 183:945-952.

34. Wilson, N. S., and J. A. Villadangos. 2005. Regulation of antigen presentation and cross-presentation in the dendritic cell network: facts, hypothesis, and immunological implications. *Adv Immunol* 86:241-305.
35. van Niel, G., R. Wubbolts, and W. Stoorvogel. 2008. Endosomal sorting of MHC class II determines antigen presentation by dendritic cells. *Curr Opin Cell Biol* 20:437-444.
36. Yu, D. T., R. J. Winchester, S. M. Fu, A. Gibofsky, H. S. Ko, and H. G. Kunkel. 1980. Peripheral blood Ia-positive T cells. Increases in certain diseases and after immunization. *J Exp Med* 151:91-100.
37. Reddy, M., E. Eirikis, C. Davis, H. M. Davis, and U. Prabhakar. 2004. Comparative analysis of lymphocyte activation marker expression and cytokine secretion profile in stimulated human peripheral blood mononuclear cell cultures: an in vitro model to monitor cellular immune function. *J Immunol Methods* 293:127-142.
38. Ferenczi, K., L. Burack, M. Pope, J. G. Krueger, and L. M. Austin. 2000. CD69, HLA-DR and the IL-2R identify persistently activated T cells in psoriasis vulgaris lesional skin: blood and skin comparisons by flow cytometry. *J Autoimmun* 14:63-78.
39. Evans, R. L., T. J. Faldetta, R. E. Humphreys, D. M. Pratt, E. J. Yunis, and S. F. Schlossman. 1978. Peripheral human T cells sensitized in mixed leukocyte culture synthesize and express Ia-like antigens. *J Exp Med* 148:1440-1445.
40. Ko, H. S., S. M. Fu, R. J. Winchester, D. T. Yu, and H. G. Kunkel. 1979. Ia determinants on stimulated human T lymphocytes. Occurrence on mitogen- and antigen-activated T cells. *J Exp Med* 150:246-255.
41. Sharrow, S. O., K. Ozato, and D. H. Sachs. 1980. Phenotypic expression of I-A and I-E/C subregion determinants on murine thymocytes. *J Immunol* 125:2263-2268.
42. Truneh, A., F. Albert, P. Golstein, and A. M. Schmitt-Verhulst. 1985. Early steps of lymphocyte activation bypassed by synergy between calcium ionophores and phorbol ester. *Nature* 313:318-320.
43. Matsushima, G. K., Y. Itoh-Lindstrom, and J. P. Ting. 1992. Activation of the HLA-DRA gene in primary human T lymphocytes: novel usage of TATA and the X and Y promoter elements. *Mol Cell Biol* 12:5610-5619.
44. Parham, P. 2005. *The Immune System*. Garland Science, New York.
45. Amlot, P. L., F. Tahami, D. Chinn, and E. Rawlings. 1996. Activation antigen expression on human T cells. I. Analysis by two-colour flow cytometry of umbilical cord blood, adult blood and lymphoid tissue. *Clin Exp Immunol* 105:176-182.
46. Holling, T. M., N. van der Stoep, E. Quinten, and P. J. van den Elsen. 2002. Activated human T cells accomplish MHC class II expression through T cell-specific occupation of class II transactivator promoter III. *J Immunol* 168:763-770.
47. Wong, A. W., N. Ghosh, K. P. McKinnon, W. Reed, J. F. Piskurich, K. L. Wright, and J. P. Ting. 2002. Regulation and specificity of MHC2TA promoter usage in human primary T lymphocytes and cell line. *J Immunol* 169:3112-3119.
48. Isaacson, J. A., K. P. Flaming, and J. A. Roth. 1998. Increased MHC class II and CD25 expression on lymphocytes in the absence of persistent lymphocytosis in cattle experimentally infected with bovine leukemia virus. *Vet Immunol Immunopathol* 64:235-248.
49. Bendali-Ahcene, S., J. L. Cadore, M. Fontaine, and J. C. Monier. 1997. Anti-alpha chain monoclonal antibodies of equine MHC class-II antigens: applications to equine infectious anaemia. *Res Vet Sci* 62:99-104.

50. Lyons, C. R., R. G. Cook, T. F. Tucker, and J. W. Uhr. 1981. Biochemical characterization of Ia alloantigens in guinea pigs. II. Comparative peptide mapping of Ia antigens from B cells, T cells, and macrophages. *J Immunol* 127:1885-1888.
51. Reizis, B., C. Schramm, I. R. Cohen, and F. Mor. 1994. Expression of major histocompatibility complex class II molecules in rat T cells. *Eur J Immunol* 24:2796-2802.
52. Broeren, C. P., M. H. Wauben, M. A. Lucassen, M. Van Meurs, P. J. Van Kooten, C. J. Boog, E. Claassen, and W. Van Eden. 1995. Activated rat T cells synthesize and express functional major histocompatibility class II antigens. *Immunology* 84:193-201.
53. Otten, L. A., F. Tacchini-Cottier, M. Lohoff, F. Annunziato, L. Cosmi, L. Scarpellino, J. Louis, V. Steimle, W. Reith, and H. Acha-Orbea. 2003. Deregulated MHC class II transactivator expression leads to a strong Th2 bias in CD4+ T lymphocytes. *J Immunol* 170:1150-1157.
54. Chang, C. H., S. C. Hong, C. C. Hughes, C. A. Janeway, Jr., and R. A. Flavell. 1995. CIITA activates the expression of MHC class II genes in mouse T cells. *Int Immunol* 7:1515-1518.
55. Lal, G., M. S. Shaila, and R. Nayak. 2005. Activated mouse T-cells synthesize MHC class II, process, and present morbillivirus nucleocapsid protein to primed T-cells. *Cell Immunol* 234:133-145.
56. Brown, K., M. Fidanboylu, and W. Wong. 2010. Intercellular exchange of surface molecules and its physiological relevance. *Arch Immunol Ther Exp (Warsz)* 58:263-272.
57. Rechavi, O., I. Goldstein, and Y. Kloog. 2009. Intercellular exchange of proteins: the immune cell habit of sharing. *FEBS Lett* 583:1792-1799.
58. Smyth, L. A., B. Afzali, J. Tsang, G. Lombardi, and R. I. Lechler. 2007. Intercellular transfer of MHC and immunological molecules: molecular mechanisms and biological significance. *Am J Transplant* 7:1442-1449.
59. Rechavi, O., M. Kalman, Y. Fang, H. Vernitsky, J. Jacob-Hirsch, L. J. Foster, Y. Kloog, and I. Goldstein. 2010. Trans-SILAC: sorting out the non-cell-autonomous proteome. *Nat Methods* 7:923-927.
60. Patel, D. M., P. Y. Arnold, G. A. White, J. P. Nardella, and M. D. Mannie. 1999. Class II MHC/peptide complexes are released from APC and are acquired by T cell responders during specific antigen recognition. *J Immunol* 163:5201-5210.
61. Game, D. S., N. J. Rogers, and R. I. Lechler. 2005. Acquisition of HLA-DR and costimulatory molecules by T cells from allogeneic antigen presenting cells. *Am J Transplant* 5:1614-1625.
62. Tsang, J. Y., J. G. Chai, and R. Lechler. 2003. Antigen presentation by mouse CD4+ T cells involving acquired MHC class II:peptide complexes: another mechanism to limit clonal expansion? *Blood* 101:2704-2710.
63. Gutierrez-Vazquez, C., C. Villarroya-Beltri, M. Mittelbrunn, and F. Sanchez-Madrid. 2013. Transfer of extracellular vesicles during immune cell-cell interactions. *Immunol Rev* 251:125-142.
64. Oviedo-Orta, E., and W. Howard Evans. 2004. Gap junctions and connexin-mediated communication in the immune system. *Biochim Biophys Acta* 1662:102-112.
65. Joly, E., and D. Hudrisier. 2003. What is trogocytosis and what is its purpose? *Nat Immunol* 4:815.
66. Revenfeld, A. L., R. Baek, M. H. Nielsen, A. Stensballe, K. Varming, and M. Jorgensen. 2014. Diagnostic and prognostic potential of extracellular vesicles in peripheral blood. *Clin Ther* 36:830-846.

67. Thery, C., M. Ostrowski, and E. Segura. 2009. Membrane vesicles as conveyors of immune responses. *Nat Rev Immunol* 9:581-593.
68. Akers, J. C., D. Gonda, R. Kim, B. S. Carter, and C. C. Chen. 2013. Biogenesis of extracellular vesicles (EV): exosomes, microvesicles, retrovirus-like vesicles, and apoptotic bodies. *J Neurooncol* 113:1-11.
69. Gyorgy, B., T. G. Szabo, M. Pasztoi, Z. Pal, P. Misjak, B. Aradi, V. Laszlo, E. Pallinger, E. Pap, A. Kittel, G. Nagy, A. Falus, and E. I. Buzas. 2011. Membrane vesicles, current state-of-the-art: emerging role of extracellular vesicles. *Cell Mol Life Sci* 68:2667-2688.
70. Valadi, H., K. Ekstrom, A. Bossios, M. Sjostrand, J. J. Lee, and J. O. Lotvall. 2007. Exosome-mediated transfer of mRNAs and microRNAs is a novel mechanism of genetic exchange between cells. *Nat Cell Biol* 9:654-659.
71. Mittelbrunn, M., C. Gutierrez-Vazquez, C. Villarroya-Beltri, S. Gonzalez, F. Sanchez-Cabo, M. A. Gonzalez, A. Bernad, and F. Sanchez-Madrid. 2011. Unidirectional transfer of microRNA-loaded exosomes from T cells to antigen-presenting cells. *Nat Commun* 2:282.
72. Davis, D. M. 2007. Intercellular transfer of cell-surface proteins is common and can affect many stages of an immune response. *Nat Rev Immunol* 7:238-243.
73. Choudhuri, K., J. Llodra, E. W. Roth, J. Tsai, S. Gordo, K. W. Wucherpfennig, L. C. Kam, D. L. Stokes, and M. L. Dustin. 2014. Polarized release of T-cell-receptor-enriched microvesicles at the immunological synapse. *Nature*.
74. Lorber, M. I., M. R. Loken, A. M. Stall, and F. W. Fitch. 1982. I-A antigens on cloned alloreactive murine T lymphocytes are acquired passively. *J Immunol* 128:2798-2803.
75. Umeshappa, C. S., H. Huang, Y. Xie, Y. Wei, S. J. Mulligan, Y. Deng, and J. Xiang. 2009. CD4+ Th-APC with acquired peptide/MHC class I and II complexes stimulate type 1 helper CD4+ and central memory CD8+ T cell responses. *J Immunol* 182:193-206.
76. Nolte-'t Hoen, E. N., S. I. Buschow, S. M. Anderton, W. Stoorvogel, and M. H. Wauben. 2009. Activated T cells recruit exosomes secreted by dendritic cells via LFA-1. *Blood* 113:1977-1981.
77. Patel, D. M., and M. D. Mannie. 2001. Intercellular exchange of class II major histocompatibility complex/peptide complexes is a conserved process that requires activation of T cells but is constitutive in other types of antigen presenting cell. *Cell Immunol* 214:165-172.
78. Buschow, S. I., E. N. Nolte-'t Hoen, G. van Niel, M. S. Pols, T. ten Broeke, M. Lauwen, F. Ossendorp, C. J. Melief, G. Raposo, R. Wubbolts, M. H. Wauben, and W. Stoorvogel. 2009. MHC II in dendritic cells is targeted to lysosomes or T cell-induced exosomes via distinct multivesicular body pathways. *Traffic* 10:1528-1542.
79. Undale, A. H., P. J. van den Elsen, and E. Celis. 2004. Antigen-independent acquisition of MHC class II molecules by human T lymphocytes. *Int Immunol* 16:1523-1533.
80. Wetzel, S. A., T. W. McKeithan, and D. C. Parker. 2005. Peptide-specific intercellular transfer of MHC class II to CD4+ T cells directly from the immunological synapse upon cellular dissociation. *J Immunol* 174:80-89.
81. Arnold, P. Y., and M. D. Mannie. 1999. Vesicles bearing MHC class II molecules mediate transfer of antigen from antigen-presenting cells to CD4+ T cells. *Eur J Immunol* 29:1363-1373.
82. Pichler, W. J., and T. Wyss-Coray. 1994. T cells as antigen-presenting cells. *Immunol Today* 15:312-315.

83. Baecher-Allan, C., E. Wolf, and D. A. Hafler. 2006. MHC class II expression identifies functionally distinct human regulatory T cells. *J Immunol* 176:4622-4631.
84. Taams, L. S., W. van Eden, and M. H. Wauben. 1999. Antigen presentation by T cells versus professional antigen-presenting cells (APC): differential consequences for T cell activation and subsequent T cell-APC interactions. *Eur J Immunol* 29:1543-1550.
85. LaSalle, J. M., P. J. Tolentino, G. J. Freeman, L. M. Nadler, and D. A. Hafler. 1992. Early signaling defects in human T cells anergized by T cell presentation of autoantigen. *J Exp Med* 176:177-186.
86. Satyaraj, E., S. Rath, and V. Bal. 1994. Induction of tolerance in freshly isolated alloreactive CD4+ T cells by activated T cell stimulators. *Eur J Immunol* 24:2457-2461.
87. Bettens, F., E. Frei, K. Frutig, D. Mauri, W. J. Pichler, and T. Wyss-Coray. 1995. Noncytotoxic human CD4+ T-cell clones presenting and simultaneously responding to an antigen die of apoptosis. *Cell Immunol* 161:72-78.
88. Chen, X., and J. J. Oppenheim. 2011. The phenotypic and functional consequences of tumour necrosis factor receptor type 2 expression on CD4(+) FoxP3(+) regulatory T cells. *Immunology* 133:426-433.
89. Hewitt, C. R., and M. Feldmann. 1989. Human T cell clones present antigen. *J Immunol* 143:762-769.
90. Lanzavecchia, A., S. Abrignani, D. Scheidegger, R. Obrist, B. Dorken, and G. Moldenhauer. 1988. Antibodies as antigens. The use of mouse monoclonal antibodies to focus human T cells against selected targets. *J Exp Med* 167:345-352.
91. Nakagawa, T. Y., and A. Y. Rudensky. 1999. The role of lysosomal proteinases in MHC class II-mediated antigen processing and presentation. *Immunol Rev* 172:121-129.
92. Riese, R. J., P. R. Wolf, D. Bromme, L. R. Natkin, J. A. Villadangos, H. L. Ploegh, and H. A. Chapman. 1996. Essential role for cathepsin S in MHC class II-associated invariant chain processing and peptide loading. *Immunity* 4:357-366.
93. Manoury, B., E. W. Hewitt, N. Morrice, P. M. Dando, A. J. Barrett, and C. Watts. 1998. An asparaginyl endopeptidase processes a microbial antigen for class II MHC presentation. *Nature* 396:695-699.
94. Sharpe, A. H., and G. J. Freeman. 2002. The B7-CD28 superfamily. *Nat Rev Immunol* 2:116-126.
95. Gotsman, I., A. H. Sharpe, and A. H. Lichtman. 2008. T-cell costimulation and coinhibition in atherosclerosis. *Circ Res* 103:1220-1231.
96. Tatari-Calderone, Z., R. T. Semnani, T. B. Nutman, J. Schlom, and H. Sabzevari. 2002. Acquisition of CD80 by human T cells at early stages of activation: functional involvement of CD80 acquisition in T cell to T cell interaction. *J Immunol* 169:6162-6169.
97. Sabzevari, H., J. Kantor, A. Jaigirdar, Y. Tagaya, M. Naramura, J. Hodge, J. Bernon, and J. Schlom. 2001. Acquisition of CD80 (B7-1) by T cells. *J Immunol* 166:2505-2513.
98. Lombardi, G., R. Hargreaves, S. Sidhu, N. Imami, L. Lightstone, S. Fuller-Espie, M. Ritter, P. Robinson, A. Tarnok, and R. Lechler. 1996. Antigen presentation by T cells inhibits IL-2 production and induces IL-4 release due to altered cognate signals. *J Immunol* 156:2769-2775.
99. Wyss-Coray, T., H. Gallati, I. Pracht, A. Limat, D. Mauri, K. Frutig, and W. J. Pichler. 1993. Antigen-presenting human T cells and antigen-presenting B cells

induce a similar cytokine profile in specific T cell clones. *Eur J Immunol* 23:3350-3357.

100. Taams, L. S., W. van Eden, and M. H. Wauben. 1999. Dose-dependent induction of distinct anergic phenotypes: multiple levels of T cell anergy. *J Immunol* 162:1974-1981.
101. Baumgarth, N., and M. Roederer. 2000. A practical approach to multicolor flow cytometry for immunophenotyping. *J Immunol Methods* 243:77-97.
102. Perfetto, S. P., P. K. Chattopadhyay, and M. Roederer. 2004. Seventeen-colour flow cytometry: unravelling the immune system. *Nat Rev Immunol* 4:648-655.
103. Moro, M., V. Cecconi, C. Martinoli, E. Dallegno, B. Giabbai, M. Degano, N. Glaichenhaus, M. P. Protti, P. Dellabona, and G. Casorati. 2005. Generation of functional HLA-DR*1101 tetramers receptive for loading with pathogen- or tumour-derived synthetic peptides. *BMC Immunol* 6:24.
104. Stockel, J., E. Meinl, C. Hahnel, J. Malotka, R. Seitz, K. Drexler, H. Wekerle, and K. Dornmair. 1994. Refolding of human class II major histocompatibility complex molecules isolated from Escherichia coli. Assembly of peptide-free heterodimers and increased refolding-yield in the presence of antigenic peptide. *J Biol Chem* 269:29571-29578.
105. Gorga, J. C., V. Horejsi, D. R. Johnson, R. Raghupathy, and J. L. Strominger. 1987. Purification and characterization of class II histocompatibility antigens from a homozygous human B cell line. *J Biol Chem* 262:16087-16094.
106. Koutna, I., P. Simara, P. Ondrackova, and L. Tesarrova. 2012. Flow Cytometry Analysis of Intracellular Protein. In *Flow Cytometry - Recent Perspectives*. I. Schmid, ed. InTech. 421-438.
107. Krutzik, P. O., and G. P. Nolan. 2003. Intracellular phospho-protein staining techniques for flow cytometry: monitoring single cell signaling events. *Cytometry A* 55:61-70.
108. Tung, J. W., K. Heydari, R. Tirouvanziam, B. Sahaf, D. R. Parks, and L. A. Herzenberg. 2007. Modern flow cytometry: a practical approach. *Clin Lab Med* 27:453-468, v.
109. Herzenberg, L. A., J. Tung, W. A. Moore, and D. R. Parks. 2006. Interpreting flow cytometry data: a guide for the perplexed. *Nat Immunol* 7:681-685.
110. Chattopadhyay, P. K., B. Gaylord, A. Palmer, N. Jiang, M. A. Raven, G. Lewis, M. A. Reuter, A. K. Nur-ur Rahman, D. A. Price, M. R. Betts, and M. Roederer. 2012. Brilliant violet fluorophores: a new class of ultrabright fluorescent compounds for immunofluorescence experiments. *Cytometry A* 81:456-466.
111. Koester, S. K., and W. E. Bolton. 2000. Intracellular markers. *J Immunol Methods* 243:99-106.
112. Livak, K. J., S. J. Flood, J. Marmaro, W. Giusti, and K. Deetz. 1995. Oligonucleotides with fluorescent dyes at opposite ends provide a quenched probe system useful for detecting PCR product and nucleic acid hybridization. *PCR Methods Appl* 4:357-362.
113. Schmittgen, T. D., and K. J. Livak. 2008. Analyzing real-time PCR data by the comparative C(T) method. *Nat Protoc* 3:1101-1108.
114. National Center for Biotechnology Information, U. S. N. L. o. M. 2014. HLA-DRB1 major histocompatibility complex, class II, DR beta 1 [*Homo sapiens* (human)].
115. Livak, K. J., and T. D. Schmittgen. 2001. Analysis of relative gene expression data using real-time quantitative PCR and the 2(-Delta Delta C(T)) Method. *Methods* 25:402-408.

116. Joergensen, M., R. Baek, S. Pedersen, E. K. Soendergaard, S. R. Kristensen, and K. Varming. 2013. Extracellular Vesicle (EV) Array: microarray capturing of exosomes and other extracellular vesicles for multiplexed phenotyping. *J Extracell Vesicles* 2.
117. Jorgensen, M. M., R. Baek, and K. Varming. 2015. Potentials and capabilities of the Extracellular Vesicle (EV) Array. *J Extracell Vesicles* 4:26048.
118. Regeczy, N., G. Gorog, and K. Paloczi. 2001. Developing an expert system for immunophenotypical diagnosis in immunodeficiency. Age-related reference values of peripheral blood lymphocyte subpopulations in Hungary. *Immunol Lett* 77:47-54.
119. Bisset, L. R., T. L. Lung, M. Kaelin, E. Ludwig, and R. W. Dubs. 2004. Reference values for peripheral blood lymphocyte phenotypes applicable to the healthy adult population in Switzerland. *Eur J Haematol* 72:203-212.
120. Crucian, B., M. Nelman-Gonzalez, and C. Sams. 2006. Rapid flow cytometry method for quantitation of LFA-1-adhesive T cells. *Clin Vaccine Immunol* 13:403-408.
121. Shimizu, Y. 2003. LFA-1: more than just T cell Velcro. *Nat Immunol* 4:1052-1054.
122. Letourneau, S., C. Krieg, G. Pantaleo, and O. Boyman. 2009. IL-2- and CD25-dependent immunoregulatory mechanisms in the homeostasis of T-cell subsets. *J Allergy Clin Immunol* 123:758-762.
123. Kuniyasu, Y., T. Takahashi, M. Itoh, J. Shimizu, G. Toda, and S. Sakaguchi. 2000. Naturally anergic and suppressive CD25(+)CD4(+) T cells as a functionally and phenotypically distinct immunoregulatory T cell subpopulation. *Int Immunol* 12:1145-1155.
124. Chen, X., J. J. Subleski, R. Hamano, O. M. Howard, R. H. Wiltrout, and J. J. Oppenheim. 2010. Co-expression of TNFR2 and CD25 identifies more of the functional CD4+FOXP3+ regulatory T cells in human peripheral blood. *Eur J Immunol* 40:1099-1106.
125. Ermann, J., P. Hoffmann, M. Edinger, S. Dutt, F. G. Blankenberg, J. P. Higgins, R. S. Negrin, C. G. Fathman, and S. Strober. 2005. Only the CD62L+ subpopulation of CD4+CD25+ regulatory T cells protects from lethal acute GVHD. *Blood* 105:2220-2226.
126. Dunham, R. M., B. Cervasi, J. M. Brenchley, H. Albrecht, A. Weintrob, B. Sumpter, J. Engram, S. Gordon, N. R. Klatt, I. Frank, D. L. Sodora, D. C. Douek, M. Paiardini, and G. Silvestri. 2008. CD127 and CD25 expression defines CD4+ T cell subsets that are differentially depleted during HIV infection. *J Immunol* 180:5582-5592.
127. Simonetta, F., A. Chiali, C. Cordier, A. Urrutia, I. Girault, S. Bloquet, C. Tanchot, and C. Bourgeois. 2010. Increased CD127 expression on activated FOXP3+CD4+ regulatory T cells. *Eur J Immunol* 40:2528-2538.
128. Walker, L. S., and D. M. Sansom. 2011. The emerging role of CTLA4 as a cell-extrinsic regulator of T cell responses. *Nat Rev Immunol* 11:852-863.
129. Dilek, N., N. Poirier, P. Hulin, F. Coulon, C. Mary, S. Ville, H. Vie, B. Clemenceau, G. Blancho, and B. Vanhove. 2013. Targeting CD28, CTLA-4 and PD-L1 costimulation differentially controls immune synapses and function of human regulatory and conventional T-cells. *PLoS One* 8:e83139.
130. Okazaki, T., and T. Honjo. 2006. The PD-1-PD-L pathway in immunological tolerance. *Trends Immunol* 27:195-201.
131. Kim, E. Y., J. J. Priatel, S. J. Teh, and H. S. Teh. 2006. TNF receptor type 2 (p75) functions as a costimulator for antigen-driven T cell responses in vivo. *J Immunol* 176:1026-1035.

132. Fleisher, T. A. 2013. Appendix 2: Laboratory reference values. In *Clinical Immunology: Principles and practice*, 4th ed. R. R. Rich, T. A. Fleisher, W. T. Shearer, H. Schroeder, A. J. Frew, and C. M. Weyond, eds. Elsevier, Maryland Heights, MO.
133. Hulspas, R., M. R. O'Gorman, B. L. Wood, J. W. Gratama, and D. R. Sutherland. 2009. Considerations for the control of background fluorescence in clinical flow cytometry. *Cytometry B Clin Cytom* 76:355-364.
134. Nimmerjahn, F., and J. V. Ravetch. 2007. Fc-receptors as regulators of immunity. *Adv Immunol* 96:179-204.
135. Swiatek-de Lange, M., W. Rist, H. F. Stahl, A. Weith, and M. C. Lenter. 2008. Comment on "MHC class II expression identifies functionally distinct human regulatory T cells". *J Immunol* 180:3625; author reply 3626.
136. Baecher-Allan, C., and D. A. Hafler. 2008. Response to Comment on "MHC Class II Expression Identifies Functionally Distinct Human Regulatory T Cells". *J Immunol* 180:3626.
137. Cheadle, W. G., M. J. Hershman, S. R. Wellhausen, and H. C. Polk, Jr. 1991. HLA-DR antigen expression on peripheral blood monocytes correlates with surgical infection. *Am J Surg* 161:639-645.
138. Filion, L. G., C. A. Izaguirre, G. E. Garber, L. Huebsh, and M. T. Aye. 1990. Detection of surface and cytoplasmic CD4 on blood monocytes from normal and HIV-1 infected individuals. *J Immunol Methods* 135:59-69.
139. Delirezh, N., E. Shojaeefar, P. Parvin, and B. Asadi. 2013. Comparison the effects of two monocyte isolation methods, plastic adherence and magnetic activated cell sorting methods, on phagocytic activity of generated dendritic cells. *Cell J* 15:218-223.
140. Sada-Ovalle, I., A. Talayero, L. Chavez-Galan, L. Barrera, A. Castorena-Maldonado, A. Soda-Merhy, and L. Torre-Bouscoulet. 2012. Functionality of CD4+ and CD8+ T cells from tonsillar tissue. *Clin Exp Immunol* 168:200-206.
141. Daubeuf, S., M. A. Lindorfer, R. P. Taylor, E. Joly, and D. Hudrisier. 2010. The direction of plasma membrane exchange between lymphocytes and accessory cells by trogocytosis is influenced by the nature of the accessory cell. *J Immunol* 184:1897-1908.
142. Daubeuf, S., A. L. Puaux, E. Joly, and D. Hudrisier. 2006. A simple trogocytosis-based method to detect, quantify, characterize and purify antigen-specific live lymphocytes by flow cytometry, via their capture of membrane fragments from antigen-presenting cells. *Nat Protoc* 1:2536-2542.
143. Hudrisier, D., A. Aucher, A. L. Puaux, C. Bordier, and E. Joly. 2007. Capture of target cell membrane components via trogocytosis is triggered by a selected set of surface molecules on T or B cells. *J Immunol* 178:3637-3647.
144. Liu, H., M. Rhodes, D. L. Wiest, and D. A. Vignali. 2000. On the dynamics of TCR:CD3 complex cell surface expression and downmodulation. *Immunity* 13:665-675.
145. San Jose, E., A. Borroto, F. Niedergang, A. Alcover, and B. Alarcon. 2000. Triggering the TCR complex causes the downregulation of nonengaged receptors by a signal transduction-dependent mechanism. *Immunity* 12:161-170.
146. Peters, P. J., J. J. Neefjes, V. Oorschot, H. L. Ploegh, and H. J. Geuze. 1991. Segregation of MHC class II molecules from MHC class I molecules in the Golgi complex for transport to lysosomal compartments. *Nature* 349:669-676.
147. Choi, D. S., D. K. Kim, Y. K. Kim, and Y. S. Gho. 2013. Proteomics, transcriptomics and lipidomics of exosomes and ectosomes. *Proteomics* 13:1554-1571.

148. Choi, D. S., D. Y. Choi, B. S. Hong, S. C. Jang, D. K. Kim, J. Lee, Y. K. Kim, K. P. Kim, and Y. S. Gho. 2012. Quantitative proteomics of extracellular vesicles derived from human primary and metastatic colorectal cancer cells. *J Extracell Vesicles* 1.
149. Bernardo, D., H. O. Al-Hassi, E. R. Mann, C. T. Tee, A. U. Murugananthan, S. T. Peake, A. L. Hart, and S. C. Knight. 2012. T-cell proliferation and forkhead box P3 expression in human T cells are dependent on T-cell density: physics of a confined space? *Hum Immunol* 73:223-231.
150. Fife, B. T., and J. A. Bluestone. 2008. Control of peripheral T-cell tolerance and autoimmunity via the CTLA-4 and PD-1 pathways. *Immunol Rev* 224:166-182.
151. Peiser, M., A. Becht, and R. Wanner. 2007. Antibody blocking of MHC II on human activated regulatory T cells abrogates their suppressive potential. *Allergy* 62:773-780.
152. Curran, M. A., W. Montalvo, H. Yagita, and J. P. Allison. 2010. PD-1 and CTLA-4 combination blockade expands infiltrating T cells and reduces regulatory T and myeloid cells within B16 melanoma tumors. *Proc Natl Acad Sci U S A* 107:4275-4280.
153. Hall, B. M., N. D. Verma, G. T. Tran, and S. J. Hodgkinson. 2011. Distinct regulatory CD4+T cell subsets; differences between naive and antigen specific T regulatory cells. *Curr Opin Immunol* 23:641-647.
154. Sawant, D. V., and D. A. Vignali. 2014. Once a Treg, always a Treg? *Immunol Rev* 259:173-191.
155. Hoeppli, R. E., D. Wu, L. Cook, and M. K. Levings. 2015. The environment of regulatory T cell biology: cytokines, metabolites, and the microbiome. *Front Immunol* 6:61.
156. Kedl, R. M., B. C. Schaefer, J. W. Kappler, and P. Marrack. 2002. T cells down-modulate peptide-MHC complexes on APCs in vivo. *Nat Immunol* 3:27-32.
157. Lanzavecchia, A. 2002. Lack of fair play in the T cell response. *Nat Immunol* 3:9-10.
158. Zhang, L., J. N. Manirarora, and C. Wei. 2014. Evaluation of immunosuppressive function of regulatory T cells using novel in vitro cytotoxicity assay. *Cell and Bioscience* 4.
159. Okoye, I. S., S. M. Coomes, V. S. Pelly, S. Czieso, V. Papayannopoulos, T. Tolmachova, M. C. Seabra, and M. S. Wilson. 2014. MicroRNA-containing T-regulatory-cell-derived exosomes suppress pathogenic T helper 1 cells. *Immunity* 41:89-103.

CHAPTER 7. APPENDICES

7.1. APPENDIX A - ADDITIONAL SCIENTIFIC WORK

A1 - Poster presentations

2013: HUPO 12th Annual World Congress, Yokohama Japan

Poster title: Phenotyping of extracellular vesicles from human monocyte-derived dendritic cells

2012: Forskningens Dag, arranged by Region Nordjylland, Aalborg University Hospital

Poster title: Funktionelle aspekter af MHC klasse II molekyler på humane T celler

A2 - Conference publications

Evo K.L. Søndergaard, Lotte H. Pugholm, Rikke Bæk, **Anne Louise S. Revenfeld**, Kim Varming, Malene M. Jørgensen (2015): "Extensive analysis of four ovarian cancer cell lines and their production of extracellular vesicles during normoxic and hypoxic conditions". *Journal of Extracellular Vesicles*, 4, 27783.

Anne Louise Revenfeld, Allan Stensballe, Malene Jørgensen, Rikke Bæk, Kim Varming (2014): "Extensive phenotyping of extracellular vesicles of extracellular vesicles from mono- and co-cultures of human dendritic cells and allogeneic CD4+ T cells". *Journal of Extracellular Vesicles*, 3, 24214.

Rikke Bæk, Malene Jørgensen, Evo K.L. Søndergaard, Lotte H. Pugholm, **Anne Louise S. Revenfeld**, Kim Varming (2014): "Preanalytical treatment of blood samples prior to phenotyping by EV Array". *Journal of Extracellular Vesicles*, 3, 24214.

A3 - Oral Presentations

2014, 3rd International Society for Extracellular Vesicles (ISEV), Rotterdam, Netherlands

Title: Extensive phenotyping of extracellular vesicles from mono- and co-cultures of dendritic cells and allogeneic CD4+ T cells

2014, Annual Meeting, Danish Society for Clinical Immunology, Middelfart, Denmark

Title: Funktionelle aspekter af MHC klasse II molekyler på T celler

2012, PhD seminar, Aalborg University

Title: Functional aspects of MHC class II molecules on T cells

2011, University of British Colombia, Department of Biochemistry and Molecular Biology

Title: Functional aspects of MHC class II molecules on T cells

7.2. APPENDIX B - MANUSCRIPTS INCLUDED IN THE THESIS

B1 - Manuscript 1

Revenfeld, A.L.S, Steffensen, R., Pugholm, L. H., Stensballe, A., Jørgensen, M.M, Varming, K. (2015): The existence of HLA-DR on circulating CD4+ T cells cannot be explained by a concurrent presence of *HLA-DRB1* expression. BMC Immunology. Accepted with revisions.

B2 - Manuscript 2

Revenfeld, A.L.S, Varming, K., Jørgensen, M.M, Stensballe, A.: Phenotypic characterization of extracellular vesicles and CD4+ HLA-DR+ responder T cells following contact-dependent and –independent allogeneic MLC. Journal of Leukocyte Biology. In preparation.

B3 - Manuscript 3

Revenfeld, A.L.S., Bæk, R., Nielsen, M. H., Stensballe, A., Varming, K., Jørgensen, M. (2014): *Diagnostic and prognostic potential of extracellular vesicles in peripheral blood*. Clin Ther; 36, 6, pp. 830-46.

B4 - Manuscript 4

Revenfeld, A.L.S., Søndergaard, E.K.L., Stensballe, A., Bæk, R., Jørgensen, M.M, Varming, K. (2015): *Characterization of a cell culturing system for the study of contact-independent vesicle communication. Journal of Extracellular Vesicles.* Submitted

B1 - Manuscript 1

Title: The existence of HLA-DR on circulating CD4+ T cells cannot be explained by a concurrent presence of *HLA-DRB1* expression

Anne LS Revenfeld[1§], Rudi Steffensen[1], Lotte H Pugholm[1], Malene M Jørgensen[1], Allan Stensballe[2], Kim Varming[1]

[1]Department of Clinical Immunology, Aalborg University Hospital, Urbansgade 34-36, 9000 Aalborg, Denmark

[2]Laboratory for Medical Mass Spectrometry, Department of Health Science and Technology, Aalborg University, Fredrik Bajersvej 7E, 9100 Aalborg, Denmark

[§]Corresponding author

Email addresses:

ALSR: anlor@rn.dk

RS: rns@rn.dk

LHP: lohap@rn.dk

MMJ: maljoe@rn.dk

AS: as@hst.aau.dk

KV: kv@rn.dk

Abstract

Background

The human major histocompatibility complex class II (MHCII) isotype HLA-DR is an activation marker for T cells. However, whether an endogenous protein expression or a molecular acquisition accounts for the presence of HLA-DR on T cells remains undetermined and controversial.

Results

Using human T cells from peripheral blood, we compared several aspects of the presence of the HLA-DR protein to the presence of mRNA for *HLA-DRB1*. Using an optimized flow cytometry setup, we determined that the HLA-DR observed on CD4+ T cells is almost exclusively membrane-associated, while for autologous CD19+ B cells, the protein could be located in the membrane as well as in the cytoplasm. In addition, negligible expression levels of *HLA-DRB1* were found in CD4+ T cells, using an allele-specific qPCR assay. Finally, the presence of HLA-DR was not confined to activated CD4+ and CD8+ T cells, as evaluated by the co-expression of CD25.

Conclusions

The functional role of the HLA-DR molecule on T cells remains enigmatic, however, this study presents evidence showing that HLA-DR on CD4+ T cells in peripheral blood could not be explained by the simultaneous presence of an endogenous protein synthesis. Although an inducible endogenous protein expression cannot be excluded, our findings suggest a more pronounced role for HLA-DR on T cells than simply as an activation marker.

Background

It has been observed for more than four decades that T cells in peripheral blood can present MHC class II (MHCII) molecules on their surface and that the number of MHCII+ T cells increases upon activation [1-4]. In line with this, one of the three human MHCII isotypes, called HLA-DR, is frequently used as a T cell activation marker along with other molecules, such as CD69 and CD25 [5-8]. Nonetheless, the functional role and significance of HLA-DR on human T cells is not fully determined and the unequivocal confirmation of an endogenous expression or a protein acquisition from other immune cells is absent. The constitutive expression of HLA-DR is limited to a few cell types, collectively called APCs [9, 10]. These cells use HLA-DR to present antigenic peptides to CD4+ T cells and consequently HLA-DR is involved in many facets of immune homeostasis such as T cell activation, peripheral tolerance, and induction of apoptosis [11].

Since the first observations of HLA-DR on T cells in the late 1970's, a number of studies have investigated aspects of the HLA-DR molecule in this particular context. Though still a subject of discussion, the general understanding is that the presence of this protein complex can be explained by either of two scenarios. The first involves an inducible *de novo*, endogenous protein synthesis, while the other encompasses a molecular acquisition from adjacent cells by currently unverified mechanisms. The studies supporting the former explanation have investigated several of the components involved in HLA-DR expression, transport, and function, including lysosomal proteases [12], antigen presentation [13, 14], and engagement of CIITA [9, 12, 15], which is reported as the master regulator of *HLA-DR* expression [16-19]. Mouse T cells do not produce MHCII, which has been explained by a lack of CIITA expression [20]. However, even when CIITA is absent, MHCII expression is still observed for several cell types [21, 22]. The second phenomenon explaining HLA-DR on T cells is investigated in several other studies, demonstrating a transfer of a fully functional protein complex from APCs [23, 24]. In accordance with this, the MHCII observed on mouse T cells is a result of an acquisition from APCs [25-27]. In addition, a number of studies have found that activated rat T cells can both synthesize and absorb MHCII molecules from adjacent cells [28-30]. The transfer of HLA-DR to human T cells has also been reported [31, 32], but a possible link between this acquisition and a potential endogenous expression of HLA-DR remains to be investigated.

Our study aimed to investigate the presence of HLA-DR in human T cells from two perspectives: At the protein level and at the transcriptional level. This was carried out to further elucidate whether an endogenous expression of HLA-DR is present in human CD4+ T cells in peripheral blood from healthy individuals. For the protein analysis, a stringent flow cytometry setup was applied to allow for unbiased identification of HLA-DR+ cells. A novel qPCR assay was developed to investigate the mRNA expression of a specific *HLA-DRB1* allele, thus minimizing the homology issues otherwise associated with analysis the *HLA-DR* genes. Though an inducible, endogenous expression cannot be excluded, the cumulative results show that HLA-

DR on CD4+ T cell in peripheral blood could not be explained by a concurrent presence of an active protein synthesis.

Results

Identification of HLA-DR in the membrane and intracellular compartment of CD3+ T cells

We initially wanted to investigate the cellular distribution of the HLA-DR antigen both in the membrane (HLA-DR mem) and in the intracellular space (HLA-DR IC) of CD3+ T cells by using flow cytometry. An initial staining of HLA-DR mem was followed by fixation, permeabilization of the cellular membrane, and a secondary staining of HLA-DR IC. To separate the two HLA-DR signals, two anti-HLA-DR antibodies of the same clone, but with different fluorophores-conjugations, were applied (anti-HLA-DR mem AF488; anti-HLA-DR IC AF647). The distribution of HLA-DR mem and HLA-DR IC in CD3+T cells was compared to the distribution in CD19+ B cells, since the HLA-DR expression pattern in this APC is well characterized. To identify the HLA-DR mem and HLA-DR IC positive events, the Fluorescence Minus One (FMO)[33] approach was applied (Figure 1). This approach is very useful for resolving weakly stained cells in multicolor panels in flow cytometry analyses [34, 35]. The applied FMO included a tube containing all markers and replacing the HLA-DR antibody of interest with an isotype control antibody. In this way, the HLA-DR single and double positive events could be determined, as exemplified in Figure 1.

Dimorphic distribution of HLA-DR in the membrane and intracellular compartment of CD3+ T cells and CD19+ B cells

Based on the abovementioned staining and gating strategy, we identified the fraction of CD3+ T cells from peripheral blood in which HLA-DR could be found in either the membrane or the intracellular compartment or in both. An identical procedure was carried out for autologous CD19+ B cells, to ensure a positive reference. A summary of these findings can be found in Table 2. From here it can be seen that the presence of HLA-DR mem on CD3+ T cells and CD19+ B cells differed significantly in terms of the percent-wise distribution. Moreover, the corresponding median fluorescence intensity (MFI) values were also markedly different with a nearly 14 times greater MFI value detected for the CD19+ B cells than the equivalent value for the CD3+ T cells. A similar tendency was also observed for the presence of HLA-DR IC. Here, the MFI for HLA-DR IC in the CD19+ B cells was approximately 5.5-fold higher compared to the MFI for the CD3+ T cells. To investigate whether the T cells, which presented membrane-associated HLA-DR to the greatest extent, also carried the largest amount of HLA-DR IC, a correlation for HLA-DR in the two compartments was made. This revealed that a positive correlation between these two proteins existed, both for CD3+ T cells and CD19+ B cells (Figure 2), with corresponding Pearson correlation coefficients of 0.73 ± 0.03 and 0.41 ± 0.03, respectively.

To validate the findings for HLA-DR mem and HLA-DR IC it was important to ensure than an initial saturation of HLA-DR mem had been obtained with the applied antibody. Hence, a saturation control was included in which all antibodies and

staining conditions were applied, only omitting the permeabilization agent. Consequently, the HLA-DR IC signal should be absent in this sample if both the HLA-DR mem staining had saturated all membrane-associated HLA-DR and no HLA-DR IC antibody entered the cell. As a general feature, a small HLA-DR IC signal could be detected in the saturation control for both the CD3+ HLA-DR mem+ T cells and CD19+ HLA-DR mem+ B cells (Figure 3). However, for the CD3+ T cells, this signal never surpassed the HLA-DR IC signal from the fully stained sample (Figure 3B) or the one in the FMO control (Figure 3A). For the CD19+ B cells, the HLA-DR IC signal in the saturation control was slightly greater than the one detected in the FMO control (Figure 3A), but was sufficiently separated from the HLA-DR IC signal observed for the fully stained sample (Figure 3A and 3B). A doubling of the applied amount of both HLA-DR antibodies did not increase or decrease the recorded intensities and cellular distributions of these markers (data not shown).

As a final investigation, the antibody staining procedure applied in the flow cytometric analysis was tested in a confocal microscopy setting. The purpose of this qualitative analysis was to visualize the separation of the fluorescence signals obtained, when targeting HLA-DR mem and HLA-DR IC with two different anti-HLA-DR antibodies. In contrast to the flow cytometric analysis, in which CD3+ T cells and CD19+ B cells from peripheral blood were the target cells, isolated CD4+ T cells and CD19+ B cells were used for the confocal microscopy investigation. With these cells it was shown that CD4+ T cells presenting HLA-DR mem could be identified (Figure 4, top panel). In contrast, CD4+ T cells presenting both HLA-DR mem and HLA-DR IC were almost absent (Additional Figure 1). To ensure that the observed HLA-DR signals in the CD4+ T cell population were not due to contaminating APCs, such as monocytes, the identification of these T cells included a CD3 antibody. For the CD19+ B cells, the HLA-DR proteins were present in both the membrane and intracellular compartment of the entire cell population (Figure 4, bottom panel). The purity of the isolated CD4+ T cells and CD19+ B cells was 97.6% ± 2.2 and 96.6% ± 0.4, respectively, as determined by flow cytometry (n=2; data not shown).

Relative contribution of CD4+ and CD8+ T cells to CD3+ HLA-DR mem+ T cell subset

In addition to the results about the presence of HLA-DR mem and HLA-DR IC for CD3+ T cells, it was investigated to which extent CD4+ and CD8+ T cells each contribute to the CD3+ HLA-DR mem+ subset. Accordingly, CD3+ CD4+ HLA-DR mem+ and CD3+ CD8+ HLA-DR mem+ T cells (hereafter referred to as CD4+ HLA-DR mem+ and CD8+ HLA-DR mem+ T cells) were identified in a flow cytometric analysis of PBMCs. The presence of HLA-DR mem was evaluated for these cells (Figure 5A, left panel) by using the FMO approach described in Figure 1. This resulted in the detection of 8.9% ± 1.6 CD4+ HLA-DR mem+ T cells and 18.7% ± 3.1 CD8+ HLA-DR mem+ T cells (n=6). Since the CD4/CD8 ratio in peripheral blood is approximately 2 for adults [36, 37], the CD4+ and CD8+ T cells each contributed roughly equally to the entire CD3+ HLA-DR mem+ T cell population.

To further characterize the HLA-DR mem-presenting CD4+ and CD8+ T cells, the co-expression of another T cell activation marker, CD25, was also investigated for these cells. Of the CD4+ HLA-DR mem+, 22.8% ± 2.3 co-expressed CD25 (Figure 5A, right panel). Additionally, CD25 was enriched in the CD4+ HLA-DR mem+ population, when compared to the corresponding CD4+ HLA-DR mem- population, for which the expression of CD25 was 12.7% ± 1.2 (Figure 5B). In contrast, the CD25 expression was greatest in the HLA-DR mem- subset of the CD8+ T cells (3.5% ± 0.8) as compared to the CD8+ HLA-DR mem+ T cells (1.3% ± 0.3).

Contrasting expression profiles of *HLA-DRB1* mRNA in CD4+ T cells and CD19+ B cells

In order to link the presence of the HLA-DR protein in T cells to its transcription, an investigation of the *HLA-DRB1* mRNA expression was performed. For this investigation, a set of primers for a qPCR assay were designed to target the transcripts of the *HLA-DRB1*03* allele (Table 1). To ensure that only the desired target was amplified, the *HLA-DRB1*03*-specific assay was initially tested on a panel of PBMCs from 13 individuals with *HLA-DRB1* alleles representative of the major DR haplotypes [38](data not shown). Accordingly, the *HLA-DRB1*03* positive individuals were selected, when they had either the homozygous *HLA-DRB1*03* genotype or the heterozygous *HLA-DRB1*03/*15* genotype. For the *HLA-DRB1*03* negative samples, individuals with either the homozygous *HLA-DRB1*15* genotype or the heterozygous *HLA-DRB1*01/*07* were selected.

Subsequently, the expression pattern of *HLA-DRB1*03* was determined for human, isolated CD4+ T cells and CD19+ B cells from peripheral blood. As for the flow cytometric analysis of HLA-DR mem and HLA-DR IC, the CD19+ B cells were included as a positive control. The qPCR analysis was performed with cells from individuals with either a positive or a negative *HLA-DRB1*03* genotype, as indicated on the section above. The results of the expression analysis are displayed in Figure 6A. The difference, which was observed between CD4+ T cells and CD19+ B cells with an *HLA-DRB1*03* positive genotype, corresponded to a 240-fold higher transcript quantity in the B cells. No detectable signal was obtained for the CD4+T cells with an *HLA-DRB1*03* negative genotype. In contrast, two of the five corresponding CD19+ B cell samples produced a detectable signal, yielding normalized expression values in a similar range as those for the CD4+ T cells from the *HLA-DRB1*03* positive individuals (Figure 6B). The corresponding Ct values were 37.18 ± 0.17 (n=2) and 36.20 ± 0.52 (n=5), respectively.

As evaluated by flow cytometry, the purity of the isolated CD4+ T cells was 98.8% ± 0.37 (n=10; data not shown). Moreover, the presence of a cellular contamination, which could contribute to the detected mRNA signal in the CD4+ T cells from the *HLA-DRB1*03* positive individuals, was also investigated. First, the amount of mRNA for *CD19* was evaluated by qPCR (Figure 6C). This B cell differentiation marker was included since B cells constitute the largest *HLA-DRB1*-expressing population in PBMCs, thus encompassing the greatest source of a possible cellular contamination. The *CD19* transcripts were approximately 1500 times more abundant

in the CD19+ B cell samples compared to the CD4+ T cell samples, regardless of *HLA-DRB1*03* genotype. Secondly, the presence of CD14+ monocytes was also assessed by flow cytometry. For the investigated samples, 0.97% ± 0.10 CD4+ CD14+ cells could be detected (n=8; all the *HLA-DRB1*01* positive donors were included).

Discussion

The presence of HLA-DR antigens on T cells has been observed for more than four decades. The expression pattern and functionality of HLA-DR is well described for APCs but in the context of T cells, many unidentified aspects still remain. With the use of a stringent staining and gating strategy for flow cytometry, this study investigated the distribution of HLA-DR in the cellular membrane (HLA-DR mem) and intracellular compartment (HLA-DR IC) of human CD3+ T cells from peripheral blood. As a positive reference, this distribution was compared to that of autologous CD19+ B cells. We hypothesized that if the cell of question contained the functional protein in both the membrane and intracellular compartment it was likely that an endogenous protein expression existed.

The flow cytometric analysis identified that approximately 18% of CD3+ T cells from peripheral blood contained HLA-DR mem (Table 2). Other studies, which investigate HLA-DR on T cells, generally report a smaller amount of HLA-DR mem+ T cells. However, these reports range widely from less than 5% [36, 37] to approximately 10% [5], but also above 15% [39, 40]. An inherent challenge of flow cytometry is to separate the true positive events from the background, especially for low-density markers. Such a case favors the use of an FMO-approach [41], thus minimizing user specific bias in the gating process. This approach was used in the present study with a consequent more accurate determination of the HLA-DR mem+ T cells than previously demonstrated. The identification of a uniformly HLA-DR mem-expressing, autologous B cell population validated the applied strategy. While only a few percent of all CD3+ T cells in peripheral blood contained HLA-DR IC, all the autologous CD19+ B cells were HLA-DR IC+ (Table 2), yet again confirming their constitutive HLA-DR expression. A positive correlation between HLA-DR mem and HLA-DR IC was observed for both CD3+ T cells and CD19+ B cells (Figure 2). However, not all CD3+ HLA-DR mem+ T cells were also HLA-DR IC+ (Table 2), which could be expected if an active protein synthesis was present.

Additional analyses revealed that CD4+ and CD8+ T cells each account for approximately 50% of the entire CD3+ HLA-DR mem+ subset in peripheral blood. Notably, HLA-DR mem was twice as enriched in the CD8+ T cells (~19% of total CD8+ population), when compared to the CD4+ T cells (~9% of total CD4+ population). Also, the presence of HLA-DR mem was seemingly not confined to activated CD4+ and CD8+ T cells, as evaluated by a co-expression CD25 (Figure 5). More than 20% of the CD4+ HLA-DR mem+ T cells co-expressed CD25, while the expression of CD25 by the CD8+ HLA-DR mem+ T cell was minimal, as observed by others [42]. In addition, the CD4+ T cells with the highest density of HLA-DR mem were also the cells with the greatest CD25 expression (Figure 5B). Although both CD4+ HLA-DR mem+ [3, 43] and CD8+ HLA-DR mem+ T cells [42] found in peripheral blood have been associated with regulatory functions, the difference in the expression of CD25 presented in this study could indicate distinct functionalities of these two cellular subsets. This relates to the observation that CD25 expression is an essential feature for regulatory CD4+ T cells, which are often identified by a CD25high phe-

notype [3, 43-45]. However, further investigations are required to substantiate this hypothesis.

In order to investigate the link between the presence of the HLA-DR protein on T cells to an endogenous expression, a transcriptional analysis of *HLA-DRB1* was performed, using a novel qPCR assay. The assay targeted a specific allele of the most prevalently expressed beta subunit of the heterodimeric HLA-DR protein, namely the beta 1 (B1) chain. For the specific allele, we chose *HLA-DRB1*03*, which is a part of the DR52 haplotype (*HLA-DRB1*03, *11, *12, *13, and *14)*[38]. The amount of *HLA-DRB1* transcripts in this haplotype is the most abundant, compared to other haplotypes [46], making it a plentiful and advantageous target. By choosing to target only one allele, it was intended to circumvent the issues associated with the extensive homology of the *HLA-DR* genes, thus providing unambiguous expression results. Whereas the protein analyses mainly focused on the entire CD3+ T cell population in peripheral blood, the qPCR centered on isolated CD4+ T cells. Hence, the basis of this investigation was a population of cells of which approximately 9% presented HLA-DR mem (Figure 5A).

With the qPCR of *HLA-DRB1*03* presented here, only minimal amounts of transcripts could be detected in the CD4+ T cells from *HLA-DRB1*03* positive individuals, while autologous CD19+ B cells clearly possessed an active gene transcription of *HLA-DRB1* (Figure 6A). To further assess the marginally positive *HLA-DRB1*03* mRNA signals for these CD4+ T cells, the results from the negative controls were evaluated. The CD4+ T cells from *HLA-DRB1*03* negative individuals did not yield any detectable signals. In contrast, for two out of the five corresponding CD19+ B cell samples all triplicates produced detectable signals, which were very similar to the *HLA-DRB1*03* positive CD4+ T cells (Figure 6B). Although much effort was put into ensuring the specificity of the applied qPCR assay, the signal from the *HLA-DRB1*03* negative CD19+ B cells illustrates that a small level of non-specificity is most likely inevitable. It was not expected that the *HLA-DRB1*03* negative CD4+ T cells could yield a similar non-specific signal, as these cells would not produce B cell-comparable amounts of *HLA-DRB1* transcripts, given the existence of such a production in the CD4+ T cells. Aside from these negative controls, it was imminent to assess the presence of a cellular contamination, which could have contributed with *HLA-DRB1*03* mRNA in the CD4+ T cell sample. The most abundant APC in peripheral blood is B cells. It is unlikely that these cells were present in the isolated CD4+ T cells, as evaluated in Figure 6C. Monocytes, however, are also known to express both HLA-DR [47] and CD4 [48] and could consequently also be isolated with the applied CD4+ positive selection kit. Approximately 1% of monocytes could be detected in the CD4+ T cell samples. Hence, it is plausible that these cells could have made a contribution to the *HLA-DRB1*03* mRNA in the relevant CD4+ T cell samples. In total, this suggests that the signal detected in the CD4+ T cells with an *HLA-DRB1*03* positive genotype could be non-specific or ascribed to a possible cellular contamination from APCs.

When correlated with the flow cytometric analysis of HLA-DR, the results from the qPCR assay signifies that the presence of HLA-DR on the surface of a rather constant-sized population of circulating CD4+ T cells in healthy individuals cannot be explained by a concomitant presence of an active gene expression. Even if the specific mRNA may have been partially degraded in the HLA-DR-presenting CD4+ T cells, it can be still be reasonably expected that these cells would give rise to a detectable *HLA-DRB1* mRNA signal, if an expression was present, as they constituted roughly 9% of the investigated cells. However, the results do not exclude the possibility that an inducible, endogenous expression of HLA-DR is present in these T cells. Nevertheless, this study showed tendencies for circulating HLA-DR-presenting CD4+ T cells in healthy individuals. These characteristics may be different for CD4+ HLA-DR mem+ T cells found in others tissues, such as in the lymph nodes, where elevated levels of HLA-DR-presenting T cells have been observed [40]. To support these theories and to fully appreciate the presence and dynamics of HLA-DR on human T cells, further analyses are required. These could include activated CD4+ T cells in lymphoid tissue, such as the palatine tonsils, or in individuals with constantly activated T cells, such as HIV-infected patients [49].

In terms of functionality, HLA-DR on T cells has mainly been associated with immunosuppressive signals, inducing either apoptosis or anergy in activated T cells [3, 50, 51]. However, reports about T cell activation can also be found [26, 32]. Nonetheless, it seems that the function of HLA-DR in APCs cannot simply be extrapolated to T cells. This is based on a number of observations from this and other studies. Here, clear differences were demonstrated for the presence of HLA-DR both at the protein and transcript level, when comparing CD4+ T cells to CD19+ B cells. Others describe how T cell-T cell and T cell-APC interactions have significantly different effects on the responder T cells. Although TCR involvement, and consequently also HLA-DR, and co-stimulatory molecules are present for both types of cellular interaction [50], the resulting cytokine production (IL-2 and IL-4) and Ca^{2+} influx differ [51-53]. Moreover, most T cell-T cell interactions seemingly result in the induction of anergy, further underlining these differences [50]. In relation to key features of APCs, the mechanism for antigen acquisition remains unidentified for T cells [12], while other studies have investigated other requirements of antigen presentation in these cells, including HLA-DM, CLIP, and proteolytic enzymes [12, 50]. Finally, the expression of essential co-stimulatory molecules, including CD80 and CD86, has been investigated. While some report an endogenous expression by T cells [50], others demonstrate an acquisition of functional molecules from APCs [32, 54, 55]. One of these studies demonstrated a simultaneous acquisition of HLA-DR by CD4+ T cells in a contact-dependent manner [32] but also a contact-independent transfer of HLA-DR has been shown [27]. Aside from underlining apparent differences between T cells and APC, related to HLA-DR and antigen-presentation, the phenomenon of intercellular transfer is very interesting from immunological point of view. It has been recognized that immune cells are particularly prone to engage in such molecular exchange, bestowing new functional phenotypes on the recipient cells [56-62]. This challenges the classical subdivision of immune cells, which is based on such functional phenotypes, and also expands the regulatory mechanisms of the immune system. In relation to HLA-DR, many studies have used allogeneic stimula-

tor cells to activate T cells, as part of a mixed lymphocyte culture (MLC), thereby inducing the presence of HLA-DR. However, if acquisition of HLA-DR and other molecules can occur in such a cell culture, it will have a major impact on future study design and interpretation of data and possibly also explain some of the contradictory results reported about HLA-DR in T cells to date [50]. Even though the results presented in this study could indicate that an intercellular protein transfer may account for the presence of HLA-DR on CD4+ T cells from peripheral blood, the exact mechanisms explaining HLA-DR on these T cells remain to be delineated.

Conclusions

In this study we further elucidated the presence of HLA-DR on human T cells. To the best of our knowledge, no study has to date investigated the direct *HLA-DRB1* expression in human CD4+ T and CD19+ B cells from peripheral blood and correlated it to the concurrent presence of HLA-DR antigens in the cell membrane and intracellular compartment. By doing so, observations about the presence of HLA-DR on T cells along with indications about its functionality can be obtained simultaneously. We observed that the HLA-DR present on CD4+ T cells from peripheral blood of healthy individuals is mainly membrane-associated. With the lack of *HLA-DRB1* mRNA expression in CD4+ T cells, it can reasonably be proposed that HLA-DR on CD4+ T cells in peripheral blood cannot be explained by the simultaneous presence of an active, endogenous protein synthesis. Moreover, HLA-DR-presentation by both CD4+ and CD8+ T cells was not confined to activated T cells. The collected data add more layers to the presence of HLA-DR on T cells, pointing to a redefinition of HLA-DR as a simple T cell activation marker.

Methods

Antibodies

The following conjugated antibodies were obtained from BD Biosciences (Mountainview, CA, USA): Anti-CD3-PE (SK7), anti-CD3-PerCP (SP34-2), anti-CD4-APC-H7 (SK3), anti-CD4-PE (RPA-T4), anti-CD8-PerCP (SK1), anti-CD8-PerCP-Cy5.5 (SK1), anti-CD14-PE-Cy7 (M5E2), anti-CD19-APC (HIB19), anti-CD19-PE (4G7), anti-CD19-PerCP-Cy5.5 (SJ25C1), anti-CD25-FITC (2A3), anti-HLA-DR-FITC (G46-6), mouse-IgG1-APC-H7 (X40), mouse-IgG1-FITC (MOPC-21), mouse-IgG2a-FITC (27-35), mouse IgG1-PE (MOPC-21), mouse-IgG2a-PE (MOPC-173), mouse IgG1-PerCP (MOPC-21), mouse IgG1-PerCP-Cy5.5 (MOPC-21), and mouse IgG1-PE-Cy7 (MOPC-21). From BD Biosciences, the unconjugated anti-CD3 (HIT3a) was also acquired. Anti-CD45-FITC (T29/33), anti-HLA-DR-PE (AB3), and mouse-IgG1-APC (DAK-GO1) were purchased from Dako A/S (Glostrup, DK). Anti-HLA-DR-Alexa Fluor (AF) 488 (L243), anti-HLA-DR-AF647 (L243), mouse-IgG2a-AF488 (MOPC-173), and mouse-IgG2a-AF647 (MOPC-173) were purchased from BioLegend (San Diego, CA, USA). Mouse-IgG1-PerCP-Cy5.5 (P3.6.2.8.1) was obtained from eBioscience (San Diego, CA, USA). The goat anti-mouse IgG-AF555 was purchased from Invitrogen (Life Technologies, Carlsbad, CA, USA).

Cells and isolation

Venous peripheral blood was obtained from healthy donors with known HLA types. The blood was collected in heparinized tubes (Vacuette®, Lithium Heparin, Greiner Bio One, DE). Isolation of PBMCs was accomplished by using Lymphoprep™ gradient centrifugation (Axis-Shield, Oslo, NO). The PBMCs were either used directly after the isolation or stored at -140 °C in a storage medium (RPMI 1640 (Gibco, Life Technologies), 40% heat-inactivated fetal calf serum (FCS) (Gibco), 10% DMSO (Merck Millipore, Darmstadt, Germany), 100 U/mL penicillin/10µg/mL streptomycin (Ampliqon, Odense, DK)). The CD4+ T cells were isolated from PBMCs using the Dynabeads® CD4 Positive Selection kit (Invitrogen) according to the manufacturer's guidelines. As an additional purification step, any residual B cells were removed from the isolated CD4+ T cells by positive selection, using Dynabeads® CD19 Pan B (Invitrogen). The purity of the isolated CD4+ T cells was evaluated by staining with fluorochrome-conjugated antibodies with subsequent flow cytometric analysis.

From the CD4+ depleted PBMCs, CD19+ B cells were isolated using the Dynabeads® Untouched™ Human B Cells kit (Invitrogen) according to the manufacturers guidelines.

Detection of membrane-bound and intracellular markers by flow cytometry

For the detection of membrane-bound and intracellular HLA-DR, $1x10^6$ PBMCs were stained with antibodies against CD3, CD19, HLA-DR (L243-AF488), or the corresponding isotype control antibodies (30 min, room temperature (RT)). Subse-

quently, 100 µl of Fixation Medium (reagent A) from FIX & PERM® Cell Fixation and Permeabilization Kit (Invitrogen) was added (15 min, RT). Following one wash with PBS (Gibco), a second antibody against HLA-DR (L243-AF647), or the corresponding isotype antibody, and 100 µl of Permeabilization Medium (reagent B) were added to the cells (20 min, RT). Finally, the cells were washed once with PBS prior to flow cytometric analysis. For the detection of membrane-bound HLA-DR on CD4+ and CD8+ T cells, the procedure only included the primary surface staining, using antibodies against CD3, CD4, CD8, CD25, and HLA-DR (L243-AF647).

The acquisition of stained cells was performed on a FACSCanto A using FACSDiva™ software (version 6.1.3, BD Biosciences). Calibration and compensation settings for the cytometer were obtained each day by using the 7-Color Setup Beads (BD Biosciences) and once a week with the FACSDiva™ CS&T Research Beads (BD Biosciences). The analysis of the data was carried out with the FlowJo software (version 10.0.7, FlowJo LLC, Ashland, OR, USA). Negative isotype controls were utilized to identify the positive events. The controls were either combined in a single tube or part of a "fluorescence minus one" (FMO) tube [33]. The median fluorescence intensity (MFI) was the statistical value of choice.

Detection of membrane-bound and intracellular HLA-DR by confocal microscopy

For all experiments, $1.5x10^5$ isolated CD4+ T cells or CD19+ B cells were left to adhere to poly-L-lysine coated slides (Sigma-Aldrich, St. Louis, MO, USA)(20 min, RT). The T cells were initially stained with anti-CD3 (HIT3a)(1:250; 45 min, RT), followed by incubation with secondary antibody (goat-anti-mouse IgG-AF555)(1:200; 45 min, RT). Slides were washed 3 times in PBS and cells were fixed in 2% paraformaldehyde (PFA)(Sigma-Aldrich)(15 min, RT). Both T and B cells were then stained with anti-HLA-DR-AF488 (L243)(1:100; 45 min, RT). Slides were washed 3 times in PBS and cells were fixed in 2% PFA (15 min, RT) followed by another round of washing and permeabilization with permeabilization buffer (1% bovine serum albumin (BSA)(Sigma-Aldrich), 0.1% saponin (Sigma-Aldrich), PBS)(8 min, RT). To visualize cytosolic HLA-DR, cells were subsequently stained with anti-HLA-DR-AF647 (L243)(1:100 in permeabilization buffer; 45 min, RT). Slides were washed 4 times in PBS and mounted with mounting medium (Sigma-Aldrich). Images were acquired on a Leica TCS SP5 confocal laser scanning microscope (Leica, Wetzlar, Germany). Images were processed using ImageJ (version 1.48, NIH, USA).

Total RNA extraction and cDNA synthesis

Total RNA was extracted from the isolated CD4+ T cells and CD19+ B cells by using the TRIzol extraction method (Invitrogen). The A260/A280 ratio was determined using a NanoDrop 1000 Spectrophotometer (Thermo Scientific, Waltham, MA, USA). Total cDNA for the quantitative PCR (qPCR) were generated from 1 µg total RNA from all samples using a mixture of poly-T and random primers with SuperScript VILO cDNA Synthesis Kit (Invitrogen) at a temperature profile of 25°C

for 10 min, 42°C for 60 min, and 85°C for 5 min according to the manufacturers guidelines.

Quantitative PCR

PCR primers for amplification of 57-136 base pairs gene-specific PCR products were used from conserved regions of the four studied genes (*HLA-DRB1*03*, *CD19*, *B2M*, and *GUSB*). Primers and FAM-labeled minor groove binder (MGB) TaqMan probes were used to detect the RNA expression level of the reference genes *B2M* and *GUSB* [67] and the target gene *HLA-DRB1*03* for which the *HLA-DRB1*03:01:01:01* mRNA sequence from the IMGT/HLA database was used as target sequence. Expression levels of *CD19* were detected using 20x probe assays mix (Life Technologies, USA). The information about primer and probe sequences are given in Table 1. The qPCR assay was applied to evaluate the gene expression profiles of the four genes and the data was analyzed using the QuantStudio 12K Flex system (Life Technologies, USA). The real-time PCR reactions were performed in a final volume of 25 µl, containing 1 µl cDNA solution, 12 µl Master Mix (TaqMan Universal PCR Master Mix, ABI, Darmstadt, Germany), 0.05 µM probe and 0.9 µM of forward and reverse primers. The PCR reaction for TaqMan gene expression assays contained 1 µl cDNA solution, 12 µl Master Mix and 1.25 µl TaqMan gene expression assay. Reactions were made up to a final volume of 25 µl with sterile water. All experiments were performed in triplicate and the real-time PCR protocol was as following: Denaturation by a hot start at 95°C for 10 min, followed by 50 cycles of a two-step program (denaturation at 95°C for 15 sec and annealing/extension at 60°C for 1 min). For all the included gene targets, only the threshold cycle (Ct) values below 40 were included in the subsequent data analysis. Gene expression of the target gene was normalized to the mean Ct of *B2M* and *GUSB* applying the formula $2^{-\Delta Ct}$, where ΔCt = Ct target gene – Ct reference genes.

Statistical analysis

The statistical analysis of data from both qPCR and flow cytometry experiments was performed using SigmaPlot (version 11, Systat Software Inc, San Jose, CA, USA). A paired or unpaired t-test was applied to test for differences between the groups of cells from the same individual or between two individuals, respectively. For non-normally distributed data, the corresponding non-parametric analysis was applied. Differences between groups were considered statistically significant, when $p < 0.05$. Unless otherwise specified, the data is presented as mean ± SEM.

List of abbreviations

APC: Antigen-presenting cell

CIITA: Class II trans-activator

CLIP: Class II-associated invariant chain peptide

Ct: Threshold cycle

CTLA-4: Cytotoxic T-lymphocyte-associated protein 4

FSC: Forward scatter

FMO: Fluorescence Minus One

HLA-DR: Human leukocyte antigen DR

HLA-DR IC: Human leukocyte antigen DR, intracellular

HLA-DR mem: Human leukocyte antigen DR, membrane-bound

IL: Interleukin

ICAM-1: Intercellular adhesion molecule 1

LFA-1: Lymphocyte function-associated antigen 1

MFI: Median fluorescence intensity

MHC: Major histocompatibility complex

MLC: Mixed lymphocyte culture

PBMC: Peripheral blood mononuclear cell

SSC: Side scatter

Competing interest

The authors declare that they have no competing interests.

Authors' contributions

ALSR designed, performed, and analyzed data from the flow cytometric analyses, qPCR, and confocal microscopy experiments and also drafted the manuscript. RS designed and performed the qPCR experiments and edited the manuscript. LHP performed the experimental procedures and the data analysis of the confocal microscopy and edited the manuscript. AS, MMJ, and KV contributed to the study design, supervised the study, and edited the manuscript. All authors read and approved the final version of the manuscript.

Acknowledgements

The authors thankfully acknowledge Dr. Svend Birkelund, Aalborg University for his invaluable help with the confocal microscopy experiments. We also thank technician Anne Elbæk, Department of Clinical Immunology, Aalborg Hospital, Denmark, for excellent technical assistance.

References

1. Evans RL, Faldetta TJ, Humphreys RE, Pratt DM, Yunis EJ, Schlossman SF: **Peripheral human T cells sensitized in mixed leukocyte culture synthesize and express Ia-like antigens.** *J Exp Med* 1978, **148:**1440-1445.
2. Ko HS, Fu SM, Winchester RJ, Yu DT, Kunkel HG: **Ia determinants on stimulated human T lymphocytes. Occurrence on mitogen- and antigen-activated T cells.** *J Exp Med* 1979, **150:**246-255.
3. Baecher-Allan C, Wolf E, Hafler DA: **MHC class II expression identifies functionally distinct human regulatory T cells.** *J Immunol* 2006, **176:**4622-4631.
4. Oshima S, Eckels DD: **Selective signal transduction through the CD3 or CD2 complex is required for class II MHC expression by human T cells.** *J Immunol* 1990, **145:**4018-4025.
5. Salgado FJ, Lojo J, Fernandez-Alonso CM, Vinuela J, Cordero OJ, Nogueira M: **Interleukin-dependent modulation of HLA-DR expression on CD4and CD8 activated T cells.** *Immunol Cell Biol* 2002, **80:**138-147.
6. Helft J, Jacquet A, Joncker NT, Grandjean I, Dorothee G, Kissenpfennig A, Malissen B, Matzinger P, Lantz O: **Antigen-specific T-T interactions regulate CD4 T-cell expansion.** *Blood* 2008, **112:**1249-1258.
7. Rea IM, McNerlan SE, Alexander HD: **CD69, CD25, and HLA-DR activation antigen expression on CD3+ lymphocytes and relationship to serum TNF-alpha, IFN-gamma, and sIL-2R levels in aging.** *Exp Gerontol* 1999, **34:**79-93.
8. Ferenczi K, Burack L, Pope M, Krueger JG, Austin LM: **CD69, HLA-DR and the IL-2R identify persistently activated T cells in psoriasis vulgaris lesional skin: blood and skin comparisons by flow cytometry.** *J Autoimmun* 2000, **14:**63-78.
9. Holling TM, van der Stoep N, Quinten E, van den Elsen PJ: **Activated human T cells accomplish MHC class II expression through T cell-specific occupation of class II transactivator promoter III.** *J Immunol* 2002, **168:**763-770.
10. Mach B, Steimle V, Martinez-Soria E, Reith W: **Regulation of MHC class II genes: lessons from a disease.** *Annu Rev Immunol* 1996, **14:**301-331.
11. Gotsman I, Sharpe AH, Lichtman AH: **T-cell costimulation and coinhibition in atherosclerosis.** *Circ Res* 2008, **103:**1220-1231.
12. Costantino CM, Ploegh HL, Hafler DA: **Cathepsin S regulates class II MHC processing in human CD4+ HLA-DR+ T cells.** *J Immunol* 2009, **183:**945-952.
13. Costantino CM, Spooner E, Ploegh HL, Hafler DA: **Class II MHC self-antigen presentation in human B and T lymphocytes.** *PLoS One* 2012, **7:**e29805.
14. Hewitt CR, Feldmann M: **Human T cell clones present antigen.** *J Immunol* 1989, **143:**762-769.
15. Wong AW, Ghosh N, McKinnon KP, Reed W, Piskurich JF, Wright KL, Ting JP: **Regulation and specificity of MHC2TA promoter usage in human primary T lymphocytes and cell line.** *J Immunol* 2002, **169:**3112-3119.
16. Harton JA, Ting JP: **Class II transactivator: mastering the art of major histocompatibility complex expression.** *Mol Cell Biol* 2000, **20:**6185-6194.
17. van den Elsen PJ, Peijnenburg A, van Eggermond MC, Gobin SJ: **Shared regulatory elements in the promoters of MHC class I and class II genes.** *Immunol Today* 1998, **19:**308-312.
18. Steimle V, Otten LA, Zufferey M, Mach B: **Complementation cloning of an MHC class II transactivator mutated in hereditary MHC class II deficiency (or bare lymphocyte syndrome).** *Cell* 1993, **75:**135-146.
19. Silacci P, Mottet A, Steimle V, Reith W, Mach B: **Developmental extinction of major histocompatibility complex class II gene expression in plasmocytes is**

mediated by silencing of the transactivator gene CIITA. *J Exp Med* 1994, **180:**1329-1336.
20. Chang CH, Hong SC, Hughes CC, Janeway CA, Jr., Flavell RA: **CIITA activates the expression of MHC class II genes in mouse T cells.** *Int Immunol* 1995, **7:**1515-1518.
21. Williams GS, Malin M, Vremec D, Chang CH, Boyd R, Benoist C, Mathis D: **Mice lacking the transcription factor CIITA--a second look.** *Int Immunol* 1998, **10:**1957-1967.
22. Arancibia-Carcamo CV, Osawa H, Arnett HA, Haskova Z, George AJ, Ono SJ, Ting JP, Streilein JW: **A CIITA-independent pathway that promotes expression of endogenous rather than exogenous peptides in immune-privileged sites.** *Eur J Immunol* 2004, **34:**471-480.
23. Umeshappa CS, Huang H, Xie Y, Wei Y, Mulligan SJ, Deng Y, Xiang J: **CD4+ Th-APC with acquired peptide/MHC class I and II complexes stimulate type 1 helper CD4+ and central memory CD8+ T cell responses.** *J Immunol* 2009, **182:**193-206.
24. Arnold PY, Davidian DK, Mannie MD: **Antigen presentation by T cells: T cell receptor ligation promotes antigen acquisition from professional antigen-presenting cells.** *Eur J Immunol* 1997, **27:**3198-3205.
25. Swartz TJ, Evavold B, Suzuki H, Yokoyama A, Quintans J: **Antigenicity of passively acquired major histocompatibility antigens on T cells.** *Transplantation* 1988, **46:**137-143.
26. Tsang JY, Chai JG, Lechler R: **Antigen presentation by mouse CD4+ T cells involving acquired MHC class II:peptide complexes: another mechanism to limit clonal expansion?** *Blood* 2003, **101:**2704-2710.
27. Nolte-'t Hoen EN, Buschow SI, Anderton SM, Stoorvogel W, Wauben MH: **Activated T cells recruit exosomes secreted by dendritic cells via LFA-1.** *Blood* 2009, **113:**1977-1981.
28. Patel DM, Arnold PY, White GA, Nardella JP, Mannie MD: **Class II MHC/peptide complexes are released from APC and are acquired by T cell responders during specific antigen recognition.** *J Immunol* 1999, **163:**5201-5210.
29. Patel DM, Dudek RW, Mannie MD: **Intercellular exchange of class II MHC complexes: ultrastructural localization and functional presentation of adsorbed I-A/peptide complexes.** *Cell Immunol* 2001, **214:**21-34.
30. Walker MR, Mannie MD: **Acquisition of functional MHC class II/peptide complexes by T cells during thymic development and CNS-directed pathogenesis.** *Cell Immunol* 2002, **218:**13-25.
31. Undale AH, van den Elsen PJ, Celis E: **Antigen-independent acquisition of MHC class II molecules by human T lymphocytes.** *Int Immunol* 2004, **16:**1523-1533.
32. Game DS, Rogers NJ, Lechler RI: **Acquisition of HLA-DR and costimulatory molecules by T cells from allogeneic antigen presenting cells.** *Am J Transplant* 2005, **5:**1614-1625.
33. Roederer M: **Spectral compensation for flow cytometry: visualization artifacts, limitations, and caveats.** *Cytometry* 2001, **45:**194-205.
34. Tung JW, Heydari K, Tirouvanziam R, Sahaf B, Parks DR, Herzenberg LA: **Modern flow cytometry: a practical approach.** *Clin Lab Med* 2007, **27:**453-468, v.
35. Hulspas R, O'Gorman MR, Wood BL, Gratama JW, Sutherland DR: **Considerations for the control of background fluorescence in clinical flow cytometry.** *Cytometry B Clin Cytom* 2009, **76:**355-364.
36. Regeczy N, Gorog G, Paloczi K: **Developing an expert system for immunophenotypical diagnosis in immunodeficiency. Age-related reference**

values of peripheral blood lymphocyte subpopulations in Hungary. *Immunol Lett* 2001, **77:**47-54.

37. Bisset LR, Lung TL, Kaelin M, Ludwig E, Dubs RW: **Reference values for peripheral blood lymphocyte phenotypes applicable to the healthy adult population in Switzerland.** *Eur J Haematol* 2004, **72:**203-212.
38. Handunnetthi L, Ramagopalan SV, Ebers GC, Knight JC: **Regulation of major histocompatibility complex class II gene expression, genetic variation and disease.** *Genes Immun* 2010, **11:**99-112.
39. Fleisher TA: **Appendix 2: Laboratory reference values.** In *Clinical Immunology: Principles and practice.* 4th edition. Edited by Rich RR, Fleisher TA, Shearer WT, Schroeder H, Frew AJ, Weyond CM. Maryland Heights, MO: Elsevier; 2013
40. Amlot PL, Tahami F, Chinn D, Rawlings E: **Activation antigen expression on human T cells. I. Analysis by two-colour flow cytometry of umbilical cord blood, adult blood and lymphoid tissue.** *Clin Exp Immunol* 1996, **105:**176-182.
41. Herzenberg LA, Tung J, Moore WA, Parks DR: **Interpreting flow cytometry data: a guide for the perplexed.** *Nat Immunol* 2006, **7:**681-685.
42. Arruvito L, Payaslian F, Baz P, Podhorzer A, Billordo A, Pandolfi J, Semeniuk G, Arribalzaga E, Fainboim L: **Identification and clinical relevance of naturally occurring human CD8+HLA-DR+ regulatory T cells.** *J Immunol* 2014, **193:**4469-4476.
43. Peiser M, Becht A, Wanner R: **Antibody blocking of MHC II on human activated regulatory T cells abrogates their suppressive potential.** *Allergy* 2007, **62:**773-780.
44. Chen X, Oppenheim JJ: **The phenotypic and functional consequences of tumour necrosis factor receptor type 2 expression on CD4(+) FoxP3(+) regulatory T cells.** *Immunology* 2011, **133:**426-433.
45. Dilek N, Poirier N, Hulin P, Coulon F, Mary C, Ville S, Vie H, Clemenceau B, Blancho G, Vanhove B: **Targeting CD28, CTLA-4 and PD-L1 costimulation differentially controls immune synapses and function of human regulatory and conventional T-cells.** *PLoS One* 2013, **8:**e83139.
46. Vincent R, Louis P, Gongora C, Papa I, Clot J, Eliaou JF: **Quantitative analysis of the expression of the HLA-DRB genes at the transcriptional level by competitive polymerase chain reaction.** *J Immunol* 1996, **156:**603-610.
47. Cheadle WG, Hershman MJ, Wellhausen SR, Polk HC, Jr.: **HLA-DR antigen expression on peripheral blood monocytes correlates with surgical infection.** *Am J Surg* 1991, **161:**639-645.
48. Filion LG, Izaguirre CA, Garber GE, Huebsh L, Aye MT: **Detection of surface and cytoplasmic CD4 on blood monocytes from normal and HIV-1 infected individuals.** *J Immunol Methods* 1990, **135:**59-69.
49. Dunham RM, Cervasi B, Brenchley JM, Albrecht H, Weintrob A, Sumpter B, Engram J, Gordon S, Klatt NR, Frank I, et al: **CD127 and CD25 expression defines CD4+ T cell subsets that are differentially depleted during HIV infection.** *J Immunol* 2008, **180:**5582-5592.
50. Holling TM, Schooten E, van Den Elsen PJ: **Function and regulation of MHC class II molecules in T-lymphocytes: of mice and men.** *Hum Immunol* 2004, **65:**282-290.
51. Taams LS, van Eden W, Wauben MH: **Antigen presentation by T cells versus professional antigen-presenting cells (APC): differential consequences for T cell activation and subsequent T cell-APC interactions.** *Eur J Immunol* 1999, **29:**1543-1550.
52. Lombardi G, Hargreaves R, Sidhu S, Imami N, Lightstone L, Fuller-Espie S, Ritter M, Robinson P, Tarnok A, Lechler R: **Antigen presentation by T cells inhibits IL-**

2 production and induces IL-4 release due to altered cognate signals. *J Immunol* 1996, **156:**2769-2775.

53. Wyss-Coray T, Gallati H, Pracht I, Limat A, Mauri D, Frutig K, Pichler WJ: **Antigen-presenting human T cells and antigen-presenting B cells induce a similar cytokine profile in specific T cell clones.** *Eur J Immunol* 1993, **23:**3350-3357.
54. Tatari-Calderone Z, Semnani RT, Nutman TB, Schlom J, Sabzevari H: **Acquisition of CD80 by human T cells at early stages of activation: functional involvement of CD80 acquisition in T cell to T cell interaction.** *J Immunol* 2002, **169:**6162-6169.
55. Sabzevari H, Kantor J, Jaigirdar A, Tagaya Y, Naramura M, Hodge J, Bernon J, Schlom J: **Acquisition of CD80 (B7-1) by T cells.** *J Immunol* 2001, **166:**2505-2513.
56. Rechavi O, Goldstein I, Kloog Y: **Intercellular exchange of proteins: the immune cell habit of sharing.** *FEBS Lett* 2009, **583:**1792-1799.
57. Gutierrez-Vazquez C, Villarroya-Beltri C, Mittelbrunn M, Sanchez-Madrid F: **Transfer of extracellular vesicles during immune cell-cell interactions.** *Immunol Rev* 2013, **251:**125-142.
58. Davis DM: **Intercellular transfer of cell-surface proteins is common and can affect many stages of an immune response.** *Nat Rev Immunol* 2007, **7:**238-243.
59. Revenfeld AL, Baek R, Nielsen MH, Stensballe A, Varming K, Jorgensen M: **Diagnostic and prognostic potential of extracellular vesicles in peripheral blood.** *Clin Ther* 2014, **36:**830-846.
60. Hudrisier D, Aucher A, Puaux AL, Bordier C, Joly E: **Capture of target cell membrane components via trogocytosis is triggered by a selected set of surface molecules on T or B cells.** *J Immunol* 2007, **178:**3637-3647.
61. Wetzel SA, McKeithan TW, Parker DC: **Peptide-specific intercellular transfer of MHC class II to CD4+ T cells directly from the immunological synapse upon cellular dissociation.** *J Immunol* 2005, **174:**80-89.
62. Dhainaut M, Moser M: **Regulation of immune reactivity by intercellular transfer.** *Front Immunol* 2014, **5:**112.
63. Rechavi O, Kalman M, Fang Y, Vernitsky H, Jacob-Hirsch J, Foster LJ, Kloog Y, Goldstein I: **Trans-SILAC: sorting out the non-cell-autonomous proteome.** *Nat Methods* 2010, **7:**923-927.
64. Thery C, Ostrowski M, Segura E: **Membrane vesicles as conveyors of immune responses.** *Nat Rev Immunol* 2009, **9:**581-593.
65. Ahmed KA, Xiang J: **Mechanisms of cellular communication through intercellular protein transfer.** *J Cell Mol Med* 2011, **15:**1458-1473.
66. Smyth LA, Afzali B, Tsang J, Lombardi G, Lechler RI: **Intercellular transfer of MHC and immunological molecules: molecular mechanisms and biological significance.** *Am J Transplant* 2007, **7:**1442-1449.
67. Beillard E, Pallisgaard N, van der Velden VH, Bi W, Dee R, van der Schoot E, Delabesse E, Macintyre E, Gottardi E, Saglio G, et al: **Evaluation of candidate control genes for diagnosis and residual disease detection in leukemic patients using 'real-time' quantitative reverse-transcriptase polymerase chain reaction (RQ-PCR) - a Europe against cancer program.** *Leukemia* 2003, **17:**2474-2486.

Figure legends

Figure 1. Improved flow cytometric gating strategy identifies HLA-DR in the membrane and intracellular compartment of CD3+ T cells and CD19+ B cells. Initially, the lymphocyte population was gated in a forward scatter (FSC)/side scatter (SSC) plot. From the lymphocytes, the CD3+ T cells and CD19+ B cells were subsequently gated. Subsequently, the CD3+ HLA-DR mem+ (17%) and CD19+ HLA-DR mem+ (99.7%) populations were identified with pre-defined gates set using the FMO control for HLA-DR mem. In the last step, it was determined, which HLA-DR mem+ cells also carried the HLA-DR protein intracellularly. For this purpose, gates set with the FMO controls were used, identifying the double positive CD3+ HLA-DR mem+ HLA-DR IC+ (15.6%) and CD19+ HLA-DR mem+ HLA-DR IC+ (95.2%) populations. For all the FMO controls, the threshold was set so that a maximum of 1% of the events fell into the double positive quadrant. The plots are from one donor as a representative example of the 10 included donors.

Figure 2. Correlation between HLA-DR mem and HLA-DR IC in CD3+ T cells and CD19+ B cells. The gating strategy presented in Figure 1 was employed to identify the HLA-DR mem+ and HLA-DR IC+ CD3+ T cells and CD19+ B cells in the presented dot plots. These plots were made to visualize a possible correlation between HLA-DR in the two cellular compartments. Moreover, a statistical correlation (Pearson) was made, correlating the HLA-DR mem value with the HLA-DR IC value for each event included in the CD3+ and CD19+ populations. This revealed a positive correlation between HLA-DR mem and HLA-DR IC for both CD3+ T cells and CD19+ T cells. Both dot plots are representative examples of the included donors (n=10).

Figure 3. Comparison of HLA-DR IC signal in CD3+ T and CD19+ B cells with/without permeabilization. To test for saturation of HLA-DR mem with the initially applied anti-HLA-DR antibody, a saturation control was made for all the included donors. For the control, the entire staining setup was applied, only omitting the permeabilization agent. Subsequently, the gating strategy displayed in Figure 1 was applied to identify the CD3+ HLA-DR mem+ T cells and CD19+ HLA-DR mem+ B cells. A) The histograms show the HLA-DR IC signals for the fully stained sample, the corresponding FMO control, and the saturation control. The histograms are a representative example of the 10 donors included in the study. B) For all the 10 donors, there was a detectable HLA-DR IC signal present in the saturation control for both the CD3+ T cells and the CD19+ B cells. However, this signal was always lower than the specific HLA-DR IC signal detected in the fully stained sample.

Figure 4. Confocal microscopy analysis of HLA-DR mem and HLA-DR IC in CD4+ T cells and CD19+ B cells. To verify the double staining procedure applied in the flow cytometric evaluation of HLA-DR mem and HLA-DR IC, confocal microscopy was performed. Isolated CD4+ T cells and CD19+ B cells were stained with anti-HLA-DR mem and anti-HLA-DR IC, using a similar procedure as that for the equivalent flow cytometric analyses. For the CD4+ T cells, an additional staining with anti-CD3 was performed. As for the flow cytometric analysis, the saturation of HLA-DR mem was evaluated prior to targeting of HLA-DR IC (Figure 3). In this control no intracellular staining was detected (data not shown). In addition, the control of the secondary antibody, applied to target the anti-CD3 antibody, showed no non-specific binding (data not shown). The presented results are representative of two independent experiments (n=2).

Figure 5. Contribution of CD4+ and CD8+ T cells to the CD3+ HLA-DR mem+ T cell population. The relative contribution of CD4+ and CD8+ T cells to the CD3+ HLA-DR mem+ T cell population was investigated by staining PBMCs with antibodies against CD3, CD4, CD8, CD25, and HLA-DR mem. A) Using the gating strategy described in Figure 1, the HLA-DR mem-presenting CD4+ and CD8+ T cells were identified (left panel). Subsequently, the co-expression of CD25 was determined for these cells and compared to the CD25 expression in the corresponding HLA-DR mem- cells. B) The highest degree of CD25 expression was observed for the CD4+ T cells, which presented the most HLA-DR mem (top panel). In contrast, CD25 was found to the greatest extent of the CD8+ T cells presenting no HLA-DR mem (bottom panel). n=6.

Figure 6. Quantifying mRNA from target genes by qPCR. A) The expression of *HLA-DRB1*03* mRNA was investigated in isolated CD4+ T cells and CD19+ B cells from donors with an *HLA-DRB1*03* positive or negative genotype (n=5 for each genotype). The expression of the target gene was normalized to the mean of two reference genes (*B2M* and *GUSB*). Data is presented as mean ± SEM. B) Normalized expression of *HLA-DRB1*03* for selected samples are depicted in this panel. The values represent each of the five *HLA-DRB1*03* positive CD4+ T cell samples and the two *HLA-DRB1*03* negative B cell samples, which yielded a detectable signal in the qPCR analysis of *HLA-DR B1*03*. C) Expression of *CD19* mRNA in T and B cells (n=10). The expression of the target gene was normalized to the mean of two reference genes (*B2M* and *GUSB*). Data are presented median and interquartile range. The bars denote the 5% and 95% percentiles. *, $p<0.05$; **, $p>0.01$; ND, Not detectable.

Tables

Table 1 Primer and probe sequences, assay id and amplicon size for the genes analyzed by qPCR. F = Forward, R = Reverse. The specificity of the *HLA-DRB1*03* assay is located in the forward primer. For *B2M*, the forward primer is located in exon 2 and reverse primer in exon 4.

Gene	Primers	FAM labeled MBG probe	Amplicon size	Exon boundary
*HLA-DRB1*03*	F: 5'-CACCTATTGCAGACACAA-3' R: 5'-AACCACTCACAGAACAGA -3'	5'-ACCTTAGGATGGACTCGC-3'	136	2-3
B2M	F: 5'-GAGTATGCCTGCCGTGTG-3' R: 5'-AATCCAAATGCGGCATCT-3'	5'-CCTCCATGATGCTGCTTACATGTCTC-3'	109	3
GUSB	F: 5´-GAAAATATGTGGTTGGAGAGCTCATT-3´ R: 5´-CCGAGTGAAGATCCCCTTTTTA-3´	5´-CCAGCACTCTCGTCGGTGACTGTTCA-3´	100	11-12
CD19	Hs01047410_g1		57	1-2

Table 1 Distribution of HLA-DR in the membrane and intracellular compartment of CD3+ T and CD19+ B cells from peripheral blood of healthy individuals. * The identified cells are from PBMCs. n = 10. ** Parent population: Lymphocyte gate *** The *p* values are given for the comparison of the differences between the percent of positive cells from the CD3+ T cells and the corresponding group from the CD19+ B cells.

Cell type*	% of parent population ± SEM	MFI ± SEM	*p*
CD3+ T cells			
CD3+**	77.8 ± 1.9		
CD3+ HLA-DR mem+	18.2 ± 4.2	1,662 ± 138	0.002
CD3+ HLA-DR mem+ HLA-DR IC+	17.9 ± 2.5	1,748 ± 152	<0.001
CD3+ HLA-DR IC+	3.0 ± 0.7	1,775 ± 145	<0.001
CD19+ B cells			
CD19+**	6.3 ± 1.0		
CD19+ HLA-DR mem+	98.8 ± 0.5	23,047 ± 2,059	
CD19+ HLA-DR mem+ HLA-DR IC+	96.9 ± 0.9	9,227 ± 596	
CD19+ HLA-DR IC+	95.9 ± 1.2	9,314 ± 680	

Additional files

Additional Figure 1. Confocal microscopy analyses of HLA-DR mem and HLA-DR IC in CD4+ T cells. Cells presenting HLA-DR both in the membrane and intracellular compartment were rarely found among the isolated CD4+ T cells. One double positive T cell was detected in one of the two independent experiments.

File name: Additional file 1

File format: TIF

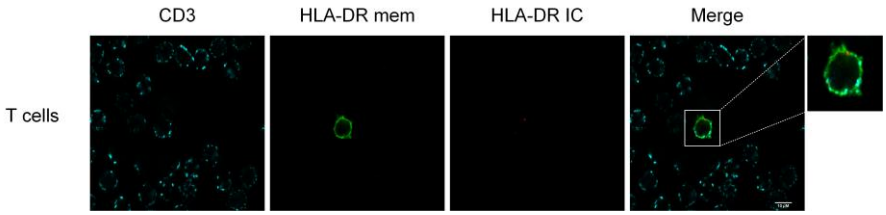

Figures

Figure 1

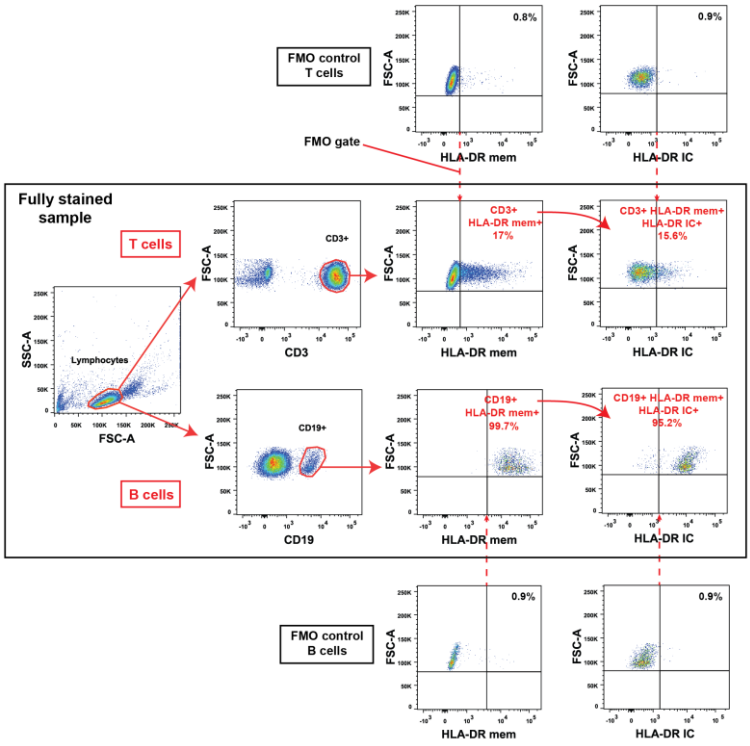

Figure 2

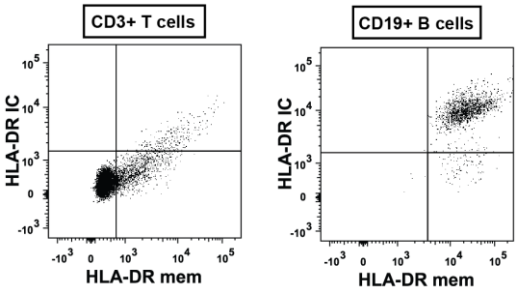

Figure 3

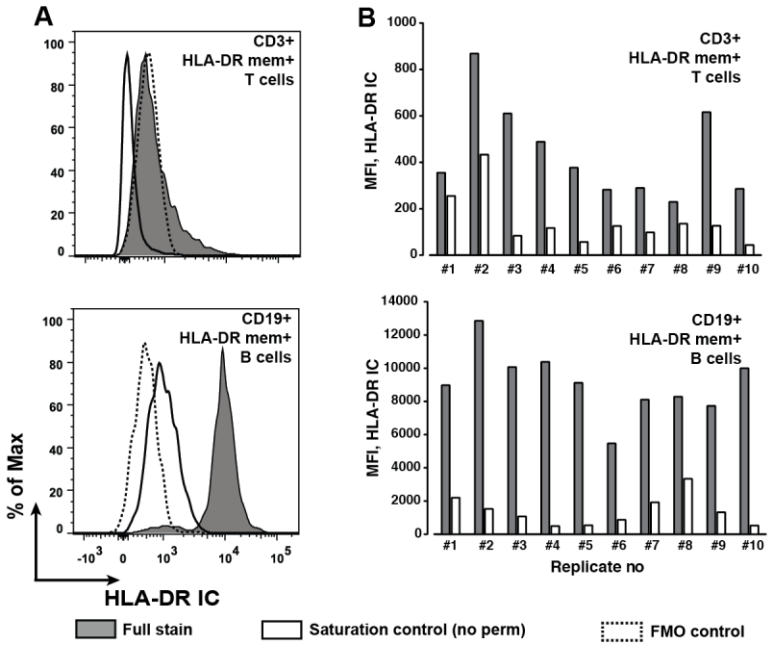

Figure 4

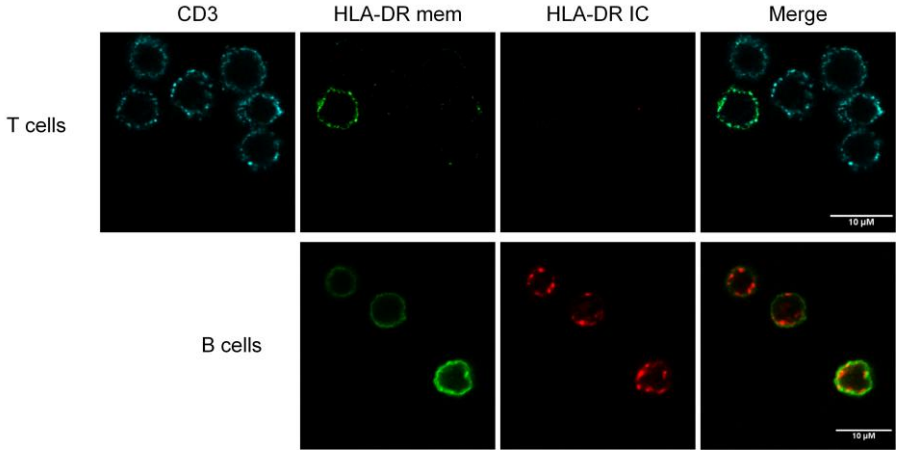

Figure 5

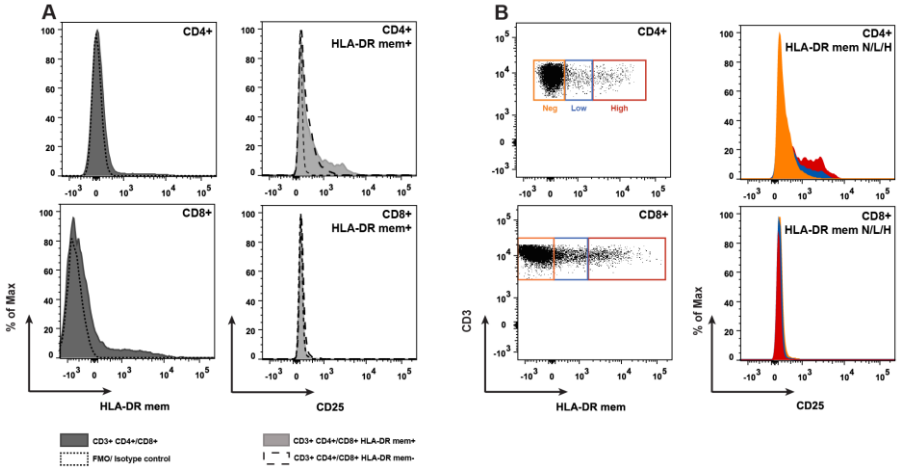

Figure 6

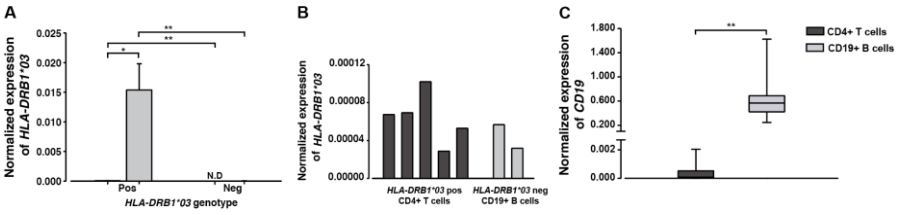

B2 - Manuscript 2

Title: Phenotypic characterization of extracellular vesicles and CD4+ HLA-DR+ responder T cells following contact-dependent and -independent allogeneic MLC

Running title: Characteristics of HLA-DR-presenting CD4+ T cells

Summary sentence: Phenotypic and functional features of HLA-DR-presenting T cells in alloresponses with indications of a role in peripheral tolerance

Journal: Journal of Leukocyte Biology

Anne Louise Schacht Revenfeld*†, Rikke Bæk†, Malene Møller Jørgensen†, Kim Varming†, Allan Stensballe*

* Department of Health Science and Technology, Aalborg University, Denmark

† Department of Clinical Immunology, Aalborg University Hospital, Aalborg, Denmark

Corresponding author:

Anne Louise Schacht Revenfeld, Department of Clinical Immunology, Aalborg University Hospital, Urbansgade 32-36, DK-9000 Aalborg, Denmark (Tel: +45 97655587; email: anlor@rn.dk)

Keywords: Peripheral tolerance, flow cytometry, EV Array, Tregs

Total character count: 25267

Total number of figures: 5

Total number of color figures: 2

Total number of references: 58

Total number of words in abstract: 199

Total number of words in summary sentence: 19

Abbreviations

APC	Antigen-presenting cell
CTLA-4	Cytotoxic T-lymphocyte associate protein 4
DC	Dendritic cell
EV	Extracellular vesicles
FBS	Fetal bovine serum
FMO	Fluorescence minus one
FoxP3	Forkhead box P3
FSC	Forward scatter
HLA-DR	Human leukocyte antigen DR
MFI	Median fluorescence intensity
MHCII	Major histocompatibility complex II
MLC	Mixed lymphocyte culture
PBMC	Peripheral blood mononuclear cells
PD-1	Programmed cell death 1
PD-L	Programmed death-ligand
PHA-P	Phytohaemagglutinin P
RT	Room temperature
SSC	Side scatter
TCR	T cell receptor
Teff	Effector T cell
TNFRII	Tumor necrosis factor receptor II
Treg	Regulatory T cell
TW	Transwell

Abstract

Although the observation of major histocompatibility complex II (MHCII) molecules on T cells is longstanding, the explanation for this occurrence remains enigmatic. As such, reports of an inducible, endogenous expression exist, as do studies demonstrating a protein acquisition from other cells by mechanisms including vesicle transfer. Here, we further characterized some of the requirements for the presence of the human MHCII isotype, human leukocyte antigen DR (HLA-DR), on human CD3+ CD4+ T cells. This was accomplished with a combination of flow cytometry of cell surface markers and extensive phenotyping of cell-derived extracellular vesicles (EVs). It was found that expression of HLA-DR could not be induced in CD3+ CD4+ T cell monocultures after both mitogenic and antigen-like stimulation. In addition, contact-dependent differences were observed for both proliferation and presence of HLA-DR on the responder CD3+ CD4+ T cells following an allogeneic mixed lymphocyte culture (MLC). The functional phenotype of the CD3+ CD4+ HLA-DR+ responder T cells indicated a possible regulatory role for these cells. Finally, the phenotype of the EVs produced during the MLCs was more heterogeneous than the investigated cellular phenotype. Nevertheless, the EV phenotype displayed contact-dependent differences, which may provides clues about their intended functionality in cellular communication.

Introduction

The expression of major histocompatibility complex II (MHCII) is essential for the specificity of the adaptive immune system. The T cell receptor (TCR) of CD4+ T cells interacts with the cognate peptide-MHCII complexes on antigen-presenting cells (APCs), thus activating the T cells. The constitutive expression of MHCII is limited to professional APCs, however, MHCII has for more than four decades also been observed on T cells [1-4]. In addition, the number of MHCII+ T cells increases upon activation [4, 5]. In line with this, the most frequently expressed MHCII molecule in humans, the human leukocyte antigen DR (HLA-DR), is commonly used as a marker for T cell activation [5-7]. It remains a subject of discussion, whether the presence of MHCII on T cells is explained by an endogenous protein synthesis or by an acquisition from adjacent cells. Furthermore, the functional consequences of MHCII on T cells are still poorly understood.

An inducible, endogenous protein synthesis of MHCII has been reported for T cells, similar to that described for APCs. The expression of MHCII has been observed for T cells from several species, including bovine [8], rat [9, 10], and human [11]. In addition, T cells can also acquire fully functional MHCII from neighboring cells by yet unconfirmed mechanisms. This molecular transfer was already observed in the 1980's [12] and since then several studies have demonstrated that the acquisition is possible for rat [13], mouse [14-16] and human T cells[17]. Moreover, it has been stated that an acquisition explains the presence of MHCII on mouse T cells [13, 15], which are known not to express MHCII endogenously even after *in vitro* stimulation [18]. The responsible mechanisms have been reported as either being a vesicle-mediated transfer [13, 19, 20] or the acquisition of entire membrane patches [21], also known as trogocytosis [22]. Regardless of an endogenous expression or protein acquisition, MHCII on T cells has mainly been associated with induction of down regulatory signals in the responder T cell [11, 23-25]. However, several studies also demonstrate that the MHCII+ T cells can activate other T cells [15, 17]. Nonetheless, these functional findings collectively suggest a more pronounced role of MHCII on T cells than being an activation marker.

The purpose of this study was to further elucidate the presence of HLA-DR on the surface of human CD3+ CD4+ T cells. In this context, the influence of APCs in this phenomenon was investigated. It was observed that the presence of HLA-DR in monocultures of primary CD3+ CD4+ T cells was not inducible following *in vivo* mitogenic and antigen-like stimulation. Moreover, contact-dependent differences were observed for both proliferation and presence of HLA-DR on CD3+ CD4+ T cells following an allogeneic mixed lymphocyte culture (MLC). Furthermore, a phenotypical characterization of the responder CD3+ CD4+ HLA-DR+ T cells also revealed contact-dependent differences as well as indicating a possible regulatory function of these T cells. The phenotype of the cell-derived extracellular vesicles (EVs) was much more heterogeneous than the cellular counterpart. However, contact-dependent differences in the EV phenotype were observed, providing clues to the vesicular communication in allogeneic MLCs.

Materials and Methods

Cells and isolation

Venous peripheral blood was obtained from healthy donors with known HLA types. The blood was collected in heparinized tubes (Vacuette, Lithium Heparin, Greiner Bio One, DE). Isolation of peripheral blood mononuclear cells (PBMCs) was accomplished by using Lymphoprep™ gradient centrifugation (Axis-Shield, Oslo, NO). The PBMCs were either used directly after the isolation or stored at -140 °C in a storage medium (RPMI 1640 (Gibco, Life Technologies, Carlsbad, USA), 40% heat-inactivated fetal bovine serum (FBS)(Gibco), 10% dimethyl sulfoxide (Merck Millipore, Darmstadt, Germany), 100 U/mL penicillin/10µg/mL streptomycin (Ampliqon, Odense, DK)). The CD4+ T cells were isolated from PBMCs using either a Dynabeads® CD4 Positive Selection kit (Invitrogen, Life Technologies, Carlsbad, CA, USA) or a Dynabeads® Regulatory CD4+ CD25+ T Cell Kit (Invitrogen), using only the CD4+ isolation part. The entire procedure was carried out according to the manufacturer's guidelines. The purity of the isolated cells was evaluated by flow cytometry.

Mitogenic and antigen-like stimulation

The isolated CD4+ T cells or PBMCs were seeded in a concentration of $7x10^5$ cells/mL in culture medium (RPMI 1640, 10% FBS, 100 U/mL penicillin/10µg/mL streptomycin) with or without mitogenic/antigen-like stimuli for 20h. Phytohaemagglutinin-P (PHA-P)(Sigma-Aldrich, St. Louis, MO, USA) was used in a final concentration of 3.3 µg/mL, while Dynabeads® Human T-Activator CD3/CD28 for T Cell Expansion and Activation (Invitrogen) was used according to the manufacturers guidelines.

Mixed lymphocyte culture

A 6-day allogeneic mixed lymphocyte culture (MLC) was performed with PBMCs from two donors with complete HLA mismatch. Prior to the MLC, the stimulator cells were irradiated (1700 rad), while the responder cells were labeled with 15 µM Cell Proliferation Dye eFluor® 450 (eBioscience, San Diego, CA, USA) according to the manufacturers guidelines. For the contact-dependent MLC (classical), $5x10^4$ of each responder and stimulator cells were mixed in a 96-well plate (Nunc, Thermo Scientific, Waltham, MA, USA) in a total volume of 150 µL culture medium (RPMI 1640, 10% FBS, 100 U/mL penicillin/10µg/mL streptomycin). For the contact-independent setup, stimulator cells and responder cells were separated by a Millicell® Hanging Cell Culture Insert with a pore size of 0.4 µm (Merck Millipore)(hereafter termed transwell (TW)) in 24-well plates (Nunc). The upper chamber contained $2.5x10^5$ stimulator cells in 400 µL of culture medium, while the lower chamber contained $5x10^5$ responder cells in 800 uL of culture medium. For the stimulator and responder control samples, $5x10^4$ of either responder or stimulator cells were seeded in a 96-well plate, as described above. On day 5, 50 µL (1 µCi, 96-well plate) or 400 µL (8 µCi, 24-well plate) of Thymidine-^{3}H (Perkin Elmer,

Waltham, MA, USA) was added to the selected wells designated for measurements of proliferation. The Thymidine-^{3}H labeled cells were harvested after 24h and radioactive incorporation was detected in a scintillation counter (TopCount NXT, Perkin Elmer). On day 6 of the MLCs, the cell culture supernatants were removed and centrifuged once at 500x*g* 10 min at room temperature (RT) to pellet cells. The cell-free supernatants were stored at -40 °C prior to vesicle phenotyping. The pelleted cells from the cell supernatant were pooled with those harvested from the MLCs and the cellular phenotyping was performed using flow cytometry.

Cellular phenotyping with flow cytometry

Antibodies for cellular phenotyping: Conjugated antibodies against the following targets were obtained from BD Biosciences (Mountainview, CA, USA): CD3-APC (UCHT1), CD3-FITC (UCHT1), CD3-PerCP (SP34-2), CD4-APC-H7 (SK3), CD4-FITC (RPA-T4), CD4-PE (RPA-T4), CD11a-FITC (G43-25B), CD25-FITC (M-A251), CD62L-FITC (DREG-56), CD127-PE (HIL-7R-M21), CD152 (CTLA-4)-PE (BNI3), CD279 (PD-1)-PE-Cy7 (EH12.1), HLA-DR-FITC (L243), HLA-DR-PE (L243), HLA-DR-PerCP-Cy5.5 (L243), mouse-IgG1-APC-H7 (X40), mouse-IgG1-FITC (MOPC-21), mouse IgG1-PE (MOPC-21), mouse IgG1-PerCP (MOPC-21), and mouse IgG1-PE-Cy7 (MOPC-21). Antibodies against HLA-DR-Alexa Fluor 647 (L243) and mouse-IgG2a-Alexa Fluor 647 (MOPC-173) were from BioLegend (San Diego, CA, USA). Mouse-IgG2a-FITC (eBM2a) and mouse-IgG2a-PE (eBM2a) were from eBioscience. Anti-TNFRII (CD120b)-PE (80M2) was from Immunotech (Beckman Coulter, Inc., Brea, CA, USA). Mouse-IgG1-APC (DAK-GO1) was from Dako A/S (Glostrup, DK).

Data acquisition and analysis: The acquisition of stained cells was performed on a FACSCanto A using FACSDiva™ software (version 6.1.3, BD Biosciences). Calibration and compensation settings for the cytometer were obtained daily by using the 7-Color Setup Beads (BD Biosciences) and once a week with the FACSDiva™ CS&T Research Beads (BD Biosciences). The analysis of the data was carried out with the FlowJo software (version 10.0.7, FlowJo LLC, Ashland, OR, USA). Negative isotype controls or fluorescence minus one (FMO) controls [26, 27] were utilized to identify the positive events. For all populations, the median fluorescence intensity (MFI) was the statistical value of choice.

EV Array analysis

Production of microarrays: Microarray printing was performed on a SpotBot® Extreme Protein Edition Microarray Printer as previously described [28].

Antibodies and proteins for vesicle phenotyping: A total of 24 anti-human antibodies and one protein were used. They are listed in the following with the corresponding product number (#) or clone. From R&D Systems (Minneapolis, MN, USA): Annexin V (#AF399), CD4 (34930), CD19 (4G7-2E3), CD45 (2D1), CD80 (37711), CD82 (#423524), CD83 (H15e), LAMP-2 (H4A3), TNFRI (#DY225), and TNFRII (#DY726). From Biolegend: Alix (3A9), CD63 (MEM-259), HLA-ABC (W6/32), and HLA-DR (L243). From LifeSpan BioSciences, Inc. (Seattle, WA, USA): CD9

(#LS-C35418), CD81 (#LS-B7347), and CTLA-4 (ANC152.2/8H5). From BD Biosciences: CD3 (Hit3a) and CD14 (M5E2). From Abcam (Cambridge, MA, USA): Flotilin-1 (#Ab41927) and TSG101 (5B7). From Santa Cruz Biotechnologies (Dallas, TX, USA): TLR-3 (TLR3.7). From Abbiotec (San Diego, CA, USA): CD11a (HI111). From eBioscience: ICAM-1 (R6.5). From Haematologic Technologies, Inc. (Essex Juncton,VT, USA): Lactadherin (protein) (#BLAC-1200). All antibodies and protein were printed in triplicates at 87.5 – 200 µg/mL diluted in PBS containing 5% glycerol.

Antibodies for semi-quantification of vesicles: For the semi-quantification, only anti-CD9, anti-CD63, and anti-CD81 were printed on the micro-array slides, as previously described [29]. In short, 18 repeated spots were printed with a cocktail of the three antibodies.

Catching and visualization: Initially, the microarray slides were blocked (50 mM ethanolamine, 100 mM Tris, 0.1% SDS, pH 9.0) prior to incubation with 100 µl of undiluted cell culture supernatant. The incubation was performed in Multi-Well Hybridization Cassettes (ArrayIt) at RT for two hours followed by overnight incubation at 4 °C. Following a wash in wash buffer (0.05% Tween 20®, PBS), the slides were incubated with biotinylated detection antibodies (diluted 1:1500, anti-human-CD9, -CD63, -CD81, (Ancell Corporation, MN, USA)) in wash buffer. After a wash, a subsequent 30 minutes incubation step with Cy5-labelled streptavidin (diluted 1:1500, Life Technologies) in wash buffer, was carried out for detection. Prior to scanning at 635 nm, the slides were washed first in washing buffer and then in MilliQ water and dried using a Microarray High-Speed Centrifuge (ArrayIt). Scanning and spot detection was performed as previously described [29].

Data analysis: Creation of graphs was carried out using GraphPad Prism (version 6.04, GraphPad Software, Inc., San Diego, CA, USA) and Excel (version 2013, Microsoft, Redmond, WA, USA). Heat maps were produced using Genesis (version 1.7.6, IGB TU Graz, Graz, Austria). For a given antibody spot, the signal intensity was calculated as the mean signal of triplicate spots in relation to the sample signal of the negative spot (PBS) in triplicate. For each spot, the signal intensity was calculated by subtracting the mean of the background (no sample/blank, washing buffer) from the mean of the foreground (spot signal). Before visualization and calculation of linearity, the antibody signal intensities were converted to log space by log2 transformation.

Statistical analysis

The statistical analysis of data was performed using SigmaPlot (version 11, Systat Software Inc, San Jose, CA, USA). To test for differences between two groups, a paired or unpaired t-test was applied to test for differences between the two groups of cells from the same individual or between two individuals, respectively. To test for differences between more than two groups, a one-way repeated measures ANOVA, followed by Tukey's post-hoc analysis, was applied. Differences between groups were considered statistically significant, when $p < 0.05$.

Results

Inducible expression of HLA-DR in isolated CD3+ CD4+ T cells

To investigate if CD3+ CD4+ T cells from peripheral blood endogenously express the HLA-DR observed on their cell surface, we attempted to induce this expression in isolated CD3+ CD4+ T cells with PHA-P or anti-CD3/anti-CD28. For both types of stimuli, an increase in the presence of HLA-DR could not be detected after 20 h of stimulation (Figure 1, filled bars). In contrast, the number of CD3+ CD4+ HLA-DR+ T cells increased when PBMCs were stimulated with either PHA-P ($p = 0.008$) or anti-CD3/anti-CD28 ($p = 0.001$), as compared to the unstimulated counterpart (Figure 1, hatched bars). Moreover, the amount of CD3+ CD4+ HLA-DR+ T cells was approximately 12 and 9 times greater in the PBMC population than in the monocultures stimulated with PHA-P (p=0.006) or anti-CD3/anti-CD28 (p=0.002), respectively. The purity of the isolated CD3+ CD4+ T cells was 94.5% ± 5.2 (n=3), as evaluated by flow cytometry (data not shown).

Requirements for MLC-induced cellular proliferation

A 6-day allogeneic MLC assay was employed to investigate the importance of APCs for CD4+ T cell activation and a subsequent presence of HLA-DR on CD4+ T cells. As an additional feature, the importance of a physical interaction between the responder cells and the stimulator cells was also evaluated. As an initial outcome measure, the cell proliferation was determined for the two MLC combinations. A prominent proliferative response was detected from the cells from the contact-dependent MLC (classic MLC), as compared to the responder control sample (Figure 2). Contrary to this observation, the responder cells from the contact-independent MLC (transwell (TW) MLC) did not proliferate above the level detected for the responder control.

Cellular phenotype of HLA-DR-presenting responder CD4+ T cells

In addition to the proliferation, the cellular phenotype of the CD4+ HLA-DR+ responder cells was characterized by a flow cytometric evaluation of seven cell surface markers related to the activity and function of both regulatory T cells (Tregs) and effector T cell (Teff). Initially, it was established that the number of HLA-DR-presenting CD3+ CD4+ T cells was highest in the contact-dependent MLC, in which 20.5% ± 2.4 CD3+ CD4+ HLA-DR+ T cells could be detected (Figure 3B), which was significantly different from the baseline measurements of 6.9% ± 2.0 (p = 0.009). For the TW MLC and the responder control sample, these numbers were lower with 13.3% ± 3.3 and 18.0% ± 1.3 CD3+ CD4+ HLA-DR+ T cells identified, respectively. When comparing the phenotype of the HLA-DR presenting responder cells from the classic MLC and the TW MLC, four of the included markers exhibited the largest difference in expression an were all enriched in the classic MLC (Figure 3C). These markers were CD25, cytotoxic T-lymphocyte associated protein 4 (CTLA-4, CD152), tumor necrosis factor receptor II (TNFRII, CD120b), and programmed cell death 1 (PD-1, CD279)(Figure 3B). The most differentially expressed marker was CD25, which exhibited almost a 2-fold increase in expression in the

classic MLC, as compared to the TW MLC. In addition, the detected CD25 expression in the classic MLC was more than 3 times greater than the corresponding expression in the responder control (9.0% ± 0.4; $p = 0.027$) and 1.6 times greater than the baseline expression (18.6% ± 4.1). For the TW MLC, these numbers were 1.7 and 0.8, respectively. For CTLA-4, the expression was approximately 50% increased in the classic MLC, when compared to the observed expression in the TW MLC (40.5% ± 3.3 and 26.6% ± 4.6; $p = 0.017$). The expression of CTLA-4 in both MLCs was also significantly different from the responder control (6.8% ± 0.3), yielding a 4-6 times higher expression in the MLCs. Moreover, when compared to the baseline measurements (2.6% ± 0.4), the expression was 10- and 15-fold higher in the TW MLC and classic MLC, respectively. With regard to TNFRII, the expression was approximately 40% greater in the classic MLC as compared to the TW MLC (51.9% ± 0.9 and 38.0% ± 5.4)(Figure 3B). However, the CD3+ CD4+ HLA-DR+ responder T cells had increased the expression of TNFRII almost 1.6 and 2 times in the TW MLC and classic MLC, respectively, as compared to the baseline measurements (24.6% ± 3.5). Finally, the expression of PD-1 was on average 25% greater in the classic MLC than in the in the TW MLC (65.2% ± 8.1 and 52.1% ± 10.4). In relation to the baseline measurements (42.8% ± 4.0), PD-1 expression was 1.2 and 1.5 times greater in the TW MLC and classic MLC, respectively.

Differential expression separates the HLA-DR- and HLA-DR+ responder T cells

In order to further characterize the MLC responder cells, the phenotypical differences between the CD3+ CD4+ HLA-DR- and CD3+ CD4+ HLA-DR+ T cells were evaluated. As shown in the correlation plots in Figure 4A, four of the investigated markers were enriched in the HLA-DR+ subsets of both MLCs, as compared to the corresponding HLA-DR- subsets. These markers were CD25, CTLA-4, TNFRII, and PD-1. Moreover, it was consistently observed for both types of MLC that the expression of CD11a was upregulated on the CD3+ CD4+ HLA-DR+ responder T cells, as compared to the corresponding HLA-DR- subsets (n=3)(Figure 4B).

Contact-dependent differences observed for the phenotype of extracellular vesicles following allogeneic MLC

In addition to the cellular phenotype of the responder cells from the MLCs, the phenotype of the extracellular vesicles (EVs) found in the cell supernatants on day 6 of the MLCs was also characterized. For the characterization, we applied the EV Array to detect the EVs, which display CD9, CD63, and/or CD81, known to be present on exosomes [30]. A summary of the additional protein markers detected on these EVs is depicted in the heat maps in Figure 5A (two of three included biological replicates; third replicate can be found in [31]). Of the three exosomal markers, only CD9 and CD81 could be detected in all samples. In addition, CD82 was also present in all EV samples. The relative distribution of these markers can be seen in the left bar plot in Figure 5B. The presence of the remaining markers included in the EV phenotyping was quite heterogeneous. However, tendencies were present for a number of these markers. As such, CD3 was predominantly detected in the EVs from the

classic MLC, while it was virtually absent in the TW MLC samples (Figure 5B, right bar plot). This trend was also applicable for the detection of CTLA-4. Nevertheless, the detectable signals for this marker were low. In the TW samples, EVs were more enriched in TNFRI, when compared to the classic MLC and the controls (Figure 5B). Apart from the heterogeneous presence of many of the included markers, several of these markers could not be detected or yielded barely detectable signals for EVs from the MLCs. These included lineage specific markers CD4 (T cells), CD19 (B cells), and CD83 (DCs)(data not shown). Moreover, the hematopoietic marker CD45 and the class I equivalent of HLA-DR, HLA-ABC, were also included in this list (data not shown). Finally, it was observed that both non-irradiated and irradiated PBMCs, such as the stimulator cells, had produced equal amounts of CD9, CD63, and CD81 on the EVs found in the cell supernatant after 6 days of cell culture (Figure 5C).

Discussion

For many years it has been believed that T cells from most species possess the ability to express HLA-DR/MHCII endogenously. However, this dogma has been challenged by several studies demonstrating that a protein acquisition either completely account for or contribute to the presence of HLA-DR on T cells. We initially addressed this discrepancy by inducing *in vitro* HLA-DR expression in CD3+ CD4+ T cells from peripheral blood, either as monoculture or part of a PBMC population. This was interesting since it has been demonstrated that HLA-DR found on the surface of CD3+ CD4+ in peripheral blood cannot be explained by a simultaneous mRNA production [32]. In the current study, the presence of HLA-DR only increased in the CD3+ CD4+ T cells in the PBMC population after mitogenic (PHA-P) or antigen-like (anti-CD3/anti-CD28) stimulation (Figure 1). Although these results cannot indisputably exclude endogenous HLA-DR expression in CD3+ CD4+ T cells, they indicate an important role of APCs, and possibly also accessory cells, in this context.

This role was addressed in more detail, focusing on the interaction between T cells and APCs. By employing an allogeneic MLC, the *in vivo* antigen-recognition by T cells was approximated to a great extent [33]. Furthermore, we investigated whether a physical interaction was required for the presence of HLA-DR on the responder CD3+ CD4+ T cells following the MLC. This was carried out to elucidate aspects of a possible transfer of HLA-DR from APCs to T cells by vesicles, as reported earlier [13, 19, 20]. Since the relative placement of the cells in the TW system can affect the vesicle phenotype [31], the cells exerting the major stimulatory function (the stimulator cells) were placed in the upper compartment of the TW system, while primary vesicle recipient (responder cells) was placed in the lower compartment. For both MLCs, three experimental outcomes were measured to evaluate the contact-dependent effects on the responder CD3+ CD4+ HLA-DR+ T cells: The proliferative capacity, the functional phenotype of these cells, and the phenotype of the extracellular vesicles (EVs) shed into the cell culture medium.

In relation to the first experimental outcome, a notable proliferative response was detected for the responder cells in the contact-dependent (classic) MLC (Figure 2). On the contrary, no proliferation could be observed for the responder cells from the contact-independent (transwell, TW) MLC. Hence, the proliferation observed in allogeneic MLCs required physical contact between T cell and APC.

For the second experimental outcome, the CD3+ CD4+ HLA-DR+ T cells were characterized by investigating the presence of seven cell surface markers. These markers included general T cell activation markers, as well as markers associated with Tregs and T cell suppression. The latter category of cell surface markers was included since HLA-DR on T cells mainly has been associated with suppressive activity [23-25], as it has been observed for HLA-DR+ Tregs [11]. In addition, anti-MHCII antibodies have been demonstrated to block the suppressive activity of activated human Tregs [34], suggesting an important role for HLA-DR on Tregs. Of the seven included markers, the differential expression was mostly pronounced for four

of these, when comparing the classic MLC to the TW MLC after the six days of incubation. These included CD25, CTLA-4, PD-1, and TNFRII (Figure 3B and 3C) and all markers were mostly enriched in CD3+ CD4+ HLA-DR+ responder T cells from the classic MLC. Moreover, the expression these markers were enhanced in the CD3+ CD4+ HLA-DR+ T cells, when compared to the corresponding HLA-DR- subsets (Figure 4A). However, as can be appreciated from Figure 3B, the number the CD3+ CD4+ HLA-DR+ T cells were quite similar for the MLCs and the responder control, although a significant increase was observed from the baseline measurements. However, the phenotype of these cells from the MLCs was not artifactually induced by the culturing conditions, as the MLCs created notably different CD25 and CTLA-4 expression than the control. Most of the investigated markers can be found on both conventional Teffs and Tregs. Due to their dissimilar functionalities, it was important to look for expressional patterns differentiating these two cellular groups. CD25 is used as a T cell activation marker and also to identify naturally occurring CD4+ Treg [35] and those induced from CD4+ CD25- precursors [36]. The function of CTLA-4 depends on its expression by either Teff or Tregs [37, 38]. For Teff, CTLA-4 is up-regulated following activation, where it provides co-inhibitory signaling by competing for the shared ligands of the co-stimulatory receptor CD28 [39]. In Tregs, expression of CTLA-4 has been linked to their suppressive activity [39, 40]. For a part of the CD3+ CD4+ HLA-DR+ cells, CD25 and CTLA-4 displayed a positive correlation (Figure 3A, top panel). However, the non-uniform correlation demonstrates how the HLA-DR-presenting CD3+ CD4+ T cells are a heterogeneous cell population. Nevertheless, further investigations are required to link this correlation to either Teff or Tregs function. Like CTLA-4, PD-1 is part of the CD28 family of proteins [41] with an essential role in T cell inhibition and consequently also in peripheral tolerance [42]. While T cells exclusively express CTLA-4 [41], both activated T and B cells can express PD-1 [42]. Moreover, T cells can express one of the two ligands for PD-1 (PD-Ls), which is also expressed by other lymphoid and non-lymphoid cells [41, 43]. A PD-1/PD-L1 ligation in T cells can result in either activation of anergy, though it is mostly asscociated with the latter [37, 41, 43, 44]. Interestingly, the ligation between PD-1 and PD-L has also been suggested to play a role in the interaction between T cells [45], though with currently unverified effects. Blocking CTLA-4 and PD-1 reduces Treg activity in melanoma patients [46] and, as previously mentioned, blocking of HLA-DR on activated Tregs has similar effects [34]. This could a suggest a link between HLA-DR, CTLA-4, PD-1, Tregs, and their suppresive capacity. However, such a relationship remains to be established. Finally, TNFRII was also enriched in the CD3+ CD4+ HLA-DR+ responder T cells in both MLCs, when compared to the HLA-DR- counterparts (Figure 4A, bottom panel). Moreover, it positively correlated with the expression of PD-1. Although TNFRII is involved in lymphocyte activation and proliferation [25], several studies have shown that TNFRII is primarily confined to Tregs in both human and mouse [47-49]. A suppressive activity of CD4+ CD25+ TNFRII+ HLA-DR+ T cells has been established with an observed co-expression of CTLA-4 [25]. Hence, a concurrent presence of HLA-DR, CD25, CTLA-4, PD-1, and TNFRII on CD4+ T cells could very likely identify a subset of cells with suppressive activity. A delineation of the suppressive activity of the CD3+ CD4+ HLA-

DR+ responder T cells observed in the present study would consequently be relevant. With regards to the contact-dependent differences observed here, it is notable that the phenotype of the CD3+ CD4+ HLA-DR+ responder T cells in the TW MLC was almost identical to the corresponding phenotype in the classic MLC, although with a delayed onset or a less prominent expression. This was observed for all of the three included biological replicates, possibly pointing to a consistent trend. However, the lack of proliferation in the TW MLC indicates functional differences. It would consequently be interesting to explore if the TW MLC response encompasses one component of the full T cell response observed in the contact-dependent, classic MLC or if it could represent an particular mechanism for immune regulation.

For the third experimental outcome, we characterized the EVs in the cell supernatants from the MLCs. This was achieved by extensively phenotyping the EVs for both vesicle-specific and cell-specific protein surface markers using the EV Array [29, 30]. With this analysis, we detected EVs containing CD9, CD81, and CD82, from all MLCs and controls. Of these three tetraspanins, CD9 and CD81 are generally accepted as markers that identify a particular subset of EVs, called exosomes [50, 51]. Moreover, CD82 has also been associated with this type of EV [52]. Exosomes are known to be key players in cellular communication, both in maintaining homeostasis and for the progression of pathological condition, including cancer [30]. Also, immunomodulatory effects of exosomes have been documented, involving transfer of proteins and other molecules, such as RNA, between cells, effectively changing the phenotype and function of the recipient cell [19, 53-55]. The detection of CD9, CD81, and CD82 in the current study indicated that production of such EVs were present in all of the cellular samples. This is relevant, since vesicle-based cellular communication has yet to be characterized in the context of allogeneic MLCs. However, the detected EV phenotypes were very heterogeneous across the biological replicates (Figure 5B, right bar plot). It has been demonstrated that EV phenotype obtained in the applied TW setup is reproducible [31], thus pointing to other factors giving rise to this heterogeneity. Pronounced inter-individual variations in the EV phenotype have been observed for the vesicles found in plasma of healthy individuals [29]. The quite different EV phenotypes detected in the present study could be a consequence of such variations. This may signify that the EV phenotype can be individually adapted, which is unlike the cellular phenotype described above, for which there were consistent trends for all individuals. However, the heterogeneity of the EV phenotypes complicates identification of their functionality. Nevertheless, there were a few contact-dependent differences, which could be detected for the EV phenotypes. Two T cell-associated proteins, CD3 and CTLA-4, were predominantly observed in the classic MLC, while TNFRI was mostly found on EVs from the TW system. Also, HLA-DR-bearing EVs were mostly observed in the TW compartment holding the stimulator cells. In terms of functionality, the down-regulation of CD3 following T cell activation [56, 57] has been associated with the production of CD3-enriched EVs, as a tool of this down-regulation [58]. Hence, EVs may be used for other purposes than intercellular communication. Though the contact-dependent differences in the EV phenotypes were subtle, they could reflect distinct functions of these vesicles in each of the MLC systems. Nonetheless, this remains to

be delineated. In the context of HLA-DR, it has been noted that vesicles possibly mediate the demonstrated transfer of HLA-DR from APCs to T cells [15-17, 19, 20]. The levels of EV-associated HLA-DR detected for both MLCs were low, either signifying a modest production of HLA-DR bearing EVs or a high uptake rate, rendering them inaccessible to analysis. With the data presented here, it is, however, not possible to support that vesicle-mediated cellular communication is important for the presence of HLA-DR on CD3+ CD4+ T cells without additional studies.

In the current study we elucidated some of the aspects of HLA-DR on human CD3+ CD4+ T cells. We found that APCs play an important role in this context and confirmed that physical contact between these two cells influence the presence of HLA-DR on T cells [17, 20]. Although the allospecific activation gave rise to a heterogeneous population of CD3+ CD4+ HLA-DR+ responder T cells, the phenotype of these cells indicated a regulatory role. We also showed that, in spite of a high degree of heterogeneity, distinct vesicle subsets are formed during alloresponses, which could mediate important cell-to-cell communication. The results of the present study show valid tendencies for the evaluated outcome measures and indicate possible interesting markers for further investigation. This may be used to gain further understanding of the mechanisms of immunologic tolerance with great importance to basic immunology as well as autoimmune diseases, transplantation, and cancer.

Authorship

A.L.S.R. designed and performed research and wrote the manuscript. R.B. performed research and revised manuscript. M.M.J. performed data analysis, contributed to the study design, and revised the manuscript. K.V. and A.S. contributed to the study design, data interpretation, and revised the manuscript

Acknowledgements

The authors gratefully acknowledge technician Anne Elbæk, Department of Clinical Immunology, Aalborg University Hospital, Denmark, for excellent technical assistance.

Conflict of interest disclosure

The authors declare no conflict of interest.

References

1. Evans, R.L., Faldetta, T.J., Humphreys, R.E., Pratt, D.M., Yunis, E.J., Schlossman, S.F. (1978) Peripheral human T cells sensitized in mixed leukocyte culture synthesize and express Ia-like antigens. *J Exp Med* **148**, 1440-5.
2. Ko, H.S., Fu, S.M., Winchester, R.J., Yu, D.T., Kunkel, H.G. (1979) Ia determinants on stimulated human T lymphocytes. Occurrence on mitogen- and antigen-activated T cells. *J Exp Med* **150**, 246-55.
3. Sharrow, S.O., Ozato, K., Sachs, D.H. (1980) Phenotypic expression of I-A and I-E/C subregion determinants on murine thymocytes. *J Immunol* **125**, 2263-8.
4. Yu, D.T., Winchester, R.J., Fu, S.M., Gibofsky, A., Ko, H.S., Kunkel, H.G. (1980) Peripheral blood Ia-positive T cells. Increases in certain diseases and after immunization. *J Exp Med* **151**, 91-100.
5. Reddy, M., Eirikis, E., Davis, C., Davis, H.M., Prabhakar, U. (2004) Comparative analysis of lymphocyte activation marker expression and cytokine secretion profile in stimulated human peripheral blood mononuclear cell cultures: an in vitro model to monitor cellular immune function. *J Immunol Methods* **293**, 127-42.
6. Ferenczi, K., Burack, L., Pope, M., Krueger, J.G., Austin, L.M. (2000) CD69, HLA-DR and the IL-2R identify persistently activated T cells in psoriasis vulgaris lesional skin: blood and skin comparisons by flow cytometry. *J Autoimmun* **14**, 63-78.
7. Shipkova, M., Wieland, E. (2012) Surface markers of lymphocyte activation and markers of cell proliferation. *Clin Chim Acta* **413**, 1338-49.
8. Isaacson, J.A., Flaming, K.P., Roth, J.A. (1998) Increased MHC class II and CD25 expression on lymphocytes in the absence of persistent lymphocytosis in cattle experimentally infected with bovine leukemia virus. *Vet Immunol Immunopathol* **64**, 235-48.
9. Broeren, C.P., Wauben, M.H., Lucassen, M.A., Van Meurs, M., Van Kooten, P.J., Boog, C.J., Claassen, E., Van Eden, W. (1995) Activated rat T cells synthesize and express functional major histocompatibility class II antigens. *Immunology* **84**, 193-201.
10. Reizis, B., Schramm, C., Cohen, I.R., Mor, F. (1994) Expression of major histocompatibility complex class II molecules in rat T cells. *Eur J Immunol* **24**, 2796-802.
11. Baecher-Allan, C., Wolf, E., Hafler, D.A. (2006) MHC class II expression identifies functionally distinct human regulatory T cells. *J Immunol* **176**, 4622-31.
12. Lorber, M.I., Loken, M.R., Stall, A.M., Fitch, F.W. (1982) I-A antigens on cloned alloreactive murine T lymphocytes are acquired passively. *J Immunol* **128**, 2798-803.
13. Patel, D.M., Arnold, P.Y., White, G.A., Nardella, J.P., Mannie, M.D. (1999) Class II MHC/peptide complexes are released from APC and are acquired by T cell responders during specific antigen recognition. *J Immunol* **163**, 5201-10.
14. Patel, D.M., Mannie, M.D. (2001) Intercellular exchange of class II major histocompatibility complex/peptide complexes is a conserved process that requires activation of T cells but is constitutive in other types of antigen presenting cell. *Cell Immunol* **214**, 165-72.
15. Tsang, J.Y., Chai, J.G., Lechler, R. (2003) Antigen presentation by mouse CD4+ T cells involving acquired MHC class II:peptide complexes: another mechanism to limit clonal expansion? *Blood* **101**, 2704-10.
16. Buschow, S.I., Nolte-'t Hoen, E.N., van Niel, G., Pols, M.S., ten Broeke, T., Lauwen, M., Ossendorp, F., Melief, C.J., Raposo, G., Wubbolts, R., Wauben, M.H.,

Stoorvogel, W. (2009) MHC II in dendritic cells is targeted to lysosomes or T cell-induced exosomes via distinct multivesicular body pathways. *Traffic* **10**, 1528-42.
17. Game, D.S., Rogers, N.J., Lechler, R.I. (2005) Acquisition of HLA-DR and costimulatory molecules by T cells from allogeneic antigen presenting cells. *Am J Transplant* **5**, 1614-25.
18. Otten, L.A., Tacchini-Cottier, F., Lohoff, M., Annunziato, F., Cosmi, L., Scarpellino, L., Louis, J., Steimle, V., Reith, W., Acha-Orbea, H. (2003) Deregulated MHC class II transactivator expression leads to a strong Th2 bias in CD4+ T lymphocytes. *J Immunol* **170**, 1150-7.
19. Arnold, P.Y., Mannie, M.D. (1999) Vesicles bearing MHC class II molecules mediate transfer of antigen from antigen-presenting cells to CD4+ T cells. *Eur J Immunol* **29**, 1363-73.
20. Undale, A.H., van den Elsen, P.J., Celis, E. (2004) Antigen-independent acquisition of MHC class II molecules by human T lymphocytes. *Int Immunol* **16**, 1523-33.
21. Wetzel, S.A., McKeithan, T.W., Parker, D.C. (2005) Peptide-specific intercellular transfer of MHC class II to CD4+ T cells directly from the immunological synapse upon cellular dissociation. *J Immunol* **174**, 80-9.
22. Joly, E., Hudrisier, D. (2003) What is trogocytosis and what is its purpose? *Nat Immunol* **4**, 815.
23. Holling, T.M., Schooten, E., van Den Elsen, P.J. (2004) Function and regulation of MHC class II molecules in T-lymphocytes: of mice and men. *Hum Immunol* **65**, 282-90.
24. Pichler, W.J., Wyss-Coray, T. (1994) T cells as antigen-presenting cells. *Immunol Today* **15**, 312-5.
25. Chen, X., Oppenheim, J.J. (2011) The phenotypic and functional consequences of tumour necrosis factor receptor type 2 expression on CD4(+) FoxP3(+) regulatory T cells. *Immunology* **133**, 426-33.
26. Roederer, M. (2001) Spectral compensation for flow cytometry: visualization artifacts, limitations, and caveats. *Cytometry* **45**, 194-205.
27. Herzenberg, L.A., Tung, J., Moore, W.A., Parks, D.R. (2006) Interpreting flow cytometry data: a guide for the perplexed. *Nat Immunol* **7**, 681-5.
28. Jorgensen, M.M., Baek, R., Varming, K. (2015) Potentials and capabilities of the Extracellular Vesicle (EV) Array. *J Extracell Vesicles* **4**, 26048.
29. Jorgensen, M., Baek, R., Pedersen, S., Soendergaard, E.K., Kristensen, S.R., Varming, K. (2013) Extracellular Vesicle (EV) Array: microarray capturing of exosomes and other extracellular vesicles for multiplexed phenotyping. *J Extracell Vesicles* **2**, 20920.
30. Revenfeld, A.L., Baek, R., Nielsen, M.H., Stensballe, A., Varming, K., Jorgensen, M. (2014) Diagnostic and prognostic potential of extracellular vesicles in peripheral blood. *Clin Ther* **36**, 830-46.
31. Revenfeld, A.L.S., Søndergaard, E.K.L., Stensballe, A., Bæk, R., Jørgensen, M.M., Varming, K. (2015) Characterization of a cell culturing system for the study of contact-independent vesicle communication. *J Extracell Vesicles* **Submitted; PhD manuscript 4**.
32. Revenfeld, A.L.S., Steffensen, R., Pugholm, L.H., Jørgensen, M.M., Stensballe, A., Varming, K. (2015) The existence of HLA-DR on circulating CD4+ T cells cannot be explained by a concurrent presence of HLA-DRB1 expression. *BMC Immunol* **Accepted with revisions; PhD manuscript 1**.
33. Felix, N.J., Allen, P.M. (2007) Specificity of T-cell alloreactivity. *Nat Rev Immunol* **7**, 942-53.

34. Peiser, M., Becht, A., Wanner, R. (2007) Antibody blocking of MHC II on human activated regulatory T cells abrogates their suppressive potential. *Allergy* **62**, 773-80.
35. Kuniyasu, Y., Takahashi, T., Itoh, M., Shimizu, J., Toda, G., Sakaguchi, S. (2000) Naturally anergic and suppressive CD25(+)CD4(+) T cells as a functionally and phenotypically distinct immunoregulatory T cell subpopulation. *Int Immunol* **12**, 1145-55.
36. Karim, M., Kingsley, C.I., Bushell, A.R., Sawitzki, B.S., Wood, K.J. (2004) Alloantigen-induced CD25+CD4+ regulatory T cells can develop in vivo from CD25-CD4+ precursors in a thymus-independent process. *J Immunol* **172**, 923-8.
37. Dilek, N., Poirier, N., Hulin, P., Coulon, F., Mary, C., Ville, S., Vie, H., Clemenceau, B., Blancho, G., Vanhove, B. (2013) Targeting CD28, CTLA-4 and PD-L1 costimulation differentially controls immune synapses and function of human regulatory and conventional T-cells. *PLoS One* **8**, e83139.
38. Tai, X., Van Laethem, F., Pobezinsky, L., Guinter, T., Sharrow, S.O., Adams, A., Granger, L., Kruhlak, M., Lindsten, T., Thompson, C.B., Feigenbaum, L., Singer, A. (2012) Basis of CTLA-4 function in regulatory and conventional CD4(+) T cells. *Blood* **119**, 5155-63.
39. Walker, L.S., Sansom, D.M. (2011) The emerging role of CTLA4 as a cell-extrinsic regulator of T cell responses. *Nat Rev Immunol* **11**, 852-63.
40. Kolar, P., Knieke, K., Hegel, J.K., Quandt, D., Burmester, G.R., Hoff, H., Brunner-Weinzierl, M.C. (2009) CTLA-4 (CD152) controls homeostasis and suppressive capacity of regulatory T cells in mice. *Arthritis Rheum* **60**, 123-32.
41. Okazaki, T., Honjo, T. (2006) The PD-1-PD-L pathway in immunological tolerance. *Trends Immunol* **27**, 195-201.
42. Fife, B.T., Bluestone, J.A. (2008) Control of peripheral T-cell tolerance and autoimmunity via the CTLA-4 and PD-1 pathways. *Immunol Rev* **224**, 166-82.
43. Freeman, G.J., Long, A.J., Iwai, Y., Bourque, K., Chernova, T., Nishimura, H., Fitz, L.J., Malenkovich, N., Okazaki, T., Byrne, M.C., Horton, H.F., Fouser, L., Carter, L., Ling, V., Bowman, M.R., Carreno, B.M., Collins, M., Wood, C.R., Honjo, T. (2000) Engagement of the PD-1 immunoinhibitory receptor by a novel B7 family member leads to negative regulation of lymphocyte activation. *J Exp Med* **192**, 1027-34.
44. Butte, M.J., Pena-Cruz, V., Kim, M.J., Freeman, G.J., Sharpe, A.H. (2008) Interaction of human PD-L1 and B7-1. *Mol Immunol* **45**, 3567-72.
45. Bennett, F., Luxenberg, D., Ling, V., Wang, I.M., Marquette, K., Lowe, D., Khan, N., Veldman, G., Jacobs, K.A., Valge-Archer, V.E., Collins, M., Carreno, B.M. (2003) Program death-1 engagement upon TCR activation has distinct effects on costimulation and cytokine-driven proliferation: attenuation of ICOS, IL-4, and IL-21, but not CD28, IL-7, and IL-15 responses. *J Immunol* **170**, 711-8.
46. Curran, M.A., Montalvo, W., Yagita, H., Allison, J.P. (2010) PD-1 and CTLA-4 combination blockade expands infiltrating T cells and reduces regulatory T and myeloid cells within B16 melanoma tumors. *Proc Natl Acad Sci U S A* **107**, 4275-80.
47. Chen, X., Subleski, J.J., Kopf, H., Howard, O.M., Mannel, D.N., Oppenheim, J.J. (2008) Cutting edge: expression of TNFR2 defines a maximally suppressive subset of mouse CD4+CD25+FoxP3+ T regulatory cells: applicability to tumor-infiltrating T regulatory cells. *J Immunol* **180**, 6467-71.
48. Chen, X., Subleski, J.J., Hamano, R., Howard, O.M., Wiltrout, R.H., Oppenheim, J.J. (2010) Co-expression of TNFR2 and CD25 identifies more of the functional CD4+FOXP3+ regulatory T cells in human peripheral blood. *Eur J Immunol* **40**, 1099-106.

49. van Mierlo, G.J., Scherer, H.U., Hameetman, M., Morgan, M.E., Flierman, R., Huizinga, T.W., Toes, R.E. (2008) Cutting edge: TNFR-shedding by CD4+CD25+ regulatory T cells inhibits the induction of inflammatory mediators. *J Immunol* **180**, 2747-51.
50. Andaloussi, S.E.L., Mager, I., Breakefield, X.O., Wood, M.J. (2013) Extracellular vesicles: biology and emerging therapeutic opportunities. *Nat Rev Drug Discov* **12**, 347-57.
51. Gyorgy, B., Szabo, T.G., Pasztoi, M., Pal, Z., Misjak, P., Aradi, B., Laszlo, V., Pallinger, E., Pap, E., Kittel, A., Nagy, G., Falus, A., Buzas, E.I. (2011) Membrane vesicles, current state-of-the-art: emerging role of extracellular vesicles. *Cell Mol Life Sci* **68**, 2667-88.
52. Escola, J.M., Kleijmeer, M.J., Stoorvogel, W., Griffith, J.M., Yoshie, O., Geuze, H.J. (1998) Selective enrichment of tetraspan proteins on the internal vesicles of multivesicular endosomes and on exosomes secreted by human B-lymphocytes. *J Biol Chem* **273**, 20121-7.
53. Nolte-'t Hoen, E.N., Buschow, S.I., Anderton, S.M., Stoorvogel, W., Wauben, M.H. (2009) Activated T cells recruit exosomes secreted by dendritic cells via LFA-1. *Blood* **113**, 1977-81.
54. Okoye, I.S., Coomes, S.M., Pelly, V.S., Czieso, S., Papayannopoulos, V., Tolmachova, T., Seabra, M.C., Wilson, M.S. (2014) MicroRNA-containing T-regulatory-cell-derived exosomes suppress pathogenic T helper 1 cells. *Immunity* **41**, 89-103.
55. Gutierrez-Vazquez, C., Villarroya-Beltri, C., Mittelbrunn, M., Sanchez-Madrid, F. (2013) Transfer of extracellular vesicles during immune cell-cell interactions. *Immunol Rev* **251**, 125-42.
56. Liu, H., Rhodes, M., Wiest, D.L., Vignali, D.A. (2000) On the dynamics of TCR:CD3 complex cell surface expression and downmodulation. *Immunity* **13**, 665-75.
57. San Jose, E., Borroto, A., Niedergang, F., Alcover, A., Alarcon, B. (2000) Triggering the TCR complex causes the downregulation of nonengaged receptors by a signal transduction-dependent mechanism. *Immunity* **12**, 161-70.
58. Choudhuri, K., Llodra, J., Roth, E.W., Tsai, J., Gordo, , S., Wucherpfennig, K.W., Kam, L.C., Stokes, D.L., Dustin, M.L. (2014) Polarized release of T-cell-receptor-enriched microvesicles at the immunological synapse. *Nature* **507**, 118-23.

Figure legends

Figure 1 Presence of HLA-DR on *in vitro* PHA or anti-CD3/anti-CD28 stimulated CD4+ T cells. Isolated CD4+ T cells or PBMCs were stimulated with PHA-P or anti-CD3/anti-CD28 for 20h. Subsequently, the presence of HLA-DR was evaluated by flow cytometry for the CD3+ CD4+ T cells in all samples. Initially, the lymphocytes were gated in a FSC/SSC plot, after which the CD3+ CD4+ cells were identified. Finally, the CD3+ CD4+ HLA-DR+ T cell population was determined. Data is presented as mean ± SEM. **, $p \leq 0.01$; n=2-6.

Figure 2 Cellular proliferation after contact-dependent and -independent MLCs. After a 6-day MLC, either contact-dependent (classic) or contact-independent (transwell; TW), the proliferation of the responder cells was determined. The proliferative response was evaluated by the incorporation of Thymidine-^{3}H from day 5 to 6 of the MLCs and for the responder control sample. Data is presented as mean ± SEM. n=3. Cpm: Counts per minute.

Figure 3 Cellular phenotypes of HLA-DR+ responder CD3+ CD4+ T cells after contact-dependent and -independent MLC. A flow cytometric analysis was used to determine the presence of HLA-DR and other selected cell surface markers on the responder cells of the contact-dependent MLC (classic) and contact-independent MLC (transwell, TW). A) Gating of the responder T cells. Initially, a lymphocyte gate was created in a forward scatter (FSC)/side scatter (SSC) plot. Next, the responder cells were identified from their eFluor 420 labeling after which the CD3+ CD4+ T cells could be selected. Finally, the HLA-DR+ events were identified with a pre-defined gate from a FMO control, in which a maximum of 1% of positive events were allowed in the double-positive quadrant. The plots are representative examples from one of the three included biological replicates. B) To compare their cellular phenotype, a flow cytometric evaluation of seven markers was performed at baseline and at day 6 for the responder HLA-DR T cells from the classic and TW MLC. Selected markers were also investigated for the responder control at day 6. Data is presented as mean ± SEM. n = 3. C) A ratio of the expression of each of the seven markers was made between the classic MLC and the TW MLC, in order to visualize which markers were up- or down-regulated in each condition. CTLA-4: Cytotoxic T-lymphocyte associated protein 4 (CD152); PD-1 Programmed cell death 1 (CD279); TNFRII: Tumor necrosis factor receptor II (CD120b). **, $p \leq 0.01$

Figure 4 Differential expression of several surface markers on HLA-DR+ and HLA-DR- responder T cells. The differential expression of the seven cell surface markers shown in Figure 3B was also investigated for the corresponding HLA-DR- responder T cell subset. These cells were identified from the top left quadrant of the last plot in Figure 3A. A) The correlation plots with adjunct histograms show the correlation between CTLA-4 and CD25 (top panel) and PD-1 and TNFRII (bottom panel) for CD3+ CD4+ HLA-DR+ responder T cells and the HLA-DR- equivalent.

All markers were enriched in the HLA-DR-presented subset in both types of MLCs. The plots are representative examples for the three biological replicates included. C) The histograms demonstrate how the expression of CD11a was increased in the CD3+ CD4+ HLA-DR+ responder T cells, when compared to the CD3+ CD4+ HLA-DR- subset. The histograms are representative for the three biological replicates included.

Figure 5 The phenotype of extracellular vesicles (EVs) from the MLCs display contact-dependent differences. The EV Array was applied to extensively phenotype the EVs from the cell supernatant from the MLCs. Antibodies targeting the listed markers were used for capturing of the EVs. The signal observed for each of the markers infers a simultaneous presence of CD9, CD63, and/or CD81, since a cocktail of antibodies against these three exosomal markers was used for detection. A) Summary of selected, investigated EV markers for two of the three included replicates. The heat map for the third replicate can be found in [31]. B) The relative distribution of selected EV markers for all MLCs and controls are visualized for the highly expressed markers (left plot) and for those with a lower expression (right plot). Data is presented as mean ± SEM. C) A semi-quantitative EV Array analysis was performed for the EVs produced by non-irradiated and irradiated PBMCs after 6 days in culture. n = 1.

Figures

Figure 1

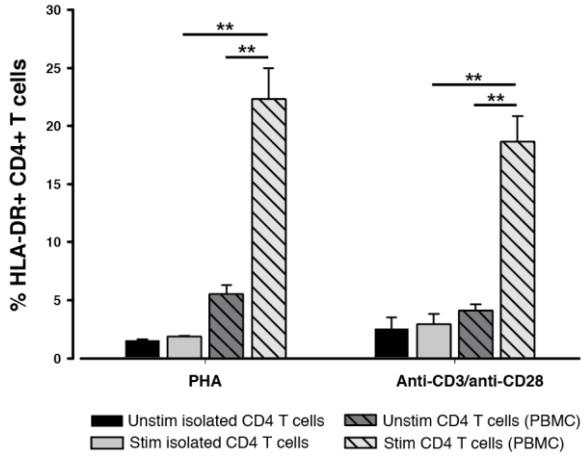

Figure 2

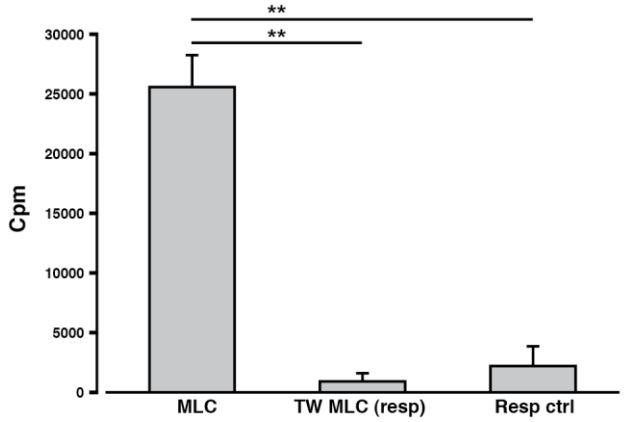

Figure 3

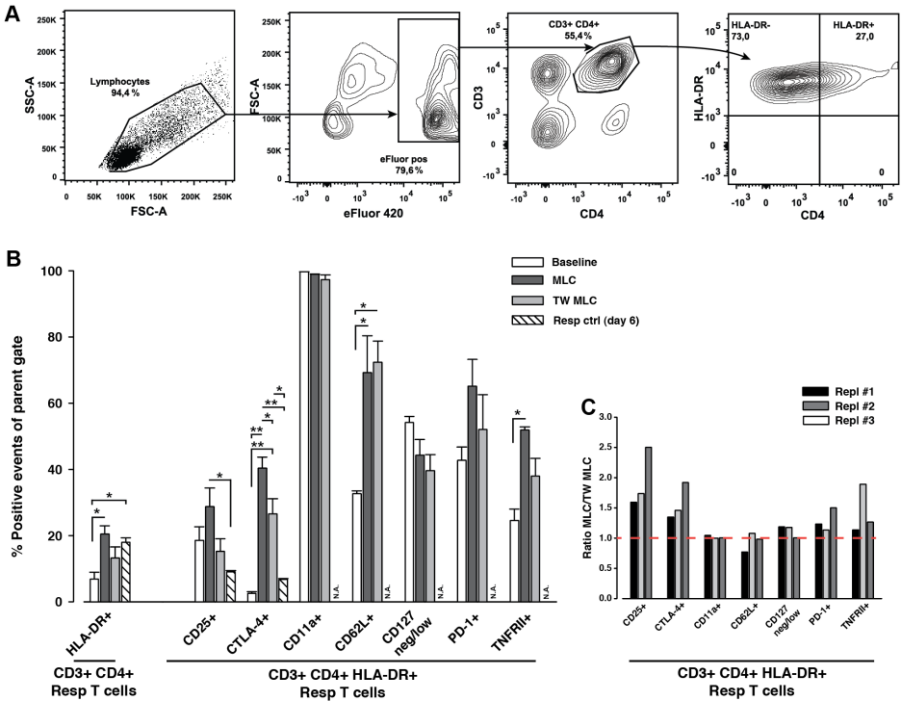
A
Lymphocytes
94,4 %
SSC-A
FSC-A
eFluor pos
79,6 %
eFluor 420
CD3+ CD4+
55,4 %
CD3
CD4
HLA-DR-
73,0
HLA-DR+
27,0
HLA-DR
B
Baseline
MLC
TW MLC
Resp ctrl (day 6)
% Positive events of parent gate
HLA-DR+
CD25+
CTLA-4+
CD11a+
CD62L+
CD127 neg/low
PD-1+
TNFRII+
N.A.
CD3+ CD4+ Resp T cells
CD3+ CD4+ HLA-DR+ Resp T cells
C
Repl #1
Repl #2
Repl #3
Ratio MLC/TW MLC
CD3+ CD4+ HLA-DR+ Resp T cells

Figure 4

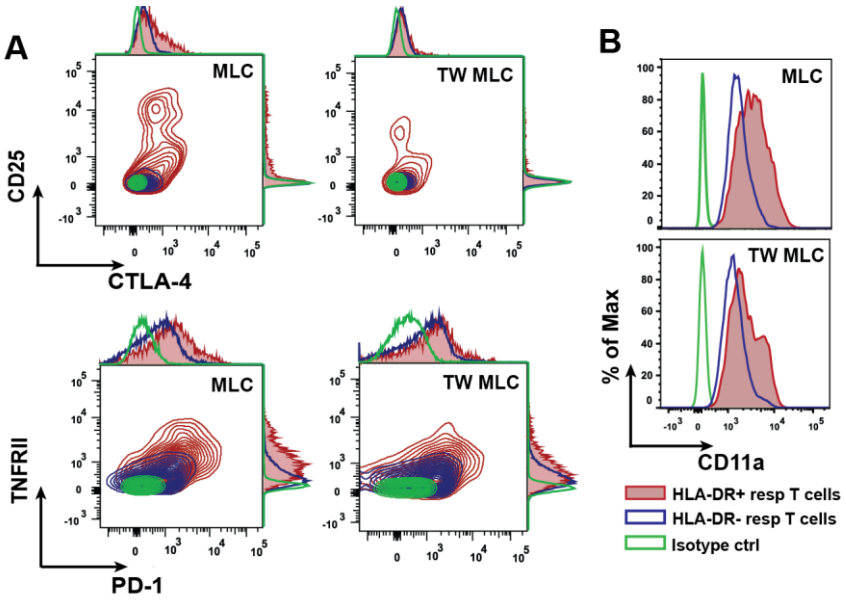
A
MLC
TW MLC
CD25
CTLA-4
MLC
TW MLC
TNFRII
PD-1
B
MLC
TW MLC
% of Max
CD11a
HLA-DR+ resp T cells
HLA-DR- resp T cells
Isotype ctrl

Figure 5

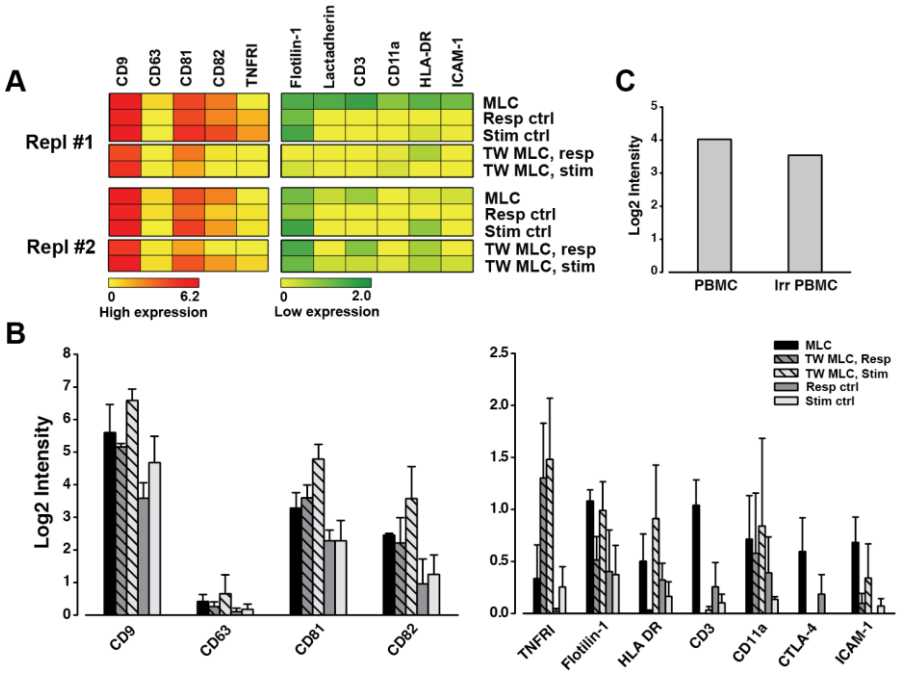
A
CD9
CD63
CD81
CD82
TNFRI
Flotilin-1
Lactadherin
CD3
CD11a
HLA-DR
ICAM-1
Repl #1
Repl #2
MLC
Resp ctrl
Stim ctrl
TW MLC, resp
TW MLC, stim
0
6.2
High expression
0
2.0
Low expression
C
Log2 Intensity
PBMC
Irr PBMC
B
Log2 Intensity
CD9
CD63
CD81
CD82
MLC
TW MLC, Resp
TW MLC, Stim
Resp ctrl
Stim ctrl
TNFRI
Flotilin-1
HLA DR
CD3
CD11a
CTLA-4
ICAM-1

B3 - Manuscript 3

Clinical Therapeutics/Volume 36, Number 6, 2014

Review Article

Diagnostic and Prognostic Potential of Extracellular Vesicles in Peripheral Blood

Anne Louise Schacht Revenfeld, MSc[1]; Rikke Bæk, MSc[2]; Morten Hjuler Nielsen, MSc[3]; Allan Stensballe, PhD[1]; Kim Varming, MD[2]; and Malene Jørgensen, PhD[2]

[1]*Laboratory for Medical Mass Spectrometry, Section for Biomedicine, Aalborg University, Aalborg, Denmark;* [2]*Department of Clinical Immunology, Aalborg University Hospital, Aalborg, Denmark; and* [3]*Department of Clinical Biochemistry, Aalborg University Hospital, Aalborg, Denmark*

ABSTRACT

Purpose: Extracellular vesicles (EVs) are small, membrane-enclosed entities released from cells in many different biological systems. These vesicles play an important role in cellular communication by virtue of their protein, RNA, and lipid content, which can be transferred among cells. The complement of biomolecules reflects the parent cell, and their characterization may provide information about the presence of an aberrant process. Peripheral blood is a rich source of circulating EVs, which are easily accessible through a blood sample. An analysis of EVs in peripheral blood could provide access to unparalleled amounts of biomarkers of great diagnostic and prognostic value. The objectives of this review are to briefly present the current knowledge about EVs and to introduce a toolbox of selected techniques, which can be used to rapidly characterize clinically relevant properties of EVs from peripheral blood.

Methods: Several techniques exist to characterize the different features of EVs, including size, enumeration, RNA cargo, and protein phenotype. Each technique has a number of advantages and pitfalls. However, with the techniques presented in this review, a possible platform for EV characterization in a clinical setting is outlined.

Findings: Although EVs have great diagnostic and prognostic potential, a lack of standardization regarding EV analysis hampers the full use of this potential. Nevertheless, the analysis of EVs in peripheral blood has several advantages compared with traditional analyses of many soluble molecules in blood.

Implications: Overall, the use of EV analysis as a diagnostic and prognostic tool has prodigious clinical potential. (*Clin Ther.* 2014;36:830–846) © 2014 The Authors. Published by Elsevier HS Journals, Inc.

Key words: Extracellular vesicles, microvesicles, exosomes, diagnostics, phenotyping, RNA cargo, enumeration.

INTRODUCTION

In recent years, interest in the characterization, biogenesis, and function of extracellular vesicles (EVs) has increased immensely. These membrane-derived vesicles play vital roles in a plethora of processes in several biological systems. In humans, EVs are pivotal to cellular communication for the maintenance of homeostasis and the development and progression of pathologic conditions, such as cancer. Consequently, this communication forms the basis for the use of EV analysis in a clinical setting because EVs seem to be a promising source of biomarkers of diagnostic and prognostic value. EV analysis can likely be used as one component of treatment surveillance. In addition, EVs have the potential of being used as drug therapy entities, delivering a tailored pharmacologic cargo to a specific target.

Accepted for publication May 15, 2014.
http://dx.doi.org/10.1016/j.clinthera.2014.05.008
0149-2918/$ - see front matter

Classification of EVs

In general, EVs are a heterogeneous population of membrane-enclosed vesicles released from a variety of cells into the extracellular space *in vivo* and *in vitro*. One general feature for these vesicles is that they are enclosed by a membrane that consists of a phospholipid bilayer. However, the EVs can be divided into a number of subpopulations each with specific characteristics, including their biogenesis, size, cellular origin, protein composition, mRNA and microRNA (miRNA) content, and/or biological function. With biogenesis as a classification tool, the EVs can be divided into 3 major groups: exosomes, microvesicles (MVs), and apoptotic bodies. Many of the properties of EVs, and in particular exosomes, have been reviewed extensively elsewhere[1–9]; therefore, the following section states the overall characteristics of these 3 EV groups.

Exosomes

Exosome is the vesicle type that has been studied most intensely. They are approximately 30 to 100 nm in diameter and originate from inward budding of the limiting membrane of multivesicular bodies, which are late endosomal compartments present in the cytosol of the cell.[4,6,10,11] When the multivesicular bodies fuse with the plasma membrane, the release of the exosomes to the extracellular space is facilitated. The biogenesis of the exosomes causes the orientation of the membrane proteins to be similar to that of the plasma membrane. The exosomal membrane is enriched in cholesterol, ceramide, and sphingomyelin and exposes the phospholipid phosphatidylserine.[6,11] In addition, exosomes contain several proteins that are currently used as markers to identify exosomes. These makers are not ubiquitously expressed on all exosomes but are found in a large proportion of these vesicles. Therefore, they are generally accepted as exosomal markers. These markers include TSG101, Alix, and the tetraspanins CD9, CD63, and CD81.[2,4] Along with these hallmark proteins, the phenotype of exosomes often reflects a molecular signature of the cell from which they originate. This cell-specific signature may provide some indication about the functionality of the exosomes because some of these signature molecules could ensure the delivery of the exosomes to the correct target cell,[12] point to a signal being transduced by a receptor-ligand interaction of exosomes and recipient cell,[13] or simply indicate which cells are the active exosome producers.[14] The composition of the exosome cargo can also be related to the potential biological function of this vesicle type. They have been known to contain proteins from both the plasma membrane and cytosol along with mRNA and the non–protein-coding miRNAs and small interfering RNAs.[2,15–17]

Microvesicles

The size of MVs ranges from 100 to 1000 nm. They are formed from outward budding of the plasma membrane, thus releasing the MVs directly into the extracellular space.[2,4,18] Hence, the membrane proteins of MVs retain the topologic features of those found in the plasma membrane. Generally, most MVs incorporate phosphatidylserine in the outer leaflet of the membrane.[4,6,10,19] This feature has frequently been used to isolate and identify MVs from biological samples along with a combination of cell-specific protein markers to determine their cellular origin.[19,20] However, several studies indicate that phosphatidylserine may only be present in some subpopulations of MVs.[21–24] Currently, there is a less extensive list of markers to identify MVs when compared with exosomes. Nonetheless, CD40 ligand, adenosine diphosphate ribosylation factor 6, and several integrins and selectins have been proposed as MV markers.[2,5,6,18,25] Like exosomes, the phenotype of MVs reflects their parent cell, and the content of the vesicle cargo also includes membrane and cytosolic proteins, mRNA, and miRNAs.[2,5]

Apoptotic Bodies

Apoptotic bodies are the largest vesicle type of the 3 major EV classification groups, with a size ranging from approximately 500 to 4000 nm.[26,27] They are formed from blebbing of the plasma membrane in cells undergoing apoptosis, releasing the apoptotic bodies straight into the extracellular space.[4] Similar to both the membrane of exosomes and MVs, phosphatidylserine can be found in the outer leaflet of the lipid bilayer of apoptotic bodies.[2,6,10,28] In terms of identifying apoptotic bodies, thrombospondin and complement component C3b are in many cases accepted apoptotic body markers.[1] Unlike the 2 other vesicle types, apoptotic bodies are distinguished by containing organelles, DNA fragments, and histones as a part of the vesicular cargo in addition to proteins and other molecules from the cytosol of the parent cell.[2,4,27,28]

EVs and the Immune System

Because some of the first reports of vesicular release were published 3 decades ago,[29,30] an

enormous amount of research has been performed to delineate all aspects of this phenomenon, however, predominantly related to exosomes and MVs. Within the field of immunology, the evidence of the immunomodulatory effects of EVs has steadily increased throughout the years. Several studies document that many of the cells of the adaptive and innate immune system release EVs, including T and B lymphocytes, dendritic cells, and mast cells.[12,15,31–33] Exosomes have in particular been implicated in several contexts of antigen presentation. T cells can be activated by major histocompatibility complex II–bearing exosomes from antigen-presenting cells,[12] and some T cells even acquire these major histocompatibility complex II molecules,[34] enabling them to present antigens to other T cells.[13] On the transcriptional level, miRNA can also be transferred from T cells to antigen-presenting cells by exosomes, and this molecular transfer changes the gene expression of the recipient cell.[13] In relation to pathologic challenges of the immune system, EVs have been associated with the spread of several types of infection. Accordingly, EVs from cells infected with HIV-1, Epstein-Barr virus, hepatitis C virus, and cytomegalovirus mediate the spread of these pathogens by entering the recipient cell.[35,36] In addition, EVs from infected cells can help initiate a proper immune response against the pathogen.[37] Numerous studies have found that tumor-derived EVs can exert immunosuppressive functions, thus promoting tumor progression.[38] This can be facilitated by modulation of T cells, including the inhibition of both function and proliferation of anti–tumor-specific T cells[39] or by promotion of suppressive subsets of T cells.[40,41] Tumor-derived EVs can also play a role in transferring oncogenic activity, as was observed with the vesicular transfer of the oncogenic epidermal growth factor receptor vIII from glioma cells.[42] This receptor could also be detected on tumor EVs in serum from a number of patients with glioblastoma.[17]

Currently, it is apparent that several aspects of the mechanisms and functional consequences of EVs have yet to be determined. Nonetheless, it is also evident from the work already performed that EVs are central to an abundance of cellular processes, including those of a pathologic nature, and consequently have great potential as targets for diagnosis, prognosis, or treatment.

DIAGNOSTIC AND PROGNOSTIC POTENTIAL OF EVs IN PERIPHERAL BLOOD

Numerous studies have established that EVs can be detected in a multitude of biological fluids, such as saliva, urine, blood, ascites, breast milk, and cerebrospinal fluid.[1,8,9] In this context, blood is an immense source of EVs, and serum is estimated to contain approximately 3×10^6 exosomes per microliter.[8] Because EVs are released constitutively into the bloodstream and this release increases on cellular activation, as well as in many pathologic conditions,[43–46] a mere enumeration of EVs may indicate the presence of an aberrant process. In many aspects of diagnostics, the use of blood samples is already implemented in the clinic because it is known that blood harbors a vast amount of biomarkers and other biologically relevant molecules. In addition, most tissues will contribute to this molecular reservoir due to dense vascularization of the body. In line with this, the analysis of EVs in peripheral blood is likely to provide an indicator of the systemic health status, which can be used in clinical settings.

Analysis of EVs in Peripheral Blood

The use of EV analysis encompasses several advantages over the traditional analyses of many soluble molecules in blood, such as hormones and cytokines. One significant advantage is the inherent protection of the EV cargo of proteins and RNA from degradation, thus rendering them intact and functional.[17] Otherwise, they would be rapidly degraded in blood.[8] This has proven to be particularly significant for the use of miRNA as valuable biomarkers because most RNA in blood exists as cargo of EVs. Regarding another aspect of stability, EVs appear to have a relatively long half-life in blood.[8] Therefore, EVs can likely be transported from any location of the body to the bloodstream, thus making them easily accessible for analysis, compared with biopsies. This also has a significant advantage for the patient because the collection of a blood sample is a minimally invasive procedure associated with much less discomfort than a biopsy. Another advantage of EVs links to the great dynamic range of molecules present in the bloodstream. It can often become an issue to detect relevant biomarkers because these diagnostic molecules frequently constitute a small part of the total amount of molecules in a blood sample.[47,48] This is also the case for EV-associated proteins, which for exosomes denote $<0.01\%$ of the plasma proteome.[9] However, on the basis of the presence of a relatively small panel of markers, EVs can be identified, and the phenotype and cargo, holding biomarkers of

otherwise undetectable amounts, can be analyzed and interpreted into clinically relevant information. Furthermore, EV size distribution, phenotype, or cargo content can seemingly change according to the progression of a disease.[43–46,49,50] The access to cell-specific and disease state–specific EV profiles of proteins and RNA from a blood sample renders a sophisticated fingerprint of a disease of diagnostic and prognostic value.

EV Analysis in Risk Stratification

Cases are emerging in which EV analyses of blood samples seem to be good candidates as a part of a diagnostic platform. In addition, some examples exist in which this type of analysis shows a promising prognostic potential. As previously mentioned, the number of detectable EVs in a blood sample seems to increase in several types of cancers compared with healthy individuals.[43–46,49,50] Moreover, in some cases the amount of EVs continuously increase as the disease progresses into later stages.[44,45] In further relation to cancer, protein and RNA biomarkers have been identified in EVs from the peripheral circulation, with the preponderance of cases that involve miRNAs found in exosomes. Accordingly, several cases reveal that either a single or a panel of differentially expressed miRNAs can significantly identify patients with cancer compared with control individuals.[46,50] A selected number of EV miRNAs, which have the potential to become biomarkers of several cancer types, are given in Table I.

Table I. miRNAs differentially expressed pathologic conditions.

miRNA	Cancer Type	Reference
miR-1	NSCLC	51
miR-15b	Melanoma	52
miR-17-3p	Colorectal cancer	53
miR-21	DLBCL	54
	Glioblastoma	17
	Ovarian cancer	55
miR-25	NSCLC	56
miR-30d	NSCLC	51
miR-92	Colorectal cancer	53
	Ovarian cancer	55
miR-93	Ovarian cancer	55
miR-141	Prostate cancer	57
miR-155	DLBCL	54
	Breast cancer	58
miR-182	Melanoma	59
miR-210	DLBCL	54
miR-223	NSCLC	56
miR-486	NSCLC	51
miR-499	NSCLC	51

DLBCL = diffuse large B-cell lymphoma; miRNA = micro-RNA; NSCLC = non-small cell lung cancer.

The use of EV protein markers in risk stratification has also been investigated. One study found that the presence of 2 exosomal proteins in exosomes from plasma distinguished patients with ovarian cancer from controls.[43] In another study, EVs from patients with gastric cancer had significantly increased expression of 2 proteins, including HER2/neu, when compared with controls.[44] From this study, an interesting notion arises, indicating that some EV markers may not exclusively be used in diagnosis but could also indicate which patients are eligible for a specific treatment. A list of disease-related EV proteins from blood is given in Table II.

CHARACTERIZATION OF EVs IN PERIPHERAL BLOOD

The characterization of EVs in peripheral blood can be based on several of their biochemical and biophysical properties. These properties include size, cargo, density, morphologic findings, lipid composition, and protein phenotype. Currently, a wide range of techniques facilitates EV analysis. Some techniques have existed for years and are being further developed to embrace the challenges of this type of analysis. Other techniques have emerged as a consequence of the increasing interest within the field. The focus of the following section is to introduce a toolbox of selected techniques that could be part of a potential platform to rapidly characterize several clinically relevant properties of EVs in peripheral blood. An overview of the steps from blood sample to output of the analysis will be presented for each technique along with advantages and pitfalls. A summary of several key features associated with the presented techniques is outlined in Figure 1.

Isolation of EVs From Peripheral Blood

One aspect that is a prerequisite for almost all techniques used for EV analysis is isolation of EVs

Table II. Selected protein extracellular vesicle markers isolated from blood.

Disease	Markers	Reference
Ovarian cancer	L1CAM, CD24, ADAM10, EMMPRIN	60
	TGFβ1, MAGE3/6	43
	Claudin-4	49
Glioblastoma	EGFRvIII	17
	EGFR, EGFRvIII, PDPN, IDH1	61
Melanoma	CD63 and Caveolin 1	62
Oral cancer	FasL	63
Gastric cancer	HER-2/neu, CCR6	44
Cancer-associated thrombosis	Tissue factor (CD142)	64
Alzheimer disease	Amyloid B	65

from the biological fluid in which they are present. Hence, it is evident that EV isolation is essential, and with no standardized protocols yet, this is a major focus in the field of EV research.[66] This section introduces the key points of EV isolation because many aspects of this procedure have been recently described elsewhere.[8,66–68] Currently, most studies of EVs use differential centrifugation for isolation, sometimes accompanied by a size filtration step.[66,68] The isolation includes numerous sequential centrifugation steps with increasing centrifugal force, thus using size and density properties of the EV subsets to separate these from other components of blood. Initially, low-speed steps (300-500*g*) are applied to remove whole cells.[43,67] This is followed by higher speeds, typically in the range of 10,000 to 20,000*g*, to remove cellular debris and to isolate larger EVs >100 nm.[43,66,68–70] Finally, one or more ultracentrifugation steps are applied to pellet the smallest EVs, using centrifugal forces in the range of 100,000 to 200,000*g*.[43,66–68] It is also possible to combine the ultracentrifugation with a density gradient, such as sucrose or iodixanol,[67] or affinity purification.[71] Nevertheless, the choice of isolation procedure may have a considerable effect on the downstream analyses of EVs from blood. In addition to isolation, the preanalytical procedures also encompass choice of anticoagulant, processing temperature, and storage before analysis. These variables are all likely to affect the dynamic material that blood constitutes, and although standardizations are in the pipeline, several recommendations have been published.[66]

PHENOTYPING AND PROTEIN VALIDATION

Several methods exist to characterize the protein composition of EVs, related to either a surface marker phenotype or the proteins present in the EV cargo. Although the EV phenotype is particularly important in the determination of cellular and subcellular origin, it can in combination with a protein cargo analysis also provide clues about the functionality of the EVs. The following section focuses on 4 techniques used for characterization of EV proteins because they have great potential as reliable methods used in EV analysis. Common to all 4 methods is the dependence and use of antibodies. Consequently, they all rely on the specificity and sensitivity of the applied antibodies. Currently, no proteins are known to be constitutively sorted into vesicles independently of the subcellular origin of the vesicle and the activation status of the producing cell. This lack of invariant housekeeping markers hampers the quantitative analysis of vesicles. In the 1990s, exosomes derived from B cells were discovered to contain the lysosomal membrane protein CD63,[72] and later other members of the tetraspanin superfamily were found to be enriched in exosomes as well.[73] These early studies also found that exosomal CD63 is present in a much lower amount compared with that of the producing cells. In contrast, CD81 was >10-fold up-regulated in exosomes.[73] The phenotyping of plasma exosomes from 7 healthy donors revealed a similar tendency, indicating that CD63 is less represented and in a heterogeneous manner in relation to CD81 and CD9.[74] This finding could challenge the common

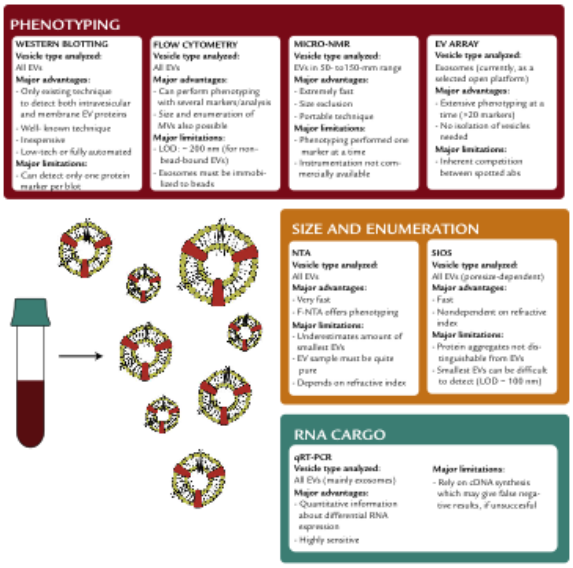

Figure 1. Overview of the techniques used to analyze extracellular vesicles (EVs) present in blood samples from a clinical and diagnostic perspective. The 3 major characterization areas are illustrated (phenotyping, size and enumeration, and RNA cargo) and the major advantages and pitfalls are outlined for each of the techniques presented in this review. abs = antibodies; cDNA = complementary DNA; LOD = limit of detection; F-NTA = fluorescence nanoparticle tracking analysis; micro-NMR = micro-nuclear magnetic resonance; MVs = microvesicles; NTA = nanoparticle tracking analysis; qRT-PCR = quantitative real-time reverse transcription–polymerase chain reaction; SIOS = scanning ion occlusion sensing.

perception of CD63 as an optimal exosomal marker,[72] which may have been attributed solely to its initial discovery and description. Consequently, it is important to choose the markers for EV phenotyping carefully.

Western Blotting

The analytical technique called Western blotting (WB) or immunoblotting is a widely accepted method used to detect specific protein markers in EVs. In general, WB is applied to validate the presence or absence of EV protein markers in purified samples based on the availability of specific antibodies.[75–80]. A major advantage of WB is the possibility of detecting intravesicular and membrane-associated proteins with the same technology (Figure 1). The basic principle of WB[81–83] is outlined in Figure 2A. The results obtained by WB are semiquantitative and can be correlated to the presence of a uniformly expressed protein. Multiple steps of centrifugation of the EV-containing

samples are generally needed before analysis.[71,80,84] In addition, the amount of EV-containing sample used for WB can vary greatly. To illustrate this, it was possible to generate 5 WBs using an EV sample of 200 µL of plasma,[84] whereas another study used WB analysis for the detection of CD63 in EVs and was able to accomplish this with approximately 0.2 µg of EV protein, equivalent to 10^8 EVs.[61] Because WB depends on a high protein concentration, sample preparation with ultracentrifugation is needed, which may be difficult in many clinical laboratories. Nonetheless, if the diagnostic or prognostic marker is of intravesicular origin, WB remains the only usable detection method of those currently applied.

Flow Cytometry

Flow cytometry is a powerful technique for multiparametric analysis of single biological particles and remains the most extensively used technique for enumeration and phenotyping of EVs in clinical samples.[85–90] By suspending particles in a hydrodynamically focused fluid stream passing a laser beam, this technique allows simultaneous analysis of the physical characteristics, including size and granularity, and expression of multiple antigens of up to thousands of particles per second.[91,92] Different approaches are applied when phenotyping either MVs or exosomes by flow cytometry. MVs are typically identified as particles with a forward scatter smaller than an internal standard that consists of approximately 1-µm beads.[93] Figure 2B illustrates how MVs can be distinguished using a blend of size-calibrated fluorescent beads. When analyzing a plasma sample, better specificity of MV detection is obtained by identifying those MVs that expose phosphatidylserine and cell-specific markers (Figure 2B). In addition, MV count per analyzed volume can easily be calculated by adding a known number of fluorescent latex beads as an internal standard. For the phenotyping of MVs by flow cytometry, use of 50 to 100 µL of platelet-free plasma is recommended.[21] Use of flow cytometry to phenotype exosomes and other EVs <200 nm normally depends on adsorption of these vesicles onto antibody-coated beads (Figure 2C). The beads are large enough to facilitate the detection of these small vesicles, which would otherwise fall below the lower limit of detection (Figure 2C). A multiparametric analysis of the EVs captured onto the beads can be performed using fluorescent-labeled antibodies against selected EV surface markers.[90] To be able to use flow cytometry for plasma exosome characterization, an isolation procedure is needed. As an example, a 3-step centrifugation isolation on 3 mL of plasma can be used as a preparatory procedure before the phenotyping.[89,90] The previous generation of flow cytometers is challenged by the small size and signals from most EVs, and several laboratories have reported that a size of 0.5 µm is the cutoff value for accurate identification.[94] However, the enhanced sensitivity of modern digital flow cytometers allows the detection of EVs in the range of approximately 200 nm to 1.0 µm[21] (Figure 1).

Micro–Nuclear Magnetic Resonance

Micro–nuclear magnetic resonance (µ-NMR) is a highly sensitive and rapid analytical technique developed for profiling circulating EVs from blood samples.[61] The technique uses size and immunoaffinity to define an EV population and favors EVs in the range of 50 to 150 nm. The EVs are labeled with target-specific magnetic nanoparticles and detected by a hand-sized NMR system[95,96] (Figure 2D). A prototype µ-NMR system has previously been used for the detection of whole tumor cells (target size range, >10 µm).[97] The output of the µ-NMR technique is a MV expression of an EV protein marker, which is calculated as the decay rate of the target protein normalized to that of a selected exosomal marker, such as CD63.[61] The output is quantitative in a relative way across samples but cannot be assigned a definitive number of vesicles or number of marker molecules on each vesicle.[61] Before loading the blood sample onto the chip, a 2-step centrifugation purification is needed. The pelleted EVs can be loaded onto the µ-NMR device for analysis, and the relative contents of a single EV marker are determined within seconds. Signals are detectable to approximately 10^4 of EVs, which is equivalent to 0.02 ng of EV protein.[61] Even if it has been established that the expression of CD63 measured by µ-NMR correlates with the number vesicles present,[61] this may not be the case with EVs from all cellular systems. Hence, care should be taken to choose the appropriate exosomal marker for normalization.

EV Array

The EV array is based on the technology of protein microarray and is capable of detecting and phenotyping

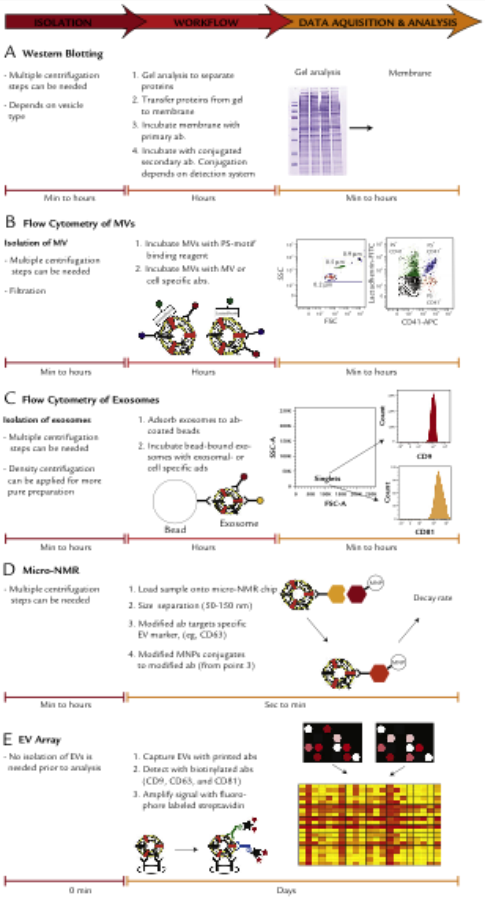

Figure 2. Outline of the workflow and timeframes for the presented techniques used for phenotyping of extracellular vesicles (EVs) from peripheral blood. (A) Western Blotting, (B) flow cytometry of microvesicles (MVs), (C) flow cytometry of exosomes, (D) micro-nuclear magnetic resonance (micro-NMR), and (E) EV Array. abs = antibodies; MNP = magnetic nanoparticles; PS = phosphatidylserine.

EVs from unpurified starting material in a high-throughput manner.[74] The technology is developed to perform multiplexed phenotyping of EVs in an open platform; however, it is optimized to analyze the exosomal EV subset. Protein microarrays are well accepted as powerful tools to search for antigens or antibodies in various sample types.[98,99] Micrometer-sized spots of capturing antibodies against known EV surface antigens are printed in a customized spot setup. The basic principle of the subsequent analysis is outlined in Figure 2E. The captured vesicles are detected using a cocktail of antibodies against the tetraspanins CD9, CD63 and CD81.[72,78] The antibodies are applied to ensure that all exosomes captured are detected, as well as excluding other types of EVs from being detected. The read-out is a fluorescence signal for each individual microarray spot (Figure 2E). The method is semiquantitative and gives the phenotype of EVs for 21 protein markers simultaneously. Plasma samples are analyzed directly without any further purification or isolation steps, and only 10 μL of plasma is needed. It has been established that only 2.5×10^4 exosomes is required for each microarray analysis.[74] The technique uses an overnight incubation to capture the EVs. Because of the incubation time and the remaining development procedure, this method takes approximately 2 days to complete, making it the slowest assay of the ones presented in this review.

ENUMERATION AND SIZE

Determination of the amount and size distribution of EVs in a blood sample is greatly valuable because of the previously mentioned observation that an increased production of EVs has been detected in several pathologic conditions. In addition, knowing the size of the EVs present can be informative because it can indicate which vesicle type is the most dominant type in an unprocessed sample and provide information about the quality of an isolation procedure.[100] Several methods exist to enumerate EVs and determine their size. The following section focuses on 2 of these because they have great potential as fast methods used in EV analysis.

Nanoparticle Tracking Analysis

Nanoparticle tracking analysis (NTA) allows for a quick size determination and quantification of EVs in a suspension. It was first introduced in 2006 and has in recent years received significant attention within the field of EV analysis.[101] The technique is based on relating the Brownian motions of a particle to its size. Brownian motions are experienced by all particles in a fluid, here constituted by EVs in a suspension. These motions can be tracked when the particles are illuminated by a laser beam and scatter the light[101–103] (Figure 3A). An image processing software subsequently calculates the size distribution and concentration of particles in the solution.[100,101,104] The NTA determines these factors most precisely for EVs in the range of 30 to 1000 nm in a concentration of approximately 10^8 to 10^9 particles/mL.[100,102] Hence, NTA seems to offer a more sensitive enumeration than other conventional methods, such as flow cytometry. For the analysis of plasma, the high content of lipoprotein particles may pose a significant problem.[101] Consequently, it is a prerequisite to isolate the EV type of interest before NTA, when analyzing these vesicles from plasma or serum.[101] As an interesting notion, selected NTA instruments allow for the expansion to fluorescence NTA in which EVs can be labeled with antibodies conjugated to stable fluorophores and subsequently be phenotyped in addition to the enumeration and concentration determination.[103]

Scanning Ion Occlusion Sensing

The scanning ion occlusion sensing (SIOS) method is a relatively new technology that facilitates a fast analysis of EV size, concentration, and biochemical composition. The technology is nonoptical, label free, and based on passing each EV through a nanopore in a membrane by means of single-molecule electrophoresis.[105] The basic principle is shown in Figure 3B. A transmembrane current drives the electrophoresis, and an ionic current through the nanopore channel can be measured.[105] The passing EV shifts this current, and the transient blockade of the pore can be translated into information about size and surface charge.[102] In addition to the size and surface charge, the total number of EVs passing the nanopore is detected, and the read-out can be depicted as a plot of concentration versus size distribution (Figure 3B). The SIOS has a reported usability for particles in the large range of 70 nm to 10 μm and in the concentration of 10^5 to 10^{12} particles/mL.[102] The use of complex samples can pose some difficulties because protein aggregates cannot be separated from MVs, which is explained by their similar size (Figure 1). In contrast to NTA,

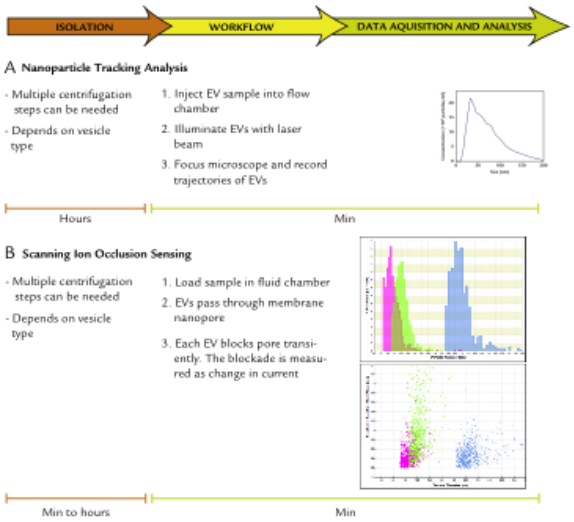

Figure 3. Outline of the workflow and timeframe for the presented techniques used for size determination and enumeration of extracellular vesicles (EVs). (A) Nanoparticle tracking analysis; (B) Scanning Ion Occlusion Sensing.

SIOS does not depend on the refractive index of the particles analyzed because it is a nonoptical technique.

RNA CARGO

Along with the increasing attention on EVs, it has become consistently apparent that their RNA cargo contributes to the potential diagnostic and prognostic value of these vesicles. As mentioned previously, several research groups have reported that the RNA present in serum and plasma is in fact protected from the highly active RNases when being stored inside the different kind of vesicles.[16,57,106,107] In addition, the major content of the EVs has been found to be small RNAs, such as mRNA and miRNA,[17,108] the latter being small non–protein-coding pieces of RNA, consisting of 18–24 nucleotides.[57,109,110] They are known to play important roles in the regulation of mRNA, which they can target for cleavage.[109] The expression of miRNAs seems to depend on the cellular function and in some cases on the cellular stage. In addition, a number of miRNAs are specific to cell type or tissue.[109] As previously mentioned, a rapidly expanding list of miRNAs as potential biomarkers is forming, in which a differential expression can be detected between healthy and pathologic conditions, in particular related to cancer. A selection of such EV miRNA markers is given in Table I. When focusing on the discovery of potential miRNA biomarkers, approaches such as microarray analyses and deep sequencing are useful techniques to perform a wide search. Such a search can be performed with pooled samples of a chosen disease group versus a control group. After single or multiple

candidates are identified, a more targeted manner is chosen to validate and quantify these findings to reveal the true diagnostic potential.[56] This is facilitated by quantitative real-time reverse transcription–polymerase chain reaction (qRT-PCR).[70] Because the qRT-PCR technique is the most relevant as a possible clinically test to characterize the EV RNA cargo, this is the focus of the following section.

qRT-PCR

The qRT-PCR technique is based on the PCR, which is used to amplify and simultaneously quantify a targeted RNA molecule.[111] For ≥1 specific sequences in a sample, qRT-PCR enables detection and quantification. The quantity can be an absolute number of copies or a relative amount when normalized to RNA input or additional reference genes. Initially, the characterization of the EV RNA cargo requires extraction of the RNA[112] and complementary DNA synthesis[113,114] before qRT-PCR (Figure 4). The output of the quantification is a signal that relates to the amount of RNA present in the sample. Because this has no unit, the results of the relative quantification can be compared across a number of different qRT-PCR analyses. A total of ≥1 reference genes are applied to correct for nonspecific variation, such as the differences in the quantity and quality of RNA used, which can affect the efficiency of reverse transcription and therefore the entire PCR process. In most of the reported work on EV RNA cargo analysis, a comprehensive isolation procedure is applied (Figure 4). The isolation often involves multiple centrifugation steps and filtration.[80,115,116] However, an optimized protocol was recently published, describing the extraction and qRT-PCR analysis of EV RNA directly from plasma and serum isolated with only a single centrifugation step at low speed and time.[70] Furthermore, the protocol describes that a 250-µL sample provides a sufficient amount of RNA to perform a qRT-PCR analysis,[70] which is of high value in a diagnostic relation. Other studies confirm that miRNAs can be extracted from both serum and plasma with similar results.[54,57]

FUTURE TECHNICAL PERSPECTIVES

The techniques presented in this review could all potentially be part of a platform to characterize EVs from peripheral blood and transform these data into clinically relevant information. However, to fully harness the diagnostic and prognostic potential of EVs, a number of aspects remain to be delineated. A fundamental aspect, which is imperative to address, is standardization.[66] The standardization relates to several areas of EV analysis and research and includes nomenclature, preanalytical conditions, and isolation procedures. This will give rise to standardized protocols and facilitate unbiased comparisons of results from different studies across laboratories. Furthermore, it will greatly aid in the development of robust clinical assays. The next challenge, before using EVs in a diagnostic manner, is to select the most

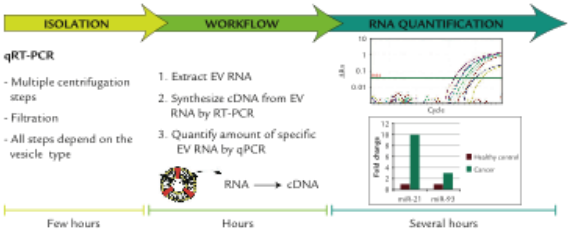

Figure 4. Outline of the workflow and timeframe for the analysis of extracellular vesicle (EV) RNA cargo by quantitative real-time reverse-transcription polymerase chain reaction (qRT-PCR). cDNA = complementary DNA.

optimal methods, concerning sample requirements, apparatus, and analysis accessibility. In addition, selection of the most optimal combination of target markers is essential to several of the methods. A common feature for all the methods outlined is the need for an extensive isolation procedure before EV analysis. In that regard, considerations should be taken concerning the loss of material and thereby valuable information. Therefore, the method of analysis should most optimally work on unpurified plasma or serum samples. A prerequisite for the incorporation of EV analysis into robust clinical assays is the discovery and validation of relevant diagnostic or prognostic EV targets. Currently, thousands of EV-related proteins and RNA components have been identified by proteomic and transcriptomic approaches.[117] In the discovery process, various cell lines have been extensively used.[7,49,71] Even if cell lines are only an approximation of the *in vivo* conditions, they serve as useful model systems and encompass a relevant source of cell surface–expressed biomarkers and intracellular proteins and RNAs, relating to cancer in particular. These *in vitro* model systems are consequently valuable in the matter of identifying which proteins and potential biomarkers are conveyed to the EVs. As an example, this strategy was adopted to identify the protein Claudin as an EV-expressed biomarker for ovarian cancer. Likewise, the model systems of cell lines have a great potential to elucidate the biogenesis of EVs and their subsequent influence on the recipient cells. This finding has been reported in a study in which a mast cell line was exposed to oxidative stress and the subsequent cell-derived EVs revealed a changed RNA profile compared with those derived from cells grown under normal conditions. This study additionally clarified that the stress-derived EVs were able to affect non-stressed cells to become more resistant to the oxidative stress.[32] Nonetheless, the use of cell lines and their autologous production of EVs must be carefully interpreted. Cell lines are kept in a closed and controlled system, mainly as monocultures, and will therefore only receive and respond to the signals specifically applied to them. Because the cells receive no signals or EVs from their original surrounding environment, they will most likely merely autocommunicate. Therefore, cell lines will only partly reflect the authenticity of the biogenesis of the EVs. In the biomarker discovery, the use of mass spectrometry (MS) has for at least 2 decades been essential for the proteomics-driven research of EVs and is the only technique available that allows EV characterization from all common clinical biospecimens, including serum, plasma, urine, synovial fluid, ascites, and feces. Accordingly, the identification of several important EV protein markers has been facilitated by MS.[118] The use of MS has also provided information about aspects of EV biogenesis along with possible pathologic functions of these vesicles.[117] Currently, technical methods for targeted MS platforms are being applied in clinical assays and include multiple reaction monitoring and selected reaction monitoring. These methods enable MS as a high-throughput technique to perform rapid analyses of EV proteins, which could also be used in a diagnostic fashion and not exclusively in the discovery phase for EV biomarkers. Nonetheless, the development of standardizations for EV analysis along with a continued effort to unravel all aspects of EV proteins and RNA will improve the understanding of the molecular mechanisms and biological functions of EVs. Despite being in its infancy, the field of EV research has undoubtedly received an enormous interest. Consequently, numerous initiatives have been implemented in the EV society, including several databases (ExoCarta,[119] EVpedia,[120] Vesiclepedia,[121] and miRandola[122]), conferences (International Society for Extracellular Vesicles conference on microvesiculation and disease), and a dedicated journal (*Journal of Extracellular Vesicles*).[123]

FUTURE CLINICAL PERSPECTIVES

The apparent role of EVs in a vast number of biological processes, along with many of their intriguing features, forms the basis of extending EV analysis beyond basic research and into a clinical and therapeutic context. Despite being a relatively new field, the potential and versatility of EV analysis are supported by an increasing number of publications. The applications of this type of analysis include the areas of diagnostics and prognostics, as well as drug therapy, regenerative medicine, and vaccines. For the purpose of diagnosis and prognosis, the use of EVs seems particularly promising because these vesicles contain a plethora of clinically relevant molecules, such as proteins and RNA from the parent cell. Thereby, the miRNA and protein patterns, which are unique for a specific pathologic condition, can be used. The analysis of EVs could accordingly be incorporated as a screening tool and applied to confirm a diagnosis.

Furthermore, EV analysis has the potential to become an element in treatment surveillance and companion diagnostics, resulting in a patient-optimized treatment. Related to therapeutics, EVs have been proposed as a new type of drug delivery system. Such a system involves engineered EVs loaded with a therapeutic cargo and expressing ligands, which target a particular tissue or cell type. The inherent protection of the cargo and tailored cellular targeting simultaneously enhance the solubility, stability, and specificity of the therapeutic agent. In another approach, the EVs constitute the therapeutic target, and the aim is to inhibit their release or to perform a systemic depletion. In terms of regenerative capabilities, EVs from stem cells have clinical potential.[124] The EVs accordingly constitute a cell-free approach, which mediates many of the regenerative properties from the stem cells. This circumvents several issues related to stem cell transplantations, consequently making handling and storage easier and increasing the stability. This cell-free approach has also been adapted in the field of vaccines and immunotherapy. Particularly in relation to cancer, EVs have been used as potent inducers of antitumor responses.[125,126] In addition, several Phase I and Phase II studies have been initiated, almost exclusively focusing on vaccination with autologous exosomes.[6] The results of these studies indicate a promising future for the use of EV-based treatment. The abovementioned examples of the clinical use of EV analysis clearly indicate its feasibility. In line with the scope of this review, the potential of using EV analysis of a simple blood sample seems encouraging, and this is particularly pronounced in relation to diagnostics. Despite the extensive amount of information, which is possible to obtain from a single blood sample, this complexity is at the same time a challenge that complicates EV analysis. Nonetheless, advances and continued research within the field allow for the development and improvement of techniques and standard protocols, which seek to meet these challenges. The increased understanding of this may lead to a paradigm shift, particularly related to immune regulation and cellular communication in cancer. Taken together, technology and biology will inevitably pave the way for the future use of EV analysis in many clinical applications.

ACKNOWLEDGMENTS

Ms. Revenfeld, Ms. Bæk, Dr. Nielsen, and Dr. Jørgensen performed the literature search, the figure creation, and wrote or contributed to the writing of the manuscript. All authors contributed to the design of the article and revised and accepted the final manuscript.

The authors gratefully acknowledge Dr. Shona Pedersen (Department of Biochemical Chemistry, Aalborg University Hospital, Aalborg, Denmark) for input and discussion of technical issues regarding size and enumeration of EVs. The authors also kindly acknowledge the editorial support provided by Dr. Lotte H. Pugholm and Dr. Evo K.L. Søndergaard (Department of Clinical Immunology, Aalborg University Hospital, Aalborg, Denmark).

CONFLICTS OF INTEREST

The authors have indicated that they have no conflicts of interest regarding the content of this article.

REFERENCES

1. Akers JC, Gonda D, Kim R, et al. Biogenesis of extracellular vesicles (EV): exosomes, microvesicles, retrovirus-like vesicles, and apoptotic bodies. *J Neurooncol*. 2013;113:1–11.
2. Andaloussi SEL, Mager I, Breakefield XO, et al. Extracellular vesicles: biology and emerging therapeutic opportunities. *Nat Rev Drug Discov*. 2013;12:347–357.
3. Raposo G, Stoorvogel W. Extracellular vesicles: exosomes, microvesicles, and friends. *J Cell Biol*. 2013;200:373–383.
4. Gyorgy B, Szabo TG, Pasztoi M, et al. Membrane vesicles, current state-of-the-art: emerging role of extracellular vesicles. *Cell Mol Life Sci*. 2011;68:2667–2688.
5. Cocucci E, Racchetti G, Meldolesi J. Shedding microvesicles: artefacts no more. *Trends Cell Biol*. 2009;19:43–51.
6. Thery C, Ostrowski M, Segura E. Membrane vesicles as conveyors of immune responses. *Nat Rev Immunol*. 2009;9:581–593.
7. Mathivanan S, Ji H, Simpson RJ. Exosomes: extracellular organelles important in intercellular communication. *J Proteomics*. 2010;73:1907–1920.
8. Vlassov AV, Magdaleno S, Setterquist R, et al. Exosomes: current knowledge of their composition, biological functions, and diagnostic and therapeutic potentials. *Biochim Biophys Acta*. 2012;1820:940–948.
9. Pant S, Hilton H, Burczynski ME. The multifaceted exosome: biogenesis, role in normal and aberrant cellular function, and frontiers for pharmacological and biomarker opportunities. *Biochem Pharmacol*. 2012;83:1484–1494.
10. Distler JH, Huber LC, Gay S, et al. Microparticles as mediators of cellular cross-talk in inflammatory disease. *Autoimmunity*. 2006;39:683–690.
11. Villarroya-Beltri C, Gutierrez-Vazquez C, Sanchez-Madrid F, et al. Analysis of microRNA and protein transfer by exosomes during an immune synapse. *Methods Mol Biol*. 2013;1024:41–51.

12. Nolte-'t Hoen EN, Buschow SI, Anderton SM, et al. Activated T cells recruit exosomes secreted by dendritic cells via LFA-1. *Blood*. 2009;113:1977–1981.
13. Arnold PY, Mannie MD. Vesicles bearing MHC class II molecules mediate transfer of antigen from antigen-presenting cells to CD4+ T cells. *Eur J Immunol*. 1999;29:1363–1373.
14. Choudhuri K, Llodra J, Roth EW, et al. Polarized release of T-cell-receptor-enriched microvesicles at the immunological synapse. *Nature*. 2014;507:118–123.
15. Mittelbrunn M, Gutierrez-Vazquez C, Villarroya-Beltri C, et al. Unidirectional transfer of microRNA-loaded exosomes from T cells to antigen-presenting cells. *Nat Commun*. 2011;2:282.
16. Valadi H, Ekstrom K, Bossios A, et al. Exosome-mediated transfer of mRNAs and microRNAs is a novel mechanism of genetic exchange between cells. *Nat Cell Biol*. 2007;9:654–659.
17. Skog J, Wurdinger T, van Rijn S, et al. Glioblastoma microvesicles transport RNA and proteins that promote tumour growth and provide diagnostic biomarkers. *Nat Cell Biol*. 2008;10:1470–1476.
18. Muralidharan-Chari V, Clancy JW, Sedgwick A, et al. Microvesicles: mediators of extracellular communication during cancer progression. *J Cell Sci*. 2010;123(pt 10):1603–1611.
19. Lynch SF, Ludlam CA. Plasma microparticles and vascular disorders. *Br J Haematol*. 2007;137:36–48.
20. Abid Hussein MN, Meesters EW, Osmanovic N, et al. Antigenic characterization of endothelial cell-derived microparticles and their detection ex vivo. *J Thromb Haemost*. 2003;1:2434–2443.
21. Nielsen MH, Beck-Nielsen H, Andersen MN, et al. A flow cytometric method for characterization of circulating cell-derived microparticles in plasma. *J Extracell Vesicles*. 2014 Feb 24. [Epub ahead of print].
22. Connor DE, Exner T, Ma DD, et al. The majority of circulating platelet-derived microparticles fail to bind annexin V, lack phospholipid-dependent procoagulant activity and demonstrate greater expression of glycoprotein Ib. *Thromb Haemost*. 2010;103:1044–1052.
23. Jimenez JJ, Jy W, Mauro LM, et al. Endothelial cells release phenotypically and quantitatively distinct microparticles in activation and apoptosis. *Thromb Res*. 2003;109:175–180.
24. Perez-Pujol S, Marker PH, Key NS. Platelet microparticles are heterogeneous and highly dependent on the activation mechanism: studies using a new digital flow cytometer. *Cytometry A*. 2007;71:38–45.
25. Muralidharan-Chari V, Clancy J, Plou C, et al. ARF6-regulated shedding of tumor cell-derived plasma membrane microvesicles. *Curr Biol*. 2009;19:1875–1885.
26. Berda-Haddad Y, Robert S, Salers P, et al. Sterile inflammation of endothelial cell-derived apoptotic bodies is mediated by interleukin-1alpha. *Proc Natl Acad Sci U S A*. 2011;108:20684–20689.
27. Hristov M, Erl W, Linder S, et al. Apoptotic bodies from endothelial cells enhance the number and initiate the differentiation of human endothelial progenitor cells in vitro. *Blood*. 2004;104:2761–2766.
28. Cline AM, Radic MZ. Apoptosis, subcellular particles, and autoimmunity. *Clin Immunol*. 2004;112:175–182.
29. Pan BT, Johnstone RM. Fate of the transferrin receptor during maturation of sheep reticulocytes in vitro: selective externalization of the receptor. *Cell*. 1983;33:967–978.
30. Harding C, Heuser J, Stahl P. Receptor-mediated endocytosis of transferrin and recycling of the transferrin receptor in rat reticulocytes. *J Cell Biol*. 1983;97:329–339.
31. Admyre C, Johansson SM, Paulie S, et al. Direct exosome stimulation of peripheral human T cells detected by ELISPOT. *Eur J Immunol*. 2006;36:1772–1781.
32. Eldh M, Ekstrom K, Valadi H, et al. Exosomes communicate protective messages during oxidative stress; possible role of exosomal shuttle RNA. *PLoS One*. 2010;5:e15353.
33. Saunderson SC, Schuberth PC, Dunn AC, et al. Induction of exosome release in primary B cells stimulated via CD40 and the IL-4 receptor. *J Immunol*. 2008;180:8146–8152.
34. Buschow SI, Nolte-'t Hoen EN, van Niel G, et al. MHC II in dendritic cells is targeted to lysosomes or T cell-induced exosomes via distinct multivesicular body pathways. *Traffic*. 2009;10:1528–1542.
35. Wurdinger T, Gatson NN, Balaj L, et al. Extracellular vesicles and their convergence with viral pathways. *Adv Virol*. 2012;2012:767694.
36. Mack M, Kleinschmidt A, Bruhl H, et al. Transfer of the chemokine receptor CCR5 between cells by membrane-derived microparticles: a mechanism for cellular human immunodeficiency virus 1 infection. *Nat Med*. 2000;6:769–775.
37. Bhatnagar S, Shinagawa K, Castellino FJ, et al. Exosomes released from macrophages infected with intracellular pathogens stimulate a proinflammatory response in vitro and in vivo. *Blood*. 2007;110:3234–3244.
38. Rak J, Guha A. Extracellular vesicles - vehicles that spread cancer genes. *Bioessays*. 2012;34:489–497.
39. Abusamra AJ, Zhong Z, Zheng X, et al. Tumor exosomes expressing Fas ligand mediate CD8+ T-cell apoptosis. *Blood Cells Mol Dis*. 2005;35:169–173.
40. Wieckowski EU, Visus C, Szajnik M, et al. Tumor-derived microvesicles promote regulatory T cell expansion and induce apoptosis in tumor-reactive activated CD8+ T

lymphocytes. *J Immunol*. 2009;183:3720–3730.
41. Szajnik M, Czystowska M, Szczepanski MJ, et al. Tumor-derived microvesicles induce, expand and up-regulate biological activities of human regulatory T cells (Treg). *PLoS One*. 2010;5:e11469.
42. Al-Nedawi K, Meehan B, Micallef J, et al. Intercellular transfer of the oncogenic receptor EGFRvIII by microvesicles derived from tumour cells. *Nat Cell Biol*. 2008;10:619–624.
43. Szajnik M, Derbis M, Lach M, et al. Exosomes in plasma of patients with ovarian carcinoma: potential biomarkers of tumor progression and response to therapy. *Gynecol Obstet (Sunnyvale)*. 2013;(Suppl 4):3.
44. Baran J, Baj-Krzyworzeka M, Weglarczyk K, et al. Circulating tumour-derived microvesicles in plasma of gastric cancer patients. *Cancer Immunol Immunother*. 2009;59:841–850.
45. Kim HK, Song KS, Park YS, et al. Elevated levels of circulating platelet microparticles, VEGF, IL-6 and RANTES in patients with gastric cancer: possible role of a metastasis predictor. *Eur J Cancer*. 2003;39:184–191.
46. Rabinowits G, Gercel-Taylor C, Day JM, et al. Exosomal microRNA: a diagnostic marker for lung cancer. *Clin Lung Cancer*. 2009;10:42–46.
47. Anderson NL, Anderson NG. The human plasma proteome: history, character, and diagnostic prospects. *Mol Cell Proteomics*. 2002;1(11):845–867.
48. Hortin GL, Sviridov D. The dynamic range problem in the analysis of the plasma proteome. *J Proteomics*. 2010;73:629–636.
49. Li J, Sherman-Baust CA, Tsai-Turton M, et al. Claudin-containing exosomes in the peripheral circulation of women with ovarian cancer. *BMC Cancer*. 2009;9:244.
50. Tanaka Y, Kamohara H, Kinoshita K, et al. Clinical impact of serum exosomal microRNA21 as a clinical biomarker in human esophageal squamous cell carcinoma. *Cancer*. 2013;119:1159–1167.
51. Hu Z, Chen X, Zhao Y, et al. Serum microRNA signatures identified in a genome-wide serum microRNA expression profiling predict survival of non-small-cell lung cancer. *J Clin Oncol*. 2010;28:1721–1726.
52. Satzger I, Mattern A, Kuettler U, et al. MicroRNA-15b represents an independent prognostic parameter and is correlated with tumor cell proliferation and apoptosis in malignant melanoma. *Int J Cancer*. 2010;126:2553–2562.
53. Ng EK, Chong WW, Jin H, et al. Differential expression of microRNAs in plasma of patients with colorectal cancer: a potential marker for colorectal cancer screening. *Gut*. 2009;58:1375–1381.
54. Lawrie CH, Gal S, Dunlop HM, et al. Detection of elevated levels of tumour-associated microRNAs in serum of patients with diffuse large B-cell lymphoma. *Br J Haematol*. 2008;141:672–675.
55. Resnick KE, Alder H, Hagan JP, et al. The detection of differentially expressed microRNAs from the serum of ovarian cancer patients using a novel real-time PCR platform. *Gynecol Oncol*. 2009;112:55–59.
56. Chen X, Ba Y, Ma L, et al. Characterization of microRNAs in serum: a novel class of biomarkers for diagnosis of cancer and other diseases. *Cell Res*. 2008;18:997–1006.
57. Mitchell PS, Parkin RK, Kroh EM, et al. Circulating microRNAs as stable blood-based markers for cancer detection. *Proc Natl Acad Sci U S A*. 2008;105:10513–10518.
58. Zhu W, Qin W, Atasoy U, et al. Circulating microRNAs in breast cancer and healthy subjects. *BMC Res Notes*. 2009;2:89.
59. Segura MF, Hanniford D, Menendez S, et al. Aberrant miR-182 expression promotes melanoma metastasis by repressing FOXO3 and microphthalmia-associated transcription factor. *Proc Natl Acad Sci U S A*. 2009;106:1814–1819.
60. Keller S, Konig AK, Marme F, et al. Systemic presence and tumor-growth promoting effect of ovarian carcinoma released exosomes. *Cancer Lett*. 2009;278:73–81.
61. Shao H, Chung J, Balaj L, et al. Protein typing of circulating microvesicles allows real-time monitoring of glioblastoma therapy. *Nat Med*. 2012;18:1835–1840.
62. Logozzi M, De Milito A, Lugini L, et al. High levels of exosomes expressing CD63 and caveolin-1 in plasma of melanoma patients. *PLoS One*. 2009;4:e5219.
63. Kim JW, Wieckowski E, Taylor DD, et al. Fas ligand-positive membranous vesicles isolated from sera of patients with oral cancer induce apoptosis of activated T lymphocytes. *Clin Cancer Res*. 2005;11:1010–1020.
64. Tesselaar ME, Romijn FP, Van Der Linden IK, et al. Microparticle-associated tissue factor activity: a link between cancer and thrombosis? *J Thromb Haemost*. 2007;5:520–527.
65. Matsubara E, Shoji M, Murakami T, et al. Platelet microparticles as carriers of soluble Alzheimer's amyloid beta (sAbeta). *Ann N Y Acad Sci*. 2002;977:340–348.
66. Witwer KW, Buzas EI, Bemis LT, et al. Standardization of sample collection, isolation and analysis methods in extracellular vesicle research. *J Extracell Vesicles*. 27 May 2013. [Epub ahead of print].
67. Momen-Heravi F, Balaj L, Alian S, et al. Current methods for the isolation of extracellular vesicles. *Biol Chem*. 2013;394:1253–1262.
68. van der Pol E, Boing AN, Harrison P, et al. Classification, functions, and clinical relevance of extracellular vesicles. *Pharmacol Rev*. 2012;64:676–705.
69. Gyorgy B, Modos K, Pallinger E, et al. Detection and isolation of

cell-derived microparticles are compromised by protein complexes resulting from shared biophysical parameters. *Blood*. 2011;117:e39–e48.
70. Moldovan L, Batte K, Wang Y, et al. Analyzing the circulating microRNAs in exosomes/extracellular vesicles from serum or plasma by qRT-PCR. *Methods Mol Biol*. 2013;1024:129–145.
71. Tauro BJ, Greening DW, Mathias RA, et al. Comparison of ultracentrifugation, density gradient separation, and immunoaffinity capture methods for isolating human colon cancer cell line LIM1863-derived exosomes. *Methods*. 2012;56:293–304.
72. Peters PJ, Neefjes JJ, Oorschot V, et al. Segregation of MHC class II molecules from MHC class I molecules in the Golgi complex for transport to lysosomal compartments. *Nature*. 1991;349:669–676.
73. Escola JM, Kleijmeer MJ, Stoorvogel W, et al. Selective enrichment of tetraspan proteins on the internal vesicles of multivesicular endosomes and on exosomes secreted by human B-lymphocytes. *J Biol Chem*. 1998;273:20121–20127.
74. Joergensen M, Baek R, Pedersen S, et al. Extracellular Vesicle (EV) Array: microarray capturing of exosomes and other extracellular vesicles for multiplexed phenotyping. *J Extracell Vesicles*. 2013 June 18. [Epub ahead of print].
75. Stoorvogel W, Geuze HJ, Griffith JM, et al. Relations between the intracellular pathways of the receptors for transferrin, asialoglycoprotein, and mannose 6-phosphate in human hepatoma cells. *J Cell Biol*. 1989;108:2137–2148.
76. Stoorvogel W, Oorschot V, Geuze HJ. A novel class of clathrin-coated vesicles budding from endosomes. *J Cell Biol*. 1996;132:21–33.
77. Blanchard N, Lankar D, Faure F, et al. TCR activation of human T cells induces the production of exosomes bearing the TCR/CD3/zeta complex. *J Immunol*. 2002;168:3235–3241.
78. Raposo G, Nijman HW, Stoorvogel W, et al. B lymphocytes secrete antigen-presenting vesicles. *J Exp Med*. 1996;183:1161–1172.
79. Heijnen HF, Schiel AE, Fijnheer R, et al. Activated platelets release two types of membrane vesicles: microvesicles by surface shedding and exosomes derived from exocytosis of multivesicular bodies and alpha-granules. *Blood*. 1999;94:3791–3799.
80. Lasser C, Eldh M, Lotvall J. Isolation and characterization of RNA-containing exosomes. *J Vis Exp*. 2012(59):e3037.
81. Laemmli UK. Cleavage of structural proteins during the assembly of the head of bacteriophage T4. *Nature*. 1970;227:680–685.
82. Towbin H, Staehelin T, Gordon J. Electrophoretic transfer of proteins from polyacrylamide gels to nitrocellulose sheets: procedure and some applications. *Proc Natl Acad Sci U S A*. 1979;76:4350–4354.
83. Renart J, Reiser J, Stark GR. Transfer of proteins from gels to diazobenzyloxymethyl-paper and detection with antisera: a method for studying antibody specificity and antigen structure. *Proc Natl Acad Sci U S A*. 1979;76:3116–3120.
84. Li Y, Jiang T, Zhang J, et al. Elevated serum antibodies against insulin-like growth factor-binding protein-2 allow detecting early-stage cancers: evidences from glioma and colorectal carcinoma studies. *Ann Oncol*. 2012;23:2415–2422.
85. Jy W, Horstman LL, Jimenez JJ, et al. Measuring circulating cell-derived microparticles. *J Thromb Haemost*. 2004;2:1842–1851.
86. Kesimer M, Scull M, Brighton B, et al. Characterization of exosome-like vesicles released from human tracheobronchial ciliated epithelium: a possible role in innate defense. *FASEB J*. 2009;23:1858–1868.
87. Mobarrez F, Antovic J, Egberg N, et al. A multicolor flow cytometric assay for measurement of platelet-derived microparticles. *Thromb Res*. 2010;125:e110–e116.
88. Orozco AF, Lewis DE. Flow cytometric analysis of circulating microparticles in plasma. *Cytometry A*. 2010;77:502–514.
89. Caby MP, Lankar D, Vincendeau-Scherrer C, et al. Exosomal-like vesicles are present in human blood plasma. *Int Immunol*. 2005;17:879–887.
90. Silva J, Garcia V, Rodriguez M, et al. Analysis of exosome release and its prognostic value in human colorectal cancer. *Genes Chromosomes Cancer*. 2012;51:409–418.
91. Lacroix R, Robert S, Poncelet P, et al. Overcoming limitations of microparticle measurement by flow cytometry. *Semin Thromb Hemost*. 2010;36:807–818.
92. Gelderman MP, Simak J. Flow cytometric analysis of cell membrane microparticles. *Methods Mol Biol*. 2008;484:79–93.
93. Shet AS, Key NS, Hebbel RP. Measuring circulating cell-derived microparticles. *J Thromb Haemost*. 2004;2:1848–1850.
94. Robert S, Poncelet P, Lacroix R, et al. Standardization of platelet-derived microparticle counting using calibrated beads and a Cytomics FC500 routine flow cytometer: a first step towards multicenter studies? *J Thromb Haemost*. 2009;7:190–197.
95. Lee H, Sun E, Ham D, et al. Chip-NMR biosensor for detection and molecular analysis of cells. *Nat Med*. 2008;14:869–874.
96. Issadore D, Min C, Liong M, et al. Miniature magnetic resonance system for point-of-care diagnostics. *Lab Chip*. 2011;11:2282–2287.
97. Haun JB, Castro CM, Wang R, et al. Micro-NMR for rapid molecular analysis of human tumor samples. *Sci Transl Med*. 2011;3. 71ra16.
98. Melton L. Protein arrays: proteomics in multiplex. *Nature*. 2004;429:101–107.

99. Hall DA, Ptacek J, Snyder M. Protein microarray technology. *Mech Ageing Dev*. 2007;128:161–167.
100. Soo CY, Song Y, Zheng Y, et al. Nanoparticle tracking analysis monitors microvesicle and exosome secretion from immune cells. *Immunology*. 2012;136:192–197.
101. Gardiner C, Ferreira YJ, Dragovic RA, et al. Extracellular vesicle sizing and enumeration by nanoparticle tracking analysis. *J Extracell Vesicles*. 2013 Feb 15. [Epub ahead of print].
102. Momen-Heravi F, Balaj L, Alian S, et al. Alternative methods for characterization of extracellular vesicles. *Front Physiol*. 2012;3:354.
103. Dragovic RA, Gardiner C, Brooks AS, et al. Sizing and phenotyping of cellular vesicles using Nanoparticle Tracking Analysis. *Nanomedicine*. 2011;7:780–788.
104. Filipe V, Hawe A, Jiskoot W. Critical evaluation of Nanoparticle Tracking Analysis (NTA) by NanoSight for the measurement of nanoparticles and protein aggregates. *Pharm Res*. 2010;27:796–810.
105. Garza-Licudine E, Deo D, Yu S, et al. Portable nanoparticle quantization using a resizable nanopore instrument - the IZON qNano. *Conf Proc IEEE Eng Med Biol Soc*. 2010; 2010:5736–5739.
106. Kosaka N, Iguchi H, Yoshioka Y, et al. Secretory mechanisms and intercellular transfer of microRNAs in living cells. *J Biol Chem*. 2010; 285:17442–17452.
107. Kogure T, Lin WL, Yan IK, et al. Intercellular nanovesicle-mediated microRNA transfer: a mechanism of environmental modulation of hepatocellular cancer cell growth. *Hepatology*. 2011;54:1237–1248.
108. Ekstrom K, Valadi H, Sjostrand M, et al. Characterization of mRNA and microRNA in human mast cell-derived exosomes and their transfer to other mast cells and blood CD34 progenitor cells. *J Extracell Vesicles*. 2012 Apr 16. [Epub ahead of print].
109. Bartel DP. MicroRNAs: genomics, biogenesis, mechanism, and function. *Cell*. 2004;116:281–297.
110. Esquela-Kerscher A, Slack FJ. Oncomirs: microRNAs with a role in cancer. *Nat Rev Cancer*. 2006;6: 259–269.
111. Gertsch J, Guttinger M, Sticher O, et al. Relative quantification of mRNA levels in Jurkat T cells with RT-real time-PCR (RT-rt-PCR): new possibilities for the screening of anti-inflammatory and cytotoxic compounds. *Pharm Res*. 2002;19: 1236–1243.
112. Eldh M, Lotvall J, Malmhall C, et al. Importance of RNA isolation methods for analysis of exosomal RNA: evaluation of different methods. *Mol Immunol*. 2012;50:278–286.
113. de Planell-Saguer M, Rodicio MC. Detection methods for microRNAs in clinic practice. *Clin Biochem*. 2013;46:869–878.
114. Chen C, Ridzon DA, Broomer AJ, et al. Real-time quantification of microRNAs by stem-loop RT-PCR. *Nucleic Acids Res*. 2005;33:e179.
115. Crescitelli R, Lasser C, Szabo TG, et al. Distinct RNA profiles in subpopulations of extracellular vesicles: apoptotic bodies, microvesicles and exosomes. *J Extracell Vesicles*. 2013 Sep 12. [Epub ahead of print].
116. Lasser C. Identification and analysis of circulating exosomal microRNA in human body fluids. *Methods Mol Biol*. 2013;1024:109–128.
117. Choi DS, Kim DK, Kim YK, et al. Proteomics, transcriptomics and lipidomics of exosomes and ectosomes. *Proteomics*. 2013;13:1554–1571.
118. Choi DS, Kim DK, Kim YK, et al. Proteomics of extracellular vesicles: exosomes and ectosomes. *Mass Spectrom Rev*. 2014 Jan 14. [Epub ahead of print].
119. Simpson RJ, Kalra H, Mathivanan S. ExoCarta as a resource for exosomal research. *J Extracell Vesicles*. 2012 Apr 16. [Epub ahead of print].
120. Kim DK, Kang B, Kim OY, et al. EVpedia: an integrated database of high-throughput data for systemic analyses of extracellular vesicles. *J Extracell Vesicles*. 2013 Mar:19. [Epub ahead of print].
121. Kalra H, Simpson RJ, Ji H, et al. Vesiclepedia: a compendium for extracellular vesicles with continuous community annotation. *PLoS Biol*. 2012;10:e1001450.
122. Russo F, Di Bella S, Nigita G, et al. miRandola: extracellular circulating microRNAs database. *PLoS One*. 2012;7:e47786.
123. Lotvall J, Rajendran L, Gho YS, et al. The launch of Journal of Extracellular Vesicles (JEV), the official journal of the International Society for Extracellular Vesicles - about microvesicles, exosomes, ectosomes and other extracellular vesicles. *J Extracell Vesicles*. 2012 Apr 16. [Epub ahead of print].
124. Yu B, Zhang X, Li X. Exosomes derived from mesenchymal stem cells. *Int J Mol Sci*. 2014;15:4142–4157.
125. Zitvogel L, Regnault A, Lozier A, et al. Eradication of established murine tumors using a novel cell-free vaccine: dendritic cell-derived exosomes. *Nat Med*. 1998;4:594–600.
126. Andre F, Chaput N, Schartz NE, et al. Exosomes as potent cell-free peptide-based vaccine, I: dendritic cell-derived exosomes transfer functional MHC class I/peptide complexes to dendritic cells. *J Immunol*. 2004;172:2126–2136.

Address correspondence to: Malene Jørgensen, PhD, Department of Clinical Immunology, Aalborg University Hospital, Urbansgade 32-36, DK-9000 Aalborg, Denmark. E-mail: maljoe@rn.dk

B4 - Manuscript 4

Title: Characterization of a cell culturing system for the study of contact-independent vesicle communication

Authors: Anne Louise S. Revenfeld[1], Evo K.L. Søndergaard[1], Allan Stensballe[2], Rikke Bæk[1], Malene M. Jørgensen[1], Kim Varming[1]

1. Department of Clinical Immunology, Aalborg University Hospital, Urbansgade 32-36, DK-9000 Aalborg, Denmark

2. Laboratory for Medical Mass Spectrometry, Department of Health Science and Technology, Aalborg University, Fredrik Bajersvej 7E, DK-9100 Aalborg, Denmark

Corresponding author

Anne Louise Schacht Revenfeld

Department of Clinical Immunology

Aalborg University Hospital

Urbansgade 32-36

DK-9000 Aalborg

Denmark

Tel: +45 97655587

Email: anlor@rn.dk

Abstract

In order to study the biological function and activity of extracellular vesicles (EVs), appropriate *in vitro* cell culturing platforms are necessary. The aim of this study was to describe an experimental system, where dynamic, vesicle-based communication between cells can be investigated. A commercially available cell-culturing system was applied to study contact-independent communication between cells, separating two cell populations by a membrane with a pore size of 0.4 μm. Some of the factors determining the vesicle transport in this cell culturing system were investigated in a cell-free setup and analyzed using the Extracellular Vesicle (EV) Array and nanoparticle tracking analysis. Furthermore, the application of the cell-culturing setup was demonstrated using human, primary cells. Here, the effects that contact-dependent and –independent cell communication had on the phenotype of EVs found in the cell supernatant were shown. Collectively, the investigations revealed that the relative placement of the two cell populations in the presented cell culturing setup is important to the biological hypothesis, which is being investigated. These observations are relevant for short-time (<24h) as well as long-time studies (several days) of vesicle-based cell communication. Moreover, the introduced cell culturing setup and analytical strategy can be used to study contact-independent vesicle communication in a reproducible manner.

Keywords

Extracellular vesicles, cell communication, contact-independent, EV Array, phenotype

Introduction

It is currently well accepted that extracellular vesicles (EVs) are released from a plethora of cell types in many biological systems (1). Furthermore, these vesicular entities can be used as a tool of intercellular communication. In line with this, EVs play an important role in many cellular processes in humans, both in physiological and pathophysiological scenarios (1-3). However, uncovering the specific biological functions of EVs is still in its infancy. Many *in vitro* experiments carried out to answer these biological questions use two different approaches: i) EVs from one cell population/ condition are isolated and added to another cell population (4-7). Subsequently, the effect of the EVs on the second population is investigated. ii) The two cell populations are co-cultured but separated by a membrane with a pore size, which allows for the transport of vesicles of a certain size, as well as soluble factors (4, 8, 9). The effect of the co-culturing can thereafter be studied on either one or both cell populations. The latter setup represents the most dynamic of the two approaches to study vesicle-based communication, since it is based on co-culture. Consequently, it incorporates the continuous communication between the studied cells, with a consequent greater resemblance to the *in vivo* conditions.

Experimental setup and aim

The cell culturing setup described in the current study is based on the co-culture approach introduced above. The principle of this setup is depicted in Figure 1. Several factors need to be taken into account, when designing such a study. A key factor, which this study investigates, is the importance of which cell population is placed in the upper and lower compartment, relative to the biological hypothesis being tested. This is relevant, since we are able to demonstrate that this placement affects the experimental outcome, both for short-time (<24h) and long-time studies (several days) of vesicle-based communication. Additionally, the subsequent analysis of the EVs must be both reliable, reproducible, and provide as much information as possible. The aim of this report is to present a combined cell culturing and analytical setup, which allows for an easy and reproducible detection of differences in EV phenotypes caused by contact-dependent and –independent cellular communication.

Materials and Methods

Co-culturing setup

Specifications: The applied cell culturing system consists of a 24-well plate (Nunc, Thermo Scientific, Waltham, MA, USA) with Millicell® Hanging Cell Culture Inserts (#PIHT 12R 48, Merck Millipore, Darmstadt, Germany) (Figure 1). The insert material is polystyrene, while the membrane in the bottom of the cell culture insert is made of polyethylene terephthalate (PET). It is tissue culture treated and gamma irradiated, thus providing a sterile device for cell culturing of both attachment-dependent cells and cells in suspension. The insert is 16 mm in height with an outer diameter of 9 mm and an inner diameter of 6.5 mm. The membrane is 12 μm thick and has an effective membrane area of 33 mm^2. Moreover, the pore size of the membrane is 0.4 μm and it has a pore density of 1 x 10^8 pores/cm^2. The recommended usage of the chosen insert includes study of cell proliferation and co-cultures as well as in transport and permeability assays.

Cell culturing: 800 μl of cells/ culture medium was added to the lower compartment of the cell culturing system. The insert was placed into the well (Figure 1) and the insert membrane was allowed to soak for a couple of minutes. 400 μl of cells/ culture medium was added to the upper compartment and the culture plate with inserts was placed in a CO_2 incubator.

Transmembrane exchange of EVs

Cell culture conditions and EV collection: Cell-free and EV-rich supernatant was obtained from the human colon cancer cell line LS180 (ATCC® CL-187™; ATCC, Manassas, VA, USA) cultured in growth medium containing RPMI 1640 (Gibco, Life Technologies, Carlsbad, CA, USA), 10% ultracentrifuged (100.000 xg, 24h, 4°C; Ti45 rotor, Beckman Coulter, Brea, USA), heat-inactivated fetal bovine serum (FBS) (Gibco), 100 U/mL penicillin, 10μg/mL streptomycin (Ampliqon, Odense, DK)). Upon collection of the EV-rich cell supernatant, the cell supernatant was centrifuged at 500 xg, 5 min, RT, to remove cells. To the cell-free supernatant, a protease inhibitor cocktail was added (EDTA-free, Roche, Basel, Switzerland, diluted 1:50 in PBS). Subsequently, the EV-rich cell supernatant was reduced in volume by using a 15 ml Amicon® Ultra filter unit with a 100k MWCO (Merck Millipore). The volume-reduced supernatant was washed twice with PBS prior to use. The final volume of the cell supernatant was approximately 1/20 of the original volume.

Dilution series to investigate transmembrane exchange of EVs: The following dilutions of the EV-rich cell supernatant from LS180 were included: 1:1 (undiluted), 1:10, 1:50, 1:100, 1:500, and 1:1000. All dilutions were made with growth medium. To describe the exchange of EVs from the lower to the upper compartment, 800 μl of cell supernatant was placed in the lower compartment of the cell culturing setup (Figure 1), as described previously. Subsequently, 400 μl of growth medium was put in the upper compartment. To describe the transmembrane exchange from the

upper to the lower compartment, the opposite setup was made. Here, the growth medium was placed in the lower compartment, while the EV-rich supernatant was put in the upper compartment. Each dilution for each combination of the compartments was made in duplicates. The culture plate holding the inserts was placed in a CO_2-incubator (temperature: 37 °C; CO_2-concentration: 5%; relative humidity: 90%) for 24h. After this, the content of each compartment was harvested into separate tubes and stored at - 40 °C until semi-quantification of the vesicles by the EV Array (see section below).

Contact-dependent and –independent mixed lymphocyte culture (MLC)

Isolation of cells: Buffy coats were obtained from healthy blood donors at Aalborg University Hospital blood bank. Each blood donor had signed a written consent form, allowing for the use of his or her blood for research purposes. The procedure was approved by local ethics legislation. Isolation of peripheral blood mononuclear cells (PBMCs) was accomplished by using gradient centrifugation with Lymphoprep™(Axis-Shield, Oslo, NO). The PBMCs were either used directly after the isolation or stored at -140 °C in a storage medium (RPMI 1640, 40% heat-inactivated FBS, 10% dimethyl sulfoxide (Merck Millipore), 100 U/mL penicillin/10µg/mL streptomycin).

Cell culture setup and EV collection: A 6-day allogeneic MLC was performed with PBMCs from two donors. The PBMCs from one donor were designated the stimulator cells, which would induce a proliferative response in the PBMCs from the second donor, entitled the responder cells. Prior to the MLC, the stimulator cells were irradiated (1700 rad). For the contact-dependent MLC (classical), $5x10^4$ of each responder and stimulator cells were mixed in a 96-well plate (Nunc) in a total volume of 150 µL culture medium. For the contact-independent setup, stimulator cells and responder cells were separated by Millicell® Hanging Cell Culture Insert. The upper chamber contained $2.5x10^5$ cells, while the lower chamber contained $5x10^5$ cells. Control samples with monocultures of both stimulator and responder cells were also included. Here, $5x10^4$ of either responder or stimulator cells were seeded in a 96-well plate, as described above. The cells were placed in a CO_2-incubator (temperature: 37 °C; CO_2-concentration: 5%; relative humidity: 90%) for 6 days. On day 6 of the MLCs, the cell culture supernatants were removed and centrifuged once at 500xg 10 min at RT to pellet cells. Protease inhibitor cocktail (EDTA-free, diluted 1:50 in PBS) was added to the cell-free supernatants prior to storage at -40 °C until vesicle phenotyping by the EV Array.

EV Array analysis

Production of microarrays: Microarray printing was performed on a SpotBot® Extreme Protein Edition Microarray Printer (Sunnyvale, ArrayIt, CA, US), as previously described (10).

Antibodies/proteins for phenotyping of vesicles: For the phenotyping, a total of 10 anti-human antibodies and one protein were used. They are listed in the following

with the corresponding product number (#) or clone. From R&D Systems (Minneapolis, MN, USA): CD82 (#423524) and TNFRI (#DY225). From Biolegend: CD63 (MEM-259) and HLA-DR (L243). From LifeSpan BioSciences, Inc. (Seattle, WA, USA): CD9 (#LS-C35418) and CD81 (#LS-B7347). From Abcam (Cambridge, MA, USA): Flotilin-1 (#Ab41927). From Haematologic Technologies, Inc. (Essex Juncton,VT, USA): Lactadherin (#BLAC-1200) (protein). From BD Biosciences: CD3 (Hit3a). From Abbiotec (San Diego, CA, USA): CD11a (HI111). From eBioscience: ICAM-1 (R6.5). All antibodies/proteins for the phenotyping were printed in triplicates at 200 µg/mL diluted in PBS containing 5% glycerol.

Antibodies for semi-quantification of vesicles: For the semi-quantification, only anti-CD9, anti-CD63, and anti-CD81 were printed on the micro-array slides, as previously described (11). In short, 18 repeated spots were printed with a cocktail of the three antibodies.

Catching and visualization: The entire procedure was performed as described previously (11). In short, the printed slides were blocked, incubated with the EV-containing sample, followed by detection of bound EVs with biotinylated anti-CD9, -CD63, and -CD81 and subsequently Cy5-labelled streptavidin.

Data analysis: Creation of graphs and statistical calculations were carried out using GraphPad Prism (version 6.04, GraphPad Software, Inc., San Diego, CA, USA), SigmaPlot (version 11, Systat Software Inc, San Jose, CA, USA), and Excel (version 2013, Microsoft, Redmond, WA, USA). Heat maps were produced using Genesis (version 1.7.6, IGB TU Graz, Graz, Austria). For a given antibody spot, the signal intensity was calculated as the mean signal of triplicate spots (18 spots for semi-quantification) in relation to the sample signal of the negative spot (PBS) in triplicate. For each spot, the signal intensity was calculated by subtracting the mean of the background (no sample/blank, washing buffer) from the mean of the foreground (spot signal). Before visualization and calculation of linearity, the antibody signal intensities were converted to log space by log2 transformation. The EV "retention" percentage, used with the semi-quantitative data, was calculated as: (Signal in EV starting compartment/ total signal in upper and lower compartment) x 100.

Nanoparticle Tracking Analysis (NTA)

Instrument details: For EV size determination, NTA was performed with a NanoSight LM10-HS system equipped with a finely tuned 405 nm laser (NanoSight Ltd., Amesbury, UK), supplied with the Nanoparticle Tracking Analysis (NTA) 3.0 0060 analytical software version, which was used for capturing and analysing the data. The camera type was EMCCD and the camera level was set to 11.

Size determination: The NanoSight was calibrated with polystyrene latex microbeads 100 nm (Thermo Scientific, Fremont, USA) prior to analysis. Dulbecco's phosphate buffered saline (DPBS) without Ca^{2+} and Mg^{+}, filtered with a 0.22 µm filter prior to use (Lonza, Verviers, Belgium) was used to dilute the microbeads (1:1000 dilution) and the EV-containing cell supernatants (1:40 dilution). The samples were manually injected into the sample chamber and a temperature-measuring

device inserted directly into the sample chamber was applied to record the temperature of sample for each run. Samples were measured with a slide shutter of 600 and with a slider gain of 300 for 60 s. The applied dilutions yielded between 20 – 100 particles/frame and each sample was measured in triplicate. Subsequently, the integrated software automatically processed the data, yielding values such as the mean, the median, the mode particle size, the value of the highest point of the peak, and the corresponding standard deviations. The detection threshold was set to 3 and the blur setting was 9 x 9.

Results

Transmembrane EV exchange between the two compartments of the cell culturing setup

Initially, the exchange characteristics of EVs between the two compartments of the cell culturing setup (Figure 1) were investigated using a cell-free setup. This was done to evaluate whether the experimental outcome is affected by the relative position of the cells in the compartments. For this purpose, volume-reduced, EV-rich cell supernatant from the human colon cancer cell line LS180 was placed in one of the compartments and growth medium in the opposite compartment. Consequently, the transport of EVs from the upper to the lower compartment, and in the reciprocal direction, was studied. After 24h, the extent of transmembrane EV exchange was evaluated in each compartment by using the EV Array to semi-quantify the content of CD9-, CD63-, and CD81-containing EVs. The results from this analysis can be seen in Figure 2. Here, the EV "retention" percentage illustrated in Figure 2A designates how much of the EV Array signal detected in the EV starting compartment constitutes of the total signal from both compartments. Consequently, an EV retention percentage of 50% indicates that the EV Array signal was similar in the two compartments, while 100% indicates that no signal could be detected in the compartment opposite to the EV starting compartment. From Figure 2A it can be deduced that the transmembrane EV exchange is far greater from the upper to the lower compartment in the investigated time frame, as compared to the reciprocal direction. This difference already becomes noticeable with the 1: 10 dilution. Furthermore, with the second dilution (1:50), practically no signal could be detected in the upper compartment, from the combination where the EVs initially were placed in the lower compartment. For the opposite combination, this tendency was observed later, at the 1:500 dilution. After 24h, the signal in the compartment, where the EV-rich supernatant had initially been placed, was similar for both combinations of the culturing setup (Figure 2B). Hence, the observed differences in the EV "retention" percentage could only be caused by the varying extent of transmembrane EV exchange for the two combinations.

As an additional investigation, the size distribution of the EVs present in each compartment after the 24h of transmembrane exchange was determined by NTA. The analyzed samples included those from the 1:50 dilution presented in Figure 2, since there was a large difference in the two EV "retention" percentages for this particular dilution. The results from the NTA can be found in Table 2. After 24h, it appears from both the mean and mode values that smaller vesicles passed from the upper to the lower compartment, as compared to the opposite direction. This correlated well with the observed signal from the EV Array (Table 1), which in this setup targeted EVs enriched with CD9, CD63, and CD81; generally accepted exosomal markers, hence identifying EVs expected to have a size between 30-100 nm (1, 12). Even though the NTA also detected vesicles in the growth medium, the mode value indicates that there is a different vesicle profile of the growth medium alone, when compared to the specific supernatants from the cell culturing setup. Moreover, the

EV Array signal obtained for the growth medium demonstrates how these vesicles do not have an impact on the specific signals from the array analysis.

Demonstration of the applicability of the cell culturing setup and analysis platform

The aim of this study was to present an experimental system in which dynamic, vesicle-based cellular communication can be studied. To demonstrate this, contact-dependent and –independent co-cultures of primary human peripheral blood mononuclear cells (PBMCs) were prepared. In this co-culture, termed a mixed lymphocyte culture (MLC), one cell population is designated the stimulator cells. These cells induce an immunological response in responder cells, constituted by the second cell population. The classical MLC is contact-dependent; hence, the two cell populations are mixed and have physical contact. For the contact-independent MLC, both combinations of the two cell populations were included. Accordingly, in one combination, the responder cells were placed in the lower compartment, while the stimulator cells were placed in the upper compartment. In the second combination, the two cell populations were reversed. After 6 days, the EV Array was used to investigate the contact-dependent changes in the EV phenotypes from the cell cultures. The results of this are depicted in Figure 3, showing a summary of the presence/ absence of 11 protein markers on EVs from the cell supernatants. As can be seen, there were several general features as well as contact-dependent differences in the EV phenotypes. For the general EV markers, CD9, CD81, and CD82 were present on EVs from all cellular setups. In particular, CD81 and CD82 were enriched in the contact-independent co-cultures. In contrast, flotilin-1 was found to the greatest extent in the contact-dependent MLC. Finally, tumor necrosis factor receptor 1 (TNFRI) was detected in the co-cultures and not in the monoculture controls. For the more cell-specific markers, there were pronounced differences, depending on the cellular contact but also interestingly on the relative placement of the two cell populations in the contact-independent co-cultures. As such, CD3 was highly enriched on EVs from the contact-dependent MLC, while CD11a was found in almost all cell cultures. HLA-DR was found mostly on EVs in the compartments holding the stimulator cells, however, to a higher degree when these cells were placed in the upper compartment. Moreover, the signal obtained for ICAM-1 for the responder cells placed in the upper compartment was three times that of the corresponding signal for the responder cells in the lower compartment.

As a final notion, the reproducibility of the presented cell culturing setup and analysis platform was evaluated. Accordingly, the contact-dependent and –independent MLCs were repeated several weeks apart, using cells from the same individuals. In Figure 4, the results of three selected markers are presented for the two technical replicates. It can be seen, that for CD9 and CD81, the detected EV signals predominantly correlated from replicate to replicate, with 12 of the 14 %CV values ranging from 1.7%-15.6% (Figure 4). The last two %CV values for CD9 and CD81 were 30% and 36.9% and they are both calculated from the stimulator cells in the lower compartment. For CD63, five of the seven %CV values could not be determined as one or both EV Array signals from the two technical replicates were below the

lower limit of detection (LOD). The last two %CV values for CD63 were 6.9 and 100.7. For the latter sample, the detected log2 signals were very close to the lower LOD (log2 values: 0.13 and 0.75).

Discussion/ conclusion

In the research field of EVs, much effort is put into deciphering the biological functions of these vesicular entities. Consequently, useful experimental and analytical platforms are of great interest. In this technical report, we present a cell culturing setup for the study of dynamic, contact-independent cell communication, focusing on the EVs involved. As depicted in Figure 1, this setup includes two compartments, where a membrane with 0.4 μm pores separates the cells. Initially, we wanted to investigate whether the transmembrane exchange of EVs were similar from both compartments. With the results presented in Figure 2, it is shown that for short time studies (<24h), the exchange of EVs is greatest from the upper to the lower compartment, than in the opposite direction. This observation is relevant because there are many studies, which investigate selected features of contact-independent cellular communication that have applied short incubation times (4, 8, 9, 12, 13). Moreover, these studies do not account for their choice of the relative placement of the cells in the two compartments, which our study indicates is highly relevant. Our study also suggests that this is important since for short times studies it may be advantageous to place the primary EV donor cells in the upper compartments, while the primary recipient cells should be placed in the lower compartment. Here, we have also demonstrated that the exchange of EVs between the two compartments must be subject to both diffusion and sedimentation, however, without determining the relative contribution of each of these two factors. In line with this, it would be logical to assume that the transport of EVs across the membrane depends on the concentration of EVs, which again depends on the rate of production and degree of uptake by the recipient cells. Hence, there are several factors affecting the more dynamic system of a co-culture than indicated by the "theoretical" EV transport described in Figure 2 and Table 1. One may therefore expect that the effects of the relative placement of two cell populations in the cell culturing setup could become less pronounced with long-time studies, i.e. over several days. Nonetheless, it would still be highly relevant to include both combinations of the compartments in a contact-independent cell culturing system to identify any major variations in the experimental outcome.

To demonstrate the applicability of the presented cell culturing setup and analytical strategy, contact-dependent and –independent co-cultures of human PBMCs were made. The aim was to investigate the resulting differences in the EV phenotypes from the two co-cultures using the EV Array. Furthermore, the effects that the relative placement of the two cell populations in the co-culture would have on the EV phenotype were also evaluated. For the 11 protein markers included in the EV phenotyping, there were clear contact-dependent differences after 6 days of co-culture (Figure 3). However, perhaps even more interesting was the observation of EV phenotype differences associated to the relative placement of the two cell populations in either the upper or lower compartment. Based on the results from the cell-free setup (Figure 2 and Table 1), it would be reasonable to place the cell population, which was expected to exert the major stimulatory function in the upper compartment, while the target cells can be placed in the lower compartment. This is

indeed supported by the fact that the EV phenotype changed for both stimulator and responder cells according to their position in the cell culturing setup. It seemed that these differences were more pronounced for the cell-specific markers (Figure 3, rightmost heat maps) than for the more general EV markers (Figure 3, leftmost heat maps). Even though the biological relevance of these observations were not investigated in more detail, it is not inconceivable that these observed differences could be important to the functional consequences of the EV-based communication between the involved cell populations. Consequently, this stresses the point that it may not be trivial how the cell populations are placed relative to each other, both for short-time and long-time studies of contact-independent cell communication.

The reproducibility of the cell-based experiments was evaluated by repeating the MLCs and the subsequent analysis after several weeks, using cells from the same individuals. As presented in Figure 4, obtained %CV values for CD9 and CD81 ranged from 1.7-36.7. However, 12 of these 14 samples had a %CV below 16, whereas the two highest values are calculated for the same sample, the stimulator cells in the lower compartment, pointing to an isolated trend for this sample. It has been established that the EV Array yields %CV values below 10, when working with plasma samples (10) and for immunoassays, %CV values below 25 have been proposed as an acceptable limit (14). However, this limit can be expanded if an experimental rationale for this is present (14), which may be the case when both technical and biological variations exist, as for this study. Nonetheless, one of the %CV values for CD63 differed somewhat more, amounting to 100.7 (Figure 4, italics). The log2 intensities from the relevant samples, forming the basis of the %CV calculation, were 0.13 and 0.75. Hence, the standard deviation was very large compared to the mean of the two intensity values, with a consequent large impact on the calculated %CV. This is an inherent issue for small intensities close to the lower LOD, which is difficult to completely circumvent. A third technical replicate may serve to improve the %CV. However, several other results from our work point to the fact that CD63 is a poor marker for EVs in general since it occurs in relatively low amount, as compared to CD9 and CD81 (unpublished data and (11)).

As part of the combined experimental setup presented here, the determination of the EV phenotype plays a major role. Using the EV Array to phenotype the vesicles provides the opportunity to gain much information about the system that is being studied. In the context of vesicle-based cell communication, the EV phenotype may be used for several purposes. First, the use of an extensive EV phenotype may aid in fine-tuning the biological hypothesis, which is being investigated. In this study, we targeted 11 protein markers. However, 60 analytes (here: antibodies) can currently be used simultaneously for each sample, when phenotyping EVs with the EV Array (10). Consequently, the EV phenotype may not only provide a large amount of information but can also be used to optimize the experimental design in an iterative fashion. Currently, the designed EV Array does not provide direct information about which cells produce the EVs and their absolute quantity. However, by linking the extensive EV phenotype to a number of additional experimental outcomes, such as the cellular phenotype or the EV RNA cargo, delineating the biological functions of the EV-based communication becomes substantial and highly relevant.

Summary

This technical report describes the use of a cell culturing setup and an analytical platform to study dynamic, contact-independent cellular communication facilitated by vesicles. From the report, a number of aspects can be summed up. First, for short-time studies (<24h), there was a greater exchange of EVs from the upper to the lower compartment of the cell culturing setup than in the opposite direction. For co-cultures, both short-time and long-time (several days) studies, it is recommended to evaluate both combinations of cells in the two compartments, to ensure that any effects of this are known. Our data suggests that it may be advantageous to place the primary EV producers in the upper compartment, while the principal vesicle recipient cells should be placed in the lower compartment. Finally, the collected experimental setup presented here provides a relevant and reproducible setup for *in vitro* studies of the functional consequences of EV-based cellular communication.

Acknowledgements

The authors thankfully acknowledge Dr. Shona Pedersen and Clinical Professor Søren Risom Kristensen (Department of Clinical Biochemistry, Aalborg University Hospital, Denmark) for their support in the NTA experiments. The authors also acknowledge technician Anne Elbæk (Department of Clinical Immunology, Aalborg University Hospital, Denmark) for excellent technical assistance.

Conflict of interest

The authors declare no conflict of interest.

References

1. Revenfeld AL, Baek R, Nielsen MH, Stensballe A, Varming K, Jorgensen M. Diagnostic and prognostic potential of extracellular vesicles in peripheral blood. Clin Ther. 2014; 36; 6:830-46.
2. Akers JC, Gonda D, Kim R, Carter BS, Chen CC. Biogenesis of extracellular vesicles (EV): exosomes, microvesicles, retrovirus-like vesicles, and apoptotic bodies. J Neurooncol. 2013 May;113; 1:1-11.
3. Andaloussi SEL, Mager I, Breakefield XO, Wood MJ. Extracellular vesicles: biology and emerging therapeutic opportunities. Nat Rev Drug Discov. 2013;12; 5: 347-57.
4. Hwang I, Shen X, Sprent J. Direct stimulation of naive T cells by membrane vesicles from antigen-presenting cells: distinct roles for CD54 and B7 molecules. Proc Natl Acad Sci U S A. 2003; 100; 11: 6670-5.
5. Nolte-'t Hoen EN, Buschow SI, Anderton SM, Stoorvogel W, Wauben MH. Activated T cells recruit exosomes secreted by dendritic cells via LFA-1. Blood. 2009;113; 9: 1977-81.
6. Mittelbrunn M, Gutierrez-Vazquez C, Villarroya-Beltri C, Gonzalez S, Sanchez-Cabo F, Gonzalez MA, et al. Unidirectional transfer of microRNA-loaded exosomes from T cells to antigen-presenting cells. Nat Commun. 2011; 2: 282.
7. Ren Y, Yang J, Xie R, Gao L, Yang Y, Fan H, et al. Exosomal-like vesicles with immune-modulatory features are present in human plasma and can induce CD4+ T-cell apoptosis in vitro. Transfusion. 2010; 51; 5: 1002-11.
8. Game DS, Rogers NJ, Lechler RI. Acquisition of HLA-DR and costimulatory molecules by T cells from allogeneic antigen presenting cells. Am J Transplant. 2005; 5; 7:1614-25.
9. Hwang I, Sprent J. Role of the actin cytoskeleton in T cell absorption and internalization of ligands from APC. J Immunol. 2001;166; 8:5099-107.
10. Jorgensen MM, Baek R, Varming K. Potentials and capabilities of the Extracellular Vesicle (EV) Array. J Extracell Vesicles. 2015; 4: 26048.
11. Jorgensen M, Baek R, Pedersen S, Soendergaard EK, Kristensen SR, Varming K. Extracellular Vesicle (EV) Array: microarray capturing of exosomes and other extracellular vesicles for multiplexed phenotyping. J Extracell Vesicles. 2013; 2: 20920.
12. Pegtel DM, Cosmopoulos K, Thorley-Lawson DA, van Eijndhoven MA, Hopmans ES, Lindenberg JL, et al. Functional delivery of viral miRNAs via exosomes. Proc Natl Acad Sci U S A.; 107; 14: 6328-33.
13. Rechavi O, Erlich Y, Amram H, Flomenblit L, Karginov FV, Goldstein I, et al. Cell contact-dependent acquisition of cellular and viral nonautonomously encoded small RNAs. Genes Dev. 2009; 23; 16: 1971-9.
14. Findlay JW, Smith WC, Lee JW, Nordblom GD, Das I, DeSilva BS, et al. Validation of immunoassays for bioanalysis: a pharmaceutical industry perspective. J Pharm Biomed Anal. 2000 ; 21; 6: 1249-73.

Figures

Figure 1

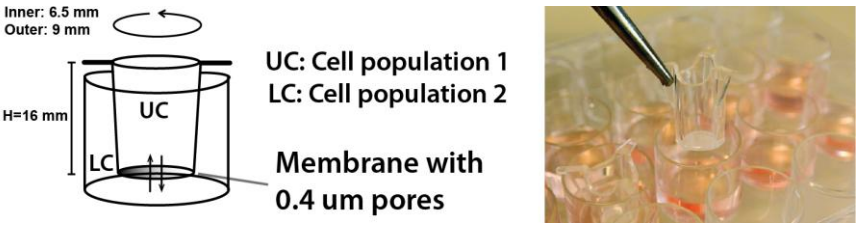

Figure 2

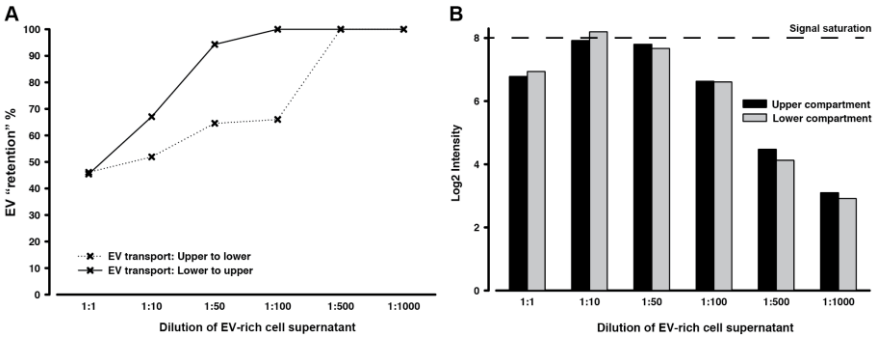

Figure 3

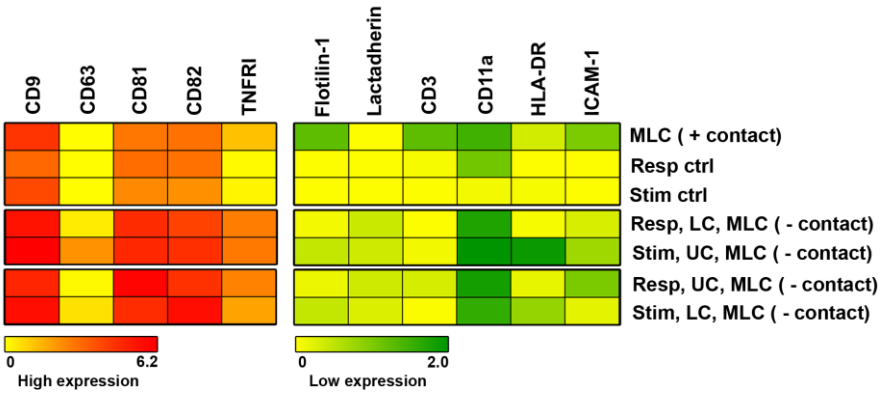

Figure 4

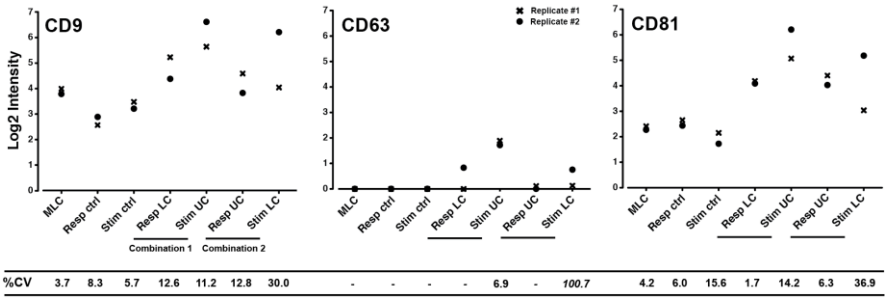

Figure legends

Figure 1 Principle of the culturing system for contact-independent cellular communication. In order to separate the two cell populations being studied, the use of cell culture inserts was applied. The insert was placed within a well of a standard culture plate (e.g. 6-well, 12-well, and 24-well plates), thus dividing the system into two compartments; an upper compartment (UC) and a lower compartment (LC). Multiple flanges at the top of the insert suspend it onto the edge of the culture plate well, which ensures that there is no direct contact between the insert and the well. A membrane is incorporated in the bottom of the insert, facilitating the cellular separation. The pore size of the membrane can vary according to the experimental design. In this report, the membrane pores are 0.4 μm in diameter, thus allowing for the passage of smaller vesicle subsets, such as exosomes (diameter 30-100 nm)[1], as well as soluble factors (indicated by the arrows).

Figure 2 Transmembrane exchange of EVs between the two compartments of the cell culturing setup. The exchange of EVs from the upper to the lower compartment of the cell culturing setup, and vice versa, was evaluated. A) An EV-rich cell supernatant from the human cell line LS180 was placed in one of the two compartments, while growth medium was placed in the opposite compartment. This was done with six dilutions of the supernatant, as indicated on the x-axis. After 24h, the content of each compartment was harvested and the amount of CD9, CD63, and CD81-enriched vesicles was semi-quantified using the EV Array. The EV "retention" percentage on the y-axis indicates how much of the total signal from the EV Array was accounted for by the signal from the compartment, where the EV-rich supernatant was put initially. B) After 24h, the EV Array signal (y-axis) from the two compartments in which the EV-rich supernatant was placed initially are shown. Each bar represents the mean of duplicates from the EV Array. The dashed line indicates signal saturation of the EV Array signal.

Figure 3 Detection of contact-dependent differences in EV phenotype. A contact-dependent and a contact-independent reaction between peripheral blood mononuclear cells from two different individuals were made. After 6 days of co-culture, the phenotypes of the produced EVs were evaluated using the EV Array to detect any contact-dependent differences. For non-specific reactions, monocultures of both stimulator (stim ctrl) and responder cells (resp ctrl) were included. Additionally, both combinations of responder and stimulator cells in the contact-independent MLC were included. As such, one combination included responder cells in the lower compartment (resp, LC) and stimulator cells in the upper compartment (stim, UC), while the other combination was reversed. Antibodies targeting the listed markers were used for capturing of the EVs. The signal observed for each of the markers infers a simultaneous presence of CD9, CD63, and/or CD81, since a cocktail of antibodies against these three exosomal markers was used for detection. For each type of MLC and controls, the mean value of two independent experiments

was used to create the heat map. The colored bars under the heat maps indicate the log2 intensity values obtained from the EV Array, where 8 is the maximum.

Figure 4 Reproducibility of the cell culturing setup and analytical platform. To demonstrate the reproducibility of the presented methodology, two independent experiments were performed of the contact-dependent and –independent mixed lymphocyte cultures (MLC)(one biological replicate). Displayed here are the results from three selected EV markers; CD9, CD63, and CD81 (also shown in Figure 3) from the EV Array analysis of the resulting cell supernatants. The corresponding %CV values are noted below each sample and were calculated based on the two technical replicates. The %CV values were not calculated for the samples with log2 signal intensities below the lower limit of detection (marked by -).

Tables

Table 1 Size distribution of the vesicles after 24h of transmembrane EV exchange. EV-rich cell supernatant was placed in either the upper (UC) or lower compartment (LC) of the cell culturing setup, while growth medium was placed in the opposite compartment. After 24h, the size of the EVs present in each compartment was determined by Nanoparticle Tracking Analysis (NTA). The data presented are from the 1:50 dilution shown in Figure 2. For each compartment, the signal from the EV Array is given along with the results from the NTA. The mean and the mode, and the corresponding standard deviations (SD), is given for triplicate measurements of each sample.

	EV Array signal	Mean size (SD) [nm]	Mode (SD) [nm]
EV transport: Upper to lower			
UC	7.8	105.9 (5.5)	88.6 (2.6)
LC	4.3	79.3 (2.7)	87.3 (9.1)
EV transport: Lower to upper			
LC	7.7	102.6 (0.6)	91.8 (5.8)
UC	0.5	97.1 (3.3)	85.3 (5.1)
Growth medium alone	0	103.9 (3.1)	102.1 (3.7)